

The structure of marine benthic food webs: Combining stable isotope techniques and inverse modeling

Dick van Oevelen



NETHERLANDS INSTITUTE OF ECOLOGY

The structure of marine benthic food webs: Combining stable isotope techniques and inverse modeling

Paranimfen:

Otto Hettinga

Maarten Jacobs

©Dick van Oevelen, Yerseke, 2005
d.vanoevelen@nioo.knaw.nl

This thesis is electronically available on the website of the University of Groningen:
<http://www.rug.nl/bibliotheek/catalogibestanden/elepubbrug/dissertaties/electronic>

The research presented in this thesis was conducted at the *Centre for Estuarine and Marine Ecology, Netherlands Institute of Ecology (NIOO-KNAW)*, Yerseke, The Netherlands. This is NIOO Thesis 44.

RIJKSUNIVERSITEIT GRONINGEN

**The structure of marine benthic food webs: Combining
stable isotope techniques and inverse modeling**

Proefschrift

ter verkrijging van het doctoraat in de
Wiskunde en Natuurwetenschappen
aan de Rijksuniversiteit Groningen
op gezag van de
Rector Magnificus, dr. F. Zwarts,
in het openbaar te verdedigen op
vrijdag 27 januari 2006
om 13.15 uur

door

Johannes van Oevelen
geboren op 15 juni 1975
te Bergen op Zoom

Promotores: Prof. dr. C. H. R. Heip
Prof. dr. J. J. Middelburg
Prof. dr. K. Soetaert

Beoordelingscommissie: Prof. dr. W. H. van der Putten
Prof. dr. P. C. de Ruiter
dr. A. F. Vézina

Contents

1	Introduction	1
1.1	The marine benthic food web	1
1.2	Stable isotopes in food web research: Natural abundance and tracer level	6
1.2.1	Stable isotopes at natural abundance level	6
1.2.2	Stable isotopes at tracer level	7
1.3	Research questions and thesis lay-out	8
2	Reconstructing food web flows using linear inverse models	11
2.1	Introduction	11
2.2	Linear inverse data assimilation in food web modeling	13
2.2.1	Ecological information	13
2.2.2	Model equations	14
2.2.3	Optimization norms	15
2.2.4	Combining the elements of LIM	16
2.3	Analysis of the inverse solution	18
2.3.1	Example food webs	18
2.3.2	Solution existence	19
2.3.3	Solution identifiability	19
2.3.4	Solution uniqueness	22
2.3.5	Solution sensitivity	24
2.4	Discussion	24
3	Carbon flow through a benthic food web: Integrating biomass, isotope and tracer data	27
3.1	Introduction	27
3.2	Methods	28
3.2.1	Study area, food web structure and data	28
3.2.2	Inverse model formulation and uncertainty analysis	30
3.3	Results	32
3.3.1	Inverse solutions and uncertainty analysis	32
3.3.2	Carbon flows in the benthic food web	35
3.4	Discussion	37
3.4.1	Field data	38
3.4.2	Extended inverse methodology, stable isotopes and tracer data	39
3.4.3	Pathways in the benthic food web	40
3.5	Appendix A: Inverse model equality and constraint equations	43
3.6	Appendix B: Introducing stable isotope and tracer data in an inverse model	47
3.6.1	Stable isotope data	47

Contents

3.6.2	Tracer data	48
3.7	Appendix C: Comparison of the inverse solutions CS, CIS and CITS	51
4	The fate of bacterial carbon in sediments: Modeling an in situ isotope tracer experiment	55
4.1	Introduction	55
4.2	Material and methods	57
4.2.1	Experimental approach	57
4.2.2	Analytical procedures	57
4.2.3	Model description	58
4.2.4	Calibration and uncertainty analysis	62
4.3	Results	63
4.3.1	Organic carbon pools	63
4.3.2	Labeling trajectories and model fits	64
4.4	Discussion	67
4.4.1	Model complexity and performance	67
4.4.2	Bacterial growth efficiency and production	68
4.4.3	Label pathways	69
4.4.4	Fate of bacterial carbon production	69
5	The trophic significance of bacterial carbon in a marine intertidal sediment: Results of an in situ stable isotope labeling study	73
5.1	Introduction	73
5.2	Materials and methods	74
5.2.1	Study site and experimental approach	74
5.2.2	Analytical procedures	75
5.2.3	Tracer model and calibration	76
5.3	Results	77
5.3.1	Label incorporation by bacteria	77
5.3.2	Meiobenthic and macrobenthic biomass	77
5.3.3	Meiobenthic and macrobenthic label incorporation	78
5.3.4	Dependence on bacterial carbon	78
5.4	Discussion	82
5.4.1	Bacteria as a carbon source	83
5.4.2	Selective feeding	85
5.4.3	Implications of the weak bacteria - benthos interaction	87
6	Fate of ¹³C labeled bacterial proteins and peptidoglycan in an intertidal sediment	89
6.1	Introduction	89
6.2	Materials and methods	90
6.2.1	Experimental setup	90
6.2.2	PLFA analysis	91
6.2.3	Amino acid analysis	91
6.3	Results and discussion	92
6.3.1	¹³ C incorporation into PLFAs, D-Ala and THAAs	92
6.3.2	Estimates of total bacterial ¹³ C uptake	93
6.3.3	Fate of bacterial ¹³ C: General trends	97
6.3.4	Fate of bacterial ¹³ C: ¹³ C-THAAs	97
6.3.5	Degradation of bacterial proteins versus peptidoglycan	99

6.3.6	Importance of peptidoglycan as a long term sink for bacterial ^{13}C	100
6.3.7	Substantial contribution of peptidoglycan to total sediment OC?	101
6.4	In summary	103
	Bibliography	104
	Summary	129
	Samenvatting	133
	Dankwoord	139
	Curriculum Vitae	141
	List of publications	143

Chapter 1

Introduction

1.1 The marine benthic food web

The marine environment is the largest ecosystem on earth, covering 71% of the earth's surface. This vast ecosystem is predominantly supported by primary production of phytoplankton in the photic zone, where it sustains the pelagic food web (Fig. 1.1). A small part of the organic carbon produced in the photic zone is exported and ultimately reaches the sediment, where it fuels the benthic community.

The benthic community is biologically diverse and consists of prokaryotic bacteria, protozoan flagellates and ciliates, and different metazoans. A rough classification of this diversity is generally based on organism size (Table 1.1 and Fig. 1.2) and is practical from several perspectives. First, abundance data of benthic communities typically show distinct size classes (Schwinghamer, 1981). Second, weight-specific physiological processes scale with body size (Peters, 1983), which makes size a useful parameter in the process of constructing energy budgets. Third, the presence of sediment particles makes sieving a practical way of separating organisms from the sediment and sieving divides a sample in size classes by definition.

Table 1.1: Size-based classification of the benthic community with size range, typical abundance level in coastal and estuarine sediments and the main groups in each size class.

Size class	Size range	Abundance	Main groups
Bacteria	0.5 - 4 μm	10^9 ml^{-1}	aerobic and anaerobic respirers, chemo-autotrophs, fermenters
Microbenthos	< 63 μm	10^3 ml^{-1}	flagellates, ciliates
Meiobenthos	63 - 1000 μm	10^6 m^{-2}	nematodes, foraminifera, copepods, turbellaria, ostracods
Macrobenthos	> 1000 μm	10^3 m^{-2}	polychaetes, bivalves, crustaceans, gastropods, echinoderms

Benthic communities in continental shelf or deep-sea sediments rely predominantly on vertical sinking of phytodetritus or horizontal bed-load transport of detritus (Graf, 1992). In contrast, estuaries and coastal systems are much shallower and therefore benthic fauna have direct access to their food sources. Benthic suspension feeders have direct access to

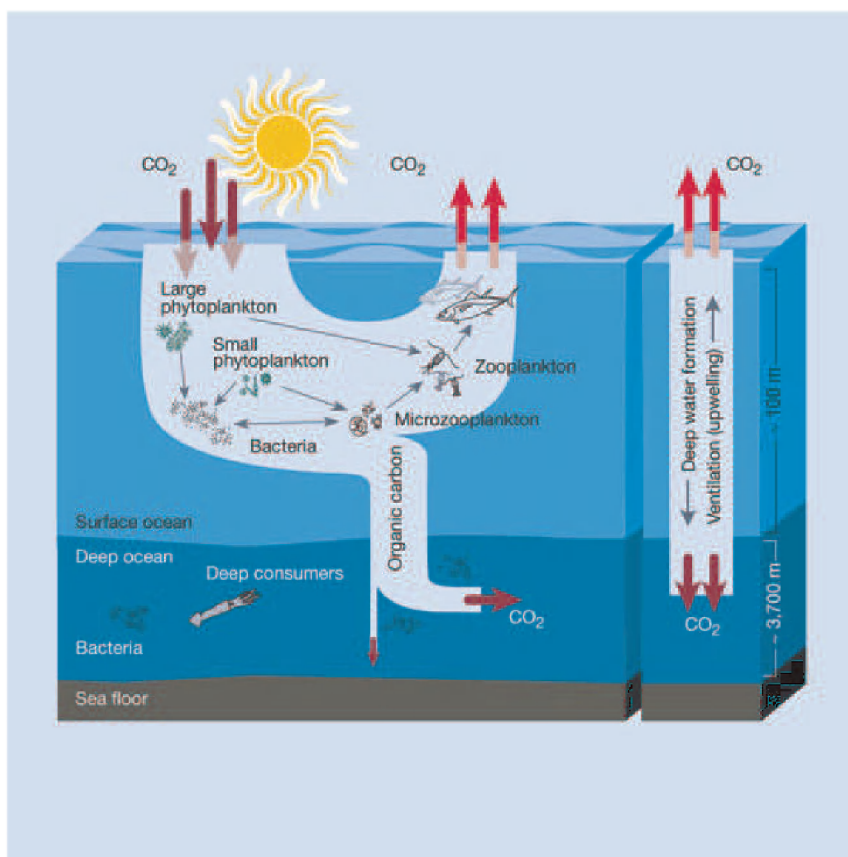


Figure 1.1: Major carbon flows in the marine ecosystem. Production of organic matter by phytoplankton supports the pelagic food web. Some organic matter escapes the surficial water layers and settles on the sediment, where it fuels the benthic food web. Remineralization of organic matter releases nutrients that are transported to the photic zone during upwelling events, where it in turn supports primary production (Chisholm, 2000).

phytoplankton and directly affect phytoplankton dynamics (Herman et al., 1999). Intertidal sediments are directly exposed to sunlight and are inhabited by microphytobenthos, unicellular eukaryotic algae and cyanobacteria, that have a high productivity (MacIntyre et al., 1996; Underwood and Kromkamp, 1999). Moreover, the close proximity of estuaries and coastal waters to other ecosystems results in additional carbon inputs. For example, salt marshes may be responsible for a large outwelling of organic carbon produced by salt marsh vegetation and river discharges bring in allochthonous organic matter derived from upstream terrestrial and freshwater ecosystems.

Our conceptual understanding of how these carbon inputs flow through the marine food web grew in complexity during the last decades. This discussion has focussed mainly on the pelagic food web, but is of equal relevance for the benthic food web. Initially, Steele (1974) developed marine food web theory on the herbivorous pathway in which phytoplankton is grazed by zooplankton which in turn is food for fish (Fig. 1.3). Another pathway that has received considerable attention is the detrital pathway. The

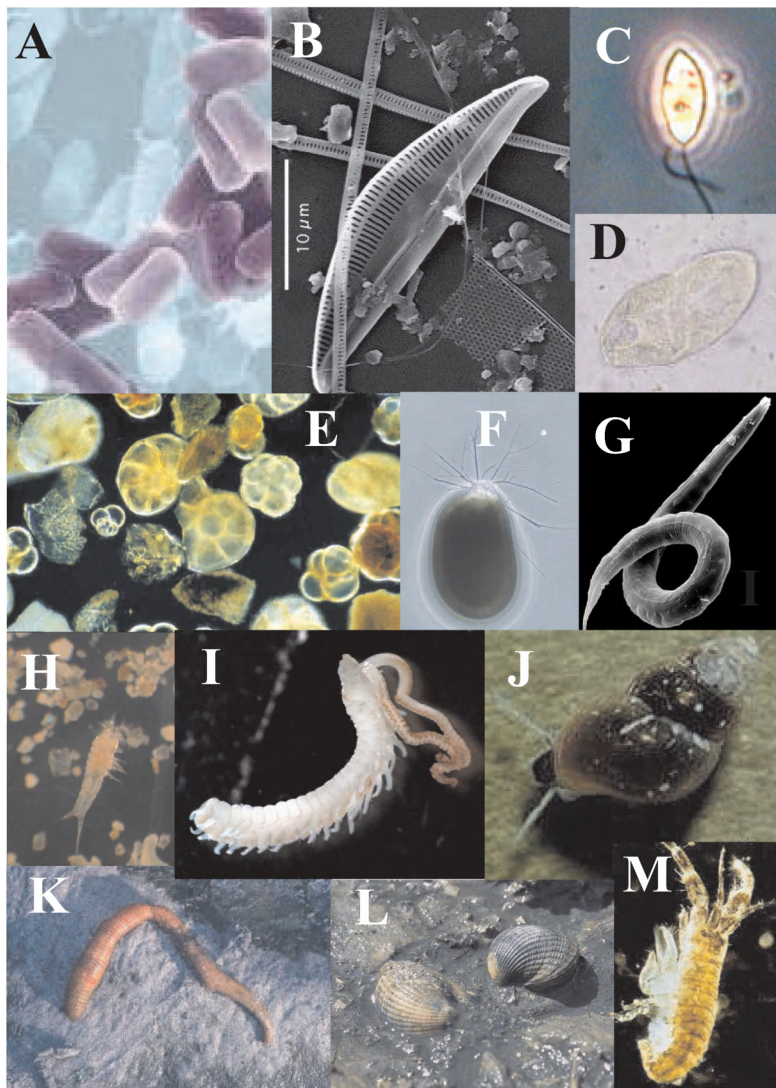


Figure 1.2: Compilation of different members of the benthic community A) bacteria, B) microphytobenthic diatoms, C) flagellates, D) ciliates, E) hard-shelled foraminifera, F) soft-bodied foraminifera, G) nematode, H) copepod, I) *Polydora cornuta* (polychaete), J) *Hydrobia ulvae* (gastropods), K) *Arenicola marine* (polychaete), L) *Cerastoderma edule* (bivalve), M) *Corophium volutator* (crustacean).

importance of detritus has been emphasized particularly for systems adjacent to salt marshes (Teal, 1962) (Fig. 1.3). Later discussion centered around the question whether assimilation of detrital carbon or attached bacteria is most important (Lopez and Levinton, 1987). The last major addition to marine food web theory has been carbon transfer through the microbial loop (Pomeroy, 1974; Azam et al., 1983) (Fig. 1.3). Dissolved organic

matter, produced by algae and bacteria, viral lysis and sloppy feeding zooplankton (Jumars et al., 1989), is assimilated by bacteria and through several transfer steps may eventually feed higher trophic levels. In this way, dissolved organic carbon that is otherwise not readily available for higher trophic levels may still contribute to the traditional food chain.

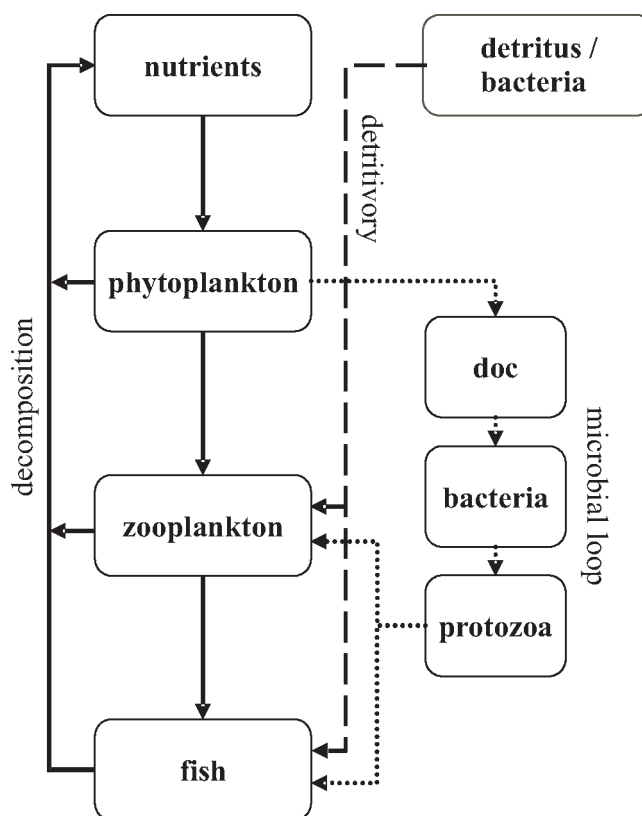


Figure 1.3: The complexity of marine food webs. In the traditional herbivorous food chain (line arrows), algal growth support zooplankton, which in turn support fish. In this view, bacteria are responsible for degradation of organic substances. The detrital pathway (long dashed arrows) is an additional carbon input to the traditional food chain by assimilation of detritus and associated bacteria. The microbial loop (dotted arrows) is assimilation of dissolved organic carbon by bacteria, subsequent grazing by protozoans and then transfer of carbon to the traditional food chain.

Our quantitative understanding of this complex 'spaghetti' of interactions in natural food webs is still very limited (Cohen et al., 1993; Polis and Strong, 1996; Herman et al., 1999; Azam and Worden, 2004; Moore et al., 2004), which is partly due to the large number of possible pathways and the difficulty to distinguish among them. Another important reason is that methodological and logistical limitations prevent from making all the necessary measurements at the same time at the same place in the field. The sedimentary environment is particularly notorious in this respect, because of high spatial and temporal variability, difficult accessibility and sampling, adsorption - desorption

1.1. The marine benthic food web

reactions and simply the presence of sediment particles that hinders the process of isolating benthic fauna. Because of these difficulties, our knowledge of benthic food webs is still limited (Herman et al., 1999). Hence, it remains a challenging task to decipher the element flows among the benthic community members and use this knowledge to come to a mechanistic and eventually predictive understanding of the structure of benthic food webs.

One way to study the structure of food webs is by means of mathematical modeling, which is taken up in this thesis by means of linear inverse modeling (LIM) and dynamic modeling. Both approaches are based on mass balances and aim to quantify the relations among the food web compartments (Fig. 1.4). In a LIM the flow values have a 'fixed' value and are considered to be a long-time average. Data are added as a value that represents the value of a flow or a combination of the flows. In a dynamic model, flows are described by mechanistic relationships and are a function of time. Data are used to fit the model parameters of the dynamic model such that the data are optimally reproduced. In general, linear inverse models have fewer data requirements and do not require detailed knowledge of mechanistic relationships (Gaedke, 1995). In contrast, dynamic models may harbor mechanistic knowledge, but require large data sets to assess the validity of the model and its parameters (Gaedke, 1995). Irrespective of the differences, both approaches have proven to be valuable tools in the quantification of food webs (Vézina and Platt, 1988; Cole et al., 2002; Van den Meersche et al., 2004). One basic requirement for effective use of these modeling approaches is the availability of data, that serve both as input for the model and as validation of the model output. Typically however, data availability is rather limited and adding new data resources that bring in additional pieces of information is a valuable strategy to increase the reliability of a food web model. In this thesis, we take advantage of developments in stable isotope techniques to increase the amount of data in our food web models. The next paragraph will briefly introduce some stable isotope techniques in food web research.

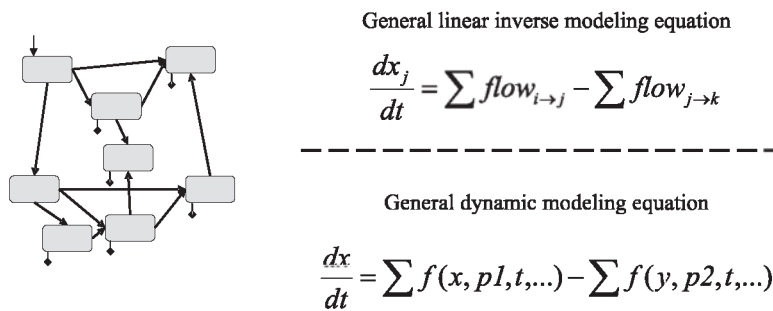


Figure 1.4: General equations for linear inverse modeling and dynamic modeling. On the left is a conceptual model of a food web. The connecting arrows define the incoming and outgoing flows for each compartment. In a linear inverse model these relationships are presumed to have a fixed value ($flow_{i \rightarrow j}$). In a dynamic model, the relationships are not fixed but expressed as a function of e.g. state variables (x), parameters ($p1$) and time (t). The resulting mass balance is a function of various different relationships with the other compartments in the food web.

1.2 Stable isotopes in food web research: Natural abundance and tracer level

1.2.1 Stable isotopes at natural abundance level

Isotopes are forms of one element, which differ in numbers of neutrons and therefore have a different atomic weight. Many isotopes are unstable and the nucleus disintegrates, releasing energy and radiation along the way, until a stable form is reached. Stable isotopes, as their name suggests, have a stable nucleus that does not disintegrate nor emits radiation. Elements that are mostly used in ecological research (C, N and S), consist for > 95 % of the lightest isotope, i.e. the stable isotope with the least number of neutrons. The isotope composition of matter is usually denoted in the δ notation; the deviation in the ratio of heavy to light isotope from a reference expressed in parts per thousand. For example the carbon $\delta^{13}\text{C}$ (‰) of a sample is

$$\delta^{13}\text{C} = \frac{\frac{^{13}\text{C}}{^{12}\text{C}}_{\text{sample}} - \frac{^{13}\text{C}}{^{12}\text{C}}_{\text{reference}}}{\frac{^{13}\text{C}}{^{12}\text{C}}_{\text{reference}}} \cdot 1000 \quad (1.1)$$

The reference material for carbon is carbonate Vienna Pee Dee Belemnite which has a isotope ratio R of $\frac{^{13}\text{C}}{^{12}\text{C}}$ of 0.0112372.

Biological processes may have different reaction rates for the heavy and the light isotope and reaction product tends to be depleted in heavy isotope with respect to its source. This process is called fractionation and resulting differences in isotope compositions may be used to trace the flow of elements through ecosystems (Peterson and Fry, 1987; Lajtha and Michener, 1994). For example, primary producers fractionate differently with respect to their inorganic carbon source and consequently have different $\delta^{13}\text{C}$ values (Fig. 1.5). Since there is limited fractionation associated with transfer up the food web, consumers have a $\delta^{13}\text{C}$ signature close to its resource according to the 'You are what you eat' principle (Post, 2002) (Fig. 1.5). Transfer of nitrogen up the food web is associated with ~ 3 ‰ enrichment per trophic level and may therefore be used to estimate trophic levels (Minagawa and Wada, 1984; Vander Zanden and Rasmussen, 1999; Post, 2002).

Several estuarine food web studies have taken benefit from stable isotopes to link producers and consumers. Peterson and Howarth (1987) clearly showed that macrobenthos in a salt marsh depended on phytoplankton and *Spartina* detritus, whereas sulfur-oxidizing bacteria and terrestrial organic matter were much less utilized. Herman et al. (2000) use the $\delta^{13}\text{C}$ difference between phytoplankton and microphytobenthos (see Fig. 1.5) to estimate dependence on local microphytobenthic production or pelagic production of an intertidal flat community. Rossi et al. (2004) used $\delta^{13}\text{C}$ signatures to demonstrate the existence of an ontogenic shift in the life-cycle of the bivalve *Macoma balthica*.

The main advantages of natural abundance stable isotope signatures are that they can be measured from comparatively small samples and isotope signatures integrate information on food sources that are assimilated in body tissues of field collected organisms over a longer period of time. However, in many cases there are more potential food sources than isotopes available to disentangle food web relationships (Phillips and Gregg, 2003). Also differences in δ signatures may be small and fractionation factors are not accurately known and may be variable (Gannes et al., 1997). An alternative way in which stable isotopes may be used to study food web dynamics is by means of a deliberate isotope tracer addition. This topic will be detailed in the next paragraph.

1.2. Stable isotopes in food web research: Natural abundance and tracer level

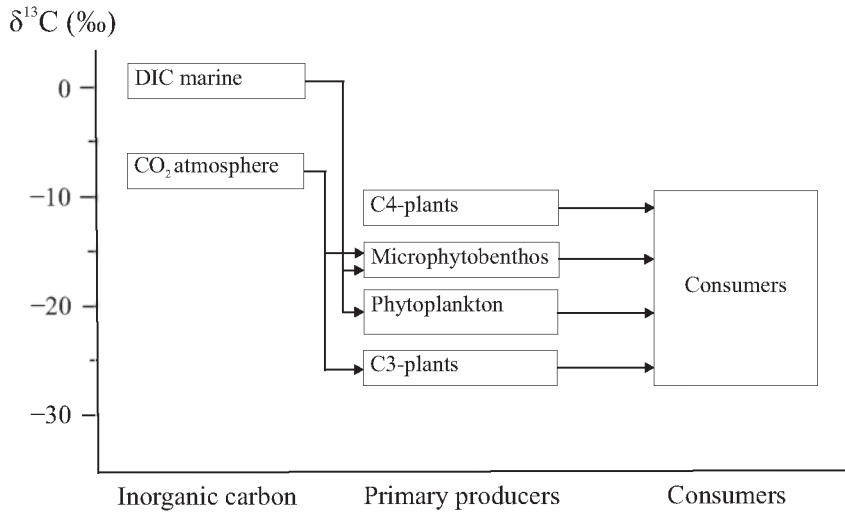


Figure 1.5: Relationship among $\delta^{13}\text{C}$ values of inorganic carbon sources, primary producers and consumers. The $\delta^{13}\text{C}$ value of the consumer depends on the importance of the different resources in its diet, e.g. a dominance of C4-plants will result in a $\delta^{13}\text{C}$ value close to -10 ‰. Adapted from Boschker and Middelburg (2002).

1.2.2 Stable isotopes at tracer level

One way to advance the use of stable isotopes in food web research is to deliberately modify the isotope composition of an (in)organic resource and monitor the transfer of this modification to other food web components. As compared to radioactive isotopes, stable isotopes have the advantage that they can be used to measure transfer rates *in situ* without legal restrictions or negative environmental effects. A change in the isotope composition compared to the background composition is denoted in the $\Delta\delta$ notation: $\Delta\delta = \delta_{\text{modified}} - \delta_{\text{background}}$. A modification of the isotope composition of an (in)organic resource will result in transfer of this modification to other food web components (see Fig. 1.6 for an example). The rate and magnitude of transfer depends on the importance of the resource for the consumer and turnover time of the consumer.

Stable isotope enrichment studies are basically done in two ways. One way is the introduction of inorganic nutrients or simple organic substrates in a food web. As such, inorganic nitrogen has been used as a tracer in rivers (Hamilton et al., 2001, 2004), estuaries (Holmes et al., 2000; Tobias et al., 2003) or sediments (Tobias et al., 2001) to quantify nitrogen transformation rates. ^{13}C -bicarbonate was used to quantify transfer up the food web of microphytobenthos in intertidal sediments (Middelburg et al., 2000) and phytoplankton in lakes (Cole et al., 2002; Pace et al., 2004). ^{13}C -acetate has been used in small streams to determine the importance of streamwater dissolved organic carbon and bacterial carbon for the invertebrate community (Hall et al., 2000). The other way is to culture algae in an isotopically enriched medium, harvesting the algae and feed them to retrieved sediment cores (Moodley et al., 2000) or *in situ* sediments (Blair et al., 1996; Levin et al., 1997; Moodley et al., 2002, 2005; Witte et al., 2003; Nomaki et al., 2005). In both cases, transfer of label to aquatic and benthic organisms is monitored in time and

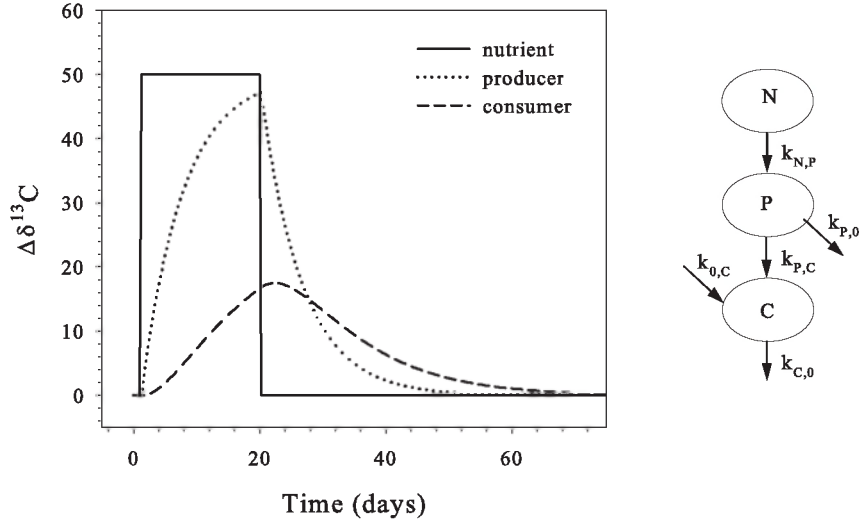


Figure 1.6: Transfer of label among a nutrient (N), producer (P) and consumer (C) compartment due to an pulse enrichment of the nutrient compartment (see Hamilton et al. (2004)): $\frac{d \Delta \delta P}{dt} = k_{N,P} \cdot \Delta \delta N - (k_{P,C} + k_{P,0}) \cdot \Delta \delta P$ and $\frac{d \Delta \delta C}{dt} = k_{P,C} \cdot \Delta \delta P - k_{C,0} \cdot \Delta \delta C$, with $k_{N,P} = k_{P,C} + k_{P,0} = 0.15$, $k_{P,C} = 0.05$ and $k_{C,0} = 0.10$, such that P obtains 100% of its nutrient requirements from N, but C obtains only 50% from P. An assumption of the model is a steady-state biomass of P and C.

used to quantify assimilation of the added substrate. These studies have revealed important insights in the structure of natural food webs through in a way that was previously not available.

1.3 Research questions and thesis lay-out

The material presented in this thesis is intended to expand our methodological capabilities to study the structure of marine benthic food webs and to apply these to answer some pressing ecological questions. The focus in this thesis is on the importance of the herbivorous, microbial and detrital pathways in an intertidal food web, with special attention for the microbial pathway. A large biological data set is required to accurately decipher the large number of carbon transfers in benthic food webs (Fig. 1.3). Therefore, we integrate a data set that consists of biomass data, process rates, natural abundance stable isotope signatures and isotope tracer data and quantify the carbon flows in the food web of the Molenplaat intertidal flat. Another important topic in benthic food web research has been the fate of bacterial carbon in marine sediments (Kemp, 1990). The main focus so far has been on transfer to grazers, but bacterivory has been found insufficient to account for measured bacterial production rates (Kemp, 1987; Epstein and Shiaris, 1992; Hondeveld et al., 1992; Hamels et al., 1998). Another possible fate is burial of bacterial carbon, e.g. Grutters et al. (2002) report the preservation of refractory cell wall components in marine sediments. However, data that allow to disentangle the possible fates of bacterial

1.3. Research questions and thesis lay-out

carbon production simultaneously are currently lacking.

Specifically, the main research questions that motivated our work were:

1. How can biomass, process rates, natural abundance and tracer stable isotope data be integrated to quantify food web flows?
2. How are the carbon flows in a intertidal flat partitioned among the herbivorous, microbial and detrital pathways?
3. What is the fate of benthic bacterial carbon production?
4. What is the importance of bacterial carbon in diets of benthic fauna?

Chapter 2 gives a review of current approaches in linear inverse modeling. The aim of these approaches is similar: reconstructing element flows in food webs from incomplete data sets. However, the inverse problem is approached from different viewpoints. We present a framework that can be used to identify the origin of these differences. In addition, several methods are proposed that allow to analyze the properties of the food web reconstruction, a topic that has been overlooked in most previous LIM applications.

Chapter 3 builds on the previous chapter and provides a case-study on how knowledge on carbon processing and carbon stocks, stable isotopes at natural abundance and tracer level can be integrated by means of linear inverse modeling. In addition, it is explicitly shown how the uncertainty in the food web reconstruction decreases when new data are added to the LIM. The ecological implications of the reconstructed benthic food web are discussed.

One conclusion in chapter 3 is that the majority of bacterial carbon production recycles back to detritus and/or dissolved organic carbon and only a limited amount of bacterial carbon production is grazed. This conclusion provided the starting point for chapter 4, in which the results from an in situ ^{13}C isotope tracer experiment that aimed to quantify the importance of different fates of benthic bacterial carbon production are presented.

The key question to be answered in chapter 5 is: How much of their carbon requirements do meiobenthos and macrobenthos derive from bacterial carbon? Data from an in situ ^{13}C labeling experiment are interpreted with a simple isotope model to estimate the dependence on bacterial carbon. The ecological implications of the bacteria-benthos interaction are discussed.

Chapter 6 compares the dynamics of different bacterial biomarkers: polar-lipid-derived fatty acids (PLFAs), D-alanine as a marker peptidoglycan and total hydrolyzable amino acids (THAA). These biomarkers represent different parts of bacterial biomass and are expected to show different degrees of degradability. The results are discussed with respect to the use of biomarkers to quantify total bacterial label uptake, the importance of carbon burial as a sink of bacterial production and differences in degradation rates of bacterial compounds.

Chapter 2

Reconstructing food web flows using linear inverse models

Dick van Oevelen, Karline Soetaert, Jack J. Middelburg. *In preparation*

2.1 Introduction

The food web is a pivotal concept in ecology. It is the formal expression of the exchanges of energy or matter among living and non-living compartments in an ecosystem. The structure of food webs has important implications for ecosystem stability (De Ruiter et al., 1995; McCann et al., 1998), biogeochemical cycling (Berg et al., 2001), fishery harvest (Ryther, 1969) and exposure to toxic chemicals (Parmelee et al., 1993). The complex nature of food webs renders their study a challenge, which is taken up by means of field observations, experimental manipulation and modeling.

Food webs can be studied at various levels of abstraction. Topological studies analyze and generalize the patterns and statistics of the linkages within food webs (Pimm et al., 1991). Theoretical ecologists apply simple mechanistic models to study food web functioning. Classical food web paradigms, such as the paradox of enrichment (Rosenzweig, 1971) and competitive exclusion (Armstrong and McGehee, 1980) arise from these Lotka-Volterra models. The realism of the model predictions is assessed by qualitative comparison to empirical data (e.g. Fox and Olsen (2000) and Diehl and Feissel (2001)) or statistical testing (e.g. Scheffer (2001) and Van de Koppel et al. (2001)).

Such theoretical and experimental studies of simple food webs have provided the core of ecological theory. However, there is a strong need for a more quantitative approach of natural food webs (Cohen et al., 1993; Hall and Raffaelli, 1993; Johnson and Omland, 2004). This trend is apparent in population modeling (Kendall et al., 1999; Persson et al., 2004), stability analysis (De Ruiter et al., 1995), nutrient cycling studies (Vanni, 2002) and research on food limitation (Gaedke et al., 2002). In addition, ecological network analysis, in which descriptive indices are derived from food web matrices (Ulanowicz, 1986; Bersier et al., 2002), relies on accurate estimates of food web flows.

Advances in our knowledge through quantifying food webs relies on the crucial merge of observations and models; the area of inverse data assimilation techniques. Data assimilation refers to data incorporation within a model structure and inverse means that

field observations (e.g. primary production) are used to reconstruct the underlying model parameters (e.g. food web flows). Inverse methods are highly valued in geophysical sciences (Menke, 1984; Sun, 1994; Wunsch, 1996; Kasibhatla et al., 1999; Lary, 1999; Wang et al., 2000), where data inferences can only be made indirectly. The essentials of inverse solutions are treated extensively in these texts. They comprise 1) solution existence, 2) solution identifiability, 3) solution uniqueness and 4) solution sensitivity. These properties reveal important information of the system at hand.

Advanced ecological applications of data assimilation in food web models are mainly found in the marine realm (e.g. Prunet et al. (1996), Vallino (2000) and Friedrichs (2002)) and rely on fitting model parameters to observed time series or spatial distribution patterns, after which the food web flows are recovered. Such non-linear inverse problems are solved with complex numerical techniques (e.g. simulated annealing, adjoint or genetic algorithms), which require significant computer time, are complicated to implement and do not always retrieve the optimal parameter set (Lawson et al., 1996; Athias et al., 2000; Vallino, 2000; Soetaert et al., 2002). Moreover, additional reasons limit the use of these mechanistic modeling approaches in ecology (Gaedke, 1995). First of all, environmental sciences typically deal with poorly or partly understood mechanisms, complicating appropriate process descriptions. Second, the model outcome can be sensitive to closure terms (Steele and Henderson, 1992), i.e. terms that describe phenomena not explicitly accounted for. Third, parameter values are often not known accurately enough to determine a start range from which they can be fitted. Fourth, data sets are usually too sparse to constrain all parameters of a mechanistic model.

In contrast, simple linear inverse box models (LIM) have fewer data requirements and regard the food web as a linear system of flows that interconnect the compartments. The flows are quantified by solving a mass balance description supplemented with site-specific and literature data on biomass and flows. Their simplicity renders these LIM a widely applied inverse technique, also known as inverse analysis (e.g. Klepper and Van de Kamer, 1987; Vézina and Platt, 1988; De Ruiter et al., 1995). In addition, ECOPATH models (Christensen and Pauly, 1992) are based on similar mass balance modeling. Even though data requirements are limited as compared to fully mechanistic models, LIM problems are initially under determined; the available measurements are insufficient to uniquely determine all flows. Dealing with this non-uniqueness and under determinacy poses the major challenge in quantitative food web studies. Moreover, the analysis of the food web solution has received comparatively limited attention in the ecological literature.

In this paper we first develop a framework of LIM by explicit distinction of its elements (1) ecological information sources, (2) equations and (3) minimization norms. This framework is used to show that inconsistency in ecological LIM approaches are rooted in the way these elements are combined when solving the non-uniqueness and under determinacy problem. Secondly, 5 published LIM of food webs will be analyzed in terms of solution existence, identifiability, uniqueness and sensitivity. This solution analysis shows the current limitations and pitfalls of the inverse method. Finally, we present some recommendations to develop further LIM in ecology.

2.2 Linear inverse data assimilation in food web modeling

The crux of linear inverse data assimilation is to optimally merge ecological data within a food web model. This definition identifies three distinct elements of LIM: 1) ecological information, 2) linear model equations and 3) an optimization norm (Fig. 2.1). These elements will be discussed in the remainder of this section.

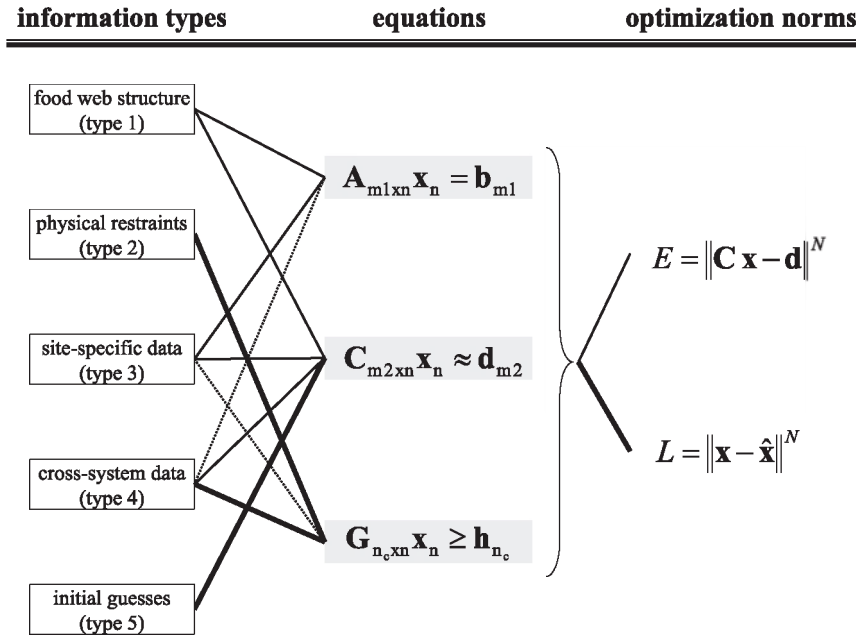


Figure 2.1: The three elements of linear inverse models in food web research: information types (see 2.2.1 Ecological information), equations (see 2.2.2 Model equations) and optimization norms (see 2.2.3 Optimization norms) and how they are combined in applications (connectors). The thickness of the connectors indicates the occurrence of a particular combination in the literature: dashed = few, solid = moderate and thick = many occurrences.

2.2.1 Ecological information

Ecological information sources relevant for food web modeling can be partitioned into 5 types, of which the first two are universal and the latter three are optional in LIM applications.

1. Food web structure consists of flows interconnecting the compartments and thereby defines a mass balance in terms of input (e.g. consumption) and output (e.g. respiration) for each compartment (Fig. 2.2).
2. Physical reality is information of physical nature, e.g. flows must be non-negative.
3. Site-specific observations are data on biomass, flows or combination of flows from the system under consideration. Typical flow measurements are production rates and community respiration.

4. Cross-system or literature data is information taken from other similar systems or from expert judgment. Typical data in this category are assimilation and production efficiencies.
5. Initial guesses are inferences about the possible values of the flows. Researchers may use measurements, literature (rate) or expert information to impose the most likely value of a flow. Initial guesses are also frequently used to find the simplest or parsimonious solution by setting them to zero. The parsimonious solution then is the solution that is closest to the initial estimates of zero.

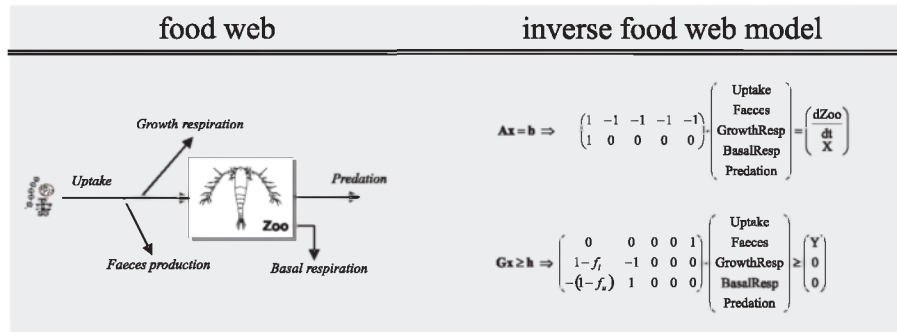


Figure 2.2: Example of a simple 'food web', implemented as a linear inverse model. Zooplankton (*Zoo*) take up algae; uptake is either lost as faeces, used for growth or growth respiration; other loss terms are predation and basal respiration. Mass balance is assured by the term accounting for the increase of biomass ($\frac{dZoo}{dt}$). X is the measured uptake by zooplankton, Y is the lower boundary imposed on the predation rate. f_l and f_u are the lower and upper bounds on the assimilation efficiency, respectively.

2.2.2 Model equations

Linear inversion allows for three types of equations: (1) a set of equations that must be satisfied exactly, (2) one that must be satisfied as closely as possible and (3) one set of inequalities (Fig. 2.1).

$$\mathbf{A}_{m_1, n} \mathbf{x}_n = \mathbf{b}_m \tag{2.1}$$

$$\mathbf{C}_{m_2, n} \mathbf{x}_n \approx \mathbf{d}_m \tag{2.2}$$

$$\mathbf{G}_{m_c, n} \mathbf{x}_n \geq \mathbf{h}_{m_c} \tag{2.3}$$

where the vector \mathbf{x} holds the n unknown flows, m_1 is the number of equalities that must be satisfied exactly, m_2 is the number of equalities that must be satisfied as closely as possible and m_c is the number of constraints. Matrices \mathbf{A} , \mathbf{C} and \mathbf{G} contain linear expressions of the flows and vectors \mathbf{b} , \mathbf{d} and \mathbf{h} hold numerical data (Fig. 2.2). The number of equations ($m_1 + m_2$) compared to the number of unknowns (n) determines the three possible states of a LIM: over determined ($m_1 + m_2 > n$), even determined ($m_1 + m_2 = n$) and under determined ($m_1 + m_2 < n$).

2.2.3 Optimization norms

In inverse theory two norms are distinguished: the prediction (or residual) norm and the solution norm. The prediction norm (E) measures the error between model predictions and observations

$$E = \| \mathbf{C}\mathbf{x} - \mathbf{d} \| ^N \quad (2.4)$$

whereas the solution norm (L) is a length measure based on the model parameters (flows)

$$L = \| \mathbf{x} - \hat{\mathbf{x}} \| ^N \quad (2.5)$$

where $\hat{\mathbf{x}}$ are the initial guesses of the flows and $\| \cdot \| ^N$ denotes some norm of power N , which generally takes the value of 1, 2 or ∞ (see below). The determinacy state principally determines which optimization norm is chosen to solve the LIM (see below); sometimes, the model solution is a compromise between both types of norms (Menke, 1984; Vézina and Platt, 1988). Vézina et al. (2004) have recently tested some optimization norms based on ecological theory (i.e. exergy and ascendancy) in a twin modeling experiment, but the results were ambiguous as no single norm was optimal under all circumstances.

Over determined model

Inevitable measurement noise implies that over determined models can never be solved with zero prediction error. Minimizing the prediction norm assures that the solution optimally agrees with all observations. The power of the prediction norm is related to the statistical distribution of the residuals. The L1 prediction norm ($N = 1$) weighs all deviations equally and is most appropriate in data sets that have a high probability of extreme data, e.g. when data are exponentially distributed (Menke, 1984). The L2 prediction norm is most commonly selected and assumes Gaussian statistics; larger deviations weigh more heavily on the norm. Successively higher powers of the norm give increasingly larger weight to the largest deviation, with the L_∞ prediction norm as most extreme case, i.e. only the equation that deviates most is optimized (Menke, 1984).

Measurement uncertainty can be used to assure that deviations from more accurate observations weigh heavier on the prediction norm. This is achieved by so-called row scaling (Wunsch, 1978; Menke, 1984; McIntosh and Rintoul, 1997)

$$\mathbf{S}_{m2 \times m2}^{1/2} \mathbf{C}_{m2 \times n} \mathbf{x}_n \approx \mathbf{S}_{m2 \times m2}^{1/2} \mathbf{d}_{m2} \quad (2.6)$$

where ideally \mathbf{S} is the error covariance matrix of the observations. As covariances are generally unknown, a diagonal matrix with the observation variance is used instead.

Even determined model

An even determined model has one unique solution that has zero prediction error.

Under determined model

An under determined model has infinite solutions with similar minimal prediction norm. Therefore, the model is solved by minimizing the prediction norm and the solution norm. When minimizing the solution norm, the power of the norm affects the weight that is given to the magnitude of the flow. Each flow weighs proportionally in the L1 solution norm, whereas large flows weigh more heavily in the L2 solution norm and with the L_∞ solution

norm only the largest flow is minimized. Following Vézina and Platt (1988), ecological applications typically solve parsimonious food webs (with initial guesses of unknown flows as zero, i.e. $\mathbf{x}_n = 0$) with the L2 solution norm. The solution is interpreted as the simplest food web satisfying mass conservation and biological constraints (Vézina and Platt, 1988). When a mixture of currencies (e.g. C and N) is used, scaling of the flows may be necessary, assuring equal weight in the solution norm (see e.g. Jackson and Eldridge, 1992). For a LIM solved with the L2 solution norm, this is achieved by (Wunsch, 1978)

$$\left(\mathbf{C}_{m2 \times m2} \mathbf{W}_{n \times n}^{-1/2} \right) \left(\mathbf{W}_{n \times n}^{1/2} \mathbf{x}_n \right) \approx \mathbf{b}_{m2} \quad (2.7)$$

which transforms to

$$\mathbf{C}'_{m2 \times n} \mathbf{x}'_n \approx \mathbf{b}_{m2} \quad (2.8)$$

from which the weighed \mathbf{x}' is solved. Subsequently, the unknowns flows are recovered with

$$\mathbf{x}_n = \mathbf{W}^{-1/2} \mathbf{x}'_n \quad (2.9)$$

Formally, \mathbf{W} is the error covariance matrix of the model parameters (Wunsch, 1978), but is usually taken to be a diagonal matrix containing column weights, for example C:N ratios to transform N flows to C equivalents (Jackson and Eldridge, 1992) or biomass such as to weigh the flows with stock size (Vézina and Savenkoff, 1999).

2.2.4 Combining the elements of LIM

The major challenge in LIM is the non-uniqueness and under determinacy of food webs. With 5 information types, 3 types of model equations and different optimization norms, there is great potential for variation in strategies to resolve these issues (Fig. 2.1). Based on this combination of LIM elements it is possible to categorize the various applications encountered in the literature.

Information type 1

Mass balances are based on the conservation of mass principle. Most applications assume that mass balances are in steady-state (i.e. input = output) over the investigated period and enforce this condition (Stone et al., 1993; Niquil et al., 1998; Diffendorfer et al., 2001; Leguerrier et al., 2003; Breed et al., 2004; Leguerrier et al., 2004; Richardson et al., 2004), whilst others allow small deviations from this condition, which are interpreted as changes in the stock over time (Vézina and Platt, 1988; Chardy et al., 1993; Vézina and Pace, 1994; Vézina and Savenkoff, 1999; Richardson et al., 2003). Other researchers start from non steady-state conditions, based on measured stock changes with time and require that the accumulation term in the mass balance is met exactly (Donali et al., 1999) or approximately (Vézina et al., 1997; Hart et al., 2000; Gaedke et al., 2002). Again others define the accumulation term as an additional unknown input or output flow to be solved in the LIM (Klepper and Van de Kamer, 1987, 1988; Jackson and Eldridge, 1992; Eldridge and Jackson, 1993; Lyche et al., 1996a,b; Vézina et al., 2000; Richardson et al., 2003).

Information type 2:

Physical constraints are always implemented in equation 2.3.

Information type 3

Site-specific observations are the most important data source for LIM as they allow discriminating the studied ecosystem from other systems. However, there is little consistency as into which equation this information is implemented. Niquil et al. (1998), Donali et al. (1999), Leguerrier et al. (2003), Breed et al. (2004), Leguerrier et al. (2004) and Richardson et al. (2004) impose that observations should be exactly reproduced in the final solution. This is in contrast with others who allow deviations from the observations (Klepper and Van de Kamer, 1987, 1988; Vézina and Platt, 1988; Jackson and Eldridge, 1992; Chardy et al., 1993; Eldridge and Jackson, 1993; Vézina and Pace, 1994; Vézina et al., 1997; Vézina and Savenkoff, 1999; Hart et al., 2000; Vézina et al., 2000; Diffendorfer et al., 2001; Gaedke et al., 2002; Richardson et al., 2003; Vézina and Pahlow, 2003). Lyche et al. (1996a,b) fitted data of a radioisotope study with a tracer model and implemented the 95 % confidence interval of each flow in the constraint equation (Eqs. 2.3). Leguerrier et al. (2003), Leguerrier et al. (2004) and Vézina et al. (2000) introduce field data also in the constraint equation (Eqs. 2.3).

Information type 4

For most processes and flows in food webs there exist data in the literature. However, the idiosyncrasy of natural food webs implies that one cannot simply assume universal validity of flow or process data across systems and seasons. Authors rate this validity and uncertainty differently. Some put this type of information on equal footing as site-specific observations and introduce these cross-system data in the same equations as their site-specific observations (Klepper and Van de Kamer, 1987, 1988; Chardy et al., 1993; Stone et al., 1993; Hart et al., 2000; Diffendorfer et al., 2001; Gaedke et al., 2002; Leguerrier et al., 2003, 2004). By doing so, the level of under determinacy decreases and the LIM may even become over determined. Others consider this type of data as rather uncertain and refer literature information to the inequality equation (Eqs. 2.3) (Vézina and Platt, 1988; Jackson and Eldridge, 1992; Eldridge and Jackson, 1993; Vézina and Pace, 1994; Lyche et al., 1996b; Vézina et al., 1997; Niquil et al., 1998; Donali et al., 1999; Vézina and Savenkoff, 1999; Vézina et al., 2000; Leguerrier et al., 2003; Richardson et al., 2003; Breed et al., 2004; Leguerrier et al., 2004; Richardson et al., 2004).

Information type 5

A suite of applications minimize the sum of squared flows (i.e. L2 solution norm) and thereby implicitly use initial guesses of zero in the solution norm (Vézina and Platt, 1988; Jackson and Eldridge, 1992; Eldridge and Jackson, 1993; Vézina and Pace, 1994; Lyche et al., 1996a,b; Vézina et al., 1997; Niquil et al., 1998; Donali et al., 1999; Vézina and Savenkoff, 1999; Vézina et al., 2000; Leguerrier et al., 2003; Richardson et al., 2003; Breed et al., 2004; Leguerrier et al., 2004; Richardson et al., 2004). Others derive initial guesses from the literature data and arrive at an over determined system, which is solved by minimizing the residual norm (Klepper and Van de Kamer, 1987, 1988; Chardy et al., 1993; Stone et al., 1993; Hart et al., 2000; Diffendorfer et al., 2001; Gaedke et al., 2002).

Power and weighting of the minimization norms

There is also some leeway in which norm is used. The L1 prediction norm has been applied by Stone et al. (1993), Hart et al. (2000), Diffendorfer et al. (2001) and Gaedke

et al. (2002) and the weighted L1 prediction norm is applied by Klepper and Van de Kamer (1987) and Klepper and Van de Kamer (1988). The L2 solution norm is applied in many studies (Lyche et al., 1996a), Niquil et al. (1998) Donali et al. (1999) Leguerrier et al. (2003) Breed et al. (2004), Leguerrier et al. (2004) and Richardson et al. (2004). The weighted L2 solution norm is used by Jackson and Eldridge (1992) and Eldridge and Jackson (1993) and the weighted L2 prediction norm is used by Chardy et al. (1993). Finally, a combination of the L2 solution and residual norm is used by Vézina and Platt (1988) and Lyche et al. (1996a) and a combination of the weighted L2 solution and prediction norm is used by Vézina and Pace (1994), Lyche et al. (1996b), Vézina et al. (1997), Vézina and Savenkoff (1999), Vézina et al. (2000) and Richardson et al. (2003).

This systematic evaluation of LIM applications shows that there is little consistency in the way LIM elements are combined (Fig. 2.1), but most prominent differences exist in

1. the amount of cross-system data, prior information and initial guesses available and how these data enter the different equations, which relates to how one overcomes the under determinacy of the model and
2. the minimization norm that is chosen to solve the resulting equations, i.e. how one singles out one solution.

2.3 Analysis of the inverse solution

The quality of parsimonious food web reconstructions and the implications of the steady-state assumption have been tested through twinning experiments in which food web flows are reconstructed from data generated by mechanistic food web models (Vézina and Pahlow, 2003). However, a rigorous analysis of the inverse food web solution is usually lacking. In what follows, a review of the literature and a systematic analysis of five published LIM according to 4 criteria is presented: solution existence, identifiability, uniqueness and sensitivity and show that such an analysis is not only informative, but also essential if we are to increase our understanding of real food web functioning. Our objective is to show that solution analysis reveals informative features of food webs and that these may aid in the evaluation of the results and illumination of potential limitations and pitfalls of the inverse method.

2.3.1 Example food webs

Five studies that applied LIM to recover carbon flows in marine (Donali et al. 1999, Niquil et al. 1998, Leguerrier et al. 2003, Chapter 3) and freshwater (Diffendorfer et al., 2001) systems were selected for analysis. The systems differed in compartment and flow resolution, number of in situ and literature flow data, number of inequalities and minimization norm (Table 2.1). The marine examples considered the benthic or pelagic food web, consisting of autotrophs, bacteria, size-class based eucaryotes (i.e. flagellates and zooplankton) and non-living compartments DOC (dissolved organic carbon) and detritus, whereas only Leguerrier et al. (2003) considered a coupled benthic-pelagic system. There were biomass estimates for most compartments and several site-specific flow measurements (e.g. primary production). Literature data were used either to increase the number of imposed flow measurements (Leguerrier et al., 2003) or to constrain respiration and production rates, assimilation and bacterial growth efficiencies and diet composition. Diffendorfer et al. (2001) restricted the analysis to a herpetological assemblage (9 groups, including salamanders, frogs and snakes), for which biomass

2.3. Analysis of the inverse solution

and diet composition data were measured or estimated. There were no direct flow measurements, but consumption and respiration rates were estimated from the literature and used to set up constraints and initial guesses. All food webs were considered to be in steady-state, except for Donali et al. (1999) who estimated rates of change through successive sampling. Van Oevelen et al. (Chapter 3) used carbon and $\delta^{13}\text{C}$ mass balances to reconstruct carbon flows in an intertidal benthic food web and two cases are considered: one where only total carbon flows were considered, one with both carbon mass balances. All food webs are implemented, solved and analyzed in the modeling environment FEMME (Soetaert et al., 2002) (see <http://www.nioo.knaw.nl/cemo/femme> for downloads).

Table 2.1: Characteristics of 5 food webs from the literature in terms of number of flows (F) and compartments (C), site-specific data, number of equations (E) and inequalities (I) and solution norm (N). References are 1) Donali et al. (1999), summer food web 2) Niquil et al. (1998), 3) Leguerrier et al. (2003), 4) Diffendorfer et al. (2001), wet prairie food web and 5) Van Oevelen et al. (Chapter 3). Abbreviations are bm = biomass pp = primary production, bp = bacterial production, zp = zooplankton production and respiration, op = oyster predation, cr = community respiration, sr = sedimentation rate, rc = rate of change, dc = diet composition, ni = natural abundance isotope data, ti = tracer isotope data.

Site characteristics ^{Reference}	F	C	Site-specific data	E	I	N
Gulf of Riga, pelagic ¹	26	7	bm, pp, bp, cr, sr, rc	14	25	L2
Takapoto Atoll, pelagic ²	32	7	bm, pp, bp, zp	15	26	L2
Marennes-Oléron Bay, tidal ³	95	16	bm, pp, zp, op	33	62	L2
Everglades, wet prairie ⁴	39	9	bm, dc	39	36	E1
Molenplaat, intertidal benthic ⁵	39	8	bm, pp, bp, cr, ni, ti	20	33	E2

2.3.2 Solution existence

Solution existence boils down to a check of the internal consistency of the various data sources and model structure. When inconsistent, the specified LIM cannot be solved; this situation might arise for example when, under steady-state, primary production is insufficient to satisfy the minimal carbon demands by herbivores. Identifying conflicts in the data set may reveal the need for better, more or alternative data. Inconsistent data sets have been dealt with in various ways. Vézina and Savenkoff (1999), Vézina et al. (1997), Vézina et al. (2000) and Richardson et al. (2003) allowed deviations from a steady state mass balance and observations. Van Oevelen et al. (Chapter 3) detected inconsistencies between two observations and adapted one to agree with the one that was regarded a better long term integrator of food web processes. Other authors change the model structure (Vézina and Pace, 1994; Richardson et al., 2003) or modify or remove some constraints from the model (Eldridge and Jackson, 1993; Vézina and Pace, 1994; Vézina and Savenkoff, 1999) in order to obtain a solution.

2.3.3 Solution identifiability

Solution identifiability deals with the question whether an inverse model contains sufficient information to identify the unknown parameters (in this case the flows). Identifiability is a quality label that allows distinguishing between flows that are well determined from those that are more uncertain. The uncertainty that surrounds inverse solutions has spurred

discussion in geophysical sciences (McIntosh and Rintoul, 1997), but is under appreciated in biological applications (but see Stone et al. (1993) and Vézina and Pahlow (2003)). There exist different measures of identifiability, here the discussion is limited to two measures that are easy to calculate and interpret: range estimation and flow resolution.

During **range estimation** an envelope around each flow is generated that depicts the feasible range that a flow can attain. The ranges are calculated by minimizing and maximizing each flow successively. Put more formally, the following is solved for each flow:

$$\text{minimize } x_i \text{ and maximize } x_i \tag{2.10}$$

subject to

$$\mathbf{Ax} = \mathbf{b} \text{ and } \mathbf{Gx} \leq \mathbf{h} \tag{2.11}$$

Note that when a flow is minimized or maximized this eliminates the need for the optimization equation (Eqs. 2.2) and data this equation does therefore not influence the outcome of the range estimation. Range estimation reveals which flows are well constrained (small range) in the LIM and which are not (large range). Thereby it also indicates which additional data can better constrain the food web. Note that flow values are not independent of each other. The linear dependency amongst flows might imply that fixing the value of one flow may fix the value of another flow or of a combination of flows. Thus, the solution space is sparse and the uncertainty is exaggerated in this type of analysis.

Klepper and Van de Kamer (1987) introduced range estimation to show that a mass-balance approach may greatly reduce the span of the initial range estimate. Stone et al. (1993) estimated ranges while changing some input data by 10 %. The potential ranges were large and they concluded that small changes in the environment may produce large changes in individual flows.

It is clear that for each of the example food webs, some of the flows are highly uncertain whereas others are much better constrained (Fig. 2.3). The food web reported by Donali et al. (1999) has the largest number of in situ measurements relative to the number of flows that have to be estimated (Table 2.1) and it is one of the best constrained food webs (Fig. 2.3A). In contrast, with 95 flows to be estimated based on only 33 equations, the food web of Leguerrier et al. (2003) is least well constrained (Fig. 2.3C). The inclusion of stable isotope data in the intertidal food web increased the number of mass balances and improved the quality of the inverse solution considerably (compare Fig. 2.3E and 2.3F, see also 2.4 Discussion).

In addition, the food web structure (the number of flows) is uncertain in all reported webs, because some flows have a lower boundary of 0 and may therefore be potentially absent from the food web. The proportion of flows with a lower boundary of 0 differed remarkably among the food webs (Table 2.2), > 30 % of the food web flows in Leguerrier et al. (2003) and Niquil et al. (1998) to < 5 % for Donali et al. (1999). In addition, the food web by Leguerrier et al. (2003) contained many flows with an infinite upper boundary (Table 2.2 en Fig. 2.3C).

2.3. Analysis of the inverse solution

Table 2.2: Summary of the range estimation of the example food webs. '0-flows' are number of flows that are zeroed in the final solution. 'Lower bound 0' is the number of flows with a lower boundary of 0 and 'Upper bound ∞ ' is the number of flows with an infinite upper boundary.

Reference	0-flows	Lower bound 0	Upper bound ∞
Donali et al. (1999)	1	8	0
Niquil et al. (1998)	4	21	0
Leguerrier et al. (2003)	26	71	19
Diffendorfer et al. (2001)	6	6	0
Van Oevelen et al. (Chapter 3)	9	16	0

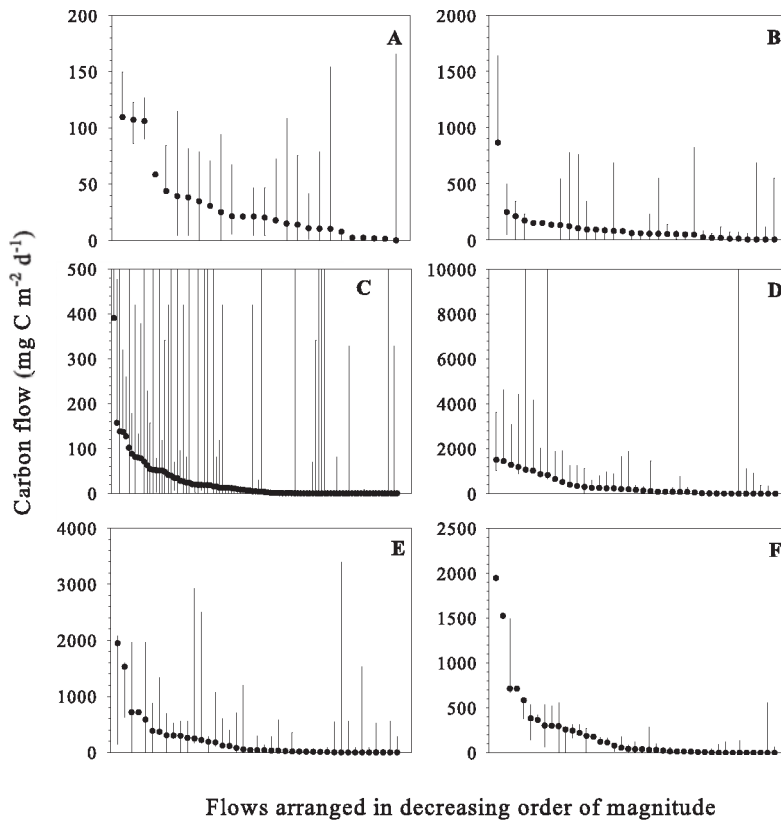


Figure 2.3: Range estimation of the example food webs A) Donali et al. (1999), B) Niquil et al. (1998), C) Leguerrier et al. (2003), flows out of scale indicate unbounded flows, D) Diffendorfer et al. (2001), flows out of scale are $> 40000 \text{ mg C m}^{-2} \text{ d}^{-1}$, E) Van Oevelen et al. (Chapter 3) without natural abundance stable isotope data and F) Van Oevelen et al. (Chapter 3) with natural abundance stable isotope data. Markers show food web flows solved with the L2 solution norm with initial estimates as zero.

Flow resolution is a measure of how well each flow is determined by information contained in the equality equation (Eqs. 2.1). The flow resolution varies between 0 and 1,

and indicates to what extent each flow is resolved independently of other flows (Menke, 1984; Vézina and Platt, 1988): 1 implies that the flow is resolved uniquely and lower values imply increasing dependence on other flows. The resolutions depend solely on the model and data structure contained in matrix \mathbf{A} and not on the numerical data in vector \mathbf{b} , hence they can be used for the optimization of sampling strategies (Menke, 1984).

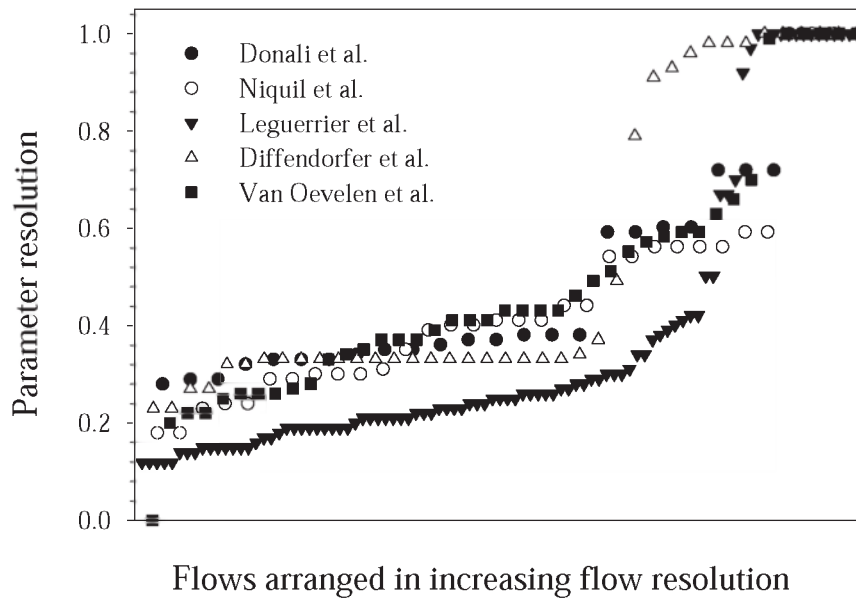


Figure 2.4: Flow resolutions of the example food webs. Flow resolutions for Van Oevelen et al. are calculated only without the stable isotope equations, because the use of stable isotope data complicates their calculation.

Reports on flow resolution are few, see Vézina and Platt (1988) and Niquil et al. (1998). The flow resolutions for all the examples show that the majority of the flows are not uniquely determined but are strongly related with other flows (i.e. most flow resolutions < 0.50 ; see Fig. 2.4). The food webs by Donali et al. (1999), Niquil et al. (1998) and Diffendorfer et al. (2001) are approximately equally resolved, whereas interdependencies are strongest in the food web by Leguerrier et al. (2003) as shown by the low resolution values. All food webs show sharp transitions in resolution patterns and these are most pronounced in Diffendorfer et al. (2001) and Leguerrier et al. (2003). In the case of Leguerrier et al. (2003) the flows related to macrobenthos are well constrained, because the relative contributions in their diet were fixed by prey biomass proportionality. Hence, it is possible to link the resolution patterns to the imposed information.

2.3.4 Solution uniqueness

Some inverse problems may have more than one optimal solution. This raises the question as to how one judges different food webs (i.e. different solutions) that equally comply with

2.3. Analysis of the inverse solution

the inverse model formulation. It appears that the question of non-uniqueness is related to the chosen norm. Quadratic minimization (L2 solution norm) should always lead to a unique solution (Lawson and Hanson, 1995), whereas linear minimization solutions are not always unique (Klepper and Van de Kamer, 1987). For example when two flows are possible, the L2 solution norm will equally divide among these possibilities, whereas when using the L1 solution norm, one combination will be arbitrarily selected.

When the example food webs were solved with linear programming techniques to find the most parsimonious solution (Eqs. 2.5) they all had a very large (probably infinite) number of optimal solutions (results not shown). Linear optimization is normally not used to calculate the most parsimonious food web, however it is commonly applied to over determined systems where the deviation from observations and initial estimates is minimized (see 2.2.4 Combining the elements of LIM) (Stone et al., 1993; Hart et al., 1997; Diffendorfer et al., 2001; Gaedke et al., 2002), and the question of non-uniqueness is usually not addressed (but see Klepper and Van de Kamer (1987)). To illustrate the issue, the example food web from Diffendorfer et al. (2001) was solved repeatedly using the L1 prediction norm with the ordering of the equations altered. Twenty-three different optimal solutions were found. Most flows retained their values (54 %), but for some their value varied considerably (Fig. 2.5). Clearly non-uniqueness should be an aspect to consider when solving an inverse model.

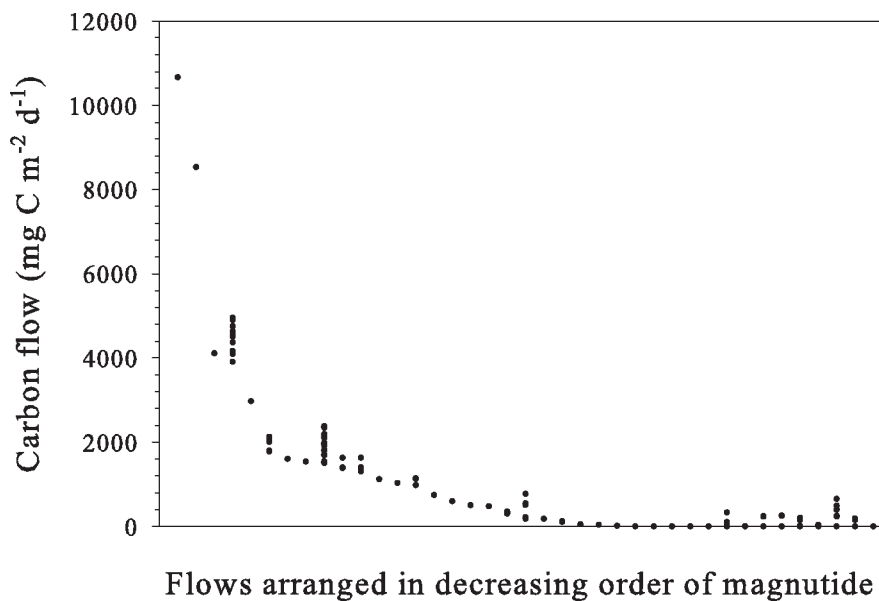


Figure 2.5: Twenty-three optimal solutions of the inverse problem by Diffendorfer et al. obtained by the L1 prediction norm.

2.3.5 Solution sensitivity

Solution sensitivity deals with the question of how (small) changes in the input propagate and change the inverse solution. A detailed ecological analysis of a food web that changes dramatically with small changes in the input data bears little relevance. Consequently, the sensitivity aspect of the solution has received considerable attention in the literature.

Systematic sensitivity analysis to test the robustness of inverse analysis range from small perturbations (10 - 20 %) of input data (Jackson and Eldridge, 1992; Niquil et al., 1998; Donali et al., 1999; Vézina and Savenkoff, 1999; Gaedke et al., 2002; Leguerrier et al., 2003; Richardson et al., 2003; Breed et al., 2004; Richardson et al., 2004) to rigorous changing or removing input values (Niquil et al., 1998; Donali et al., 1999; Vézina and Savenkoff, 1999; Hart et al., 2000; Vézina et al., 2000). Others have tested the sensitivity of the assumed food web structure (Vézina et al., 1997; Niquil et al., 1998; Richardson et al., 2003) or the imposed constraints (Leguerrier et al., 2004). The main conclusion for food webs solved with the L2 solution norm is that sensitivity to structure, input data and constraints is generally limited, although individual flows may change considerably.

Stone et al. (1993) and Diffendorfer et al. (2001) tested the sensitivity of an over determined model solved with the L1 residual norm. Stone et al. (1993) identified large changes in some individual flows as obtained by range estimation. The L2 solution norm assessment studies did not use range estimation and these ranges may be large (see 2.3.3 Solution identifiability), which complicates a direct comparison with the results of Stone et al. (1993). Diffendorfer et al. (2001) tested how much a constraint was allowed to change before a structural change in the food web was detected. The sensitivity appeared to be highly dependent on which constraint was perturbed, some did not give significant structural changes whereas others did. The potential non-uniqueness of linear programming problems (see 2.3.3 Solution identifiability) was not explicitly addressed in these L1 residual norm based sensitivity studies and this might have affected the analysis.

2.4 Discussion

There is a growing appreciation in the ecological literature for a more quantitative approach to natural food webs. Linear inverse modeling (LIM) is frequently used in food web research to quantify energy and elemental flows among ecological compartments. A systematic evaluation of inverse problems in ecology identified methodological aspects of LIM that have remained hidden or were under appreciated in the ecological literature. A general framework based on data sources, model equations and minimization norms was developed to distinguish different LIM approaches and reveal the essential choices that are to be made during the modeling process. In the literature there are major differences in the way these elements are used and combined to solve the food web model (Fig. 2.1). The alternatives imply a quality appraisal of the site-specific (type 3) and literature (type 4 - 5) data. The number of equations relative to the number of flows to be estimated is the major factor governing the quality of the inverse solutions. Researchers have therefore adopted strategies to include non-site specific, i.e. cross-system, literature (type 4) data in the equalities to increase the level of determination. Other applications select the parsimonious solution (e.g. Vézina and Platt, 1988) and in fact impose initial estimates as zero and the optimal solution is the one that meets these initial estimates as closely as possible.

An alternative approach is to include additional site-specific (type 3) data in the mass balance equalities, for instance, based on ecological stoichiometry (Sturner and Elser, 2002). Although the dynamic nature of unbalanced growth of autotrophs is not readily

implemented in a linear mass balance representation, homeostasis of consumers (bacteria, heterotrophic eukaryotes) can be used to link carbon, nitrogen and phosphorus flows in the food web (e.g. Vézina and Savenkoff, 1999; Eldridge and Jackson, 1993; Gaedke et al., 2002). Another promising approach involves the use of biomarkers, such as fatty acids (Iverson et al., 2004) or stable isotopes to quantify the contribution of different food sources in an organisms diet (Post, 2002). As these data fix relative proportions of diet sources, they increase the equations without increasing the number of unknowns and thereby narrow the uncertainty of the food web flows. Van Oevelen et al. (Chapter 3) pioneered the use of stable isotopes (both natural abundance and tracer data) in an inverse analysis of a benthic food web and show that the uncertainty in the inverse solution decreased considerably (compare Fig. 2.3E and F). Stable isotope and fatty acid signatures are becoming standard tools in food web ecology and their incorporation in LIMs is straightforward (Van Oevelen et al. (Chapter 3)).

Although LIMs are now frequently used to reconstruct element flows in food webs, there is comparatively little attention for the quality and properties of the inverse solution. Vézina and Pahlow (2003) tested the accuracy of the commonly used L2 solution norm reconstructed using twin-modeling experiments. Kones et al. (Accepted) uses factorial analysis on a large set of generated solutions of two under determined inverse models to reveal general patterns in these two sets of solutions. The factor analysis revealed that a few groups of flows, or sub-food webs, explain a large part of the variation in the set of different solutions. This means that different structures that may exist in these sub-food webs explain the uncertainty observed in the large complex food webs. This can be used to gain insight into the uncertainty of the complex food web and aid in developing a sampling strategy for further constraining the model.

In addition however, inverse theory has provided criteria such as identifiability and uniqueness to analyze inverse solutions, but these are not often applied in ecological applications. The systematic analysis of solutions of five previously quantified food webs revealed some important aspects. First of all, these inverse problems are strongly under determined and a large uncertainty surrounds most of the reconstructed food web flows (Fig. 2.3). These uncertainties should be considered when the solutions of the models are input to subsequent food web analysis, such as ecological network analysis (Ulanowicz, 1986; Bersier et al., 2002). Secondly, in all the revisited examples, most of the flows were strongly related to other flows and were not uniquely determined. Last but not least, when linear programming is used to single out an optimal solution, several alternative solutions may exist (Fig. 2.5).

Chapter 3

Carbon flow through a benthic food web: Integrating biomass, isotope and tracer data

Dick van Oevelen, Karline Soetaert, Jack J. Middelburg, P. M. J. Herman, Leon Moodley, Ilse Hamels, Tom Moens and Carlo H. R. Heip. *Submitted to Journal of Marine Research*

3.1 Introduction

The food web is a central concept in ecology and the herbivorous, detrital and microbial pathways are among its major carbon transfers. Much ecological theory is centered around the herbivorous food chain, in which primary producers sustain higher trophic levels (Ryther, 1969; Steele, 1974; Oksanen et al., 1981). The importance of the detrital pathway has been emphasized by Teal (1962) and Odum (1969) and is supported by empirical evidence (Polis and Hurd, 1996; Pace et al., 2004). More recently, the microbial loop was formalized as the transfer of dissolved organic matter, originating from phytoplankton exudation or sloppy feeding (Jumars et al., 1989), through bacterial assimilation and several grazing transfers to larger zooplankton (Azam et al., 1983). In natural food webs these three pathways are linked in many ways (Polis and Strong, 1996) and elucidating these linkages poses a major challenge in community ecology (Legendre and Rassoulzadegan, 1995; Polis and Strong, 1996; Herman et al., 1999; Cebrian, 2004; Moore et al., 2004).

Temperate intertidal flat communities are heterotrophic systems (Heip et al., 1995) and receive carbon inputs from local primary production by microphytobenthos, deposition of high-quality phytodetritus and low-quality organic matter associated with suspended particles from the water column and active filtration by suspension feeders (Herman et al., 1999). The high metabolic activity driven by this wide spectrum of organic matter sources renders intertidal flats excellent arenas to study the importance of the different pathways in natural food webs.

However, quantifying natural food webs is a notorious problem, as methodological and logistical limitations impede simultaneous measurement of all flows. Klepper and Van de Kamer (1987) and Vézina and Platt (1988) pioneered inverse analysis, a data assimilation technique that merges field observations and a priori literature information in a food web

structure, to quantify the unmeasured flows. Inverse analysis has been developed in the geophysical sciences (Wunsch and Minster, 1982; Menke, 1984) and has proven to be a robust means to capture the main food web characteristics (Vézina and Pahlow, 2003; Vézina et al., 2004).

In this paper we first extend the inverse methodology, to resolve not only conventional standing stock and process measurements, but also natural abundance stable isotope signatures and transient tracer data. This extended methodology was applied to a large data set on the food web of the Molenplaat intertidal flat (The Netherlands) (Herman et al., 2001). The data set contained different types of data: biomass of the benthos, carbon production and processing (Herman et al., 2001), integrated diet information from stable isotope signatures (Herman et al., 2000; Moens et al., 2002) and tracer data on the fate of recently fixed carbon by local primary producers (Middelburg et al., 2000). The use of all these data resulted in a significantly better constrained food web, as shown by uncertainty analysis. The resulting food web characteristics are discussed with respect to the importance of and linkages among the herbivorous, detrital and microbial pathways.

3.2 Methods

3.2.1 Study area, food web structure and data

The Molenplaat intertidal flat is located in the saline part (salinity 20-25) of the turbid, nutrient-rich and heterotrophic Scheldt estuary (Belgium, The Netherlands). The study site (station MP2 in the ECOFLAT-project) has a silt content of 38 % and organic carbon content of 0.70 % wt/wt. Herman et al. (2001) provide detailed information on the study site.

The specification of food web compartments is based on the conventional distinction based on size classes (e.g. Schwinghamer (1981)) and we consider microphytobenthos, bacteria, microbenthos (i.e. flagellates and ciliates), nematodes and other meiobenthos (copepods, ostracods and foraminifera) and macrobenthos (deposit and suspension feeders) (Fig. 3.1). Nematodes are treated separately from the other meiobenthos, because data on feeding preferences and tracer incorporation were available only for nematodes. Additionally, two abiotic carbon compartments are defined: particulate detritus and dissolved organic carbon (DOC), the latter including extracellular polymeric substances (EPS).

Extensive sampling was conducted between 1996 and 1999. Carbon stocks of detritus and all biotic compartments were determined from sediment cores. Total carbon processing was measured with field and laboratory incubations, yielding data on benthic primary production, bacterial secondary production, bacterivory by microbenthos and community respiration (Table 3.1). Nematode mouth morphology was investigated to determine the feeding preferences of the nematode community (Steyaert et al., 2003).

Natural abundance $\delta^{13}\text{C}$ isotope signatures provide an integrated measure of the different diet contributions to an organism. The $\delta^{13}\text{C}$ of nematodes, meiobenthos and macrobenthos was determined from hand-picked specimens and the bacterial $\delta^{13}\text{C}$ was derived from the $\delta^{13}\text{C}$ of bacterial specific polar lipid derived fatty acids (PLFAs) (Table 3.1). The $\delta^{13}\text{C}$ of detritus was calculated from depth profiles of $\delta^{13}\text{C}$ of total particulate organic matter (Table 3.1).

The fate of microphytobenthic carbon was quantified by an in situ pulse-chase experiment (Middelburg et al., 2000). Intertidal microphytobenthos only fixes carbon during the sunlit period of emersion, because the high turbidity of the Scheldt

3.2. Methods

estuary prevents light from reaching the sediment during submersion. During emersion, $^{13}\text{C-HCO}_3^-$ was sprayed on the surface of the tidal flat and was fixed by microphytobenthos. Subsequently, the ^{13}C tracer was tracked in bacteria, nematodes and macrobenthos, providing quantitative data on the transfer of recently fixed microphytobenthic carbon through the food web.

In addition to site-specific data, an extensive literature review was conducted to obtain quantitative information on processes for which direct field observations were not available and these data were used to constrain unknown flows within biological realistic bounds. Constraints were placed on 1) respiration and EPS excretion by microphytobenthos, 2) bacterial growth efficiency, 3) production rates, growth efficiency and assimilation efficiency of microbenthos, nematodes, meiobenthos and macrobenthos and 4) feeding preferences of nematodes and macrobenthos. Appendix A provides a complete listing, including references.

Table 3.1: Field observations used in the inverse analysis. Depth is the depth of integration. Sources are 1) Middelburg et al. (2000), 2) Hamels et al. (1998), 3) Hamels et al. (2004), 4) Steyaert et al. (2003), 5) L Moodley (unpub data), 6) Herman et al. (2000), 7) Hamels et al. (1998), 8) Dauwe et al. (2001), 9) Moens et al. (2002) and 10) PMJ Herman (unpub data).

Stocks mg C m⁻²	Depth (cm)	Value	Source
Microphytobenthos ^a	8.5	2090	1
Bacteria	4.0	4097	2
Microbenthos	4.0	140	2,3
Nematodes	6.0	156	4
Microvores		4.0	
Ciliate feeders		59.2	
Deposit feeders		27.6	
Epistrate feeders		25.6	
Facultative predators		32.8	
Predators		7.2	
meiobenthos	1.0	259	5
Copepods		59.8	
Ostracods		38.5	
Foraminifera		161.1	
macrobenthos	20.0	12172	6
Suspension feeders		3639	
Deposit feeders		6270	
Surface deposit feeders		2264	
detritus	5.0	130660	6
doc ^b	5.0	336	
Rates mg C m⁻² d⁻¹	Depth (cm)	Value	Source
Gross primary production	-	714	7
Community respiration	-	2112	8
Bacterial production ^c	0.3	598	2
Bacterial production	4.0	4121	2
Bacterivory microbenthos	4.0	13	2
$\delta^{13}\text{C}$ values	Depth (cm)	Value	Source
Microphytobenthos	-	-15.0	6
Bacterial PLFA	3.0	-20.4	1
Nematodes	4.0	-17.4	9

Meiobenthos	1.0	-15.3	5
Macrobenthos	20.0	-17.8	6
Detritus	30.0	-21.2	10
Phytoplankton	-	-21.0	6
Suspended particulate matter	-	-24.0	6

^a Taken from the depth integrated chlorophyll *a* and assuming a carbon to chlorophyll *a* ratio of 40

^b Assuming a DOC concentration of 800 $\mu\text{mol C l}^{-1}$ for porewater and a porosity of 0.70

^c Bacterial production used in the model is integrated to 0.3 cm (see 3.3 Results and 3.4 Discussion)

3.2.2 Inverse model formulation and uncertainty analysis

The goal of an inverse model is to quantify all flows that are present in a food web. The starting point is a topological food web. A topological web is a food web with flows being either present or absent and defines the mass balance for each food web compartment. Subsequently, quantitative information is added to the inverse model. For example, an equation can be added such that the sum of respiration flows equals the measured community respiration. Additionally, data from the literature are used to put biologically realistic bounds on the unmeasured flows, e.g. the assimilation efficiency can be constrained between a lower and upper boundary.

In this paper we develop the inverse model in three successive steps. First, the conventional methodology is applied, in which data on biomass and total carbon processing are used together with literature data to quantify the food web. Secondly, $\delta^{13}\text{C}$ stable isotope data are appended to the inverse model. Thirdly, data from an isotope tracer experiment are assimilated in the food web reconstruction. The inverse solutions will be referred to as: CS (Conventional Solution), CIS (Conventional and stable Isotope Solution) and CITS (Conventional, stable Isotope and Tracer Solution). The inverse models are implemented in the modeling environment FEMME (Soetaert et al., 2002) and can be freely downloaded from <http://www.nioo.knaw.nl/ceme/femme>.

Conventional inverse analysis (CS)

An inverse analysis model is expressed as 1) a set of linear equality equations

$$\mathbf{A}_{m,n}\mathbf{x}_n = \mathbf{b}_m \quad (3.1)$$

and 2) a set of linear constraint equations

$$\mathbf{G}_{m_c,n}\mathbf{x}_n \geq \mathbf{h}_{m_c} \quad (3.2)$$

Each element in \mathbf{x} represents a food web flow and inverse analysis quantifies all n flows in \mathbf{x} . The equality equation (Eqs. 3.1) contains both the topological food web (i.e. the mass balances) and the field observations consisting of process data (Vézina and Platt (1988)). Each mass balance or observation fills one row in \mathbf{A} and \mathbf{b} , m is therefore total number of mass balances and observations. A mass balance is expressed on row i of \mathbf{A} as a combination of the food web flows in \mathbf{x} : the element $a_{i,j}$ is -1 when flow j is an outflow, 0 when flow j is not part of the mass balance or 1 when flow j is an inflow. The

increase or decrease of a compartment with time (i.e. $\frac{dC}{dt}$) enters b_i . Here we assume steady-state, which means that the sum of inflows equals the sum of outflows and $\frac{dC}{dt}$ is zero. Process data are added similarly as the mass balances: the elements in \mathbf{A} express the contribution of the different flows to the process, e.g. community respiration is the sum of all respiration flows and the numerical data enter \mathbf{b} . The constraint equation is used to place upper or lower bounds on single flows or combinations of flows and these bounds will be respected in the inverse solution. The absolute values of the bounds are in vector \mathbf{h} and the constraints coefficients, signifying whether and how much a flow contributes to the constraint, are in matrix \mathbf{G} .

Inverse food web models have typically less equality equations than unknown flows (i.e. $m < n$, Vézina and Platt (1988)), this means that an infinite number of solutions obey the equality and constraint equations. The conventional procedure is to select the solution (CS) that is minimal in the sum of squared flows (i.e. $\sum_{i=1}^n x_i^2$). This solution is regarded as the simplest or most parsimonious food web (Vézina and Platt, 1988). Appendix A contains all inverse model equations and constraints.

Introducing stable isotope data (CIS)

Natural abundance stable isotope data are typically interpreted by means of a linear mixing model to estimate diet contributions of a consumer (Phillips, 2001; Post, 2002). The $\delta^{13}\text{C}$ signature of a consumer ($\delta^{13}\text{C}_j$) is expressed as a weighted average of the isotope signatures of its resources ($\delta^{13}\text{C}_i$), fractionation (Δ_i) and the associated flow ($f_{i \rightarrow j}$)

$$\delta^{13}\text{C}_j = \frac{\sum_i (\delta^{13}\text{C}_i + \Delta_i) f_{i \rightarrow j}}{\sum_i f_{i \rightarrow j}} \quad (3.3)$$

Fractionation of ^{13}C with trophic level is very small ~ 0.4 ‰ (Post, 2002) and is therefore neglected in our analysis. When all stable isotope signatures are known, they are easily implemented in the equality equation (Eqs. 3.1), but when isotope data for some compartments are missing a more complicated procedure is required (details in Appendix B). Briefly, an upper and lower boundary for each missing signature is assigned and the resulting parameter space is scanned with a grid search to locate the most parsimonious solution. Hence, the CIS is the parsimonious solution that satisfies the conventional and stable isotope data.

Assimilating deliberate tracer data (CITS)

Jackson and Eldridge (1992) simulated the fate of a tracer introduced in a pelagic food web inferred by inverse analysis. This approach inspired us to further increase the amount of data used in the food web reconstruction by adding data from a pulse-chase labeling of microphytobenthic carbon (see Appendix B for a detailed methodological description). Briefly, we generated a large set of inverse food webs and each food web was different in its flow values, but all satisfied the conventional and stable isotope data. Subsequently, each food web was fed to a tracer model that simulates tracer dynamics in each compartment. The modeled tracer dynamics were evaluated against the experimental data and the food web solution that optimally reproduced the tracer data was accepted as CITS.

Whereas in the tracer model of Jackson and Eldridge (1992) all incoming tracer instantly and homogeneously mixes in the receiving compartment, it is commonly found that metabolic processes are paid from a small pool with a comparatively fast turnover, e.g. respiration (Kooijman, 2000). Similarly, it is recently fixed carbon that is excreted as

extracellular polymeric substances (EPS) by microphytobenthos (Wolfstein et al., 2002). Therefore we assumed that respiration, excretion and faeces production have a tracer concentration equal to that of the incoming flows. Other outgoing flows, i.e. grazing, predation or export have the tracer concentration of the biotic compartment. Appendix B contains all model equations.

Uncertainty analysis

In accordance with the three step inverse analysis approach, we calculated the uncertainty for each food web. The uncertainty is expressed as flow ranges of the conventional solution (CSrange), ranges of conventional and stable isotope solution (CISrange) and ranges of conventional, stable isotope and tracer solution (CITSrange). The uncertainty analysis of CSrange and CISrange is based on subsequently minimizing and maximizing each flow (see Klepper and Van de Kamer (1987) and Stone et al. (1993))

$$\text{minimize } x_i \quad \text{and} \quad \text{maximize } x_i$$

under the conditions

$$\mathbf{Ax} = \mathbf{b}, \quad \mathbf{Gx} \geq \mathbf{h}$$

This analysis produces an envelope around each flow, which is interpreted as the potential range that a flow can attain given the data specified in the equality (either without (CSrange) or with (CISrange) the stable isotope signatures) and constraint equation. From all food webs that were ran in the tracer model, the best 10 % were used to determine CITSrange. The CITSrange was defined as the minimum and maximum of each flow found within the set of best solutions.

The effect of the uncertainty of the food webs on the tracer dynamics is presented in two ways: 1) as the lower and upper extremes in tracer dynamics found for each compartment when evaluating the large set of generated inverse solutions, therefore this represents the uncertainty in the tracer simulation of CIS and 2) after assimilating the tracer data as the lower and upper extremes in tracer dynamics for each compartment from the set of 10 % best food webs (CITSrange).

3.3 Results

3.3.1 Inverse solutions and uncertainty analysis

An initial attempt to solve the inverse model failed as a result of inconsistencies between field and literature data. Reconciliation of the depth-integrated bacterial production and community respiration required a bacterial growth efficiency of > 0.66 , far above the imposed limit of 0.32. The bacterial production measured in the top 3 mm was consistent with community respiration and was therefore used to solve the inverse model. This is extensively treated in the discussion.

The increasing use of available data resulted in differences among the CS, CIS and CITS and a large decrease in the uncertainty associated with these food webs. Main differences were found between the CS on the one hand and CIS and CITS on the other hand: 62 % of the flows in CIS and CITS differed more than ± 50 % from the CS (see 3.7 Appendix C). The large and small flows of the CIS and CITS agree well and differences mainly occur in flows of intermediate magnitude. The sum of carbon flows increased from 7670 (CS) to 8322 (CIS) to 8398 (CITS) $\text{mg C m}^{-2} \text{ d}^{-1}$.

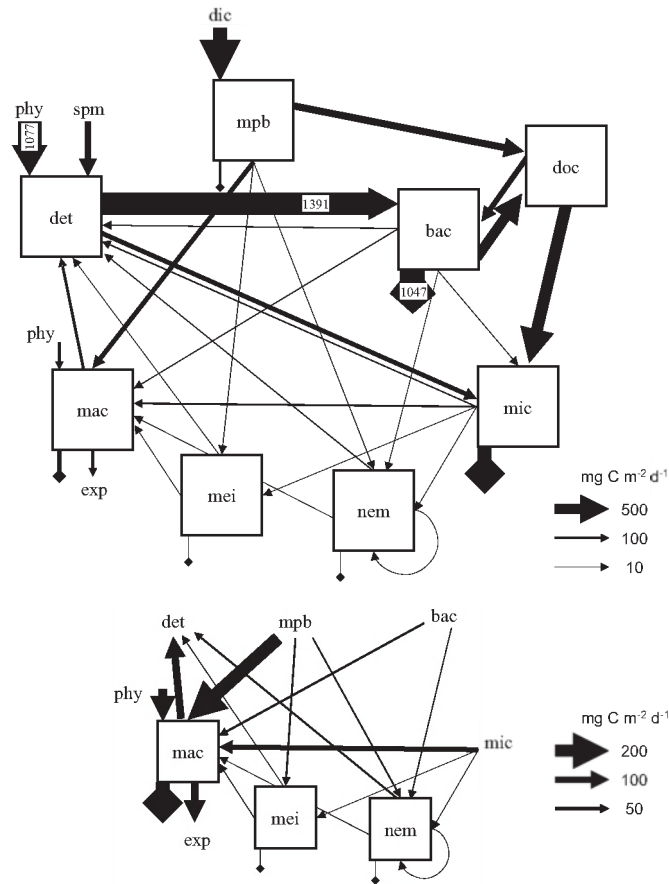


Figure 3.1: The inverse solution for the intertidal food web with flows based on assimilating biomass, stable isotope and tracer experiment data (CITS). Abbreviations: mpb is microphytobenthos, bac is bacteria, mic is microbenthos, nem is nematodes, mei is meiobenthos, mac is macrobenthos, doc is dissolved organic carbon, det is detritus, phy is phytoplankton, spm is suspended particulate matter, dic is dissolved inorganic carbon and exp is export from the system. Carbon inputs are primary production by microphytobenthos, macrobenthic suspension feeding on phytoplankton, phytoplankton and suspended particulate matter deposition. DOC is produced through EPS excretion by microphytobenthos and bacteria and consumed by bacteria and microbenthos. Detritus is consumed and produced (death and faeces production) by all heterotrophic compartments. Microphytobenthos and bacteria are grazed by microbenthos, nematodes, meiobenthos and macrobenthos. Microbenthos is grazed by nematodes, meiobenthos and macrobenthos, nematodes are grazed by predatory nematodes and macrobenthos, and meiobenthos is grazed by macrobenthos. Carbon outflows are respiration (diamond head arrows), macrobenthic export (e.g. consumption by fish or birds) and bacterial burial. Only non-zero flows are pictured. The arrows with indicated values are not scaled, because their dominance would otherwise mask the thickness differences among the other arrows. The lower panel shows nematodes, meiobenthos and macrobenthos on a different scale to better indicate the flow structure.

The uncertainty in CS is large: 51 % of the flows has a range of $> 500 \text{ mg C m}^{-2} \text{ d}^{-1}$ and 29 % a range of $> 1000 \text{ mg C m}^{-2} \text{ d}^{-1}$ (Table 3.2). The stable isotope data constrained the uncertainty significantly (Fig. 3.2): the ranges decreased $> 50 \%$ for 60

Chapter 3. Carbon flow through a benthic food web

% of the flows and > 75 % for 34 % of the flows. In the CISrange, 25 % of the unknown flows still have a range larger than $200 \text{ mg C m}^{-2} \text{ d}^{-1}$, but the range for > 50 % of the flows is $< 70 \text{ mg C m}^{-2} \text{ d}^{-1}$. The inclusion of the tracer data constrained some flows more than others (Fig. 3.2). The range of 37 % of the flows decreased > 50 % as compared to the CISrange, in particular carbon flows related to microphytobenthos, nematodes and macrobenthos were better constrained in the CITSrange. The largest ranges in CITSrange are associated with phytoplankton deposition (between 799 and $1640 \text{ mg C m}^{-2} \text{ d}^{-1}$), detritus uptake by bacteria (between 1314 and $1913 \text{ mg C m}^{-2} \text{ d}^{-1}$) and the fate of ungrazed bacterial production (detritus, DOC or burial range between 0 and $570 \text{ mg C m}^{-2} \text{ d}^{-1}$) (Table 3.2). In addition, flows associated with microbenthos have fairly large ranges: detritus and DOC ingestion by microbenthos have ranges of 555 and $495 \text{ mg C m}^{-2} \text{ d}^{-1}$, respectively. Detritivorous flows are very well constrained for nematodes ($< 1 \text{ mg C m}^{-2} \text{ d}^{-1}$), meiobenthos ($< 5 \text{ mg C m}^{-2} \text{ d}^{-1}$) and macrobenthos ($< 40 \text{ mg C m}^{-2} \text{ d}^{-1}$). Respiration fluxes are well constrained for nematodes (3 - $8 \text{ mg C m}^{-2} \text{ d}^{-1}$), meiobenthos (13 - $60 \text{ mg C m}^{-2} \text{ d}^{-1}$) and macrobenthos (226 - $323 \text{ mg C m}^{-2} \text{ d}^{-1}$), but less for bacteria (993 - $1466 \text{ mg C m}^{-2} \text{ d}^{-1}$) and microbenthos (290 - $763 \text{ mg C m}^{-2} \text{ d}^{-1}$). Finally, EPS excretion by microphytobenthos is well constrained and is between 300 and $398 \text{ mg C m}^{-2} \text{ d}^{-1}$.

The uncertainty in the tracer simulation based on the CISrange was large for microphytobenthos and bacteria, but particularly large for nematodes and macrobenthos (Fig. 3.3). The uncertainty in the tracer simulation based on CITSrange was smaller for all compartments, clearly demonstrating that the addition of tracer data further increased the reliability of the reconstructed food web. The optimal tracer simulation (CITS) describes the entire set of observations quite reasonably. The tracer dynamics of microphytobenthos fit the observations well, which means that the turnover time in our inverse solution is similar to that in the field. The food web model reproduces the quick tracer incorporation by bacteria and the peak labeling at 1-2 days. The modeled magnitude of nematode tracer incorporation is very similar to that observed in the field. However, the rapid initial enrichment is not reproduced and the modeled incorporation rate seems slightly higher than in the field. Macrobenthos tracer incorporation is somewhat overestimated as compared to the one field observation available.

Table 3.2: The intertidal benthic food web (CITS) and the associated uncertainty (CITSrange) ($\text{mg C m}^{-2} \text{ d}^{-1}$). Flows in italics are field measurements and are therefore fixed in the solution. Abbreviations as in Fig. 3.1.

Flow	CITS	CITSrange	
		min	max
doc → bac	253	120	322
doc → mic	601	171	666
det → bac	1391	1314	1913
det → mic	210	0	555
det → nem	0	0	1
det → mei	0	0	5
det → mac	0	0	40
phy → det	1077	799	1640
phy → mac	139	139	218
spm → det	304	264	537
dic → mpb	<i>714</i>	<i>714</i>	<i>714</i>
mpb → dic	114	114	172

mpb → doc	348	300	398
mpb → det	0	0	52
mpb → mic	0	0	71
mpb → nem	17	17	64
mpb → mei	25	23	99
mpb → mac	210	155	258
bac → dic	1047	993	1466
bac → doc	506	0	571
bac → det	37	0	571
bac → mic	13	13	13
bac → nem	14	14	48
bac → mei	0	0	6
bac → mac	28	0	59
bac → bur	0	0	566
mic → dic	710	290	763
mic → det	38	0	86
mic → nem	0.4	0.4	5
mic → mei	2	0	8
mic → mac	75	62	156
nem → dic	3	3	8
nem → det	24	24	112
nem → nem	3	2	8
nem → mac	4	0	7
mei → dic	13	13	60
mei → det	6	6	43
mei → mac	8	8	23
mac → dic	226	226	323
mac → det	116	116	229
mac → exp	122	122	141

3.3.2 Carbon flows in the benthic food web

Bacteria dominate carbon flows at the Molenplaat and obtain 85 % of their carbon from detritus and the remainder from DOC (Fig. 3.1 and Table 3.2). DOC originates from microphytobenthic and bacterial EPS production and bacterial mortality. Bacteria assimilated $2122 \text{ mg C m}^{-2} \text{ d}^{-1}$ and their growth efficiencies on detritus and DOC were 0.32 and 0.63, respectively. Only 9 % of the total bacterial production is grazed and the majority of the production is recycled between DOC and bacteria. Microbenthos ingestion ($825 \text{ mg C m}^{-2} \text{ d}^{-1}$) is mostly DOC (73 %), supplemented with detritus (26 %) and bacteria (2 %). Nematode ingestion ($35 \text{ mg C m}^{-2} \text{ d}^{-1}$), comprises a small fraction of total heterotrophic ingestion (1 %). The main nematode food sources are microphytobenthos (50 %) and bacteria (39 %). Nematode predation forms 10 % of total nematode ingestion. The other meiobenthos (i.e. ostracods, copepods and foraminifera) play a marginal role in carbon cycling; the ingestion rate is restricted to $27 \text{ mg C m}^{-2} \text{ d}^{-1}$ (1 % of total heterotrophic ingestion), with dominant carbon sources being microphytobenthos (93 %) followed by microbenthos (7 %). As they have a high biomass, macrobenthos play an important role in carbon cycling and their ingestion is around 15 % of total heterotrophic ingestion. Important macrobenthic carbon sources are microphytobenthos (45 %) and

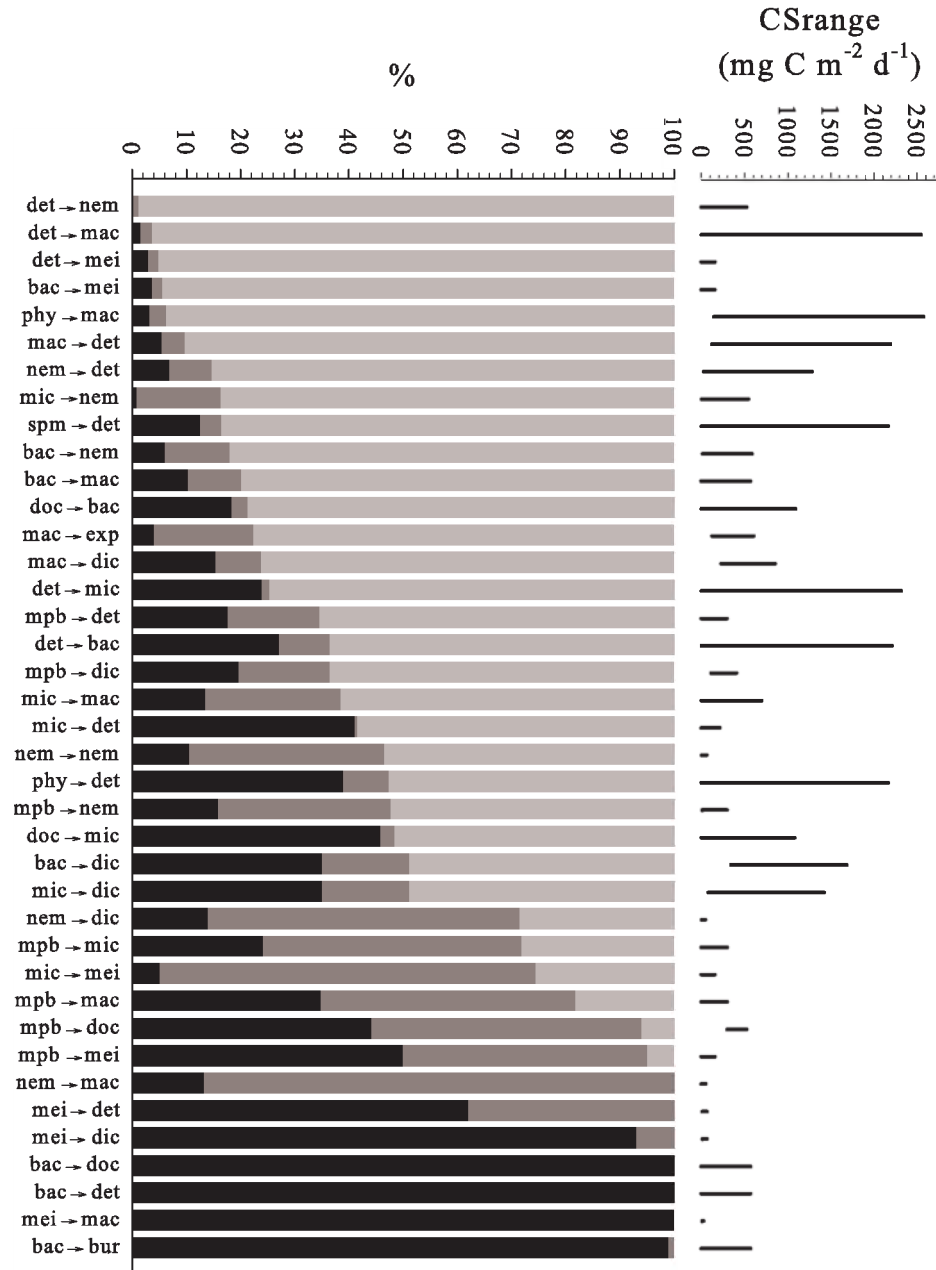


Figure 3.2: Absolute CSrange for each flow (upper panel) and the relative reduction of this CSrange (light grey) to CISrange (dark grey) to CITSrange (black) (lower panel). Abbreviations as in Fig. 3.1

phytoplankton (30 %). Ingestion of bacteria (6 %), microbenthos (16 %), nematodes (1 %) and meiobenthos (2 %) completes their diet. Surprisingly, the results show no ingestion of detritus by nematodes, meiobenthos nor macrobenthos.

The Molenplaat is heterotrophic and is supported by suspended particulate matter deposition (14 %), local primary production by microphytobenthos (32 %), suspension feeding by macrobenthos (6 %) and phytoplankton deposition (48 %) (Table 3.2). Respiration is dominated by bacterial respiration (50 %) with microbenthos as second contributor (34 %). The contribution of other compartments is smaller with 11 % for macrobenthos, 5 % for microphytobenthos and < 1 % for nematodes and meiobenthos (Table 3.2). Total secondary production amounts to $826 \text{ mg C m}^{-2} \text{ d}^{-1}$ and is again dominated by bacteria (74 %), followed by macrobenthos (15 %), microbenthos (10 %), nematodes (1 %) and other meiobenthos (1 %).

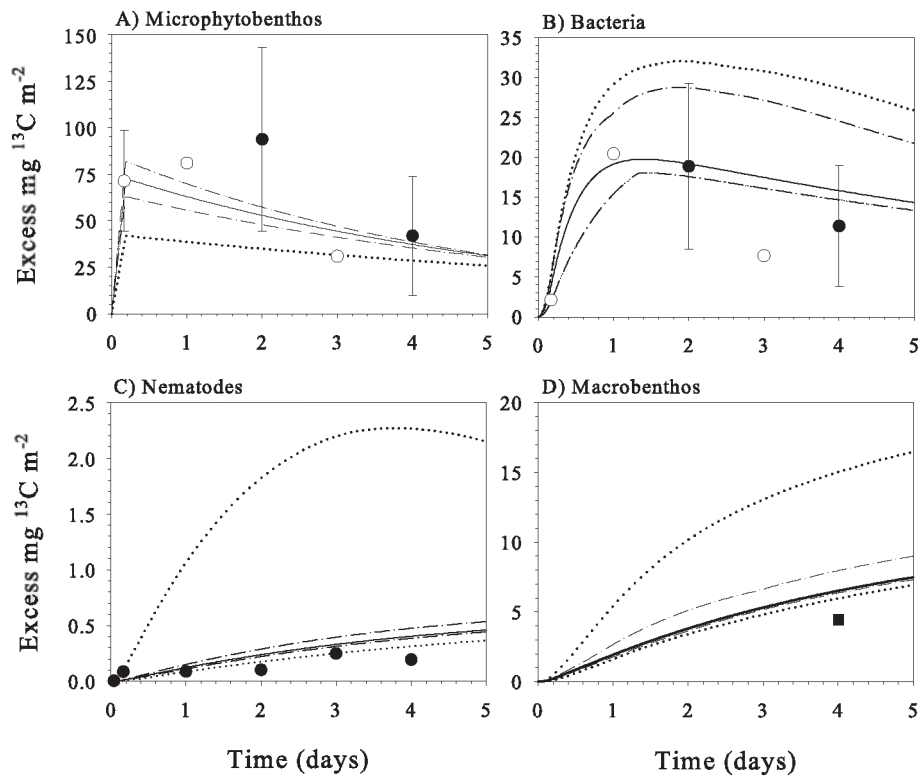


Figure 3.3: Tracer dynamics in the Molenplaat as measured in the top 5 mm (open circles), top 20 mm (filled circles) and top 20 cm (filled squares) and simulated based on the CITS (dark line). Also indicated are the range of tracer dynamics based on CISrange (dotted lines) and CITSrange (dashed dotted lines). The upper tracer dynamics ranges for CISrange and CITSrange overlap for microphytobenthos, while the lower ranges overlap for bacteria. When present, error bars denote standard deviations.

3.4 Discussion

The Molenplaat is one of the best-studied intertidal flats with comprehensive data on its physical, chemical and biological characteristics (Herman et al., 2001). Despite this extensive data set, producing a 'coherent and well-constrained' food web was ambiguous.

This ambiguity relates to data quality and availability and the inverse methodology. Hence, these will be discussed first, followed by a discussion on the importance of the herbivorous, detrital and microbial pathways in the benthic food web.

3.4.1 Field data

Spatial and temporal data acquisition

There is considerable heterogeneity in temporal and spatial sampling in the data set. The data have been collected in the period 1996 - 1999, some measurements were performed only once (e.g. $\delta^{13}\text{C}$ signatures and meiobenthic biomass), others are season-averaged (e.g. bacterial production, bacteria and microbenthos stock) and sampling depth ranged from 0-1 cm (meiobenthos) to 0-20 cm (macrobenthos). These temporal and spatial differences in data acquisition may partly explain some of the encountered discrepancies. However, several studies indicate no changes in microphytobenthic (Hamels et al., 1998), meiobenthic (M Steyaert, pers. com.) and macrobenthic (Herman et al., 2000) biomass and composition during the study period.

Bacterial production and community respiration

The inverse methodology identified the inconsistency between depth-integrated bacterial production (BP) and sediment community oxygen consumption (SCOC). Even when assuming that all respiration is bacterial, anomalously high growth efficiencies are needed. This inconsistency has frequently been reported in studies measuring both BP and SCOC (Van Duyl and Kop, 1990; Cammen, 1991; Alongi, 1995; Boon et al., 1998). Some potential problems with BP measurements are unbalanced growth and non-specificity or catabolism of the radioactive substrate that is added to measure BP (Kemp, 1990; Dixon and Turley, 2001). Moreover, BP is based on comparatively short incubations (~ 30 minutes). Compared to these uncertainties, SCOC measurements are more robust (Dauwe et al., 2001). SCOC integrates aerobic (direct oxygen consumption) and anaerobic (re-oxidation of reduced compounds) mineralization pathways over time scales in the order of days to weeks. The SCOC based on intact contact core incubations ranged from 1806 to 2406 $\text{mg C m}^{-2} \text{d}^{-1}$ and compares well with independent community respiration measurements based on CO_2 production in slurry incubations ($\sim 2400 \text{ mg C m}^{-2} \text{d}^{-1}$) (Dauwe et al., 2001). As two different SCOC measures gave similar results and SCOC integrates heterotrophic activity over a longer time scale than BP measurements, it is therefore taken as the most appropriate measure to constrain total benthic activity at the expense of the depth integrated BP. In addition, a long-term ^{13}C -glucose labeling experiment yielded a BP of 798 $\text{mg C m}^{-2} \text{d}^{-1}$ in the top 10 cm of the sediment (Chapter 4), which compares favorably to the BP adopted here (598 $\text{mg C m}^{-2} \text{d}^{-1}$).

Bacterial $\delta^{13}\text{C}$ signature

Measuring the bacterial $\delta^{13}\text{C}$ poses difficulties as this can only be assessed using bacterial specific biomarkers as proxy (Boschker and Middelburg, 2002). A critical assumption is that the isotope signature of such specific fatty acids (PLFAs) reflects that of bacterial biomass. Hayes (2001) reviews the results of *Escherichia coli* culture studies and finds a depletion of PLFAs as compared to total biomass of 3 to 8 %. A similar depletion has been found in culture studies using an inoculate of a natural bacterial community (Boschker et al., 1999). Whether these results may be translated to the field is unclear (Bouillon et al.,

2004), as fractionation depends amongst others on the relative abundance of lipids (Hayes, 2001), substrate utilization (DeNiro and Epstein, 1977) and oxygen concentration (Teece et al., 1999). For microbial substrate use in soils, it has been suggested that there is no depletion of PLFAs with respect to the substrate and that therefore the average $\delta^{13}\text{C}$ of different PLFAs is a good indicator of the $\delta^{13}\text{C}$ of the microbial substrate (Burke et al., 2003). Here, we choose for the latter approach for two reasons. First, assuming a typical depletion of 5 ‰ would lead to a bacterial $\delta^{13}\text{C}$ of -14.5 ‰, which could not be resolved with respect to the other observations. Second, such heavy bacterial $\delta^{13}\text{C}$ values would point to microphytobenthos as the dominant carbon source for bacteria. This is unlikely as (1) bacterial respiration outbalances microphytobenthos production and (2) the $\delta^{13}\text{C}$ of bacterial biomarkers did not show a depth gradient.

3.4.2 Extended inverse methodology, stable isotopes and tracer data

Food web studies taking a quantitative ecosystem perspective have revealed important insights in the structure of natural food webs (Lindeman, 1942; De Ruiter et al., 1995; Pauly et al., 1998; Gaedke et al., 2002) and inverse models are increasingly used to quantify food webs. However, a major problem is that a unique solution is selected by a parsimonious criterium (Vézina and Platt, 1988) or by upgrading site-specific data with literature data (Chapter 2). The methodology presented here, aims to increase the amount of site-specific data by additionally incorporating stable isotope and tracer data. The incorporation of the tracer data made the parsimonious criterium redundant, since the inverse solution with an optimal fit to the tracer data was chosen rather than the parsimonious solution.

Mixing models have become standards in ecology to estimate trophic position (Minagawa and Wada, 1984; Vander Zanden and Rasmussen, 1999) or diet contribution of $x + 1$ resources from x different isotopes (Peterson et al., 1986; Fry, 1991; Herman et al., 2000; Phillips, 2001; Post, 2002). When more than $x + 1$ resources are available to a consumer, it is impossible to uniquely estimate the resource diet contributions based on x different isotopes. For such situations, Phillips and Gregg (2003) propose a grid search technique to estimate a feasible range and frequency distribution for the contributions of different resources, rather than calculating a unique solution. In our study we similarly take advantage of a grid search technique (Appendix B), but use data on total carbon processing as additional constraints. This serves two purposes. First, while previous isotope applications have been very fruitful in quantifying the *relative* trophic position or *relative* contribution of a resource, we also quantify the absolute magnitude of all food web flows. Two, combining stable isotope and total carbon processing data increases the data resolution such that the uncertainty in the food web reconstruction decreases.

The integration of tracer experiments and modeling has proven to provide quantitative insight in food web interactions (Cole et al., 2002; Van den Meersche et al., 2004). Although the data from the tracer experiment provided quantitative information on the transfer of recently fixed carbon (Middelburg et al., 2000), sampling in itself was insufficient to quantify all food web flows. Instead, a tracer model was used to identify the inverse solution that optimally reproduced these tracer data. In general, the correspondence between model and data is acceptable (Fig. 3.3). The correspondence for microphytobenthos suggests that its turnover time and the fraction of the primary production excreted as EPS are accurately modeled. The general data - model agreement for bacteria gives credit to our previously discussed assumptions regarding bacterial

production and bacterial $\delta^{13}\text{C}$. Although the magnitude of nematode labeling is reproduced by the model, the initial incorporation lags slightly behind the observations. This may be explained by ingestion of DOC (not modeled) or selective ingestion of active, highly labeled microphytobenthos cells.

Modeled macrobenthic label incorporation was overestimated by a factor 1.5, as compared to the one observation. Several explanations for this discrepancy may apply. First, due to the limited spatial scale of the experiment, 30 % of the deposit feeders (e.g. *Arenicola marina*) were not present in the samples from the tracer experiment and their label incorporation could not be assessed. Second, only 19 % of the deposit feeders classify as surface deposit feeders and had access to the highly labeled microphytobenthos in the top layer of the sediment. An implicit assumption in the tracer model is that the total deposit feeding community has direct access to the labeled microphytobenthos and therefore the model likely overestimates label incorporation. As there is only one observation and several plausible explanations for an overestimation of modeled label incorporation, we feel that the discrepancy is not strong enough to question the results.

The addition of stable isotope and tracer data changed the solutions, 62 % of the flows in CIS and CITS differed more than ± 50 % from the CS. The sum of carbon flows increased from 7670 (CS) to 8322 (CIS) to 8398 (CITS) $\text{mg C m}^{-2} \text{ d}^{-1}$, corroborating the results from twin-modeling that show underestimation of flows in the parsimonious solution in recycling webs (Vézina and Pahlow, 2003). Moreover, inclusion of tracer data in the inverse solution made the parsimonious criterium redundant. The CITS food web is therefore free from the bias known to be introduced by such a criterium (Niquil et al., 1998). Finally, the integration of biomass, process, stable isotope and tracer data significantly reduced the uncertainty in the food web.

3.4.3 Pathways in the benthic food web

The biomass of bacteria, microbenthos, meiobenthos and macrobenthos for the Molenplaat can be considered representative for temperate estuarine tidal flats (Epstein and Shiaris, 1992; Heip et al., 1995; Soetaert et al., 1995; Herman et al., 1999). This also holds for bacterial production (Van Duyl and Kop, 1990), primary production and sediment oxygen consumption (Heip et al., 1995). Accordingly, the food web structure and functioning can be generalized and in this last section we discuss the importance of the herbivorous, detrital and microbial pathways.

Herbivorous pathway. The primary producers microphytobenthos and phytoplankton supported nematodes, other meiobenthos and macrobenthos in this heterotrophic benthic food web. Recent studies of food webs in estuaries (Thompson and Schaffner, 2001; Sobczak et al., 2002; Chanton and Lewis, 2002), streams (Tank et al., 2000) and lakes (Cole et al., 2002) report a similar dominant contribution of autochthonous production in diets of metazoan grazers. These results suggest that the algal-grazer link is the most important food web interaction to consider for higher trophic levels.

Microphytobenthos excrete 49 % of their carbon production as EPS, which enters the microbial pathway as dissolved organic carbon.

Microbial pathway. Bacteria dominate carbon flows and account for 74 % of secondary production and 50 % of respiration. This agrees with earlier reports on the bacterial dominance of production (Schwinghamer et al., 1986; Chardy and Dauvin, 1992) and respiration (Smith, 1973; Schwinghamer et al., 1986; Moodley et al., 2002). Grazing by higher trophic levels on bacteria is restricted and therefore bacterial production is a sink rather than a link of carbon in the benthic food web. Short-term bacterivory

studies of micro-, meio- or macrobenthos report similar limited transfer of bacterial carbon production (Kemp, 1987; Epstein and Shiaris, 1992; Hondeveld et al., 1995; Epstein, 1997a). The fate of bacterial production, other than grazing, was poorly constrained in this food web. Bacterial carbon might be recycled back to DOC or detritus or buried in the sediment. Several papers indicate that bacterial biomass and production rates are closely coupled to the distribution of viruses (e.g. Paul et al., 1993; Fischer et al., 2003) and viral lysis of bacterial cells might explain the recycling fluxes to the abiotic compartments. Although burial of recalcitrant bacterial cell-wall remnants is observed in ocean margin sediments (Parkes et al., 1993; Grutters et al., 2002), it is unknown whether this is a quantitatively important sink of bacterial production.

Microbenthos has a comparatively high carbon demand due to their high specific production and low growth efficiency. Their low rate of bacterivory implies that bacteria constitute 2 to 3 % of their diet. This is surprisingly low, given that microbenthos biomass at this study site is dominated by flagellates, which are typically seen as bacterivores. Consequently, either other carbon sources form their main food source or reported production rates are overestimates for field situations. The contribution of other resources (microphytobenthos, detritus and DOC) are poorly constrained, but DOC seems to form an important resource for microbenthos. Although flagellates are known for their capability to use dissolved organic substances (Sherr, 1988), its significance in sediments remains to be established. In the Molenplaat food web, microbenthos carbon production was transferred higher up the food web (Fig. 3.1). Hamels et al. (2001a) found evidence for such a transfer in laboratory incubations, in which nematodes heavily grazed ciliates. Hence, the microbial loop seems to have a dead end in bacteria, but there is potential transfer of DOC through microbenthos to higher trophic levels.

Detrital pathway. Semi-labile detritus supported the majority of bacterial carbon production and some of the microbenthos production. The rapid transfer of tracer to bacteria observed in the labeling experiment is fully explained by labile EPS excretion by microphytobenthos and subsequent assimilation by bacteria. However, DOC represents only 15 % of the total bacterial carbon demand. The importance of semi-labile detritus for bacterial production found in this intertidal flat food web can be explained from a biogeochemical viewpoint. Oxygen is rapidly consumed in the top millimeters of coastal sediments. Detritus is therefore predominantly degraded in the bacterial domain of suboxic and anoxic metabolic pathways (e.g. Canfield et al., 1993). Moreover, the labile part of detritus is degraded in the top layer of the sediment and therefore the most likely bacterial resource under suboxic/anoxic is semi-labile detritus.

Although the intertidal flat food web supports a large population of deposit feeding nematodes, meiobenthos and macrobenthos, these organisms appear to selectively assimilate high quality resources such as microphytobenthos, phytoplankton and to a lesser extent bacteria. Selective assimilation of high quality carbon has been demonstrated directly using $\delta^{13}\text{C}$ labeled phytodetritus (Blair et al., 1996; Levin et al., 1999; Herman et al., 2000; Moodley et al., 2002; Witte et al., 2003). This high selectivity suggests that bulk organic matter is a poor indicator of resource availability for deposit feeding organisms and refined descriptions, based on organic matter quality, are required for estimates of food availability.

The conceptual model of Mayer et al. (2001) is especially interesting when trying to explain the observed resource partitioning between bacteria and higher organisms. They relate digestive differences between deposit feeders (digestive tract) and bacteria (extra-cellular enzymes) to resource quality and suggest that deposit feeders benefit from high quality resources and that bacteria can better handle low quality resources. Their

Chapter 3. Carbon flow through a benthic food web

predictions match the general picture that emerges for this intertidal food web. Whether their concept is indeed the mechanism that explains our results is an intriguing, yet open, question.

In summary, we find two major food web pathways in our intertidal flat with comparatively limited interaction. The semi-labile detrital pathway dominates carbon flows in the food web and supports the majority of the bacterial secondary production. Transfer of bacterial carbon to higher trophic levels is very restricted and instead recycles back to detritus and DOC. The herbivorous pathway is the second dominant pathway, in which microphytobenthos and phytoplankton supply labile carbon to the food web. Nematodes, meiobenthos and macrobenthos feed selectively on this particulate carbon production. Although many species in these benthos groups classify as deposit feeder, this selectivity results in a virtual absence of detritivory. The observed separation of carbon pathways suggests that they function rather autonomously.

3.5 Appendix A: Inverse model equality and constraint equations

This appendix contains all inverse model equations (Table 3.3) and constraints (Table 3.4) with references. Some equations and constraints require additional explanation, which is given below.

Bacterial growth efficiency (BGE) varies considerably among carbon sources (del Giorgio and Cole, 1998). Therefore different BGE for growth on detritus (BGE_{det}) and DOC (BGE_{doc}) are assumed, however, with the restriction that BGE_{doc} is two times BGE_{det} . The BGE ranges for growth on DOC and detritus in a comprehensive literature review indeed show such a pattern (del Giorgio and Cole, 1998). This pattern is consistent with the notion that detritus uptake is a two-step process: 1) detritus dissolution and 2) subsequent assimilation, whereas DOC uptake only involves the second step. The ratio BGE_{doc} to BGE_{det} is fixed to two in order to reduce the number of free parameters in the grid search from 4 to 3 (see Appendix B). This saves considerably on the required calculations in the grid search, while still being a good approximation of reality.

The respiration flows for microbenthos, nematodes, meiobenthos and macrobenthos are described as the sum of two processes: maintenance and growth respiration. Maintenance costs are taken proportional to biomass (Table 3.3). It is often found that respiration rates in starved heterotrophic organisms drop to less than a few percent of their biomass per day (Fenchel, 1982; Kristensen, 1989; Nielsen et al., 1995), hence the specific maintenance respiration is fixed to 1 % of the biomass per day. Respiration costs related to growth processes can be considerably higher and are modeled as a fixed fraction of assimilated carbon. This fraction equals $1 - NGE$, with NGE being the net growth efficiency.

Table 3.3: Inverse model equations. Abbreviations: *mpb* is microphytobenthos, *bac* is bacteria, *mic* is microbenthos, *nem* is nematodes, *mei* is meiobenthos, *mac* is macrobenthos, *doc* is dissolved organic carbon, *det* is detritus, *dic* is dissolved inorganic carbon, *phy* is phytoplankton, *spm* is suspended particulate matter, *exp* is export and *bur* is burial. All mass balances are assumed to be in steady state. Flows are designated as *source* \rightarrow *sink*.

Mass balances

$$\begin{aligned} \frac{d \text{mpb}}{dt} = 0 &= \text{dic} \rightarrow \text{mpb} - \text{mpb} \rightarrow \text{dic} - \text{mpb} \rightarrow \text{doc} - \text{mpb} \rightarrow \text{det} \\ &\quad - \text{mpb} \rightarrow \text{mic} - \text{mpb} \rightarrow \text{nem} - \text{mpb} \rightarrow \text{mei} - \text{mpb} \rightarrow \text{mac} \\ \frac{d \text{bac}}{dt} = 0 &= \text{doc} \rightarrow \text{bac} + \text{det} \rightarrow \text{bac} - \text{bac} \rightarrow \text{dic} - \text{bac} \rightarrow \text{doc} \\ &\quad - \text{bac} \rightarrow \text{det} - \text{bac} \rightarrow \text{bur} - \text{bac} \rightarrow \text{mic} - \text{bac} \rightarrow \text{nem} \\ &\quad - \text{bac} \rightarrow \text{mei} - \text{bac} \rightarrow \text{mac} \\ \frac{d \text{mic}}{dt} = 0 &= \text{mpb} \rightarrow \text{mic} + \text{bac} \rightarrow \text{mic} + \text{doc} \rightarrow \text{mic} + \text{det} \rightarrow \text{mic} \\ &\quad - \text{mic} \rightarrow \text{dic} - \text{mic} \rightarrow \text{det} - \text{mic} \rightarrow \text{nem} \\ &\quad - \text{mic} \rightarrow \text{mei} - \text{mic} \rightarrow \text{mac} \\ \frac{d \text{nem}}{dt} = 0 &= \text{mpb} \rightarrow \text{nem} + \text{bac} \rightarrow \text{nem} + \text{mic} \rightarrow \text{nem} + \text{det} \rightarrow \text{nem} \\ &\quad - \text{nem} \rightarrow \text{dic} - \text{nem} \rightarrow \text{det} - \text{nem} \rightarrow \text{mac} \\ \frac{d \text{mei}}{dt} = 0 &= \text{mpb} \rightarrow \text{mei} + \text{bac} \rightarrow \text{mei} + \text{mic} \rightarrow \text{mei} \\ &\quad + \text{det} \rightarrow \text{mei} - \text{mei} \rightarrow \text{dic} - \text{mei} \rightarrow \text{det} - \text{mei} \rightarrow \text{mac} \\ \frac{d \text{mac}}{dt} = 0 &= \text{mpb} \rightarrow \text{mac} + \text{bac} \rightarrow \text{mac} + \text{mic} \rightarrow \text{mac} + \text{nem} \rightarrow \text{mac} \\ &\quad + \text{mei} \rightarrow \text{mac} + \text{det} \rightarrow \text{mac} + \text{phy} \rightarrow \text{mac} \\ &\quad - \text{mac} \rightarrow \text{dic} - \text{mac} \rightarrow \text{exp} \\ \frac{d \text{doc}}{dt} = 0 &= \text{mpb} \rightarrow \text{doc} + \text{bac} \rightarrow \text{doc} - \text{doc} \rightarrow \text{bac} - \text{doc} \rightarrow \text{mic} \end{aligned}$$

Chapter 3. Carbon flow through a benthic food web

$$\begin{aligned} \frac{d \det}{dt} = 0 = & phy \rightarrow det + spm \rightarrow det + mpb \rightarrow det + bac \rightarrow det \\ & + mic \rightarrow det + nem \rightarrow det + mei \rightarrow det + mac \rightarrow det \\ & - det \rightarrow bac - det \rightarrow mic - det \rightarrow nem \\ & - det \rightarrow mei - det \rightarrow mac \end{aligned}$$

Isotope mass balances

$$\begin{aligned} \delta^{13}C-bac &= \frac{BGE_{doc \cdot doc \rightarrow bac}}{BGE_{doc \cdot doc \rightarrow bac} + BGE_{det \cdot det \rightarrow bac}} \cdot \delta^{13}C-doc \\ &+ \frac{BGE_{det \cdot det \rightarrow bac}}{BGE_{doc \cdot doc \rightarrow bac} + BGE_{det \cdot det \rightarrow bac}} \cdot \delta^{13}C-det \\ \delta^{13}C-mic &= \frac{doc \rightarrow mic}{doc \rightarrow mic + det \rightarrow mic + mpb \rightarrow mic + bac \rightarrow mic} \cdot \delta^{13}C-doc \\ &+ \frac{det \rightarrow mic}{doc \rightarrow mic + det \rightarrow mic + mpb \rightarrow mic + bac \rightarrow mic} \cdot \delta^{13}C-det \\ &+ \frac{mpb \rightarrow mic}{doc \rightarrow mic + det \rightarrow mic + mpb \rightarrow mic + bac \rightarrow mic} \cdot \delta^{13}C-mpb \\ &+ \frac{bac \rightarrow mic}{doc \rightarrow mic + det \rightarrow mic + mpb \rightarrow mic + bac \rightarrow mic} \cdot \delta^{13}C-bac \\ \delta^{13}C-nem &= \frac{det \rightarrow nem}{det \rightarrow nem + mpb \rightarrow nem + bac \rightarrow nem + mic \rightarrow nem} \cdot \delta^{13}C-det \\ &+ \frac{mpb \rightarrow nem}{det \rightarrow nem + mpb \rightarrow nem + bac \rightarrow nem + mic \rightarrow nem} \cdot \delta^{13}C-mpb \\ &+ \frac{bac \rightarrow nem}{det \rightarrow nem + mpb \rightarrow nem + bac \rightarrow nem + mic \rightarrow nem} \cdot \delta^{13}C-bac \\ &+ \frac{mic \rightarrow nem}{det \rightarrow nem + mpb \rightarrow nem + bac \rightarrow nem + mic \rightarrow nem} \cdot \delta^{13}C-mic \\ \delta^{13}C-mei &= \frac{det \rightarrow mei}{det \rightarrow mei + mpb \rightarrow mei + bac \rightarrow mei + mic \rightarrow mei} \cdot \delta^{13}C-det \\ &+ \frac{mpb \rightarrow mei}{det \rightarrow mei + mpb \rightarrow mei + bac \rightarrow mei + mic \rightarrow mei} \cdot \delta^{13}C-mpb \\ &+ \frac{bac \rightarrow mei}{det \rightarrow mei + mpb \rightarrow mei + bac \rightarrow mei + mic \rightarrow mei} \cdot \delta^{13}C-bac \\ &+ \frac{mic \rightarrow mei}{det \rightarrow mei + mpb \rightarrow mei + bac \rightarrow mei + mic \rightarrow mei} \cdot \delta^{13}C-mic \\ \delta^{13}C-mac &= \sum_{in\ flow} \frac{det \rightarrow mac}{in\ flow} \cdot \delta^{13}C-det + \sum_{in\ flow} \frac{phy \rightarrow mac}{in\ flow} \cdot \delta^{13}C-phy \\ &+ \sum_{in\ flow} \frac{mpb \rightarrow mac}{in\ flow} \cdot \delta^{13}C-mpb + \sum_{in\ flow} \frac{bac \rightarrow mac}{in\ flow} \cdot \delta^{13}C-bac \\ &+ \sum_{in\ flow} \frac{mic \rightarrow mac}{in\ flow} \cdot \delta^{13}C-mic + \sum_{in\ flow} \frac{nem \rightarrow mac}{in\ flow} \cdot \delta^{13}C-nem \\ &+ \sum_{in\ flow} \frac{mei \rightarrow mac}{in\ flow} \cdot \delta^{13}C-mei \\ &\text{with } \sum_{in\ flow} = det \rightarrow mac + phy \rightarrow mac + mpb \rightarrow mac \\ &\quad + bac \rightarrow mac + mic \rightarrow mac + nem \rightarrow mac + mei \rightarrow mac \end{aligned}$$

Equations

Gross primary production	$dic \rightarrow mpb = 714$
Bacterivory by microbenthos	$bac \rightarrow mic = 12.8$
Sediment respiration	$mpb \rightarrow dic + bac \rightarrow dic + mic \rightarrow dic$ $+ nem \rightarrow dic + mei \rightarrow dic + mac \rightarrow dic = 2112$
Bacterial growth efficiency	$BGE_{doc} = 2 \cdot BGE_{det}$
Bacterial production	$BGE_{det} \cdot det \rightarrow bac +$ $BGE_{doc} \cdot doc \rightarrow bac = 598$
Maintenance respiration	$0.01 \cdot biomass$

3.5. Appendix A: Inverse model equality and constraint equations

Table 3.4: Constraints imposed on the benthic food web. Sources are 1) Langdon (1993), 2) Goto et al. (1999), 3) del Giorgio and Cole (1998), 4) Toolan (2001), 5) Verity (1985), 6) Zubkov and Sleigh (1999), 7) Wieltchnig et al. (2001), 8) Capriulo (1990), 9) Fenchel (1982), 10) Straile (1997), 11) Sleigh and Zubkov (1998), 12) Anderson (1992), 13) Herman and Vranken (1988), 14) Heip et al. (1985), 15) Woombs and Laybourn-Parry (1985), 16) Woombs and Laybourn-Parry (1984), 17) Gerlach (1971), 18) Schiemer (1982), 19) Schiemer et al. (1980), 20) Vranken and Heip (1986), 21) Vranken et al. (1986), 22) Heip et al. (1982), 23) Schiemer (1983), 24) Moens and Vincx (1997), 25) Landry et al. (1983), 26) Conover (1966), 27) Cowie and Hedges (1996), 28) Fleeger and Palmer (1982), 29) Feller (1982), 30) Ceccherelli and Mistri (1991), 31) Herman and Heip (1985), 32) Banse and Mosher (1980), 33) Herman et al. (1983), 34) Ikeda et al. (2001), 35) Vidal (1980), 36) Herman et al. (1984), 37) Nielsen et al. (1995), 38) Kristensen (1989), 39) Arifin and Bendell-Young (2001), 40) Hummel et al. (2000), 41) Loo and Rosenberg (1996), 42) Lopez and Cheng (1983), 43) Arifin and Bendell-Young (1997), 44) Lopez and Levinton (1987), 45) Jordana et al. (2001), 46) Sprung (1993), 47) Heip et al. (1995), 48) Thompson and Schaffner (2001), 49) Robertson (1979), 50) Vedel and Riisgård (1993), 51) Calow (1977).

Process	Flow/units	Lower boundary	Upper boundary	Sources
Microphytobenthos				
Respiration	$mpb \rightarrow dic$	$0.16 \cdot dic \rightarrow mpb$		1
Excretion	$mpb \rightarrow doc$	$0.42 \cdot dic \rightarrow mpb$	$0.73 \cdot dic \rightarrow mpb$	2
Bacteria				
BGE_{det}^a	-	0.06	0.32	3,4
Microbenthos				
AE^b	-	0.91	1.0	5
PB^c	d^{-1}	0.50	5.0	6–9
$NGE^{d,e}$	-	0.10	0.50	6,10–12
Nematodes				
AE^b	-	0.06	0.30	13–16
PB^c	d^{-1}	0.05	0.40	13,15,17–22
NGE^d	-	0.60	0.90	13–15,23
Bacterivory ^f	$bac \rightarrow nem$	$\frac{bac}{bac+mic} \frac{nem_{mic}}{nem} C_{nem}$		24
Microbenthos ^f	$mic \rightarrow nem$	$\frac{mic}{bac+mic} \frac{nem_{mic}}{nem} C_{nem}$		24
Herbivory ^f	$mpb \rightarrow nem$	$\frac{nem_{epi}}{nem} C_{nem}$		24
Predation ^f	$nem \rightarrow nem$	$\frac{nem_{pre}}{nem} C_{nem}$	$\frac{nem_{pre}+nem_{fac}}{nem} C_{nem}$	24
Meiobenthos				
AE^b	-	0.57	0.77	25–27
PB^c	d^{-1}	0.03	0.09	28–33
NGE^d	-	0.30	0.50	31–36
Macrobenthos				
AE^b	-	0.40	0.75	41–45
PB^c	d^{-1}	0.01	0.05	37,41,46–50
NGE^d	-	0.50	0.70	37,51
Phytoplankton ^g	$phy \rightarrow mac$	$\frac{mac_{sus}}{mac} C_{mac}$		

^a The range of BGE_{det} is determined from the range of values for seaweeds (del Giorgio and Cole, 1998), this range covers the range in BGE for phytoplankton and faeces as well.

^b AE is assimilation efficiency and is defined as $\frac{\sum inflow - loss\ to\ detritus}{\sum inflow}$.

^c PB is production to biomass ratio.

Chapter 3. Carbon flow through a benthic food web

^d NGE is net growth efficiency and is defined as $\frac{\sum inflow - loss\ to\ detritus - respiration}{\sum inflow - loss\ to\ detritus}$.

^e data on gross growth efficiency (GGE) are the quartiles of the box-whisker plot for flagellates and ciliates in Straile (1997), i.e. 10 % and 45 %. Subsequently net growth efficiency is calculated as $NGE = \frac{GGE}{AE}$.

^f bac is bacterial biomass, mic is microbenthos biomass, nem_{mic} is the biomass of the nematode feeding groups microvores and ciliate feeders, nem_{epi} is the biomass of the nematode epistrate feeding group, nem_{pre} is the biomass of the nematode predator feeding group, nem_{fac} is the biomass of the nematode facultative predator feeding group, nem is nematode biomass and C_{nem} is the total consumption by nematodes.

^g mac_{sus} is the biomass of the macrobenthos suspension feeding group, mac is the macrobenthos biomass and C_{mac} is the total consumption by macrobenthos.

3.6 Appendix B: Introducing stable isotope and tracer data in an inverse model

3.6.1 Stable isotope data

First it is detailed how isotope mass balances are set up in the inverse model. Mixing models require that isotope data of all components are available, which is generally not the case in complex food webs. Second, we therefore explain how a grid search can be used in case some isotope signatures are lacking. Finally, we describe the method to assimilate tracer data in the food web reconstruction.

Isotope mass balances

Isotope signatures are commonly expressed in the delta notation, which is a ‰ deviation from a reference material

$$\delta^h I = \frac{\left(\frac{^h I}{^l I}\right)_{sample} - \left(\frac{^h I}{^l I}\right)_{reference}}{\left(\frac{^h I}{^l I}\right)_{reference}} \cdot 1000 \quad (3.4)$$

where $\frac{^h I}{^l I}$ is ratio of the heavy isotope ($^h I$, e.g. ^{13}C , ^{15}N or ^{34}S) to the more common and lighter isotope ($^l I$, e.g. ^{12}C , ^{14}N or ^{32}S) in the sample and reference material.

The common formulation of an isotope mixing model for a consumer that feeds on n resources is

$$\delta^h I_j = \sum_{i=1}^n (\delta^h I_i + \Delta_i) \cdot \alpha_i \quad (3.5)$$

where $\delta^h I_j$ is the isotope signature of consumer j , $\delta^h I_i$ is the isotope signature of resource i , Δ_i is the fractionation factor and α_i is the relative contribution of resource i in the diet of consumer j . Necessarily, the relative diet contributions sum to 1, i.e. $\sum_{i=1}^n \alpha_i = 1$.

This mixing model is easily extended to a form that includes the flows as unknowns. For this, the relative contribution resource is defined as

$$\alpha_i = \frac{flow_{i \rightarrow j} \cdot \varepsilon_i}{\sum_{i=1}^n flow_{i \rightarrow j} \cdot \varepsilon_i} \quad (3.6)$$

where $flow_{i \rightarrow j}$ is the flow of resource i to consumer j and ε_i is the incorporation efficiency of resource i into the biomass of consumer j . With this definition, the linear mixing model becomes a function of the food web flows as

$$\delta^h I_j \cdot \sum_{i=1}^n (flow_{i \rightarrow j} \cdot \varepsilon_i) = \sum_{i=1}^n ((\delta^h I_i + \Delta_i) \cdot flow_{i \rightarrow j} \cdot \varepsilon_i) \quad (3.7)$$

Note that when the growth efficiency (ε_i) is taken equal for the different resources, it drops from the equation. As this equation is a linear expression of the food web flows, it is easily appended to the equality equations of the inverse model (see Table 3.3).

Dealing with unknown isotope values

From the isotope mass balance description it is clear that the isotope composition of all resources are required and the growth efficiencies for each food source should either be the same or known. For the Molenplaat case study there were four unknown parameters: $\delta^{13}\text{C}$ -microbenthos, $\delta^{13}\text{C}$ -DOC, BGE_{det} and BGE_{doc} . This number was reduced to three by assuming $BGE_{doc} = 2 \cdot BGE_{det}$ (see Appendix A for justification). To overcome these data deficiencies we developed approach based on a grid search. This method resembles the approach proposed by Phillips and Gregg (2003), who used a grid search to estimate the importance of different resources for a consumer, in case no unique solution could be found.

First, the potential range of each parameter was determined. The range on bacterial growth efficiency on detritus was taken from the literature (0.06 - 0.32, see Appendix A). The isotope signatures ranges were taken from the available isotope signatures of other compartments. From the food web structure, all the potential resource compartments were identified and the minimal and maximal isotope signatures from the resources were selected. The possible sources for DOC are bacteria ($\delta^{13}\text{C}$ of -20.4) and microphytobenthos ($\delta^{13}\text{C}$ of -15.0). Hence, the $\delta^{13}\text{C}$ -DOC should lie between -20.4 and -15.0. The end members for microbenthos in terms of their isotope signature are detritus ($\delta^{13}\text{C}$ of -21.2) and microphytobenthos ($\delta^{13}\text{C}$ of -15.0).

The ranges of these three parameters span a 3 dimensional space of all possible combinations. These initial ranges are not yet affected by the information implemented in the inverse model. To delineate the combinations of isotope signatures that are compatible with the other inverse model equations and constraints, we performed a grid search. Each parameter range was discretized (step size for isotopes 0.10 and for BGE 0.05) on a grid and the inverse model solved for every parameter combination. When the other data in the inverse model are not compatible with a certain parameter combination, the model residuals are not zero (i.e. the model cannot be solved without deviation from the imposed data). The model residual was calculated as the deviation from the linear equality and inequality equations

$$Residual\ norm = (\mathbf{Ax} - \mathbf{b})^T(\mathbf{Ax} - \mathbf{b}) + (\mathbf{Gx} - \mathbf{h})^T\Gamma(\mathbf{Gx} - \mathbf{h}) \quad (3.8)$$

Γ is a diagonal matrix whose diagonal elements are unity when the argument is negative, and zero when the argument is positive

$$\Gamma_{i,i} = \begin{cases} 0, & (\mathbf{Gx} - \mathbf{h})_i \geq 0 \\ 1, & (\mathbf{Gx} - \mathbf{h})_i < 0 \end{cases} \quad (3.9)$$

This ensures that only the inequalities that are violated add to the residual norm. By performing this evaluation for each possible parameter combination, one can delineate the possible parameter combinations that are compatible with the other data. The parameter combination that has a zero residual norm and is minimal in $\sum_{i=1}^n x_i^2$, is the simplest or parsimonious food web (sensu Vézina and Platt (1988)).

3.6.2 Tracer data

The output of an inverse model is a food web in which all flows are quantified. These flow values, in combination with the stock size of the compartments, determine how a tracer flows through the food web. The inverse food web model with conventional and stable isotope data is an under determined system. This implies that, within the limits set

3.6. Appendix B: Introducing stable isotope and tracer data in an inverse model

by these data, there is an infinite amount of different food webs that all satisfy these data equally well. Put otherwise, there is no one unique solution that optimally reproduces the data in the inverse model, but an infinite amount. However, each food web has different flow values and will therefore differ in the way a tracer flows through it. In the final step of quantifying the intertidal food web, we aim to find the food web whose tracer dynamics optimally resemble the observations from the tracer experiment.

First, the inverse model, with conventional and isotope data, was repeatedly solved and during each run the minimization function that weighted the different flows was varied

$$J = \sum_{i=1}^n w_i x_i^2 \quad (3.10)$$

where \mathbf{w} contains n weighting factors (Lawson and Hanson, 1995). The elements of \mathbf{w} were randomly varied between 1 and 100 for each run (when $\mathbf{w} = 1$ this corresponds to finding the parsimonious solution). As the contribution of a flow in the minimization function differed with each run, numerous different inverse solutions were generated (618393 in this case for practical reasons). These generated inverse solutions covered $> 91\%$ of the CISrange of all flows, except for the flows microbenthos to nematodes (84 % covered) and microbenthos to meiobenthos (73 % covered) (data not shown). This means that each flow range (CISrange) was sufficiently covered in our attempt to find the food web that optimally reproduces the tracer data.

Second, a tracer model was set up to simulate tracer flow through each food web. A specific rate constant ($\tau_{i \rightarrow j}$, d^{-1}) was calculated for each flow

$$\tau_{i \rightarrow j} = \frac{flow_{i \rightarrow j}}{stock_i} \quad (3.11)$$

in which $flow_{i \rightarrow j}$ is the flow from compartment i to j and $stock_i$ is the stock size of compartment i . These rate constants were used to set up the tracer model (Table 3.5). In the tracer model the processes respiration, excretion and faeces production have a tracer concentration equal to that of the incoming flows. Other outgoing flows, i.e. grazing, predation or export have the tracer concentration of the biotic compartment (Table 3.5). To initialize the tracer simulation, the incorporation rate of $^{13}C\text{-HCO}_3^-$ into microphytobenthos was set to the observed fixation rate of $32 \text{ mg } ^{13}C \text{ m}^{-2} \text{ h}^{-1}$ during a period of 4.5 hours. The model was solved in the modeling environment FEMME (Soetaert et al., 2002) and can be downloaded from <http://www.nioo.knaw.nl/ceme/femme>.

Table 3.5: Model equations of the dynamic tracer model. FixRate is the observed fixation rate of microphytobenthos ($32 \text{ mg } ^{13}C \text{ m}^{-2} \text{ h}^{-1}$ during 4.5 hours). The tracer concentration in a compartment is denoted as $stock^{tr}$. Abbreviations as in Fig. 3.1

$$\begin{aligned} \tau_{i \rightarrow j} &= \frac{flow_{i \rightarrow j}}{stock_i} \\ \frac{d \text{ mpb}^{tr}}{dt} &= \Gamma \cdot \text{FixRate} \cdot \left(1 - \frac{\text{mpb} \rightarrow \text{doc} + \text{mpb} \rightarrow \text{dic}}{\text{dic} \rightarrow \text{mpb}}\right) \\ &\quad - \text{mpb}^{tr} \cdot (\tau_{\text{mpb} \rightarrow \text{det}} + \tau_{\text{mpb} \rightarrow \text{mic}} + \tau_{\text{mpb} \rightarrow \text{nem}} + \tau_{\text{mpb} \rightarrow \text{mei}} + \tau_{\text{mpb} \rightarrow \text{mac}}) \\ \text{with } \Gamma &= \begin{cases} 0, & t > \frac{4.5}{24} \\ 1, & t \leq \frac{4.5}{24} \end{cases} \\ \frac{d \text{ bac}^{tr}}{dt} &= \text{BGE} \text{ doc} \cdot \text{doc}^{tr} \cdot \tau_{\text{doc} \rightarrow \text{bac}} + \text{BGE} \text{ det} \cdot \text{det}^{tr} \cdot \tau_{\text{det} \rightarrow \text{bac}} \\ &\quad - \text{bac}^{tr} \cdot (\tau_{\text{bac} \rightarrow \text{doc}} + \tau_{\text{bac} \rightarrow \text{det}} + \tau_{\text{bac} \rightarrow \text{bur}} + \tau_{\text{bac} \rightarrow \text{mic}}) \\ &\quad - \text{bac}^{tr} \cdot (\tau_{\text{bac} \rightarrow \text{nem}} + \tau_{\text{bac} \rightarrow \text{mei}} + \tau_{\text{bac} \rightarrow \text{mac}}) \\ \frac{d \text{ mic}^{tr}}{dt} &= \text{mpb}^{tr} \cdot \tau_{\text{mpb} \rightarrow \text{mic}} + \text{bac}^{tr} \cdot \tau_{\text{bac} \rightarrow \text{mic}} \end{aligned}$$

$$\begin{aligned}
 & +det^{tr} \cdot \tau_{det \rightarrow mic} + doc^{tr} \cdot \tau_{doc \rightarrow mic} \\
 & - \frac{\sum_i stock_i^{tr} \cdot \tau_{i \rightarrow mic}}{\sum_i flow_{i,mic}} \cdot (\tau_{mic \rightarrow dic} + \tau_{mic \rightarrow det}) \\
 & - mic^{tr} \cdot (\tau_{mic \rightarrow nem} + \tau_{mic \rightarrow mei} + \tau_{mic \rightarrow mac}) \\
 \frac{d\ nem^{tr}}{dt} & = mpb^{tr} \cdot \tau_{mpb \rightarrow nem} + bac^{tr} \cdot \tau_{bac \rightarrow nem} \\
 & + mic^{tr} \cdot \tau_{mic \rightarrow nem} + det^{tr} \cdot \tau_{det \rightarrow nem} \\
 & - \frac{\sum_i stock_i^{tr} \cdot \tau_{i \rightarrow nem}}{\sum_i flow_{i,nem}} \cdot (\tau_{nem \rightarrow dic} + \tau_{nem \rightarrow det}) - nem^{tr} \cdot \tau_{nem \rightarrow mac} \\
 \frac{d\ mei^{tr}}{dt} & = mpb^{tr} \cdot \tau_{mpb \rightarrow mei} + bac^{tr} \cdot \tau_{bac \rightarrow mei} \\
 & + mic^{tr} \cdot \tau_{mic \rightarrow mei} + det^{tr} \cdot \tau_{det \rightarrow mei} \\
 & - \frac{\sum_i stock_i^{tr} \cdot \tau_{i \rightarrow mei}}{\sum_i flow_{i,mei}} \cdot (\tau_{mei \rightarrow dic} + \tau_{mei \rightarrow det}) - mei^{tr} \cdot \tau_{mei \rightarrow mac} \\
 \frac{d\ mac^{tr}}{dt} & = mpb^{tr} \cdot \tau_{mpb \rightarrow mac} + bac^{tr} \cdot \tau_{bac \rightarrow mac} \\
 & + mic^{tr} \cdot \tau_{mic \rightarrow mac} + nem^{tr} \cdot \tau_{nem \rightarrow mac} \\
 & + mei^{tr} \cdot \tau_{mei \rightarrow mac} + det^{tr} \cdot \tau_{det \rightarrow mac} \\
 & - \frac{\sum_i stock_i^{tr} \cdot \tau_{i \rightarrow mac}}{\sum_i flow_{i,mac}} \cdot (\tau_{mac \rightarrow dic} + \tau_{mac \rightarrow det}) - mac^{tr} \cdot \tau_{mac \rightarrow exp} \\
 \frac{d\ doc^{tr}}{dt} & = \Gamma \cdot FixRate \cdot \frac{mpb \rightarrow doc}{dic \rightarrow mpb} + \frac{\sum_i stock_i^{tr} \cdot \tau_{i \rightarrow bac}}{\sum_i flow_{i,bac}} \cdot \tau_{bac \rightarrow doc} \\
 & - doc^{tr} \cdot (\tau_{doc \rightarrow bac} + \tau_{doc \rightarrow mic}) \\
 \frac{d\ det^{tr}}{dt} & = mpb^{tr} \cdot \tau_{mpb \rightarrow det} + bac^{tr} \cdot \tau_{bac \rightarrow det} \\
 & + \sum_i (stock_i^{tr} \cdot \tau_{i \rightarrow mic}) \cdot \frac{mic \rightarrow det}{\sum_i flow_{i \rightarrow mic}} \\
 & + \sum_i (stock_i^{tr} \cdot \tau_{i \rightarrow nem}) \cdot \frac{nem \rightarrow det}{\sum_i flow_{i \rightarrow nem}} \\
 & + \sum_i (stock_i^{tr} \cdot \tau_{i \rightarrow mei}) \cdot \frac{mei \rightarrow det}{\sum_i flow_{i \rightarrow mei}} \\
 & + \sum_i (stock_i^{tr} \cdot \tau_{i \rightarrow mac}) \cdot \frac{mac \rightarrow det}{\sum_i flow_{i \rightarrow mac}} \\
 & - det^{tr} \cdot (\tau_{det \rightarrow bac} + \tau_{det \rightarrow mic} + \tau_{det \rightarrow nem} + \tau_{det \rightarrow mei} + \tau_{det \rightarrow mac})
 \end{aligned}$$

Finally, the output of each tracer model was evaluated against the experimental data by means of a weighted cost function

$$J = \sum_{i=1}^{nv} \sum_{j=1}^{no} \left(\frac{Mod_{ij} - Obs_{ij}}{\sigma_i \cdot Obs_{ij}} \right)^2 \quad (3.12)$$

where nv is the number of variables, no is the number of observations, Mod_{ij} is the modeled value of the observed counterpart Obs_{ij} and σ_i is the relative weighting factor. Relative errors could not be assessed from the observations but were assigned based on conversion protocols: 0.15 for microphytobenthos and bacteria, 0.10 for nematodes and 0.05 for macrobenthos. Different weighting scenarios were tested but this did not alter the results significantly. The run with the lowest cost function was accepted as CITS.

3.7 Appendix C: Comparison of the inverse solutions CS, CIS and CITS

The inverse solutions, CS, CIS and CITS, are obtained using different data sets and therefore the solutions differ from each other (Table 3.6). The sum of all flows increases with increasing data resolution from 7670 (CS), 8322 (CIS) to 8398 (CITS). The main differences are found between CS and both CIS and CITS (Fig. 3.4). Differences are found over the whole range of flows, the correlation coefficients for CS versus CIS are 0.82 and 0.79 for CS versus CITS. The correlation coefficient for CIS versus CITS amounts 0.99 (Fig. 3.5). While the flows at the lower and higher end agree reasonably, there are still differences between the CIS and the CITS for intermediate sized flows (Fig. 3.5).

Table 3.6: Flow values ($\text{mg C m}^{-2} \text{ d}^{-1}$) of the inverse solutions CS, CIS and CITS.

Flow	CS	CIS	CITS
doc → bac	586	253	249
doc → mic	129	601	487
det → bac	695	1391	1370
det → mic	515	210	275
det → nem	1	0	0
det → mei	24	0	0
det → mac	20	0	0
phy → det	500	1077	987
phy → mac	520	139	198
spm → det	500	304	334
dic → mpb	714	714	714
mpb → dic	406	114	114
mpb → doc	300	348	300
mpb → det	0	0	0
mpb → mic	0	0	0
mpb → nem	9	17	18
mpb → mei	0	25	25
mpb → mac	0	210	257
bac → dic	683	1047	1021
bac → doc	416	506	436
bac → det	31	37	135
bac → mic	13	13	13
bac → nem	32	14	14
bac → mei	55	0	0
bac → mac	51	28	0
bac → bur	0	0	0
mic → dic	587	710	678
mic → det	0	38	22
mic → nem	9	0	1
mic → mei	33	2	2
mic → mac	29	75	71
nem → dic	8	3	3
nem → det	36	24	24
nem → nem	2	3	2

nem → mac	5	4	6
mei → dic	63	13	13
mei → det	26	6	6
mei → mac	23	8	8
mac → dic	365	226	283
mac → det	162	116	135
mac → exp	122	122	122

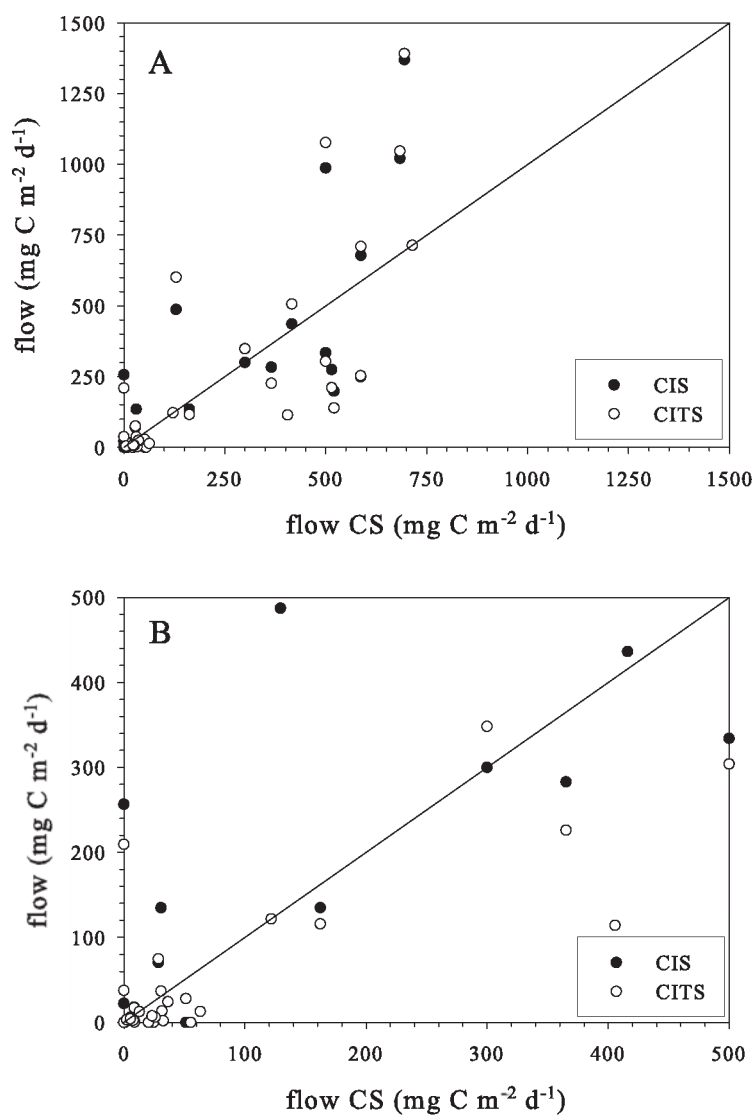


Figure 3.4: Comparison of CIS and CITS with CS on A) a scale from 0 - 1500 mg C m⁻² d⁻¹ and B) a scale from 0 - 500 mg C m⁻² d⁻¹.

3.7. Appendix C: Comparison of the inverse solutions CS, CIS and CITS

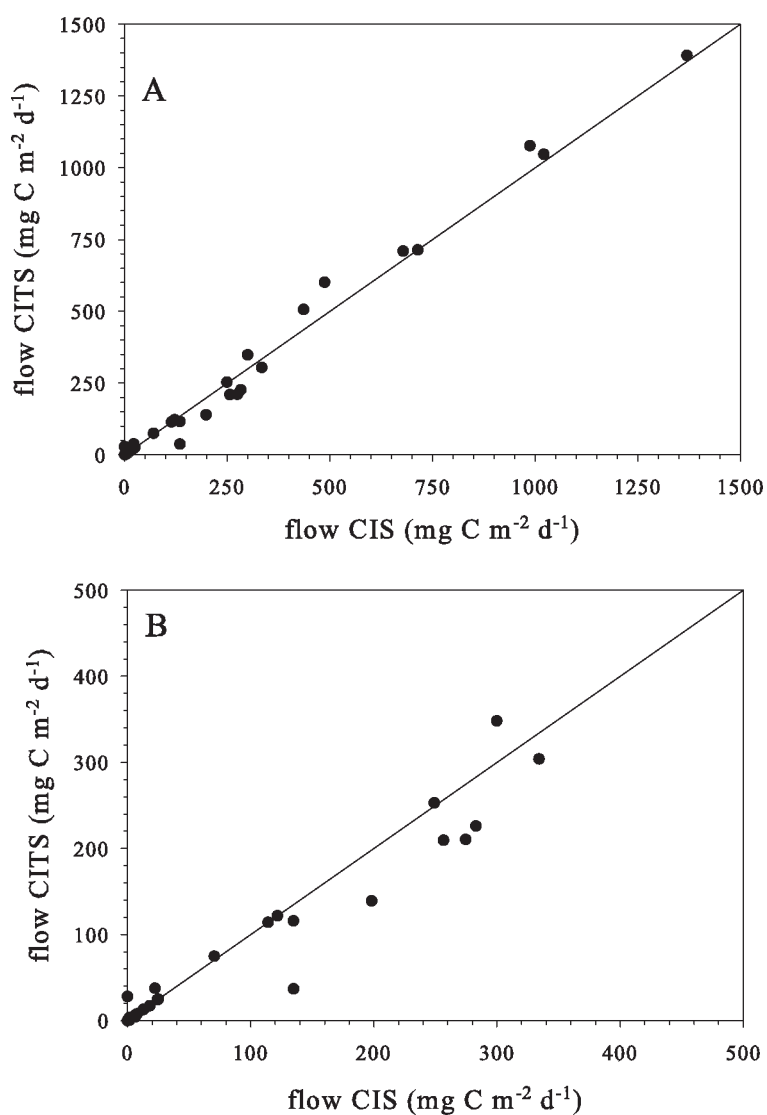


Figure 3.5: Comparison of the CIS with the CITS on A) a scale from 0 - 1500 mg C m⁻² d⁻¹ and B) a scale from 0 - 500 mg C m⁻² d⁻¹.

Chapter 4

The fate of bacterial carbon in sediments: Modeling an in situ isotope tracer experiment

Dick van Oevelen, Jack J. Middelburg, Karline Soetaert and Leon Moodley. *Accepted by Limnology and Oceanography*

4.1 Introduction

Biogeochemical cycling in marine soft sediments is dominated by heterotrophic bacterial communities (Smith, 1973). Although being highly diverse in terms of species (Torsvik et al., 1996; Li et al., 1999) and metabolic strategies (Fenchel et al., 1998), total bacterial numbers are comparatively constant at around 10^9 bacteria ml^{-1} porewater (Schmidt et al., 1998). Irrespective of this constancy, specific growth rates vary by four orders of magnitude (Sander and Kalff, 1993). The importance of bacteria in early diagenetic processes and their potential as food source has generated ample interest in the processes affecting bacterial carbon in sediments, a topic that is basically approached from at least three directions: 1) bottom-up control, 2) biogeochemical approach and 3) top-down control.

The bottom-up approach has focussed on finding linear relationships between particulate organic matter and bacterial biomass or production. These relationships may be spurious for various reasons (Bird and Duarte, 1989; Flemming and Delafontaine, 2000), but when standardized to volumetric units, significant relationships explain 25 - 60 % of the observed variation in bacterial biomass (Schallenberg and Kalff, 1993) and production (Sander and Kalff, 1993), suggesting that substrate availability impacts bacterial dynamics.

Biogeochemists usually focus on hydrolysis rates of standardized substrates (Meyer-Reil, 1986; Sawyer and King, 1993; Arnosti and Holmer, 1999) or sediment dissolved organic matter (Alperin et al., 1994; Burdige et al., 1999), production of bacterial biomass (Dixon and Turley (2001) and references therein), respiration and growth efficiency (Jahnke and Craven, 1995; del Giorgio and Cole, 1998). Hence, the biogeochemical approach resolves rates of oxic, suboxic and anoxic mineralization pathways, but the fate of bacterial production is not explicitly studied.

Chapter 4. The fate of bacterial carbon in sediments

In the top-down approach, bacterial carbon is assumed to be regulated by higher trophic levels of the benthic food web, a topic which has a long-standing interest dating back to the 1930's (MacGinitie, 1932; ZoBell, 1938). In a seminal review on bacterivory, Kemp (1990) asserted that bacteria do not form an important constituent of the macrobenthic diet and concluded that reports for meiobenthos (mostly nematodes) were conflicting. It was however noted that quantitative bacterivory data of meiobenthos and protozoans were either sparse or lacking. Methodological advances have been made such as the use of fluorescent stained sediment (Starink et al., 1994) and radioactively labeled substrates (Montagna, 1995). Using these methods, quantitative data on bacterivory by small-sized grazers have been gathered (Epstein et al., 1992; Sundback et al., 1996; Hamels et al., 2001b). In general, only 1 - 20 % of the bacterial production is grazed, although grazing intensity may fluctuate seasonally (Hondeveld et al., 1995; Epstein, 1997b; Hamels et al., 2001b). Grazing studies are generally focussed on the top cm of the sediment and are based on comparatively short time incubations (minutes to hours) in retrieved and/or slurried sediments, rendering translation to the field and longer periods cumbersome. In addition, bacterial production is measured by other methods than bacterivory and therefore do not form an integral part of the grazing studies.

Another top down agent that has received interest is viral infection (Maranger and Bird, 1996; Fischer et al., 2003; Hewson and Fuhrman, 2003), which potentially exerts control on bacteria through infection and subsequent cell lysis (Weinbauer, 2004). This mechanism may set upper limits on bacterial biomass or production, but leaves unexplained the subsequent fate of the bacterially derived carbon. Studies carried out in continental margin sediments show burial of recalcitrant bacterial cell wall remnants (Grutters et al., 2002). However, Novitsky (1986) reported rapid mineralization of dead microbial biomass in a tropical marine beach sediment.

It is clear that several regulating factors act upon sedimentary bacteria and a comprehensive understanding calls for the integration of bottom-up, biogeochemical and top-down approaches. Boudreau (1999) provided such an integration by developing spatial and temporal mass balance equations of bacterial carbon in sediments and used these in a theoretical investigation to explain the observed linear relationships between bacterial biomass and sediment particulate organic carbon (POC). The parameters of this linear relationship are non-linear composites of parameters describing exchange processes, bacterial growth efficiency and biological processes including growth, mortality and grazing.

We report the results of a ^{13}C -glucose labeling experiment and use these data in a tracer model to quantify the fate of sedimentary bacterial carbon. ^{13}C -glucose was injected in intertidal sediments and traced into bacterial specific polar-lipid-derived fatty acids (PLFAs), total organic carbon, meiobenthos, macrobenthos and respired carbon during a period of 4.5 months. The modeled processes were selected based on the comprehensive analysis by Boudreau (1999). The combined modeling - ^{13}C tracer study allowed us to quantify bacterial production, bacterial growth efficiency, mortality, resuspension and bacterial grazing by meiobenthos and macrobenthos.

4.2 Material and methods

4.2.1 Experimental approach

The Molenplaat intertidal flat was chosen as the study site since detailed physical and biological background data are available (Herman et al., 2001). The intertidal flat is located in the saline part (salinity 20-25) of the turbid, heterotrophic and nutrient-rich Scheldt estuary. The sampling site is located in the muddy center of the flat (51°26.25' N, 3°57.11' E), has a median grain size of 77 μm , organic carbon content of ~ 0.5 wt % and exposure time of about 7 hours per tidal cycle.

Prior to labeling, two 0.25 m^{-2} metal frames (0.5x0.5x0.08 m) were inserted in the sediment. On 21 May 2003, the upper 10 cm was labeled in two hours with ^{13}C by injecting 0.4 ml glucose solution (23.5 $\text{mmol } ^{13}\text{C l}^{-1}$) into four hundred 6.25 cm^{-2} squares plot $^{-1}$, which resulted in a flux of 15.3 $\text{mmol } ^{13}\text{C m}^{-2}$ per labeling day. Labeling was performed daily for 5 consecutive days to ensure sufficient label incorporation by bacteria, but labeling on day 2 had to be canceled due to bad weather. S

Sampling frequency was high initially (day 0, 0.2, 2, 3, 4, 5, 6, 8, 12, 18) and lower thereafter (day 36, 71, 136). On each sampling day, one sampling core was taken per plot. Sampling positions within the plots were determined a priori by a randomization procedure. A sampling core (\varnothing 5 cm) was inserted 10 cm deep, filled with filtered sea water and closed with a gas impermeable rubber stopper. A metal core (\varnothing 9 cm) was inserted around the sampling core to prevent disturbance of the plot and remained in place during the experiment. The sampling core was transported in a dark cool container to the laboratory. The ^{13}C -DIC flux was estimated from the difference in ^{13}C -DIC in the overlying water in the field and the laboratory. Sediment was sliced into three depth intervals (0-2, 2-5 and 5-10 cm), homogenized and sampled for POC, ^{13}C -POC, PLFAs and ^{13}C -PLFAs (5-10 ml wet sediment), porewater DIC and ^{13}C -DIC (15-20 ml wet sediment), meiobenthic biomass and label incorporation (10 ml wet sediment). The remaining sediment (~ 15 ml for 0-2 cm, ~ 35 ml for 2-5 cm and ~ 75 ml for 5-10 cm) was used to measure label incorporation by macrobenthos. Meiobenthic and macrobenthic samples were fixed with formalin (final concentration 4 %). In this paper we will present total uptake by meiobenthos and macrobenthos, while uptake rates of meiobenthic taxa and macrobenthic species will be presented in a paper that focusses on the importance of bacteria in individual diets (Chapter 5).

4.2.2 Analytical procedures

Sediment samples were weighed, freeze-dried, weighed again and converted to porosity assuming a dry sediment density of 2.55 g cm^{-3} . Organic carbon content and stable isotope ratios of sediment POC, meiobenthos and macrobenthos were measured by elemental analyzer - isotope ratio mass spectrometry (EA-IRMS) (Middelburg et al., 2000). Label incorporation into bacteria was calculated from incorporation in specific bacterial PLFA biomarkers (i14:0, i15:0, a15:0, i16:0 and 18:1 ω 7c). Lipids were extracted from 3 g dry sediment using a Bligh and Dyer extraction, from which the PLFA fraction was isolated by sequentially rinsing the lipid extract on a silicic acid column with chloroform, acetone and methanol. The PLFA extract was derivatized to volatile fatty acid methyl esters (FAME) and measured by gas chromatography-isotope ratio mass spectroscopy (GC-IRMS) for PLFA concentration and $\delta^{13}\text{C}$ -PLFA. Full methodological details can be found in Boschker et al. (1999) and Middelburg et al. (2000). Porewater was extracted by centrifugation (Saager et al., 1990) and transferred to a helium flushed headspace vial,

Chapter 4. The fate of bacterial carbon in sediments

acidified (0.1 ml H_3PO_4 ml^{-1} porewater) and stored upside down. A 3 ml headspace was created in the DIC/ ^{13}C -DIC bottom water samples by replacing water with He and acidified as described above. DIC and ^{13}C -DIC were determined by EA-IRMS (Moodley et al., 2000).

Meiobenthic samples were sieved (38 μm) and sub-sampled. Specimens of each meiobenthic group were handpicked, typically 15-30 per group, for stable isotope measurements, cleaned of adhering detritus, rinsed (0.2 μm filtered water), transferred to silver boats and stored frozen. Prior to isotope analysis the samples were thawed, acidified for carbonate removal with 20 μl 2.5 % HCl, oven-dried (50 °C) and pinched closed. Meiobenthic biomass was estimated as in Moodley et al. (2002): the carbon content of individual specimens of each meiobenthic group was determined from the carbon signal from the EA-IRMS (calibrated with Cs_2CO_3 standards) and multiplied by the number of organisms in the whole sample. Processing the meiobenthic samples proved to be very time consuming and some sacrifices were made: stable isotope data are based on samples from one plot only and the biomass is estimated from the samples taken at day 0, 0.2, 2, 4 and 6.

All macrobenthos specimens were handpicked from the sample and stored in filtered water and preserved with formalin. The sorted sample was transferred to a petri dish, from which a species sample was taken, rinsed, transferred to a silver boat and stored frozen. Bivalves were placed in an acidified bath (1 mmol HCl) to dissolve the carbonate shell, cleaned of debris, rinsed thoroughly and either whole specimens (small specimens) or flesh samples (large specimens) were transferred to silver boats and stored frozen. Sample treatment prior to isotope analysis was similar to that for meiobenthos. Macrobenthos biomass could not be accurately determined from the small sampling cores and was therefore determined by a dedicated sampling on 27th of May 2003: 12 cores (\varnothing 10 cm) were taken close to the experimental plots, sliced into 0-2, 2-5, 5-10, 10-20 and > 20 cm intervals, fixed with formalin (4 % final concentration), sieved (1 mm), sorted, weighed for wet weight and finally converted to C units using species specific conversion factors available from a large database at the Netherlands Institute of Ecology.

Delta values are expressed relative to the carbon isotope ratio (R: $^{13}\text{C}/^{12}\text{C}$) of Vienna Pee Dee Belemnite (VPDB): $\delta^{13}\text{C} = (\text{R}_{\text{sample}}/\text{R}_{\text{VPDB}} - 1) \times 1000$, R_{VPDB} is 0.0112372. Label incorporation is presented as total label content in $\text{mmol } ^{13}\text{C m}^{-2}$ in the top 10 cm (I), where I is calculated as $(\text{F}_{\text{sample}} - \text{F}_{\text{background}}) \times \text{S}$, where F is the ^{13}C fraction ($^{13}\text{C}/(^{13}\text{C} + ^{12}\text{C}) = \text{R}/(\text{R}+1)$) and S is the total carbon stock (mmol C m^{-2}) of the respective compartment.

All C and ^{13}C data reported are integrated over the top 10 cm of the sediment and are the mean of the two plots, except for meiobenthos. Errors are reported as standard deviation.

4.2.3 Model description

A mechanistic model was used to simulate the transfer of label among the biotic and abiotic compartments. The model structure was inspired by the bacterial mass balance description of Boudreau (1999), but was assumed to be zero-dimensional as the incorporated processes did not require more complexity. Particulate organic carbon (POC), dissolved organic carbon (DOC) and bacterial carbon dynamics are implemented as C and excess ^{13}C balances, whereas meiobenthos and macrobenthos are modeled only as excess ^{13}C under the assumption that their total biomass is at steady-state (Fig. 4.1). All model variables are listed in Table 4.1, model parameters are in Table 4.2, parameter values are in 4.4 and

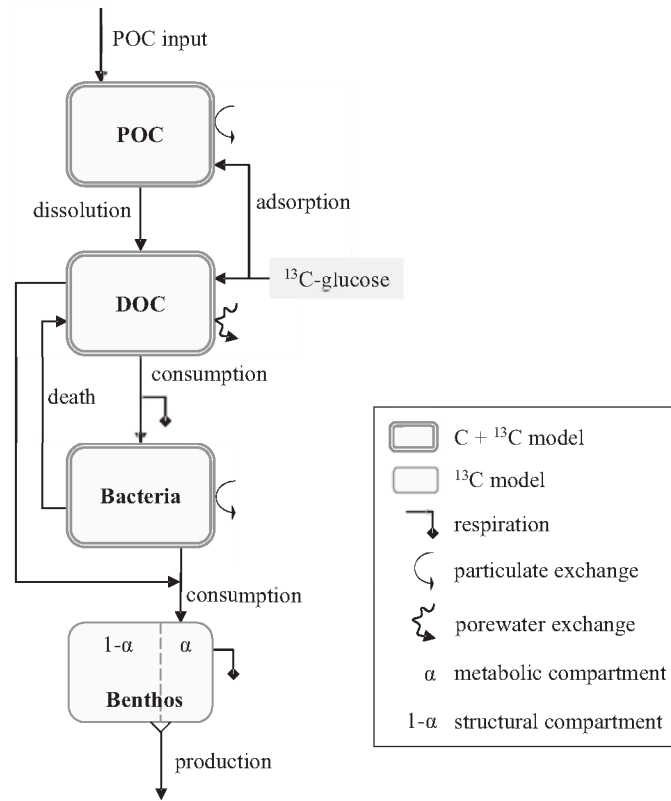


Figure 4.1: Schematic of the model showing the pathways among particulate organic carbon (POC), dissolved organic carbon (DOC), bacteria and benthos. Meiobenthos and macrobenthos are modeled separately but pictured together as benthos for simplicity.

model equations of state variables (s#) and variables (v#) are in Table 4.3.

Table 4.1: Model state variables, variables and forcing functions. The symbol X has a variable interpretation which is detailed in the description.

State variables	Unit	Description
P	mmol C m^{-2}	particulate organic carbon (POC)
D	mmol C m^{-2}	dissolved organic carbon (DOC)
B	mmol C m^{-2}	bacterial biomass
P_{13C}	$\text{mmol }^{13}\text{C m}^{-2}$	excess ^{13}C in POC
D_{13C}	$\text{mmol }^{13}\text{C m}^{-2}$	excess ^{13}C in DOC
B_{13C}	$\text{mmol }^{13}\text{C m}^{-2}$	excess ^{13}C in bacterial biomass
MxE_{13C}	$\text{mmol }^{13}\text{C m}^{-2}$	excess ^{13}C in metabolic fraction of meio- or macrobenthos
MxS_{13C}	$\text{mmol }^{13}\text{C m}^{-2}$	excess ^{13}C in structural fraction of mass of meio- or macrobenthos
DIC_{13C}	$\text{mmol }^{13}\text{C m}^{-2}$	Accumulated respired excess ^{13}C
Variables	Unit	Description
F_x	$^{13}\text{C}/\text{C}$	fraction ^{13}C of total C

$f(T)$	-	in compartment x temperature effect
Me_{13C}	mmol $^{13}C\ m^{-2}$	excess ^{13}C in meiobenthos
Ma_{13C}	mmol $^{13}C\ m^{-2}$	excess ^{13}C in macrobenthos
Org	mmol C m^{-2}	sum of P , D , B , Me , and Ma
Org_{13C}	mmol $^{13}C\ m^{-2}$	sum of P_{13C} , D_{13C} , B_{13C} , Me_{13C} , and Ma_{13C}
$disP_{P,D}$	mmol C $m^{-2}\ d^{-1}$	dissolution of POC
$adsGlu_{Glu,P}$	mmol $^{13}C\ m^{-2}\ d^{-1}$	injected glucose adsorbed to POC
$disGlu_{Glu,D}$	mmol $^{13}C\ m^{-2}\ d^{-1}$	injected glucose dissolved as DOC
$uptD_{D,B}$	mmol C $m^{-2}\ d^{-1}$	uptake of DOC by bacteria
$morB_{B,D}$	mmol C $m^{-2}\ d^{-1}$	bacterial mortality
$graM_{B,M}$	mmol C $m^{-2}\ d^{-1}$	bacterial grazing by meio- and macrobenthos
$sorM_{D,M}$	mmol C $m^{-2}\ d^{-1}$	DOC uptake by meio- and macrobenthos
$proMx$	mmol C $m^{-2}\ d^{-1}$	production by meio- (Me) or macrobenthos (Ma)
$excX$	mmol $^{13}C\ m^{-2}\ d^{-1}$	exchanges of ^{13}C -POC, ^{13}C -DOC or ^{13}C -bacteria
Forcings	Unit	Description
$Temp$	$^{\circ}C$	temperature
$GluInj$	mmol $^{13}C\ m^{-2}\ d^{-1}$	flux of injected ^{13}C labeled glucose
$POCinput$	mmol C $m^{-2}\ d^{-1}$	POC input

The biological processes are influenced by temperature using the Q_{10} formulation (v1). Carbon input to POC is constant (v2), but ^{13}C -glucose injection occurs in a period of 2 hours (v4). POC dissolution (v5) and uptake of DOC by bacteria (v8) are first order processes, which is conceptually equivalent to the common formulation in diagenetic models (Boudreau, 1999). Adsorption of a part of the injected glucose (v3) occurs immediately after amendment (Henrichs and Sugai, 1993). A fixed fraction of the DOC uptake by bacteria is respired and the remainder is incorporated into bacterial biomass (s3, s9). Bacterial mortality is a first order process (v6) and the bacterially derived organic carbon flows to DOC (s2). Exchange processes are a dilution term acting on ^{13}C -POC (e.g., advection, resuspension), ^{13}C -DOC (e.g., diffusion, bioirrigation) and ^{13}C -bacteria (e.g., advection, resuspension) (v11), under the assumption that exchanged labeled carbon is replaced by unlabeled carbon. Most organic matter and bacteria are attached to sediment grains, therefore the exchange rate for POC and bacteria is taken as equal (v11). Meiobenthic and macrobenthic biomass are assumed to be in steady-state. Their biomass, PB ratio and growth efficiency generate a carbon demand (v12), which is fulfilled partly by DOC (v9) and bacteria (v10). The steady-state assumption implies that secondary production by meiobenthos and macrobenthos is balanced by loss processes such as mortality or grazing by higher trophic levels (e.g., fish and birds). In the model, meiobenthos and macrobenthos consist of two compartments: a metabolic and a structural compartment. All assimilated carbon enters the metabolic compartment, turnover of this compartment is due to respiration and production (s7). A continuous flow feeds the structural compartment, of which the turnover is solely due to production (s8).

The model was implemented in the modeling environment FEMME (Soetaert

et al., 2002), the environment and model code can be downloaded from <http://www.nioo.knaw.nl/ceme/femme>. The model was solved with a 4th order Runge-Kutta integration method with a fixed time step of 0.01 d. A spin-up period of 300 days successfully damped the effect of initial conditions.

Table 4.2: Model parameters.

Symbol	Unit	Description
F_{Glu}	mmol ¹³ C m ⁻² d ⁻¹	Glucose injection rate
Q_{10}	-	Temperature dependence
ε_{Glu}	-	Injection efficiency
F_{POC}	mmol C m ⁻² d ⁻¹	Input of POC
ε_M	-	Growth efficiency benthos
Me	mmol C m ⁻²	Meiobenthic biomass
Ma	mmol C m ⁻²	Macrobenthic biomass
K_{Glu}	-	Glucose adsorption
$d_{P,D}$	d ⁻¹	POC dissolution
λ_P	d ⁻¹	POC exchange
λ_D	d ⁻¹	DOC exchange
$r_{D,B}$	d ⁻¹	Bacterial DOC uptake
ε_B	-	Bacterial growth efficiency
m_B	d ⁻¹	Mortality rate
α	-	Metabolic part of biomass
PB_{Me}	d ⁻¹	Production rate meiobenthos
β_{Me}	-	Bacteria in meiobenthos diet
ρ_{Me}	-	DOC in meiobenthos diet
PB_{Ma}	d ⁻¹	Production rate macrobenthos
β_{Ma}	-	Bacteria in macrobenthos diet
ρ_{Ma}	-	DOC in macrobenthos diet

Table 4.3: Model equations. The miscellaneous symbol X is specified for every state variable or variable. The symbol Mx stands for both Me and Ma .

(v1)	$f(T) = Q_{10}^{\frac{T_{emp}-20}{10}}$
(s1)	$\frac{dP}{dt} = POCinput + adsGlu_{Glu,P} - disP_{P,D}$
(v2)	$POCinput = Flux_{POC}$
(v3)	$adsGlu_{Glu,P} = \varepsilon_{Glu} \cdot K_{Glu} \cdot GluInj$
(v4)	$GluInj = Flux_{Glu} \cdot H(t)$
	with $H(t) = \begin{cases} 1, & 0 \leq t \leq 0.08, 2 \leq t \leq 2.08, 3 \leq t \leq 3.08, 4 \leq t \leq 4.08 \\ 0, & otherwise \end{cases}$
(v5)	$disP_{P,D} = d_{P,D} \cdot f(T) \cdot P$
(s2)	$\frac{dD}{dt} = disP_{P,D} + morB_{B,D} + disGlu_{Glu,D} - uptD_{D,B} - sorM_{D,M}$
(v6)	$morB_{B,D} = m_B \cdot f(T) \cdot B$
(v7)	$disGlu_{Glu,D} = \varepsilon_{Glu} \cdot (1 - K_{Glu}) \cdot GluInj$
(v8)	$uptD_{D,B} = r_{D,B} \cdot f(T) \cdot D$
(v9)	$sorM_{D,M} = f(T) \cdot \varepsilon_M^{-1} \cdot (\rho_{Me} \cdot PB_{Me} \cdot Me + \rho_{Ma} \cdot PB_{Ma} \cdot Ma)$
(s3)	$\frac{dB}{dt} = \varepsilon_B \cdot uptD_{D,B} - morB_{B,D} - graM_{B,M}$

$$\begin{aligned}
 \text{(v10)} \quad & \text{gra}M_{B,M} = f(T) \cdot \varepsilon_M^{-1} \cdot (\beta_{Me} \cdot PB_{Me} \cdot Me + \beta_{Ma} \cdot PB_{Ma} \cdot Ma) \\
 \text{(s4)} \quad & \frac{dP_{13C}}{dt} = \text{ads}Glu_{Glu,P} - (\text{dis}P_{P,D} + \text{exc}P) \cdot F_P \\
 \text{(v11)} \quad & \text{exc}X = \lambda_X \cdot X \text{ with } \lambda_X \text{ for } \lambda_P \text{ and } \lambda_D, \text{ and } X \text{ for } P, D, \text{ and } B \\
 \text{(s5)} \quad & \frac{dD_{13C}}{dt} = \text{dis}Glu_{Glu,D} + \text{dis}P_{P,D} \cdot F_P + \text{mor}B_{B,D} \cdot F_B \\
 & - (\text{upt}D_{D,B} + \text{sor}M_{D,M} + \text{exc}D) \cdot F_D \\
 \text{(s6)} \quad & \frac{dB_{13C}}{dt} = \varepsilon_B \cdot \text{upt}D_{D,B} \cdot F_D - (\text{mor}B_{B,D} + \text{gra}M_{B,M} + \text{exc}B) \cdot F_B \\
 \text{(s7)} \quad & \frac{dM_{xE_{13C}}}{dt} = \text{gra}M_{x_{B,Mx}} \cdot F_B + \text{sor}M_{x_{D,Mx}} \cdot F_D - \varepsilon_M^{-1} \cdot \text{pro}M_x \cdot F_{M_{xE}} \\
 \text{(v12)} \quad & \text{pro}M_x = f(T) \cdot PB_{Mx} \cdot M_x \\
 \text{(s8)} \quad & \frac{dM_{xS_{13C}}}{dt} = (1 - \alpha) \cdot \text{pro}M_x \cdot (F_{M_{xE}} - F_{M_{xS}}) \\
 \text{(v13)} \quad & M_{x13C} = M_{xE_{13C}} + M_{xS_{13C}} \\
 \text{(s9)} \quad & \frac{dDIC_{13C}}{dt} = (1 - \varepsilon_B) \cdot \text{upt}D_{D,B} \cdot F_D + \left(\frac{1 - \varepsilon_M}{\varepsilon_M} \right) \cdot \text{pro}M_x \cdot F_{M_{xE}} \\
 \text{(v14)} \quad & \text{Org} = P + D + B + Me + Ma \\
 \text{(v15)} \quad & \text{Org}_{13C} = P_{13C} + D_{13C} + B_{13C} + Me_{13C} + Ma_{13C}
 \end{aligned}$$

4.2.4 Calibration and uncertainty analysis

Initial ranges of parameter values were taken from the literature (Table 4.4). The optimal parameter set was subsequently selected from these ranges by minimization of a weighted cost function

$$J = \sum_{i=1}^{NVar} \sum_{j=1}^{NObs} \frac{(M_{ij} - O_{ij})^2}{\sigma_i} \quad (4.1)$$

in which all (*NObs*) model (M_{ij}) versus observation (O_{ij}) deviations are squared and weighed by the standard deviation σ_i for all variables (*NVar*). The σ_i is the average standard deviation for each variable. The parameter set which had the lowest cost function produces the best fit to the data.

Pools of bacterial carbon and POC show significant variation over the season and when the model is fitted to these data, this variation dominates the cost function. The first order model described here is suitable to track exponential-like tracer kinetics, but is inappropriate to model short-term temporal and spatial variation. To alleviate the impact of varying bacterial and POC pools on the cost function, the season-averaged pool size and standard deviation have been evaluated in the cost function instead of the original data (see also 4.4 Discussion). This ensures a correct order of magnitude pool size, but moderates the impact on the cost function. A pseudo-random calibration method (25000 runs and population size 500) was chosen because of its ability to locate the global minimum in a large parameter space (Price, 1979). The calibration ended with 250 runs of the Levenberg-Marquardt gradient method (Press et al., 1992), because of its ability to quickly converge to the minimum, once in a valley.

Parameter uncertainty, induced by fitting a model to uncertain data, was estimated by Bayesian inference (Gelman et al., 2003), using a Markov Chain Monte Carlo technique (Gilks et al., 1998). The Markov chain was initiated with the best-fit solution resulting from the calibration; it was terminated when 2000 draws were selected. The mean and standard deviation of the model parameters were then calculated from the selected draws.

Table 4.4: The initial ranges of the model parameters taken from the literature sources 1) Widdows et al. (2004), 2) review in Van Oevelen et al. (Chapter 3), 3) Henrichs and Sugai (1993), 4) Westrich and Berner (1984), 5) Henrichs and Doyle (1986), 6) Dauwe et al. (2001), 7) Widdows et al. (2000), 8) Martin and Banta (1992), 9) Schluter et al. (2000), 10) Meile et al. (2001), 11) Arnosti and Holmer (1999), 12) del Giorgio and Cole (1998), 13) Anderson and Williams (1999), 14) Fischer et al. (2003), 15) Mei and Danovaro (2004) and 16) Van Oevelen et al. (Chapter 5). Bayesian analysis (see 4.2 Material and methods) produces a set of accepted parameter values, which are presented as mean \pm standard deviation. Parameters with no initial range were fixed in the simulations.

Symbol	Initial range	Value	Source
F_{Glu}		183	
Q_{10}		2	
ε_{Glu}		0.74	^a
F_{POC}		52	1
ε_M		0.50	2
Me		188	sampled
Ma		1624	sampled
K_{Glu}	0.29-0.39	0.34 ± 0.025	3
$d_{P,D}$	0.0005-0.003	0.0024 ± 0.00024	4,5,6
λ_P	0.0-0.093	0.0085 ± 0.0024	7
λ_D	0.05-1.00	0.58 ± 0.14	8,9,10
$r_{D,B}$	0.08-2.67	0.46 ± 0.12	11
ε_B	0.40-0.75	0.50 ± 0.03	12
m_B	0.0-0.14	0.07 ± 0.02	13,14,15
α	0.0-0.50	0.31 ± 0.11	assumed
PB_{Me}	0.03-0.09	0.065 ± 0.014	2
β_{Me}	0.05-0.15	0.097 ± 0.024	16
ρ_{Me}	0.0-0.15	0.036 ± 0.012	assumed
PB_{Ma}	0.01-0.05	0.028 ± 0.009	2
β_{Ma}	0.08-0.30	0.20 ± 0.05	16
ρ_{Ma}	0.0-0.15	0.094 ± 0.032	assumed

^a defined as the amount of label recoverable after the first 4 hours

4.3 Results

4.3.1 Organic carbon pools

Sediment POC content averaged 0.48 % wt/wt and porosity was 0.50, corresponding to a POC pool of $46.6 \text{ mol C m}^{-2}$ in the upper 10 cm of the sediment. The benthic community was dominated by macrobenthos ($1624 \text{ mmol C m}^{-2}$), followed by bacteria ($781 \text{ mmol C m}^{-2}$) and meiobenthos ($188 \text{ mmol C m}^{-2}$) (Table 4.5). Meiobenthic biomass was dominated by nematodes and foraminifera. Macrobenthic was dominated by large specimens of the bivalve *Macoma balthica* and the polychaetes, *Heteromastus filiformis* and *Pygospio elegans*.

Table 4.5: Biomass of bacteria, meiobenthos and macrobenthos (mmol C m^{-2}).

Compartment	Biomass
Bacteria	781
Meiobenthos	188
Nematodes	67
Hard-shelled foraminifera	62
Juveniles <i>Heteromastus filiformis</i>	34
Unknown	9
Soft-bodied foraminifera	6
Turbellaria	4
Polychaetes	4
Copepods	3
Macrobenthos	1624
<i>Macoma balthica</i> (> 7 mm)	671
<i>Heteromastus filiformis</i>	597
<i>Pygospio elegans</i>	215
<i>Polydora cornuta</i>	34
<i>Macoma balthica</i> (\leq 7 mm)	28
<i>Hydrobia ulvae</i>	24
<i>Nereis (Hediste)</i> spp.	21
<i>Eteone</i> sp.	16
<i>Corophium</i> spp.	16
<i>Streblospio benedicti</i>	1

4.3.2 Labeling trajectories and model fits

Excess ^{13}C in the total organic carbon pool, comprising excess ^{13}C in DOC, POC and benthos, increased steadily during the labeling period (except for the dip at day 2 caused by the canceled injection) and peaked at $26.5 \text{ mmol } ^{13}\text{C m}^{-2}$ on day 5 at the end of the labeling period (Fig. 4.2A). At day 5, about 50 % of the total injected $61.1 \text{ mmol } ^{13}\text{C m}^{-2}$ was recovered as excess organic (44 %) and respired (8 %) carbon. The initial ^{13}C -POC decrease was high, but slowed after day 20, reflecting turnover differences of the organic carbon pools. After 4.5 months, almost no excess ^{13}C was detected in the organic carbon pool. Bacterial label incorporation was linear over the first 8 days and reached a maximum of $5.1 \text{ mmol } ^{13}\text{C m}^{-2}$ corresponding to $0.62 \text{ mmol } ^{13}\text{C m}^{-2} \text{ d}^{-1}$, after which it decreased in an exponential fashion (Fig. 4.2B). Meiobenthic label incorporation was swift and peaked around day 10 at $0.07 \text{ mmol } ^{13}\text{C m}^{-2}$ (Fig. 4.2C), representing 0.02 % of the label in the organic carbon pool. The excess ^{13}C in meiobenthos decreased exponentially and returned to background levels at the end of the experiment. Macrobenthic labeling was rapid within the first 10 days and reached $0.78 \text{ mmol } ^{13}\text{C m}^{-2}$ at day 5. The labeling variability was mainly caused by variable labeling of the biomass dominating large *M. balthica* (species data not shown). Label decreased exponentially with time and after 4.5 months, $0.1 \text{ mmol } ^{13}\text{C m}^{-2}$ resided in macrobenthos (Fig. 4.2D). The injected ^{13}C -glucose was rapidly respired to ^{13}C -DIC, as evidenced by the $0.46 \text{ mmol } ^{13}\text{C m}^{-2}$ respiration in the first 6 hours of the experiment (Fig. 4.2E). The respiration rate of ^{13}C label was highest during the injection period, in which $4.7 \text{ mmol } ^{13}\text{C m}^{-2}$ was respired. The respiration rate slowed down after the ^{13}C -glucose injection and decreased further after day 36, when a

total of 7 mmol $^{13}\text{C m}^{-2}$ had been respired. In the whole experimental period a total of 8.9 mmol $^{13}\text{C m}^{-2}$ was respired, which corresponds to 15 % of the total ^{13}C addition.

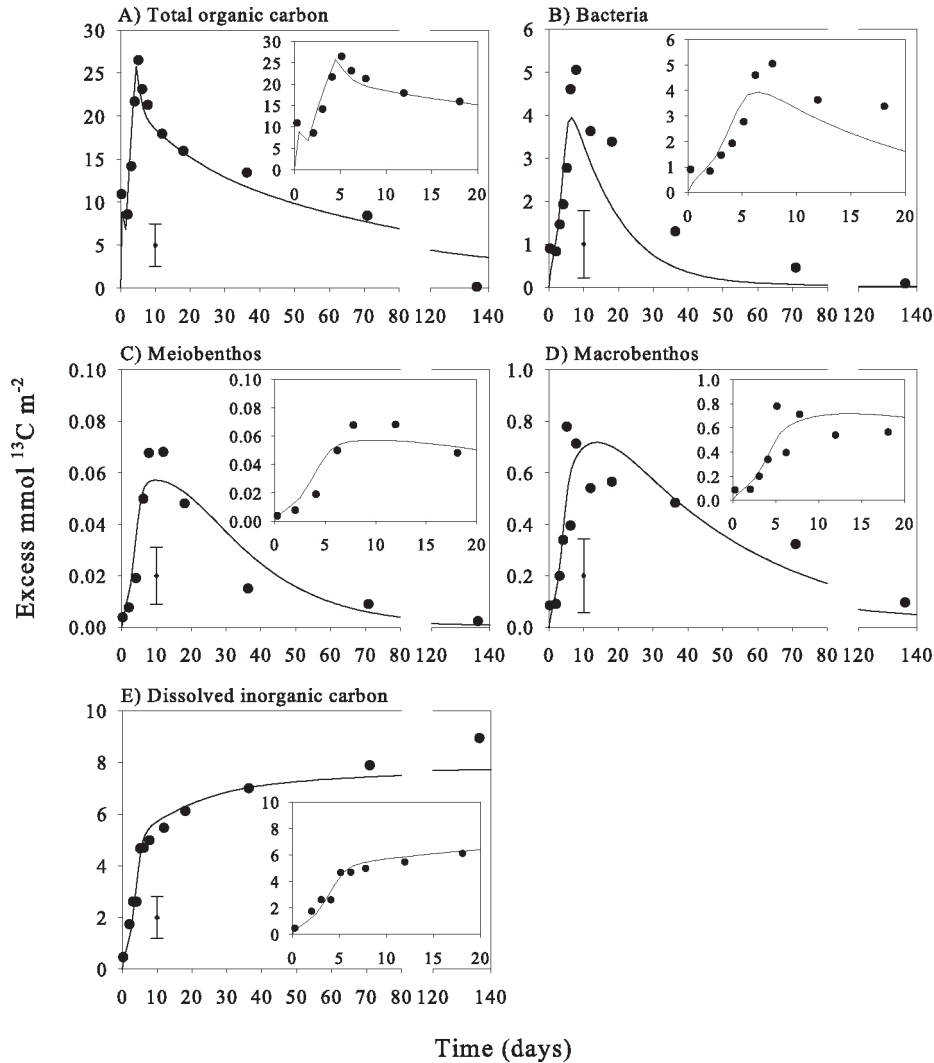


Figure 4.2: Excess ^{13}C in the compartments total organic carbon, bacteria, meiobenthos, macrobenthos and dissolved inorganic carbon with model-derived lines. Plotted data are averages from the two plots and error bars in the plot are the average standard deviations used in the calibration routine (see 4.2 Material and methods). Note the scale break in the time axis. The insets detail the temporal evolution in the first 20 days.

The ^{13}C dynamics of the organic carbon pool were accurately reproduced by the model in the first two months, but excess ^{13}C is overestimated by the model at day 136 (Fig. 4.2A). Modeled bacterial label incorporation tracks the observations during the first 6 days of the experiment, but the observations show a continued incorporation until day 8, which is not well reproduced by the model (Fig. 4.2B). This initial underestimation of label incorporation has repercussions for the prediction during the remainder of the

experiment. The rate at which label disappears from the bacterial compartment also seems higher than observed in the field. Bacterial secondary production averaged $66.5 \text{ mmol C m}^{-2} \text{ d}^{-1}$ and bacterial growth efficiency (BGE) was estimated at 0.50 ± 0.03 (Table 4.4). The label trajectories of meiobenthos and macrobenthos are accurately described, as the magnitude of labeling and their dynamics correspond well to the field observations (Fig. 4.2C and 4.2D). Secondary production by meiobenthos and macrobenthos averaged $11.5 \text{ mmol C m}^{-2} \text{ d}^{-1}$ and $42.5 \text{ mmol C m}^{-2} \text{ d}^{-1}$, respectively. Respiration of ^{13}C label is very well described during the first 3 months, but the model underestimates the respiration slightly thereafter (Fig. 4.2E). Overall, a plot of model predictions versus field observations reveals a highly significant linear relation that covers data over 4 orders of magnitude, with a slope not significantly different from 1 (Fig. 4.3).

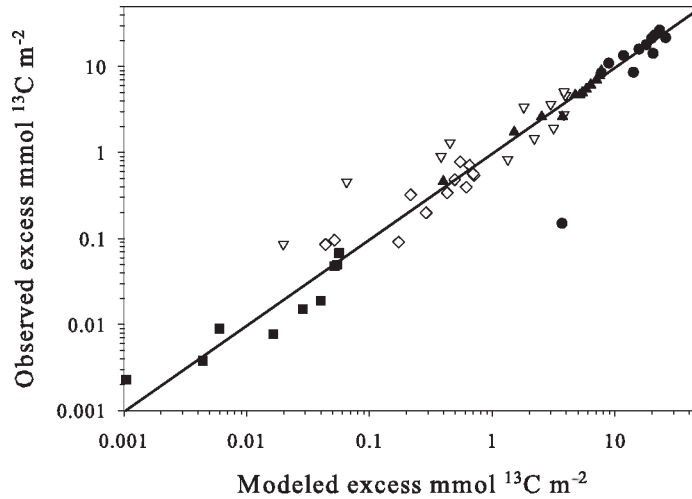


Figure 4.3: Observed versus modeled values of excess $\text{mmol } ^{13}\text{C m}^{-2}$ in the various model compartments. The line represents the linear regression of all data points ($y = 0.97x, r^2 = 0.95, p < 0.0001, n = 58$).

Some model parameters are more constrained by the observations than others (Table 4.4). The standard deviation relative to the mean is $\leq 10 \%$ for the parameters bacterial growth efficiency (ε_B), glucose adsorption (K_{Glu}) and POC dissolution rate ($d_{P,D}$) and between 24 - 37 % for the other parameters, which is similar to the relative error of the observations. Although many parameters have a high relative standard deviation, they are well constrained with regard to their initial range. The parameters POC dissolution rate ($d_{P,D}$), POC exchange rate (λ_P), bacterial DOC uptake rate ($r_{D,B}$), bacterial mortality (m_B), fraction DOC in meiobenthic diet (ρ_{Me}) and macrobenthos production rate (PB_{Ma}) are well constrained as compared to their initial range. However, for the parameters α (metabolic fraction of benthos), β_{Me} (bacterial fraction in meiobenthic diet), PB_{Me} (production rate meiobenthos), ρ_{Ma} (DOC fraction in macrobenthos diet) and K_{Glu} (glucose adsorption constant) the standard deviation is still high as compared to the initial range and these parameters are less constrained by the observations.

4.4 Discussion

This is the first in situ study on the short and long-term fate of benthic bacterial carbon production (BP). Tracking BP was achieved by injecting ^{13}C -glucose into the sediment as a stable isotope tracer and subsequently following this tracer in bacteria, meiobenthos, macrobenthos, total organic carbon and inorganic carbon. Labeling was conducted on several consecutive days to follow uptake kinetics and to ensure sufficient labeling of the bacteria. Subsequently, label appearance and retention was monitored over a period of 4.5 months to provide information on transfer among and turnover of the different compartments. We interpret this extensive data set by means of a mechanistic model that resolves most bacterial gain and loss processes. A mechanistic model requires an explicit description of its structure, underlying assumptions and contains interpretable parameters. Simpler models can be used, but these only use a subset of the available data. For example, label disappearance can be fitted with an exponential decay model to obtain the compartments turnover rate. In this simpler analysis however, data on uptake kinetics are ignored, rate constants represent net turnover as uptake of label continues after label injection, and the model fit is not constrained by any of the other observations. Moreover, the use of a mechanistic model allows us to derive information on unmeasured processes. For instance, bacterial mortality was not measured explicitly, but was derived from the model.

Inherent in benthic microbial ecology are methodological shortcomings and our experimental approach is no exception. These are partly caused by our intention to conduct this experiment over a long time scale in situ, which precludes core incubations. Label was introduced to the sediment in injection wells at a high resolution, but heterogeneous label distribution is inevitable. However, injection is the preferred method to introduce label, while minimizing sediment disturbance (Dobbs et al., 1989). Label uptake by non-grazing processes has been reported by Carman (1990) and therefore poisoned controls have been recommended to distinguish among the uptake pathways (Montagna, 1995), but such controls are not possible on the scale of this experiment. However, turnover time of glucose (\sim hours) is much shorter than that of bacteria (\sim weeks), which allows to distinguish direct uptake of glucose from bacterial grazing at the time scale of the experiment. Another concern was the potential use of respired ^{13}C by microphytobenthos. Fixation of ^{13}C -DIC enriches microphytobenthos into an alternative ^{13}C resource, thus complicating the interpretation of carbon transfer from bacteria to meiobenthos and macrobenthos. Microphytobenthos labeling was assessed through the PLFA biomarkers C20:5 ω 3 (Middelburg et al., 2000), which increased in $\delta^{13}\text{C}$ from -22.8 to 19.8 ‰ (day 8) and remained above 5.0 ‰ till day 23. This labeling is lower than the $\delta^{13}\text{C}$ of most grazers (Van Oevelen et al., (Chapter 5)) and much lower than the $\delta^{13}\text{C}$ of bacterial biomarkers (between 100 - 500 ‰ during the first month). Hence, recycling of ^{13}C via microphytobenthos does not seriously complicate the interpretation. Finally, glucose addition was truly at tracer level, as the rate of label incorporation ($0.62 \text{ mmol } ^{13}\text{C m}^{-2} \text{ d}^{-1}$) represented 0.9 % of total bacterial production ($66.5 \text{ mmol C m}^{-2} \text{ d}^{-1}$).

4.4.1 Model complexity and performance

Model complexity was a compromise between biological realism and data availability. The 0-D representation was one way to minimize model complexity. Among the depth intervals there were minor and quasi-random differences in bacterial and organic carbon $\delta^{13}\text{C}$. Therefore, the information gain in a 1-D representation would not outweigh the

necessary additional model parameters. Moreover, a 1-D model description in terms of biomass, feeding and mixing of meiobenthos and macrobenthos is not straightforward.

Sediment organic carbon is characterized by large differences in reactivity (Westrich and Berner, 1984; Middelburg, 1989). Two pools with different lability were distinguished: labile DOC and less reactive POC. This distinction is required as glucose is very labile compared to bulk sediment organic carbon. The fitted rate constant for the DOC pool (0.46 d^{-1} , Table 4.4) is somewhere between the high rate constant of injected glucose and lower rate of DOC that is derived from bacteria or POC. However, data on ^{13}C were only available for total organic carbon and more complexity than two organic carbon pools could therefore not be justified.

Bacterial biomass varied considerably and was generally between $500 - 1300 \text{ mmol C m}^{-2}$. The bacterial biomass in the model was fitted to a constant overall average ($781 \text{ mmol C m}^{-2}$) and the model output therefore showed little variation ($600 - 800 \text{ mmol C m}^{-2}$). There were several reasons for this approach. There was hourly/daily variation and a more seasonal-like trend on the scale of weeks/months. Short-term variation of a factor 2-3 is inherent in many bacterial biomass estimates and likely contains an important spatial component. This variation cannot be reproduced using the first-order 0-D model that is designed to reproduce excess ^{13}C patterns. The long-term variation shows a general increase in biomass during the first 2-3 weeks of the experiment and then a decrease. Temperature dependence alone cannot explain the biomass evolution because temperature increased during the initial 3 months. We ran simulations with higher bacterial carbon ($1000 \text{ mmol C m}^{-2}$) than the season-average, which clearly improved the fit of excess ^{13}C in bacteria, but did not change the general conclusions as presented here. Therefore it is likely that the model fit of the excess bacterial ^{13}C would improve, if the bacterial biomass evolution were better reproduced.

The faunal biomass was modeled as two compartments: a metabolic and a structural compartment (s7 and s8 in Table 4.3). Turnover is faster in the metabolic pool as this pool fuels respiration. This formulation was chosen for its higher realism (Conover, 1961), success in earlier applications (Lehman et al., 2001; Pace et al., 2004), better resemblance to the dynamic energy budget theory (Kooijman, 2000) and improved capability of reproducing the observations.

Finally, it should be stressed that different data weighting schemes and model scenarios were thoroughly tested to assess the robustness of the model results. Model scenarios with no DOC sorption by the benthos typically show a lag in labeling, delayed peak labeling and higher loss rate as compared to the observations. In general, the model results are robust and accurately describe the general trends in the labeling patterns.

4.4.2 Bacterial growth efficiency and production

The bacterial dominance of benthic secondary production has been reported earlier (e.g. Schwinghamer et al. (1986)) and is confirmed in this study with bacteria accounting for 55 % of the secondary production. The parameter BGE was calibrated at 0.50, but as the calibration is based on the respiration of relatively labile compounds (^{13}C -glucose and bacterially derived DOC), the derived BGE is likely an overestimate of the overall BGE.

The regression models presented by Sander and Kalff (1993) predict bacterial production ($66.5 \text{ mmol C m}^{-2} \text{ d}^{-1}$) reasonably when based on bacterial carbon ($91 \text{ mmol C m}^{-2} \text{ d}^{-1}$) or POC ($42 \text{ mmol C m}^{-2} \text{ d}^{-1}$), but their temperature model ($15 \text{ mmol C m}^{-2} \text{ d}^{-1}$) underestimates our bacterial production.

Boudreau (1999) presented detailed mass balances of bacterial carbon in sediments

and scaled the mass balance terms to arrive at a linear relation between bacteria and POC. The parameters of this linear relation are composed of parameters for irrigation, advection, bacterial production, mortality, grazing and bacterial growth efficiency. When the parameters obtained in our study are implemented in Boudreau's scaled linear model, the predicted ratio between bacterial biomass and POC is 0.005, consistent with, but at the lower end of the observed ratios, ranging from 0.005 to 0.024. The predicted bacterial biomass to POC ratio is based on interpretative and measurable parameters, rather than regression parameters. The general agreement is certainly encouraging, but additional data sets are required to test the general predictive power.

4.4.3 Label pathways

The use of a mechanistic model not only allow to reproduce the observations and derive useful model parameters, but also provided detailed information on the relative contributions of the different ^{13}C pathways (Fig. 4.4). The importance of the ^{13}C loss pathways from the sediment changed considerably with time. Initially, label loss occurs mainly through exchange of DOC (75 %) and respiration (20 %) but after a few days POC resuspension dominates (Fig. 4.4A). Meiobenthos and macrobenthos turnover account for maximal 10 % of the label loss. The importance of the pathways differed with time, indicating that extrapolation from short-term experiments should be done with caution. The fate of bacterial carbon production was rather invariant during the experiment and was partitioned among resuspension (8 %), meiobenthos grazing (3 %), macrobenthos grazing (24 %) and mortality (65 %) (Fig. 4.4B). The label sources for macrobenthos (very similar for meiobenthos) reflect the different turnover rates of DOC and bacteria. During the first 5 day period of label addition, 75 % of label incorporation was related to sorption of DOC, but within 2 days of ending the label injections bacterivory dominated label incorporation (90 %) and remained high thereafter (Fig. 4.4C).

4.4.4 Fate of bacterial carbon production

The microbial loop has been formalized as bacterial assimilation of dissolved organic matter and subsequent transfer up the food web by bacterivory and predation on bacterivores (Azam et al., 1983). The significance and efficiency of this loop has focussed on a link or sink debate: is bacterial production a carbon link or sink in the food web? The intractable benthic environment has made experimental studies difficult and studies therefore have tended to focus on a subset of potential grazers, such as heterotrophic flagellates (Hondeveld et al., 1995; Hamels et al., 2001b), meiobenthos (Montagna, 1995) or macrobenthos species (Kemp, 1987; Grossmann and Reichardt, 1991). These studies dealing with a subset of the grazers revealed that 1 - 20 % of the bacterial production is grazed. For the present study site, bacterial grazing by the total benthic community in the top 10 cm of the sediment was quantified. We estimate that ~ 30 % of the bacterial production was grazed: 1 - 2 % by microbenthos ($1.1 \text{ mmol C m}^{-2} \text{ d}^{-1}$ from Hamels et al. (1998)), 3 % by meiobenthos (this study) and 24 % by macrobenthos (this study). As meiobenthos and macrobenthos biomass at our study sites are high as compared to other sediments (Heip et al., 1995), we assert that bacterivory is comparatively intense. Given the accumulated evidence, grazing can be regarded as a minor to moderate fate of bacterial production in sediments.

Our combined experimental and modeling approach allowed us to distinguish among the bacterial loss pathways grazing, resuspension and mortality. Bacterial mortality

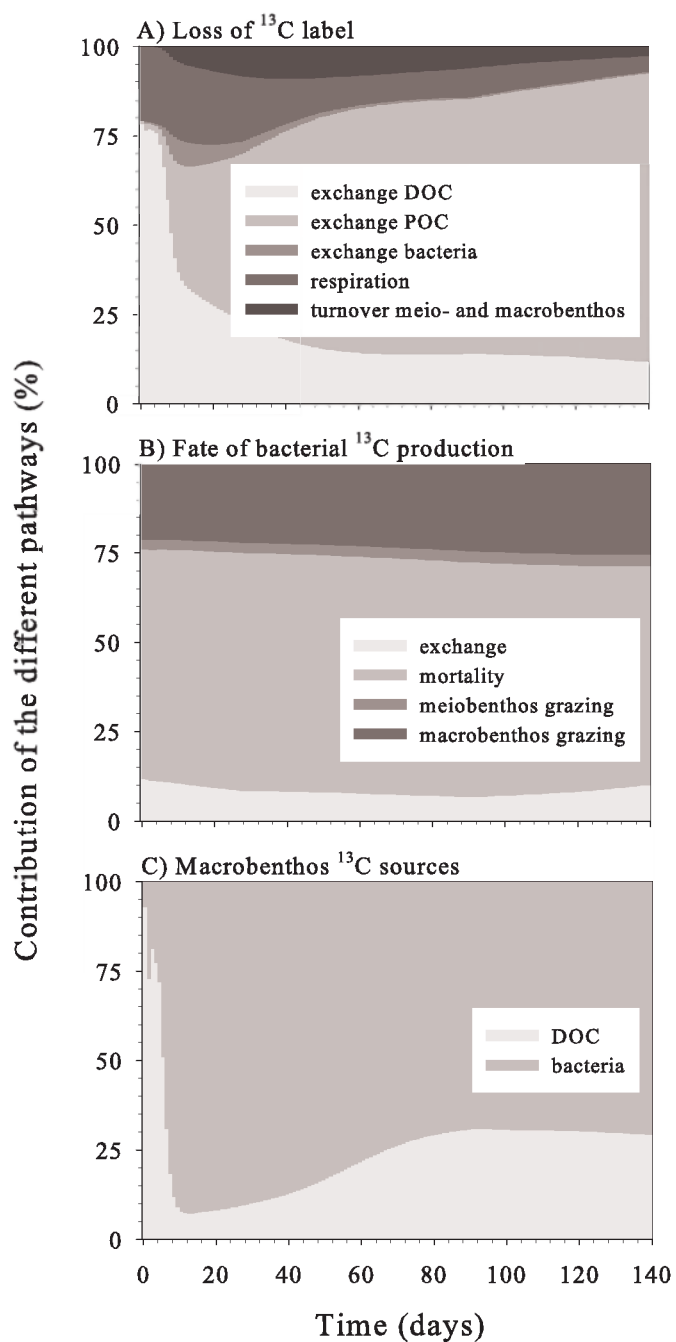


Figure 4.4: Percentage contribution of excess ^{13}C pathways in the A) loss of ^{13}C from the sediment, B) fate of bacterial ^{13}C production and C) macrobenthos ^{13}C sources.

appeared to dominate and represented a sink of 65 % of the bacterial production. However, the cause of bacterial mortality remains unexplained. Several mortality causes are known. Bacterial cell lysis resulting from a lytic infection by viruses is a major cause of bacterial

mortality in pelagic systems (Weinbauer, 2004), and was thought to be similarly important in sediments, because of higher viral and bacterial abundances (Paul et al., 1993; Maranger and Bird, 1996; Mei and Danovaro, 2004). Recent estimates on the contribution of viral lysis to bacterial mortality show a large range of 0 - 40 % (Ricciardi-Rigault et al., 2000; Hewson and Fuhrman, 2003; Glud and Middelboe, 2004). Therefore, viral lysis may be an important cause of bacterial mortality but large differences in reported contributions do not warrant generalization of the importance of this process. Programmed cell death, mortality caused by triggering an intracellular genetic code, has been found in bacterial cultures (Yarmolinsky, 1995; Engelberg-Kulka and Glaser, 1999), but remains to be quantified for natural bacterial populations. Similarly, environmental factors such as the presence of toxic compounds and thermal or salinity stress may cause mortality, but their quantitative importance remains unknown. Several factors causing bacterial mortality, other than grazing, are not yet or only recently being explored and their importance remains to be established. Irrespective of the cause of death, non-grazing mortality results in the release of bacterially derived carbon that is potentially available for recycling back to DOC.

Recycling in the DOC - bacteria loop was evaluated by a recycling efficiency, defined as $E = \frac{\text{Bacterial death}}{\text{Bacterial DOC uptake}}$ and the average number of cycles in the loop of a carbon molecule as $R = \frac{\text{Bacterial death}}{\text{POC dissolution} + \text{DOC exchange}}$, both based on season-averaged flow values. The recycling efficiency may vary between 0 (no recycling) and 1 (full recycling) and R between 0 (molecule cycles zero times) and ∞ (molecule cycles infinitely). The recycling efficiency for the DOC - bacterial loop was moderate (0.36). Note that respiration losses cap E to a maximum of 0.50 (i.e. $\varepsilon_B = 0.50$, Table 4.4), which implies that 72 % (i.e. $0.36/0.50$) of the bacterial production is recycled back to the DOC pool. Despite moderate recycling, R was comparatively low (0.17) due to the high exchange rate of DOC that dominates over the flux from bacteria to DOC. Recycling of bacterially derived carbon is consistent with observations that bacterial lysate is readily degraded by natural communities (Novitsky, 1986; Middelboe et al., 2003). However, several studies document the accumulation of the bacterial cell wall derived D-Alanine in oceans (McCarthy et al., 1998) and continental margin sediments (Grutters et al., 2002). In a companion paper (Veuger et al. (Chapter 6)), the ^{13}C in D-Alanine is compared with that in labile PLFAs and the results suggest that burial of bacterial remnants is not a major sink for bacterial carbon, but instead is recycled back to the DOC pool.

Alongi (1994) speculated on the role of bacterial cycling in tropical benthic systems and asserted that the majority of bacterial production remains ungrazed but instead lyses and the lysate is recycled within the bacterial community. Such a bacterial-viral loop was recently also proposed for pelagic food webs (Fuhrman, 2000). Our comprehensive study on the fate of benthic bacterial carbon production agrees with this concept, although the cause of death may not necessarily be viral lysis. The observed recycling is also consistent with the well documented efficient recycling of ammonium in sediments with net rates of regeneration being a fraction of gross ammonification (Blackburn and Henriksen, 1983).

Finally, the advent of diagenetic models that explicitly include bacterial biomass (Talin et al., 2003) requires an appropriate parametrization of benthic bacterial dynamics. The correspondence between the mass balance model developed by Boudreau (1999) and our results suggests a promising avenue for further exploration.

Chapter 5

The trophic significance of bacterial carbon in a marine intertidal sediment: Results of an in situ stable isotope labeling study

Dick van Oevelen, Leon Moodley, Karline Soetaert and Jack J. Middelburg. *In revision for Limnology and Oceanography*

5.1 Introduction

Deposit feeding organisms face the formidable task of gathering digestible resources that are diluted with minerals and refractory organic matter (Lopez and Levinton, 1987). Bacteria are ubiquitous in marine sediments and because of their high abundance, production and nutritional value they are considered an important resource for sediment dwelling fauna (ZoBell and Feltham, 1937; Gerlach, 1978; Tsuchiya and Kurihara, 1979).

Transfer of bacterial carbon to benthos is often discussed from the bacterial side: is bacterial carbon production a link or sink in the benthic food web (Kemp, 1990)? This bias in favor of the fate of bacterial carbon is also reflected in the methods in use: incubations with ^{14}C organic substrates (Montagna, 1995) or fluorescently labeled bacteria (Starink et al., 1994) measure the amount of bacterial carbon that is grazed per unit of time. These studies show that grazing losses are generally restricted to < 20 % of total bacterial production (Epstein and Shiaris, 1992; Hondeveld et al., 1995; Sundback et al., 1996; Hamels et al., 2001b).

Although bacterial grazing represents a minor fate of bacterial production, one may pose the complementary question whether bacterially derived carbon fulfills a significant part of the total carbon requirements of benthic fauna. However, estimates for the relative importance of bacterial carbon for meiobenthos are scant or are based on qualitative gut content analysis (e.g. for nematodes, Moens and Vincx (1997)). Quantitative data are available for some macrobenthic deposit feeders, based on laboratory measurements of

sediment ingestion rate, bacterial abundance and bacterial digestion efficiency on the one and physiological data on carbon requirements on the other hand (Cammen, 1980; Kemp, 1987; Andresen and Kristensen, 2002). Most of these studies show that bacterial carbon contributes < 10 % of the total requirements. However, deposit feeders are known for their selective uptake of high quality and organic rich particles (Lopez and Levinton, 1987; Neira and Höpner, 1993), which may contain elevated levels of bacteria and therefore the bacterial contribution in their diets may have been underestimated. For example, Hall and Meyer (1998) showed with an in situ ^{13}C -acetate tracer experiment that many stream invertebrates derived more than 50 % of their carbon from bacteria, which is much more than previously anticipated (Baker and Bradnam, 1976). Moreover, the contribution of bacterially derived carbon may differ among the different taxa, for example subsurface deposit feeders that ingest relatively refractory organic matter may be more dependant on bacteria for labile carbon and essential nutrients. Therefore, quantitative data on the bacteria - benthos links are essential for understanding the extent to which this trophic link may structure sediment communities.

In situ stable isotope labeling experiments have proven to be an excellent tool to study element transfer (Blair et al., 1996; Hall and Meyer, 1998; Middelburg et al., 2000). Here we employ stable isotope labeling in a marine intertidal sediment to estimate the amount of carbon that meiobenthic taxa and macrobenthic species derive from bacteria. ^{13}C -glucose was injected into the sediment to tag the bacterial community, incorporation of ^{13}C -glucose by bacteria was traced through ^{13}C enrichment of bacterial specific phospholipids derived fatty acids (PLFAs). Subsequent transfer of bacterial-derived ^{13}C to benthic fauna was followed through ^{13}C enrichment of hand-picked specimens. A simple isotope model was used to recover the dependency on bacterial carbon from the observed tracer dynamics. Specifically, we will focus on the following questions: (1) How much does bacterial carbon contribute to the carbon requirements of meiobenthic and macrobenthic species? (2) Is the contribution of bacteria derived carbon related to feeding/living depth in the sediment? (3) Are there indications for selective feeding by the benthic fauna?

5.2 Materials and methods

5.2.1 Study site and experimental approach

The Molenplaat intertidal flat was chosen as study site and is located in the saline part (salinity 20-25) of the turbid, heterotrophic and nutrient-rich Scheldt estuary. The sampling site is located in the silty center of the flat (51°26.25' N, 3°57.11' E), which has a median grain size of 77 μm , organic carbon content of ~ 0.5 % wt/wt and exposure time of about 7 hours per tidal cycle (see Herman et al. (2001) for detailed information).

The data presented here have been collected in the frame of an experiment on the fate of bacterial carbon production and two companion papers deal with the fate of bacterial carbon production (Chapter 4) and the fate of bacterial phospholipids, peptidoglycan and proteins (Chapter 6). Methodological details are provided in chapter 4. In short, two 0.25 m^2 square metal frames were inserted in the sediment. On 21 May 2003, the upper 10 cm was labeled with ^{13}C by injecting a glucose solution with a syringe (one injection per 6.25 cm^2), resulting in a flux of 15.3 $\text{mmol } ^{13}\text{C m}^{-2}$ per labeling day. Labeling was performed daily for 5 consecutive days to ensure sufficient label incorporation by bacteria, but labeling on day 2 had to be canceled due to bad weather. Ten samples (day 0.3, 2, 3, 4, 5, 6, 8, 12, 18 and 36 after the first injection) were collected from each plot in the first weeks from a priori randomly assigned positions. A sampling core (\varnothing 5 cm) was

inserted 10 cm deep, filled with filtered sea water and closed with a stopper. A metal core (\varnothing 9 cm) was inserted around the sampling core, which successfully prevented disturbance of the rest of the plot and remained in place during the experiment. The sampling core was carefully withdrawn and transported in a dark cool container to the laboratory. In the laboratory, sediment cores were sliced (0-2, 2-5 and 5-10 cm), homogenized and sampled for $\delta^{13}\text{C}$ -PLFA, meiobenthic biomass and label incorporation and macrobenthos label incorporation. Samples for $\delta^{13}\text{C}$ -PLFA were frozen, freeze-dried and stored frozen. Meiobenthic and macrobenthic samples were fixed with formalin (final concentration 4 %). Background $\delta^{13}\text{C}$ for PLFA, meiobenthos and macrobenthos were taken from the $t = 0$ sampling core. Some macrobenthos species were not present in the $t = 0$ samples, in which case background $\delta^{13}\text{C}$ was taken from Herman et al. (2000). Macrobenthic biomass could not be accurately determined from the small cores taken from the experimental plots and was therefore based on 12 separate cores (\varnothing 10 cm) taken in close proximity of the experimental plot.

5.2.2 Analytical procedures

Lipids were extracted from 3 g dry sediment using a Bligh and Dyer extraction, from which the PLFA fraction was isolated. The PLFA extract was derivatized to volatile fatty acid methyl esters and measured by gas chromatography-isotope ratio mass spectroscopy (GC-IRMS) for PLFA isotope values (details in Boschker et al. (1999)). The bacterial isotope signature was determined from the weighted average of the specific bacterial PLFA biomarkers i14:0, i15:0, a15:0, i16:0 and 18:1 ω 7c (Middelburg et al., 2000). PLFAs are present in the membrane and comprise roughly 6 % of the total carbon in a bacterial cell, the bacterial-specific PLFAs together account for 28 % of the carbon in all bacterial PLFAs (Middelburg et al., 2000). These conversion factors are used to convert PLFA concentration to bacterial biomass and label incorporation in PLFAs to total bacterial label incorporation (Middelburg et al., 2000).

Meiobenthic samples were sieved (38 μm) and sub-sampled. Specimens for stable isotope measurements, typically 15-30, were handpicked, cleaned of adhering detritus, rinsed (0.2 μm filtered water), transferred to silver boats and stored frozen. Processing meiobenthic samples proved to be very time consuming and only one of the two plots was therefore processed for stable isotope and biomass data, as described in Moodley et al. (2000).

Macrobenthic specimens were handpicked, stored in filtered water and preserved with formalin. The sorted sample was transferred to a petri-dish, a species sample was taken, cleaned from debris, rinsed, transferred to a silver boat and stored frozen. Bivalves and Gastropods were placed in an acidified bath (1 mmol HCl) to dissolve their carbonate shell and either whole specimens (*Macoma balthica* (< 7 mm) and *Hydrobia ulvae*) or flesh samples (*M. balthica* (\geq 7 mm)) were taken. Meiobenthic and macrobenthic samples were thawed, acidified for carbonate removal with 20 μl 2.5 % HCl and oven-dried (50 $^{\circ}\text{C}$) prior to isotope analysis. Stable isotope ratios were measured by elemental analyzer - isotope ratio mass spectrometry (EA-IRMS) (Middelburg et al., 2000).

Delta values are expressed relative to the carbon isotope ratio ($R: \frac{^{13}\text{C}}{^{12}\text{C}}$) of Vienna Pee Dee Belemnite (VPDB): $\delta^{13}\text{C} = \left(\frac{R_{\text{sample}}}{R_{\text{VPDB}}} - 1 \right) \cdot 1000$, with $R_{\text{VPDB}} = 0.0112372$. Label uptake by organisms is reflected as enrichment in ^{13}C and is presented as $\Delta\delta^{13}\text{C}$, which indicates the increase in $\delta^{13}\text{C}$ of the sample as compared to its natural background value and is calculated as: $\Delta\delta^{13}\text{C} = \delta^{13}\text{C}_{\text{sample}} - \delta^{13}\text{C}_{\text{background}}$. Hence, positive $\Delta\delta^{13}\text{C}$ values indicate that the organism has acquired some of the introduced ^{13}C label.

5.2.3 Tracer model and calibration

The relative contribution of bacteria derived carbon was estimated from comparing the $\Delta\delta^{13}\text{C}$ of a consumer ($\Delta\delta^{13}\text{C}_{con}$) with that of bacteria ($\Delta\delta^{13}\text{C}_{bac}$). If the $\Delta\delta^{13}\text{C}_{bac}$ and $\Delta\delta^{13}\text{C}_{con}$ have reached steady-state, the ratio indicates the fraction of total carbon in the consumer that is derived from bacteria. However, this steady-state assumption is not valid for all organisms within an experimental time frame of several weeks (Hall and Meyer, 1998) and an isotope model that simulates tracer dynamics in a consumer is then a better option (Hamilton et al., 2004). The isotope model can however, only be applied for frequently sampled species due to its higher data requirements. Therefore, dependence on bacterial carbon for species that were encountered repeatedly in the time series samples was estimated by means of the isotope model. For species that were only occasionally encountered, contribution of bacteria derived carbon was estimated from the ratio $\frac{\Delta\delta^{13}\text{C}_{con}}{\Delta\delta^{13}\text{C}_{bac}}$, because they were not sampled frequent enough to justify fitting the data with the isotope model. The isotope model reads (Hamilton et al., 2004)

$$\frac{d \Delta\delta^{13}\text{C}_{con}}{dt} = k_b \cdot \Delta\delta^{13}\text{C}_{bac} - k_c \cdot \Delta\delta^{13}\text{C}_{con} \quad (5.1)$$

The first term in the right hand side of the equation denotes label uptake by grazing on bacteria and the second label loss through turnover of the consumer. The dynamics of the PLFA bacterial biomarkers are used as a proxy for $\Delta\delta^{13}\text{C}_{bac}$ data and are imposed as a forcing function. The turnover rate constant (k_c) determines the total carbon requirements of the consumer and the ratio $\frac{k_b}{k_c}$ denotes the relative contribution of bacterial carbon to total carbon requirements. If bacteria fulfill all carbon requirements, i.e. $\frac{k_b}{k_c} = 1$, the $\Delta\delta^{13}\text{C}_{con}$ approaches the $\Delta\delta^{13}\text{C}_{bac}$ with time and when bacteria do not contribute (i.e. $\frac{k_b}{k_c} = 0$), there is no label uptake by the consumer (see Hamilton et al. (2004) for detailed model demonstrations).

Plausible parameter ranges were large to assure a complete coverage of potential growth rates and were $0.05 - 0.50 \text{ d}^{-1}$ (k_c) and $0.0 - 0.50$ (k_b) for meiobenthos and $0.025 - 0.25$ (k_c) and $0.0 - 0.25 \text{ d}^{-1}$ (k_b) for macrobenthos. The parameters were calibrated by minimizing the sum of squared differences between the data points and the model prediction.

It proved impossible to calibrate the model parameters k_b and k_c individually, as different combinations gave similar optimal fits, indicating that the parameters are correlated. To resolve this issue we employed Bayesian analysis. Bayesian analysis is a statistical technique that updates a prior probability distribution of a parameter with observations to arrive at a posterior probability distribution (Gelman et al., 2003). The update makes the posterior better constrained than the prior. The prior probability distributions are the initial parameter ranges for which we assume equal probability for each value within this range. The Bayesian analysis starts with a model run with a certain parameter combination, a Markov Chain Monte Carlo technique (Gilks et al., 1998) then takes random steps in parameter space and the model is solved with each parameters set. If a parameter combination gives a better fit to the data than the previous parameter combination, the run is accepted and used as new starting point for a following random step. If the new parameter combination fits worse, it can be accepted with a probability equal to the ratio of probabilities of the tested versus the existing parameter combination. The distribution of parameter values in the set of accepted runs is the posterior probability distribution of each parameter. We ran the model for each species 10000 times, which typically gave ~ 1000 accepted runs. The mean and standard deviation of the ratio

$\frac{k_b}{k_c}$ for a species was then calculated from the accepted model runs. The model was implemented in the freely available simulation environment FEMME (Soetaert et al. (2002), <http://www.nioo.knaw.nl/ceme/femme>).

To test whether dependence on bacterial carbon for meiobenthos increases with depth in the sediment, the data of a meiobenthic group of a respective depth interval was fitted with the bacterial $\Delta\delta^{13}\text{C}$ from the respective interval. For macrobenthos it is difficult to directly link their presence in a certain depth interval with their feeding depth because the size of these species (\sim cm) is comparable to that of the depth intervals. Therefore we used the feeding classification for macrobenthos species (Fauchald and Jumars, 1979; Pearson, 2001) and compared surface deposit and subsurface deposit feeders. When appropriate, data from all depth layers were pooled and used to calculate dependence on bacterial carbon.

5.3 Results

5.3.1 Label incorporation by bacteria

The $\Delta\delta^{13}\text{C}$ of different bacterial PLFAs were weighted with their respective concentration to obtain a proxy for bacterial $\Delta\delta^{13}\text{C}$. Dynamics of bacterial $\Delta\delta^{13}\text{C}$ were very consistent between plots and intervals for the upper two depth intervals (0-2, 2-5 cm) but the deepest interval (5-10 cm) showed differences between the plots and was somewhat higher labeled than the upper two intervals (Fig. 5.1A). Due to the lower concentration of PLFAs in the deepest interval (374, 181, 227 mmol C m⁻² in the depth intervals 0-2, 2-5 and 5-10 cm, respectively), its influence on the average bacterial $\Delta\delta^{13}\text{C}$ is limited (Fig. 5.1A). The average forcing function, weighted with concentration and thickness of the depth interval, for bacterial $\Delta\delta^{13}\text{C}$ was used in the isotope model or ratio calculations, because the results did not depend critically on whether distinctions were made among intervals or plots (see 5.4 Discussion). The bacterial $\Delta\delta^{13}\text{C}$ increased during and shortly after the ¹³C-glucose injection period, peaked at 519 ‰ on day 5 and decreased to 173 ‰ at day 36.

5.3.2 Meiobenthic and macrobenthic biomass

Meiobenthic biomass was 188 mmol C m⁻² and was dominated by nematodes (35 %), hard-shelled foraminifera (33 %) and juvenile *Heteromastus filiformis* (18 %) (Table 5.1). Copepods, soft-bodied foraminifera, small polychaetes and turbellaria each comprised \leq 5 % of the meiobenthic biomass. The meiobenthic biomass was highest in the top interval (0 - 2 cm, 72 % of total meiobenthic biomass) and all meiobenthic groups were present here (Table 5.1). The number of meiobenthic groups decreased with depth, with only nematodes, hard-shelled and soft-bodied foraminifera present in the deepest layer. Nematodes dominated biomass in the top two intervals (37 % and 58 %, respectively), whereas hard-shelled foraminifera clearly dominated in the deepest interval (91 %) (Table 5.1). *H. filiformis* juveniles represented a significant amount of the meiobenthic-sized biomass in the top layer (24 %), but they vanished in the middle depth interval.

Macrobenthic biomass was 1684 mmol C m⁻², label uptake was measured in species representing 96 % of the biomass, albeit with different frequencies. The remaining 4 % of the biomass was made up of species that were not sampled with the experimental cores. Large specimens of the bivalve *Macoma balthica* (\geq 7 mm, 41 %) and the polychaetes

Heteromastus filiformis (37 %) and *Pygospio elegans* (13 %) dominated the macrobenthic biomass (Table 5.1). Macrobenthic biomass did not show a pronounced trend with depth in the sediment, because the biomass important species *M. balthica* (≥ 7 mm) and *H. filiformis* have their biomass maxima in the middle and deepest depth interval, respectively. This compensates the strong decrease in biomass with depth for other species, such as *P. elegans*, *Polydora cornuta*, *M. balthica* (< 7 mm), *Hydrobia ulvae* and *Corophium* spp., which all had more than 80 % of their biomass in the top layer. The species *Arenicola marina*, *Eteone* spp. and *Cyatura carinata* and *M. balthica* (≥ 7 mm) had their highest biomass in the middle depth interval.

5.3.3 Meiobenthic and macrobenthic label incorporation

All sampled species acquired ^{13}C label, but $\Delta\delta^{13}\text{C}$ dynamics differed among groups and species (Fig. 5.1). Among the meiobenthos, polychaetes (Fig. 5.1N) and copepods (Fig. 5.1I) only marginally increased in $\Delta\delta^{13}\text{C}$ and remained below 20 ‰ during the experiment. Juvenile *Heteromastus filiformis*, soft-bodied and hard-shelled foraminifera (Fig. 5.1L, K, J) showed similar label dynamics with a steady increase to 60 ‰ followed by an exponential-like decrease to almost background levels at day 36. Among the macrobenthos, *Macoma balthica* (< 7 mm, Fig. 5.1E) attained highest $\Delta\delta^{13}\text{C}$ values (217 ‰ at day 7), but returned to almost background values at day 18 (22 ‰). In contrast, *H. filiformis* incorporated label slowly and its $\Delta\delta^{13}\text{C}$ remained constant at ~ 50 ‰ over a month (Fig. 5.1D). Labeling of large *M. balthica* (≥ 7 mm, Fig. 5.1F) specimens was highly variable, but overall lower than labeling of small specimens (Fig. 5.1E). Label incorporation by *Corophium* spp. was very rapid and peaked at 82 ‰, but its $\Delta\delta^{13}\text{C}$ signal rapidly decreased in an exponential fashion when the ^{13}C -glucose injection had ended (Fig. 5.1B). The $\Delta\delta^{13}\text{C}$ dynamics of *Polydora cornuta* and *Pygospio elegans* resemble each other with a steady increase during the first 10 days, followed by a slow decrease (Fig. 5.1G, H).

5.3.4 Dependence on bacterial carbon

As pointed out earlier, fitting the individual parameters k_b and k_c of the isotope model proved impossible due to the strong correlation between both parameters. For example, many combinations give an acceptable fit of the observed $\Delta\delta^{13}\text{C}$ values for *Heteromastus filiformis* (Fig. 5.1D, 5.2A). However, the relative contribution of bacterial carbon to the consumers total carbon requirements, i.e. $\frac{k_b}{k_c}$, is our prime interest and this ratio is much better constrained than the individual parameters (Fig. 5.2). The distribution of the ratios in the accepted set of Bayesian runs approximates a normal distribution, from which the average and standard deviation can be derived (Fig. 5.2B). The histograms for the other species/groups are not shown, but all give a similar picture. The $\Delta\delta^{13}\text{C}$ dynamics of most consumers could be readily fitted with the simple isotope turnover model (Fig. 5.1). Good visual fits were however not obtained for *Macoma balthica*, in particular the small (< 7 mm) specimens (Fig. 5.1E), and *Corophium* spp. (Fig. 5.1B), for which peak labeling and label loss rate were underestimated by the model.

Both the results from the isotope model (Eqs. 5.1) and ratio estimates ($\frac{\Delta\delta^{13}\text{C}_{\text{con}}}{\Delta\delta^{13}\text{C}_{\text{bae}}}$) show that dependence on bacterial carbon was limited (Table 5.1). The dependencies for meiobenthos were ≤ 0.14 and averaged at 0.08. The estimates for macrobenthos were more variable, ranging from 0.00 to 0.23, but averaged at 0.11 (Table 5.1). The dependence for small *M. balthica* (< 7 mm) was higher (0.36), but we consider this estimate unreliable

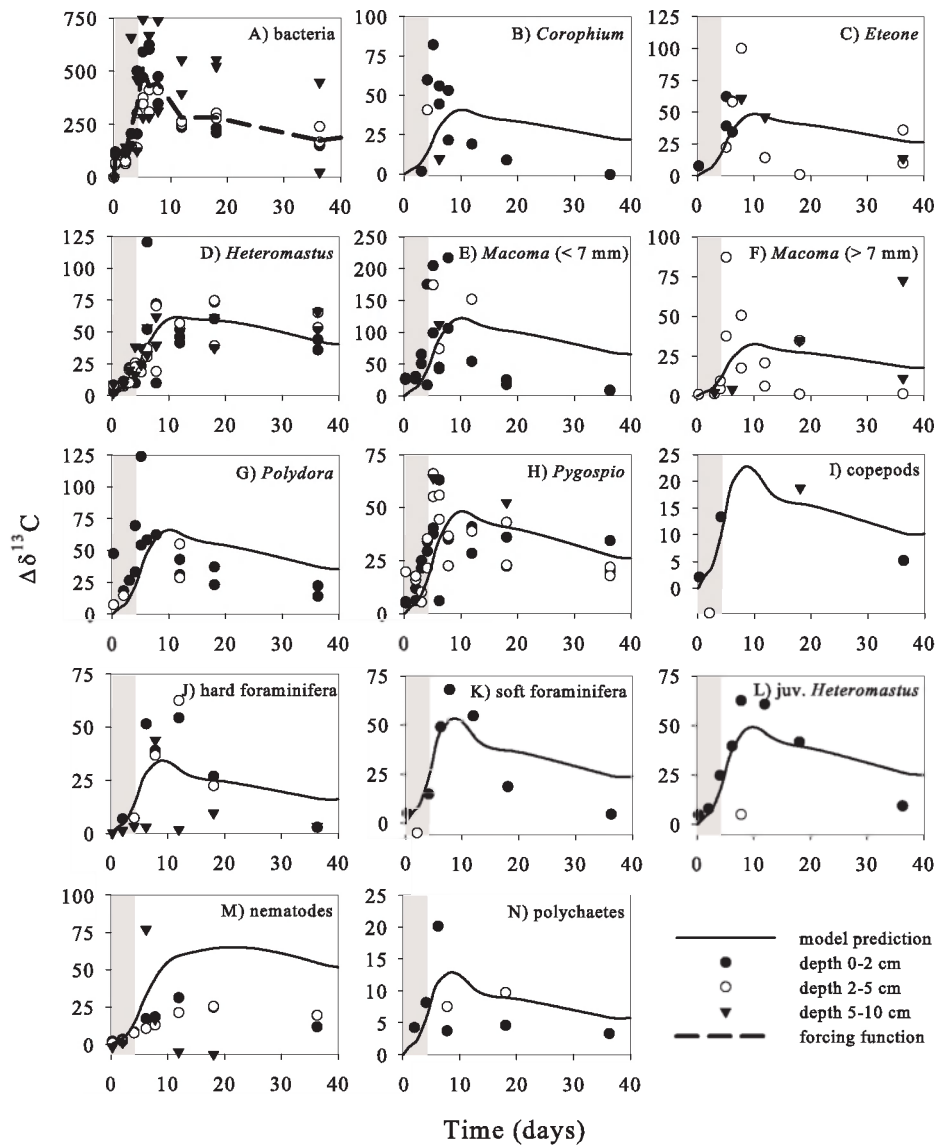


Figure 5.1: A) Observed data and forcing function of $\Delta\delta^{13}\text{C}$ of bacteria. B-N) Observations and best-fit for the macrobenthos species (B) *Corophium* spp. (n = 12). (C) *Eteone* spp. (n = 15). (D) *Heteromastus filiformis* (n = 58). (E) *Macoma balthica* (< 7 mm) (n = 23). (F) *M. balthica* (\geq 7 mm) (n = 18). (G) *Polydora cornuta* (n = 19). (H) *Pygospio elegans* (n = 41) and meiobenthic groups (I) copepods (n = 5). (J) hard-shelled foraminifera (n = 20). (K) soft-bodied foraminifera (n = 8). (L) juvenile *H. filiformis* (n = 9). (M) nematodes (n = 22) and (N) small polychaetes (n = 8). Shown are data pooled from both plots in the three depth intervals. Shaded area indicates period of ^{13}C -glucose injection.

because of the poor fit to the data (see 5.4 Discussion). Despite the variability in the $\Delta\delta^{13}\text{C}$ data, bacterial carbon contributions to diets could be readily estimated for most species, as most standard deviations are between 25 and 30 % of the mean.

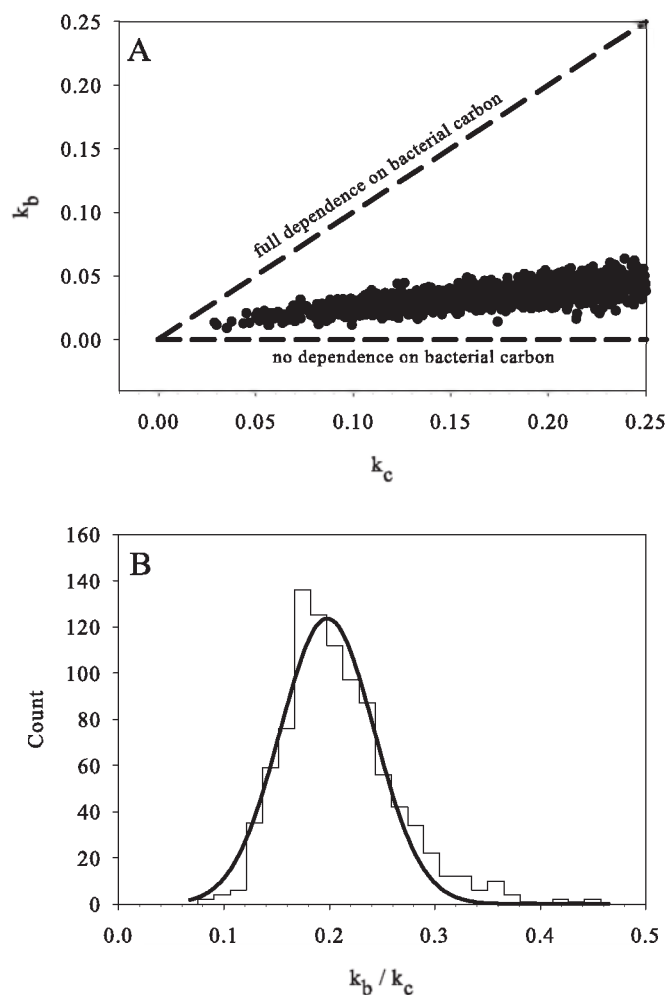


Figure 5.2: A) Scatter plot of the accepted Bayesian runs of the model parameters k_b and k_c for *Heteromastus filiformis*. the linear relationship among both parameters shows that the ratio of the parameters is better constrained than the individual parameter values. B) histogram of the ratio $\frac{k_b}{k_c}$ from the data in Fig. 5.2A and the fitted normal distribution. Histograms for the other organisms fit the normal distribution equally or better.

Nematodes and hard-shelled foraminifera were encountered frequently enough in all depth interval samples to use the isotope model to examine whether dependence on bacterial carbon changed with depth in the sediment. Nematodes did not show differences with regard to living depth (0.08 ± 0.02 , 0.08 ± 0.02 and 0.06 ± 0.04 for 0-2, 2-5 and 5-10 cm, respectively). Hard-shelled foraminifera dependence on bacteria was similar for the upper two sediment layers (0.13 ± 0.03 and 0.15 ± 0.05), but was much lower in the deepest sediment layer (0.03 ± 0.02), where they dominated meiobenthic biomass. Other meiobenthic groups had ≤ 3 observations in the middle or deepest depth layer, which does

5.3. Results

not allow reliable fitting with the isotope model. However, the ratio $\frac{\Delta\delta^{13}C_{con}}{\Delta\delta^{13}C_{bac}}$ of all samples was smaller or similar to estimated dependence on bacterial carbon estimated for the top sediment layer for each group (data not shown), indicating no increase in dependence with depth for these meiobenthic groups.

There were also no clear differences in dependence on bacterial carbon among macrobenthic feeding modes (Table 5.1), although the subsurface feeders *Heteromastus filiformis* (0.21) and *Arenicola marina* (0.23) seem to have a slightly higher dependence on bacterial carbon as compared to surface feeders (typically between 0.10 and 0.15, table 5.1). As an additional check, the ratio $\frac{\Delta\delta^{13}C_{con}}{\Delta\delta^{13}C_{bac}}$ of all macrobenthic species was evaluated in each depth layer and this confirmed that there was no trend in dependence on bacterial carbon with respect to depth (data not shown).

Table 5.1: Dependence on bacterial carbon by the benthic community. Biomass (mmol C m^{-2}) is shown as depth integrated (B) and partitioned over the three depth intervals (d1: 0-2 cm, d2: 2-5 cm, d3: 5 - 10 cm). Feeding modes (FM) for macrobenthos are surface deposit feeder (SDF), predator (P), subsurface deposit feeder (SSDF), suspension feeder (SF) or omnivore (O). The ratio $\frac{k_b}{k_c}$ is the contribution of bacterial carbon to total carbon demands as average \pm standard deviation derived from Bayesian analysis (see 5.2.3 Tracer model and calibration). Numbers in italic indicate a poor model fit (see section 5.4). The ratio $\frac{\Delta\delta^{13}C_{con}}{\Delta\delta^{13}C_{bac}}$, with bracketed day number, is shown for all sampled meiobenthos and macrobenthos.

Species/group	B	d1	d2	d3	FM	$\frac{k_b}{k_c}$	$\frac{\Delta\delta^{13}C_{con}}{\Delta\delta^{13}C_{bac}}$
copepods	3	2	0.1	-		0.06 \pm 0.02	0.03 (36)
foraminifera (hard)	62	31	6	25		0.09 \pm 0.03	0.02 (36)
foraminifera (soft)	5	4	0.5	0.6		0.14 \pm 0.04	0.03 (36)
juv <i>H. filiformis</i>	34	32	2	-		0.14 \pm 0.03	0.05 (36)
nematodes	67	50	15	2		0.06 \pm 0.02	0.09 (36)
small polychaetes	4	4	0.2	-		0.03 \pm 0.01	0.02 (36)
turbellaria	4	4	-	-			0.14 (18)
unknown species	9	7	2	-			0.02 (36)
<i>Corophium</i> spp.	4	3	1	0.2	SDF	<i>0.12\pm0.05</i>	0.00 (36)
<i>Eteone</i> spp.	15	2	13	0.3	P	0.15 \pm 0.04	0.11 (36)
<i>Heteromastus filiformis</i>	597	10	194	393	SSDF	0.21 \pm 0.05	0.30 (36)
<i>M. balthica</i> (< 7 mm)	28	28	0.2	-	SDF	<i>0.36\pm0.09</i>	0.05 (36)
<i>M. balthica</i> (\geq 7 mm)	671	-	612	59	SDF	0.11 \pm 0.04	0.16 (36)
<i>Polydora cornuta</i>	34	33	0.5	-	SF/SDF	0.20 \pm 0.04	0.10 (36)
<i>Pygospio elegans</i>	215	185	30	0.1	SDF	0.15 \pm 0.03	0.14 (36)
<i>Arenicola marina</i>	0.2	0.09	0.1	-	SSDF		0.23 (8)
<i>Cyatura carinata</i>	7	3	4	0.2	P		0.00 (6)
<i>Hydrobia ulvae</i>	24	24	-	0.2	SDF		0.01 (18)
<i>Nereis (Hediste)</i> spp.	21	0.3	-	21	O		0.05 (36)
<i>Streblospio benedicti</i>	1	0.2	0.8	-	SDF		0.01 (18)
<i>Tharyx marioni</i>	3	0.3	2	-	SDF		0.06 (36)

5.4 Discussion

Sediment organic matter is a complex mixture of pools that differ in lability, nutritional value and origin and it is very difficult to link carbon sources to the sediment dwelling community in situ. We have successfully employed a long-term stable isotope labeling approach to quantify the importance of bacteria as a carbon source for the benthic community.

One of the assumptions of the isotope turnover model is that bacteria are the only ^{13}C source for the benthic fauna. However, benthic organisms might have acquired label by direct utilization of the added ^{13}C -glucose, which would complicate the interpretation of the label dynamics. In this respect it is relevant to compare the time scale of the experiment (\sim weeks) with turnover times of ^{13}C -glucose (\sim minutes, Sawyer and King (1993)) and bacteria (\sim weeks, Schallenberg and Kalff (1993)). These time scale differences imply that direct ^{13}C -glucose uptake would be characterized by immediate labeling that stops shortly after the glucose injection period, whereas ^{13}C -bacteria uptake would be characterized by a somewhat delayed but longer lasting label uptake.

Small *Macoma balthica* (< 7 mm) and *Corophium* spp. showed rapid labeling with peak labeling shortly after the end of the ^{13}C -glucose injection and a very rapid loss of label which cannot be explained by bacterial grazing. These are indications of direct ^{13}C -glucose uptake. Indeed, the fact that the data could not be fitted with the bacterial $\Delta\delta^{13}\text{C}$ dynamics as forcing function (Fig. 5.1B and E), suggest alternative routes of label uptake. For these reasons we regard the estimates for *M. balthica* (< 7 mm) and *Corophium* spp. as unreliable. However, these results do also suggest that only these two species may utilize dissolved organic matter (DOC), whereas this was not evident for other species. Data on $\Delta\delta^{13}\text{C}$ of DOC are not available, so that the relative importance of this carbon source for *M. balthica* (< 7 mm) and *Corophium* spp. cannot be evaluated.

Most species continued to take up label after completion of label injection and some $\Delta\delta^{13}\text{C}$ trajectories approached a rather constant level (Fig. 5.1). These are both indications of transfer of bacterial ^{13}C rather than direct ^{13}C -glucose uptake and suggest that our estimates of dependence on bacterial carbon are reliable. The ratio $\frac{\Delta\delta^{13}\text{C}_{con}}{\Delta\delta^{13}\text{C}_{bac}}$ was used to quantify dependence on bacterial carbon for infrequently sampled groups/species, which is valid approach only at or close to steady-state. Data availability limited quantitative evaluation of the $\Delta\delta^{13}\text{C}_{con}$ dynamics to assess possible inference of ^{13}C -glucose uptake or whether or not steady-state has been reached and these estimates should therefore be viewed with more caution as compared to estimates derived from the isotope model.

Another potential problem is uptake of ^{13}C -glucose by epicuticular bacteria (i.e. bacteria attached to the body surface), a potential artifact that was reported for ^{14}C -acetate in copepods bacterivory experiments (Carman, 1990). However, to explain a $\Delta\delta^{13}\text{C}$ of 50 ‰ (a typical value for benthos, Fig. 5.1) and assuming that epicuticular bacteria have a $\Delta\delta^{13}\text{C}$ similar to sedimentary bacteria (280 - 519 ‰), thoroughly cleaned meiobenthic and macrobenthic specimens would have consisted of 11 to 22 % of epicuticular bacteria. Therefore, although epicuticular bacteria might elevate the $\Delta\delta^{13}\text{C}$ signal of consumers, it is unlikely that this would explain the dominant part of the signal. Moreover, arguments with regard to the short turnover time of ^{13}C -glucose as given above, also apply here.

Although not considered a major artifact here, direct uptake of ^{13}C -glucose and via epicuticular bacteria uptake would result in an overestimation of the dependence on bacterial carbon. As a final remark, model simulations taking possible DOC uptake into account, indicate that the total meiobenthic and total macrobenthic derive 10 % and 20 %, respectively, of their total carbon demands from bacteria (Chapter 4), consistent with the

results presented here for the individual groups/species.

$\Delta\delta^{13}\text{C}$ labeling patterns of bacteria were very consistent between the two plots for the upper two depths, but were more variable for the deepest depth layer (Fig. 5.1A). The average bacterial $\Delta\delta^{13}\text{C}$ captures the overall dynamics well, particularly for the upper two depths where most of the grazing has taken place. Nevertheless, labeling of some grazers was rather variable (Fig. 5.1), though at a level which is typical for in situ labeling experiments (Hall and Meyer, 1998; Middelburg et al., 2000). To examine the effect of this variability on our results, the observations of the frequently sampled *Heteromastus filiformis* were fitted separately for each plot with the bacterial $\Delta\delta^{13}\text{C}$ for the respective plot as forcing function. The derived dependencies were similar for both plots (0.21 ± 0.04 versus 0.21 ± 0.06). Because other species have a similar level of variability, we assert that our results are robust, despite the high variability inherent in this type of experiments.

5.4.1 Bacteria as a carbon source

Due to methodological difficulties in measuring bacterivory and total carbon demand requirements simultaneously, there are few studies that have quantified the importance of bacterial carbon for the benthic community. Sundback et al. (1996) measured grazing rates on microphytobenthos and bacteria by the meiobenthic groups nematodes, harpacticoids and 'others' in a microtidal sandy sediment. Grazing on microphytobenthos exceeded that on bacteria to the extent that the contribution of bacterial carbon was generally restricted to $< 10\%$. Our results agree very well with these estimates, especially for nematodes and other meiobenthic groups. The nematode community at our study site was dominated by *Tripyloides gracilis*, *Viscosia viscosa*, *Ptycholaimellus ponticus* and *Daptonema tenuispiculum* (Steyaert et al., 2003). Moens and Vincx (1997) used gut contents analysis to identify particulate food sources of nematodes and report no or only a limited importance of bacteria for these species. We find a contribution of bacterial carbon of 0.06 ± 0.02 and thus corroborate the results from gut content analysis. It will be interesting to see whether this type of labeling approaches confirm the importance of bacterial carbon for nematodes that have been classified as bacterivores. Moens and Vincx (1997) suggested that DOC uptake may potentially be important for some nematodes, this was however not evident in our study (Fig. 5.1M).

Among meiobenthic groups, highest dependence on bacterial carbon was found for hard-shelled and soft-bodied foraminifera (9 and 14 %, respectively, Table 5.1). These protozoans gather food particles through a network of pseudopodia and actively select particles before they are ingested (Moodley et al. (2000) and references therein). The selected nutritious particles might be highly populated by bacteria, which might explain their relatively high dependence on bacterial carbon.

Most estimates of importance of bacteria as carbon source exist for macrobenthic deposit feeders and are based on measured sediment ingestion rate and bacterial abundance in relation to carbon requirements assessed from physiological measurements or literature data (Cammen, 1980; Kemp, 1987; Plante et al., 1989; Cheng and Lopez, 1991; Andresen and Kristensen, 2002). Cammen (1980) found that bacteria supply between 7 and 10 % of the carbon requirements of the deposit feeder *Nereis succinea*. Due to fragmentation of the specimens we were not able to distinguish between *N. diversicolor* and *N. succinea*, but the ratio $\frac{\Delta\delta^{13}\text{C}_{con}}{\Delta\delta^{13}\text{C}_{bac}}$ of 0.05 (day 36) confirms the limited dependence of *Nereis* (*Hediste*) spp. on bacterial carbon (Table 5.1).

Arenicola marina exhibits strong bacteriolytic activity in its midgut section (Plante and Mayer, 1994), reducing the ambient bacterial density up to 70 % during transition of

the digestive tract (Aller and Yingst, 1985; Grossmann and Reichardt, 1991). However, gut contents analysis and subsequent carbon budget calculations show that bacteria fulfill only 3 - 8 % of the total carbon requirements of *A. marina* (Andresen and Kristensen, 2002). Due to the low density of *A. marina* at our study site we obtained only one $\Delta\delta^{13}\text{C}$ observation (day 8), from which we estimate a contribution on bacterial carbon of 0.23 (Table 5.1). This figure should be taken with extreme caution due to limited sampling, but suggests that bacteria might sometimes be a more important carbon source. It will be interesting to apply the labeling approach in areas densely populated with *A. marina* to examine in situ the importance of bacterial carbon.

Clough and Lopez (1993) investigated the importance of potential carbon sources for *Heteromastus filiformis*. Bacterial carbon was not considered important, because only 26 % of the ingested bacteria were assimilated during gut passage. This figure alone is not sufficient to quantify dependence on bacterial carbon, because the ingestion rate of bacterial carbon is also required. Following their budget calculations for organic matter and assuming that bacterial carbon is 1 % of sedimentary organic carbon one arrives at a contribution of ~ 3 % in the budget of *H. filiformis*. This is much lower than our estimate of 21 % (Table 5.1). Fecal casts of *H. filiformis* are several times enriched in organic carbon, nitrogen and protein content relative to sediments at feeding depth, which clearly shows selective feeding capabilities of *H. filiformis* (Neira and Höpner, 1994; Wild et al., 2005). If these worms select preferentially reactive organic matter with associated bacteria, this could explain why we find higher dependence on bacterial carbon as compared to the dependencies based on indiscriminate feeding in the budget calculations. Moreover, Aller and Yingst (1985) reported that bacterial densities are greatly reduced in fecal pellets as compared to the surrounding sediment, implying efficient use of bacterial carbon. Because uptake of several potential carbon sources was insufficient to account for the carbon requirements of *H. filiformis*, Clough and Lopez (1993) and Neira and Höpner (1994) suggested that dissolved organic carbon (DOC) might be an important additional carbon source. There were however no signs of direct ^{13}C -glucose uptake in our experiment (Fig. 5.1D). In fact, *H. filiformis* was sampled very frequently ($n = 58$) and these observations could be accurately fitted with bacterial $\Delta\delta^{13}\text{C}$ as forcing function (Fig. 5.1D). Therefore we surmise that it is unlikely that DOC is an important carbon source of *H. filiformis*.

Another way to follow the carbon sources utilized by organisms is to examine their fatty acid composition in which specific biomarker fatty acid of different sources such as algal, bacterial or vascular plants can be traced (e.g. Meziane et al., 1997)). Bacterial specific fatty acids have consistently been found in fatty acids of macrobenthos from mangroves (Meziane and Tsuchiya, 2000; Bachok et al., 2003) and intertidal sediments (Meziane et al., 1997), comprising roughly 5 to 15 % of the total macrobenthic fatty acids. Similarly, bacterial specific fatty acids were encountered in all foraminifera at our study site (Moodley et al. in prep). However, converting specific fatty acids to a contribution of bacterial carbon in diets is not straightforward. Conversion factors are needed to upscale specific fatty acids to total carbon contribution, assimilation efficiencies may differ among fatty acids and assimilated fatty acids can be metabolized or stored in adipose tissue by the consumer (Iverson et al., 2004). Therefore a direct comparison with our data is cumbersome, but the presence of bacterial specific fatty acids in benthic fauna evidently confirms transfer of organic compounds from bacteria to benthos.

The amount of labile carbon usually decreases with sediment depth and therefore we hypothesized that subsurface feeders would have a higher dependence on labile bacterial carbon as compared to surface feeders. Nematodes did not show important differences

with regard to living depth (0.08 ± 0.02 , 0.08 ± 0.02 and 0.06 ± 0.04 for 0 - 2, 2 - 5 and 5 - 10 cm, respectively). Hard-shelled foraminifera dependence on bacteria was similar for the upper two sediment layers (0.13 ± 0.03 and 0.15 ± 0.05), but contrary to our expectations was lower for the deepest sediment layer (0.03 ± 0.02). There were also no clear differences in dependence on bacterial carbon among macrobenthic feeding modes (Table 5.1). Although the subsurface feeders *Heteromastus filiformis* (0.21) and *Arenicola marina* (0.23) seem to have a somewhat higher dependence on bacterial carbon as compared to surface feeders (0.10 to 0.15 on average), it remains to be seen whether these small differences are ecological relevant. We conclude that there are no clear differences in the dependence on bacterial carbon with respect to depth for metazoan meiobenthos nor macrobenthos.

Although our results show that the contribution of bacterial carbon to total carbon requirements of intertidal meiobenthos and macrobenthos is limited to < 10 - 15 %, bacteria might be a source of essential compounds (Lopez and Levinton, 1987). For example, some foraminifera only reproduce when bacteria are present as food source (Muller and Lee, 1969). Advances in the analysis of stable isotopes in lipids (Boschker and Middelburg, 2002) and amino acids (Veuger et al., 2005) may be used to address this issue. For example, when applying an isotope tracer approach, compounds that are predominantly derived from bacteria are expected to have an elevated $\Delta\delta^{13}\text{C}$ as compared to the $\Delta\delta^{13}\text{C}$ of compounds that are assimilated from other resources. Furthermore, it remains to be established whether our results also apply in sediments that receive more refractory organic matter (e.g. deep-sea sediments). From the information available, we found on the one hand, no effect of living/feeding depth, which suggests that more refractory organic carbon does not increase dependence on bacterial carbon. On the other hand, many invertebrates of a small leaf-litter dominated stream food web relied for > 50 % on bacterial carbon, as shown by a stream water ^{13}C -acetate enrichment (Hall and Meyer, 1998). Their estimates are consistently higher than ours, which does suggest that dependence on bacteria is more important in systems that are dominated by refractory organic matter with a high C:N ratio. This comparison is admittedly crude and more data sets are required to single out the factors that control dependence on bacterial carbon in other benthic systems.

5.4.2 Selective feeding

The marginal dependence on bacterial carbon was surprisingly general among the benthic fauna encountered in the intertidal sediment (Table 5.1). This generality hints at a mechanism that prevents a greater exploitation of bacterial carbon. One possible explanation may be the dilution of bacterial carbon due to its attachment to inedible sediment grains. As suggested by Cammen (1980), a greater bacterial carbon exploitation may be limited by the processing rate of sediment particles by the benthos. For our study site, we estimated fauna processing rates as follows: total meiobenthic and macrobenthic biomass in the upper 10 cm of the sediment was $1872 \text{ mmol C m}^{-2}$, which translates to a volume of $\sim 300 \text{ cm}^3 \text{ m}^{-2}$ ($0.5 \text{ g C} = 1 \text{ g DW}$, $0.15 \text{ g DW} = 1 \text{ g WW}$ and $1 \text{ g WW} = 1 \text{ cm}^3$). If we assume a relative gut volume of 0.10 (Kooijman, 2000) and a gut residence time of 2 hour (Bock and Miller, 1999), 0.36 % of the sediment passes a digestive tract on a daily basis. If we further assume a homogeneous bacteria - sediment mixture, indiscriminate feeding by benthos results in a grazing rate of 0.0036 d^{-1} of the bacterial stock. With the average bacteria biomass of $781 \text{ mmol C m}^{-2}$ (Chapter 4), the expected grazing rate from indiscriminate feeding is $2.8 \text{ mmol C m}^{-2} \text{ d}^{-1}$. Assuming maintenance carbon

requirements of $19 \text{ mmol C m}^{-2} \text{ d}^{-1}$ (0.01 of benthic biomass d^{-1} , Nielsen et al. (e.g. 1995)), bacterial grazing of $2.8 \text{ mmol C m}^{-2} \text{ d}^{-1}$ is far below maintenance requirements alone and shows that processing rates by indiscriminate feeding by benthos may indeed limit a greater exploitation of bacterial carbon.

However, benthic fauna do not feed indiscriminately (Lopez and Levinton, 1987) and we therefore examined our data for evidence of selective feeding. From quantitative modeling the experimental data, we derived a grazing rate of $18 \text{ mmol C m}^{-2} \text{ d}^{-1}$ on bacteria by the benthic community (Chapter 4), which is about $6\times$ the expectation of indiscriminate feeding ($2.8 \text{ mmol C m}^{-2} \text{ d}^{-1}$), clearly showing selective ingestion by benthic fauna. However, since bacteria comprise only a small part of the total carbon requirements of benthos, it is likely that selection occurs for food patches that have a higher organic matter content or quality rather than selection for bacteria as such. The contribution of bacterial carbon to organic matter increases with increasing quality (Findlay et al., 2002; Fischer et al., 2002), therefore one may use dependence on bacteria as proxy for the quality of the organic matter that is selected. As a result, feeding on high quality organic matter would result in a concomitant increase in dependence on bacterial carbon.

Foraging theory predicts that feeding niches are defined by body size: small organisms rely on small but high quality patches and larger organisms on larger but lower quality patches (Ritchie, 1998; Ritchie and Olff, 1999). From this prediction a decreasing dependence on bacterial carbon with increasing body size is expected. The expected relationship was not evident in our data (Fig. 5.3). Although this exercise is speculative, it suggests that benthic fauna collectively select for high quality resources.

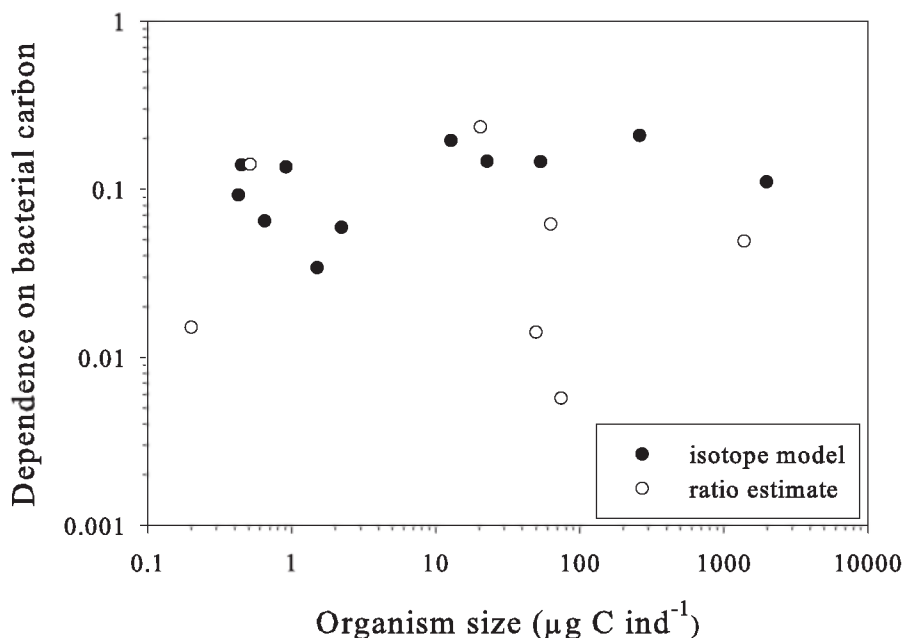


Figure 5.3: Relative dependence on bacterial carbon as a function of body size.

5.4.3 Implications of the weak bacteria - benthos interaction

In accordance with earlier observations, our results show that bacteria are a limited carbon source benthic fauna. The limited transfer of bacterial carbon to the benthos implies that there is no important direct influence of bacterial abundance or production on the dynamics of benthic fauna. Bacteria are found to be dominant processors of labile microphytobenthic carbon (Middelburg et al., 2000) and phytodetritus (Moodley et al., 2002, 2005), but also of refractory lignocellulosic detritus from vascular plants (Benner et al., 1986). On the one hand, this suggests a competitive interaction between bacteria and benthic fauna for labile carbon resources, given that also the latter rapidly assimilate labile phytodetritus (Blair et al., 1996; Herman et al., 2000; Moens et al., 2002; Witte et al., 2003). The limited transfer of bacterial carbon implies that labile carbon assimilated by bacteria, is effectively lost for the metazoan food web. On the other hand, transfer of bacterial carbon might provide a means through which refractory and otherwise indigestible detritus may enter the traditional metazoan food web (Hall and Meyer, 1998). The characteristics of the benthic system, in particular the lability of the detritus pool, will eventually determine whether the bacteria - benthos interaction will be a net gain or loss for the benthic fauna.

In terms of food web relations in intertidal sediments, the observed weak bacteria - benthos interaction should not be viewed as a predatory relation, but is more likely to be of competitive nature with respect to labile carbon sources. As described earlier, benthic fauna fed selectively, but the lack of a relationship between body size and dependence on bacterial carbon suggests that benthic organisms compete for organic matter of similar quality. Therefore, intertidal benthic food webs seem to be regulated predominantly by competitive interactions for labile resources among bacteria, meiobenthos and macrobenthos.

Chapter 6

Fate of ^{13}C labeled bacterial proteins and peptidoglycan in an intertidal sediment

Bart Veuger, Dick van Oevelen, Jack J. Middelburg and Henricus T. S. Boschker. *In revision for Limnology and Oceanography*

6.1 Introduction

Bacteria constitute a major pool of biomass in marine sediments and play a central role in ecological and biogeochemical processes. Although rates of bacterial secondary production and respiration in sediments vary over orders of magnitude, bacterial abundance is relatively constant at $\sim 10^9$ cells ml^{-1} (Schmidt et al., 1998). This suggests that bacterial production is balanced by various loss processes. Such losses include bacterial grazing by benthic fauna (Kemp, 1990), mortality due to viral lysis (Fischer et al., 2003; Hewson and Fuhrman, 2003), programmed cell death (Yarmolinsky, 1995) and other unidentified causes. Generally, $< 20\%$ of bacterial production is removed by grazing (Epstein and Shiaris, 1992; Hondeveld et al., 1995; Sundback et al., 1996). Consequently, after cell death most bacterial C stays in the sediment organic carbon (OC) pool as bacterial cell remnants, where it can be subject to degradation and recycling. Bacterial cells contain a variety of components, some of which will be readily degraded, while others are more resistant to degradation ('refractory'). The refractory nature of peptidoglycan makes it a potentially important contributor to total sediment OM just like it is thought to be an important contributor to total DOM in seawater (McCarthy et al. 1998, Amon et al. 2001, Dittmar et al. 2001). Increasing D/L-AA ratios with sediment depth reflect the selective preservation of peptidoglycan relative to protein at longer time scales (10-10.000 years), but do not provide direct information on the degradability of peptidoglycan or its significance as a potential long term sink for bacterial C and N.

An alternative approach that does provide a direct indication of the degradability of peptidoglycan is to study degradation of peptidoglycan in bacterial cultures (Jorgensen et al., 2003) or marine waters (Nagata et al., 2003). This approach showed that peptidoglycan is degraded slower than proteins and can be characterized as 'semi-labile'. However, these studies used peptidoglycan and proteins extracted from cultures and were

performed *in vitro*. This does not provide a direct indication of the degradability of peptidoglycan and proteins from sediment bacteria *in situ*, since this is also dependent on their presence in macromolecules and by interactions with particles (Borch and Kirchman, 1999; Arnarson and Keil, 2005).

In this study, we combine the two approaches mentioned above by ^{13}C labeling bacterial biomass in a tidal flat sediment and subsequent analysis of the *in situ* fate of the ^{13}C in three different bacterial cell components: 1) D-Ala, an amino acid unique to peptidoglycan that has only recently been used as a bacterial biomarker in combination with stable isotope labeling (Veuger et al., 2005). In this study, ^{13}C -D-Ala is used as an indicator for ^{13}C -peptidoglycan. 2) Total hydrolyzable amino acids (THAAs) comprises a pool of 14 HAAs (including D-Ala). Except for D-Ala, these HAAs are common protein amino acids that have very limited biomarker potential, as they are present in all organisms (Cowie and Hedges, 1992). However, as the ^{13}C -glucose labeling in this study specifically tagged bacteria, ^{13}C -THAAs could be used as an indicator for bacterial ^{13}C -proteins. 3) Bacteria-specific phospholipid-derived fatty acids (PLFAs) are a more established group of biomarkers that have been used in various ^{13}C -labeling studies to estimate total bacterial ^{13}C incorporation (Boschker et al., 1998; Middelburg et al., 2000; Pelz et al., 2001). Since PLFAs are rapidly degraded after cell death (Parkes, 1987; Moodley et al., 2000), they are restricted to living organisms, which makes them true 'ecological biomarkers' as opposed to D-Ala, which is more of a 'biogeochemical biomarker' as it is also present in bacterial cell remnants (Boschker and Middelburg, 2002). In this study, bacteria-specific PLFAs are used as an indicator for living bacteria and thereby serve as a reference to determine the fate of bacterial cell remnants (proteins and peptidoglycan).

The unique comparison of ^{13}C in the different bacterial components allowed us to compare the *in situ* fate of bacterial proteins (THAA) and peptidoglycan (D-Ala) derived from sediment bacteria and to link this with the accumulation of D-Ala in sediments. In addition to analysis of their long term fate, this study also allows direct comparison of ^{13}C incorporation into the different bacterial components. Comparison of estimates of total bacterial ^{13}C incorporation from bacteria-specific PLFAs and D-Ala provides a validation of the use of these bacterial biomarkers and their accompanying conversion factors in stable isotope labeling studies.

6.2 Materials and methods

6.2.1 Experimental setup

The material presented in this publication is part of a larger ^{13}C labeling study (see also chapter 4 and 5). In May 2003, two 0.25 m² sediment plots were selected at a silty part of the Molenplaat intertidal mudflat in the turbid, nutrient rich and heterotrophic Scheldt estuary (The Netherlands). Plots were confined by steel frames and the upper 10 cm was injected with ^{13}C glucose (1 injection per 6.25 cm², 0.4 ml of 24 mmol l⁻¹ ^{13}C per injection) at days 0, 2, 3 and 4, resulting in a ^{13}C flux of 15.3 mmol ^{13}C m⁻² per injection event. During the label addition period and in the days, weeks and months after label addition (up to 136 days), plots were sampled regularly by taking sediment cores (Ø 50 mm). Before removing sample cores from the plots, larger cores (Ø 90 mm) were placed around the sample cores to prevent disturbance of surrounding sediment. Sample cores were transported to the laboratory and sliced into three layers (0-2 cm, 2-5 cm and 5-10 cm) that were analyzed for total C and ^{13}C in POC (by EA-IRMS after removal

of carbonates by acidification), pore water DIC and PLFAs as well as ^{13}C in meio- and macrobenthos. Further details on the experimental setup and analytical procedures can be found in chapter 4. Samples from the 2-5 cm layer from one plot were also analyzed for ^{13}C in HAAs, including D-Ala. Since this paper focuses on comparison of ^{13}C in bacteria-specific PLFAs, D-Ala and THAAs, it only deals with results for the 2-5 cm layer.

6.2.2 PLFA analysis

Lipids were extracted from 3 g of dry sediment in chloroform-methanol-water using a modified Bligh and Dyer method and fractionated on silicic acid into different polarity classes. The most polar fraction, containing the PLFAs, was derivatized by mild methanolysis yielding fatty acid methyl esters (FAMES) that were analyzed by gas-chromatography-combustion-isotope ratio mass spectrometry (GC-c-IRMS). Further details on PLFA extractions and analysis can be found in Boschker (2004). Data were processed as in Middelburg et al. (2000). Although analysis included a wide range of PLFAs, we only present results for bacteria-specific PLFAs i14:0, i15:0, a15:0, i16:0 and 18:1 ω 7c.

6.2.3 Amino acid analysis

Samples for GC-c-IRMS analysis of ^{13}C in HAAs (including D-Ala) were processed following the protocol presented in Veuger et al. (2005). Briefly, samples (1 g) of freeze-dried sediment were washed with HCl (2 mol l $^{-1}$) and Milli-Q water, followed by hydrolysis in HCl (6 mol l $^{-1}$) at 110 °C for 20 h. After purification by cation exchange chromatography, amino acids were derivatized with isopropanol (IP) and pentafluoropropionic anhydride (PFA) and further purified by solvent extraction. Amino acid D- and L-enantiomers were separated by gas chromatography using a Chirasil-L-Val column. Flame ionization detection (GC-FID) was used for concentration measurements, while a selection of samples was also analyzed with a quadrupole mass spectrometer (GC-MS) to verify peak identity and purity. ^{13}C abundance was measured by GC-c-IRMS and expressed as $\delta^{13}\text{C}$ (‰): $\delta^{13}\text{C} = \left(\frac{R_{\text{sample}}}{R_{\text{VPDB}}} - 1 \right) \cdot 1000$, where $R = \frac{^{13}\text{C}}{^{12}\text{C}}$ and $R_{\text{VPDB}} = 0.0112372$.

During derivatization, extra (unlabeled) C atoms are added to the original amino acids, which changes their $\delta^{13}\text{C}$ (Silfer et al., 1991; Pelz et al., 1998). It is possible to correct for the effect of the added C (Silfer et al., 1991; Pelz et al., 1998) using the following mass-balance equation: $\delta^{13}\text{C}_{AA} = \delta^{13}\text{C}_{DAA} \cdot (C_{AA} + C_{IP} + C_{PFA}) - \frac{\delta^{13}\text{C}_{IP+PFA} \cdot (C_{IP} + C_{PFA})}{C_{AA}}$, where C_{AA} = number of C atoms in the original amino acid, D_{AA} = derivatized amino acid, C_{IP} = number of C atoms added by esterification with IP and C_{PFA} = number of C atoms added by acylation with PFA. However, the change in $\delta^{13}\text{C}$ during derivatization is also influenced by additional kinetic fractionation during acylation (addition of C from PFA). The effect of this fractionation depends on the %C derived from PFA (i.e. the number of added C atoms from PFA relative to the number of C atoms in the original amino acid). As this effect is not included in the mass balance equation, it requires empirical correction. This was done by measuring the $\delta^{13}\text{C}$ of three amino acid standards (D-Ala, D-Glu and D-Ser) before and after derivatization by EA-IRMS, which allowed us to determine empirical $\delta^{13}\text{C}_{CIP+PFA}$ values for these three amino acids. These values showed a strong linear correlation with the %C from PFA, which is similar to results by Silfer et al. (1991). Subsequently, this relation was used to determine empirical $\delta^{13}\text{C}_{CIP+PFA}$ values for the other amino acids which were then

used to calculate their original $\delta^{13}\text{C}$ values using the mass balance equation. Our empirical $\delta^{13}\text{C}_{CIP+PFA}$ values ranged between -52 and -45 ‰, which is lighter than those in Silfer et al. (1991), because we used PFA for acylation, which contains more C than the TFA used by Silfer et al. (1991) and because the used PFA was very depleted in ^{13}C ($\delta^{13}\text{C}$: -55 ‰, measured by EA-IRMS).

After correction, $\delta^{13}\text{C}$ values were used to calculate $\Delta\delta^{13}\text{C}$: $\Delta\delta^{13}\text{C}_{sample}$ (‰) = $\delta^{13}\text{C}_{sample} - \delta^{13}\text{C}_{unlabeled\ sample}$ and the atom percentage of ^{13}C : $\text{at}\%^{13}\text{C} = [100 \cdot R_{standard} \cdot ((\delta^{13}\text{C}_{sample} / 1000) + 1)] / [1 + R_{standard} \cdot ((\delta^{13}\text{C}_{sample} / 1000) + 1)]$. Subsequently, $\text{at}\%^{13}\text{C}$ was used to calculate the absolute amount of incorporated excess ^{13}C : $\text{excess } ^{13}\text{C} = (\text{at}\%^{13}\text{C}_{sample} - \text{at}\%^{13}\text{C}_{control}) \cdot \text{AA-C concentration}_{sample}$. Amino acid concentrations and excess ^{13}C are expressed in nmol carbon per gram dry sediment (nmol C gdw^{-1}).

6.3 Results and discussion

The aim of the whole ^{13}C labeling experiment was to investigate production and fate of bacterial C in the sediment of the Molenplaat tidal flat. While two companion papers discuss and model the overall turnover and fate of total bacterial ^{13}C (Chapter 4) and bacterial grazing by meio- and macrobenthos (Chapter 5), this paper focuses on the fate of ^{13}C -labeled bacterial proteins and peptidoglycan during the 4.5 months after labeling, using bacteria-specific PLFAs as an indicator for living bacteria.

Below, we first discuss ^{13}C incorporation into the different bacterial components and validate their use to estimate total excess ^{13}C incorporated by bacteria, including their respective conversion factors. Thereafter, we discuss the fate of bacterial proteins (^{13}C -THAAs) versus peptidoglycan (^{13}C -D-Ala) to clarify the role of peptidoglycan as a potential long term sink for bacterial C and its contribution to total sediment OC.

6.3.1 ^{13}C incorporation into PLFAs, D-Ala and THAAs

Injection of ^{13}C glucose into the sediment resulted in rapid and steady ^{13}C enrichment of bacteria-specific PLFAs, D-Ala and THAAs (represented by L-Ala) with the same general trends for these different bacterial components (Fig. 6.1, 6.2 and 6.3). Enrichment was well above natural abundance for D-Ala ($\delta^{13}\text{C}$ -8 ‰), other amino acids (Leu, Ile, Tyr and Thr+Val: -35 to -30 ‰, L-Ala, Lys, Glu+Phe and Pro: -25 to -20 ‰, Asp, Ser and Gly: \sim -10 ‰), bacteria-specific PLFAs (-19.6 ± 1.3 ‰) and bulk OC (-24 ‰). The measured range of natural abundance $\delta^{13}\text{C}$ values for the different HAAs is comparable with that reported by Keil and Fogel (2001).

Trends for ^{13}C incorporation into the five bacteria-specific PLFAs were the same and absolute differences in excess ^{13}C in these PLFAs were proportional to their concentrations (Fig. 6.3). Therefore, 18:1 ω 7c was used as a representative for the five bacteria-specific PLFAs for comparison with D-Ala and L-Ala/THAAs (Fig. 6.1). Although 18:1 ω 7c can also be present in certain algae (Moodley et al., 2000), this did not affect results in this study since ^{13}C uptake by algae was negligible (see below).

The strong increase in $\Delta\delta^{13}\text{C}$ during the labeling period (day 0 to 4) shows that ^{13}C from ^{13}C glucose was readily incorporated into bacterial biomass (Fig. 6.1) and that ^{13}C incorporation rates were the same for cell membranes (PLFAs), proteins (THAAs) and cell walls (D-Ala). This indicates that the experimental time scale (days) exceeded the time required for bacteria to produce complete cells, meaning that results were not biased by differences in synthesis rates for different cellular components.

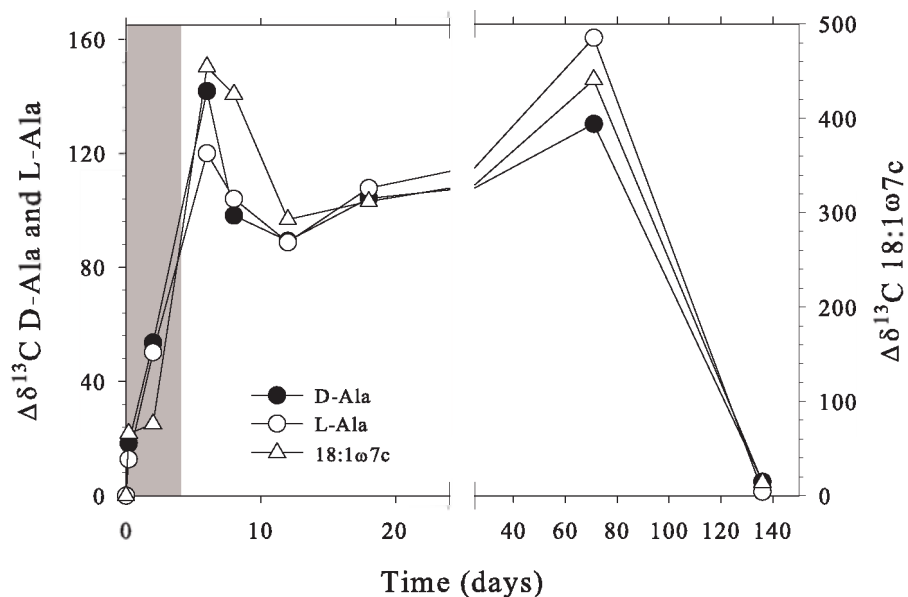


Figure 6.1: $\Delta\delta^{13}\text{C}$ values for D-Ala, L-Ala and bacteria-specific PLFA 18:1 ω 7c. Grey area indicates labeling period.

Trends for $\Delta\delta^{13}\text{C}$ values in D-Ala, L-Ala and bacteria-specific PLFAs were very similar (Fig. 6.1). The close correlation between PLFAs and D-Ala indicates that these two different bacterial biomarkers represented the same active bacterial community. Furthermore, these results confirm that uptake of ^{13}C glucose was dominated by bacteria (i.e. additional uptake by other organisms was negligible), because: 1) Trends for $\Delta\delta^{13}\text{C}$ values for D-Ala and PLFAs (bacterial biomarkers) were closely correlated with L-Ala (Fig. 6.1). Since L-Ala is a common amino acid that is present in bacteria as well as other organisms and given that bacteria normally show highest turnover rates, additional ^{13}C incorporation by non-bacteria likely would have resulted in a different trend in $\Delta\delta^{13}\text{C}$ for L-Ala than for the bacterial biomarkers. 2) Excess ^{13}C in D- versus L-Ala (Fig. 6.2B) showed a D/L-Ala ratio of $\sim 5\%$ (until day 71), which is a typical D/L-Ala ratio for a mixed marine bacterial community (Veuger et al., 2005). Substantial ^{13}C incorporation by other organisms would have resulted in a higher excess ^{13}C in L-Ala and thus in a lower excess ^{13}C D/L-Ala ratio. 3) $\Delta\delta^{13}\text{C}$ values for biomarker PLFAs from other groups of organisms, mainly microphytobenthos (20:5 ω 3) and benthic fauna (20:4 ω 6), were an order of magnitude lower than those for the bacteria-specific PLFAs, which confirms that ^{13}C incorporation by organisms other than bacteria was negligible (data not shown).

6.3.2 Estimates of total bacterial ^{13}C uptake

The excess ^{13}C incorporated into bacteria-specific PLFAs, D-Ala and THAAs can be used to estimate total bacterial ^{13}C incorporation, which requires conversion from these specific components to total bacterial biomass. This study provides the opportunity to compare estimates derived from the three different bacterial components and thereby serve as a validation of the use of these components and their respective conversion factors (Fig. 6.4).

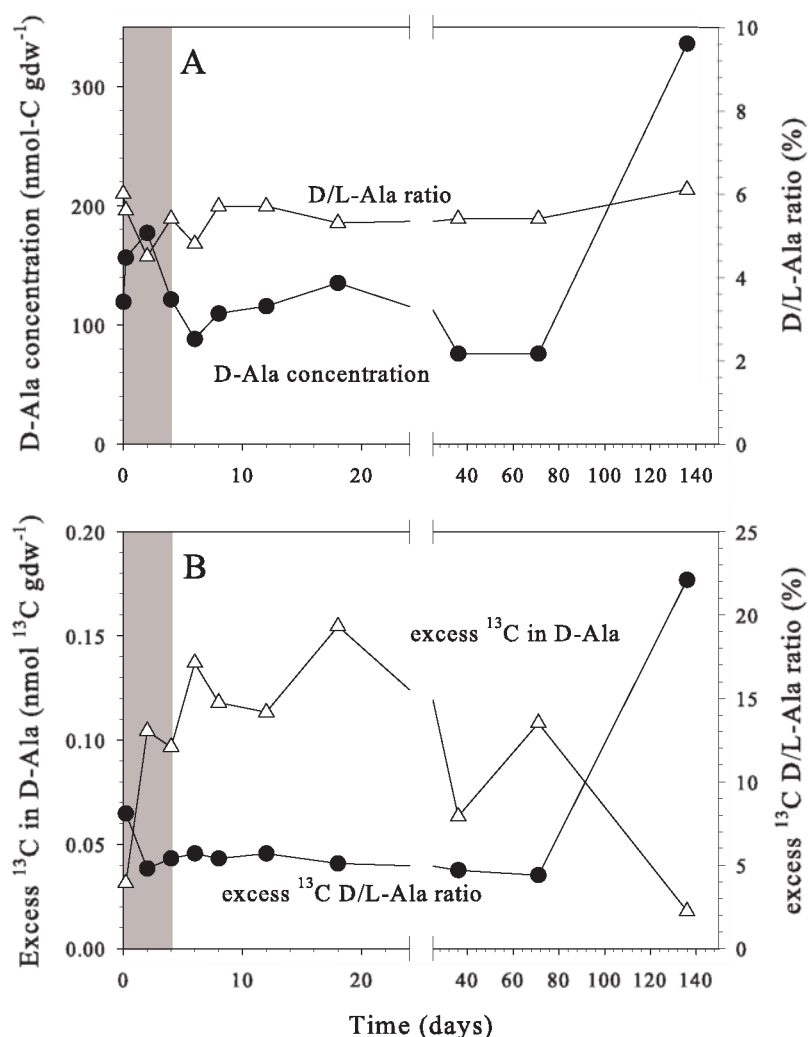


Figure 6.2: A) D-Ala concentrations and ratio between concentrations of D-Ala and L-Ala. B) excess ^{13}C in D-Ala and ratio between excess ^{13}C in D-Ala and L-Ala. Grey area indicates labeling period.

For this comparison, average values for day 6-18 were used (i.e. freshly labeled bacteria) to avoid bias from potential selective removal and/or degradation. Below, we discuss the conversion factors used in Fig. 6.4.

Conversion from excess ^{13}C in bacteria-specific PLFAs to total bacterial excess ^{13}C is the product of two separate conversion steps. The first step is conversion from bacteria-specific PLFA-C to total bacterial PLFA-C. The used value of $\times 3.6$ (28 %) is relatively robust (E Boschker, unpub data), has been used in various studies (e.g. Middelburg et al., 2000; Moodley et al., 2000) and was confirmed by the contribution of excess ^{13}C in bacteria-specific PLFAs to excess ^{13}C in total PLFAs in this study ($31 \pm 2\%$). The second step is conversion from total bacterial PLFA-C to total bacterial-C. Assuming that bacteria in the 2-5 cm layer were predominantly anaerobic, a conversion

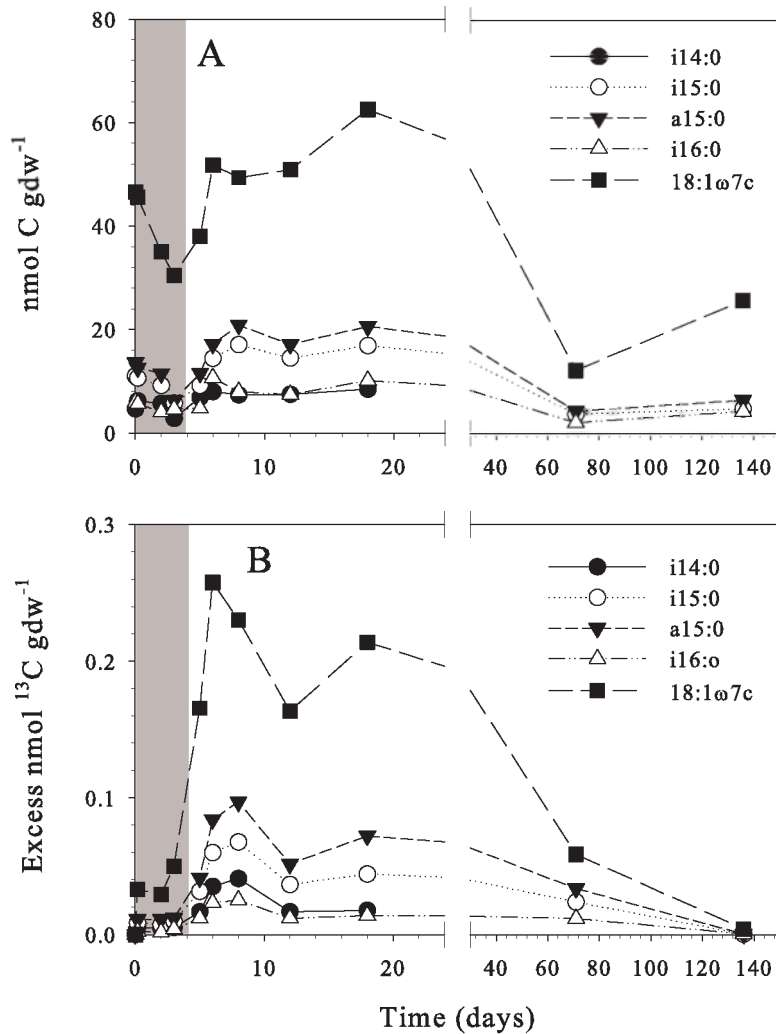


Figure 6.3: A) Concentrations and B) excess ^{13}C for bacteria-specific PLFAs. Grey area indicates labeling period.

of $\times 26$ (3.8 %) was used, which is based on the PLFA content of a mixed bacterial culture grown under anaerobic conditions (Brinch-Iversen and King, 1990). Similar values from Brinch-Iversen and King (1990) have successfully been used in various other studies (e.g. Middelburg et al., 2000; Van den Meersche et al., 2004). For this study, the first and second step together yield a total conversion of $\times 94$ (Fig. 6.4).

In contrast to estimates from the bacterial biomarkers, estimates of total bacterial excess ^{13}C from ^{13}C -THAAs require only a small conversion since THAAs are $\sim 50\%$ of total bacterial-C (Cowie and Hedges, 1992; Madigan et al., 2000), resulting in a conversion of $\times 2$. Conversion from D-Ala to total bacterial-C can be derived from measured D-Ala contents of bacterial cultures as presented in Veuger et al. (2005). However, these cultures showed rather variable D-Ala contents, while conversion based on the average D-Ala content for these cultures ($1.9 \text{ mg D-Ala gdw}^{-1}$) yielded an estimate of total bacterial

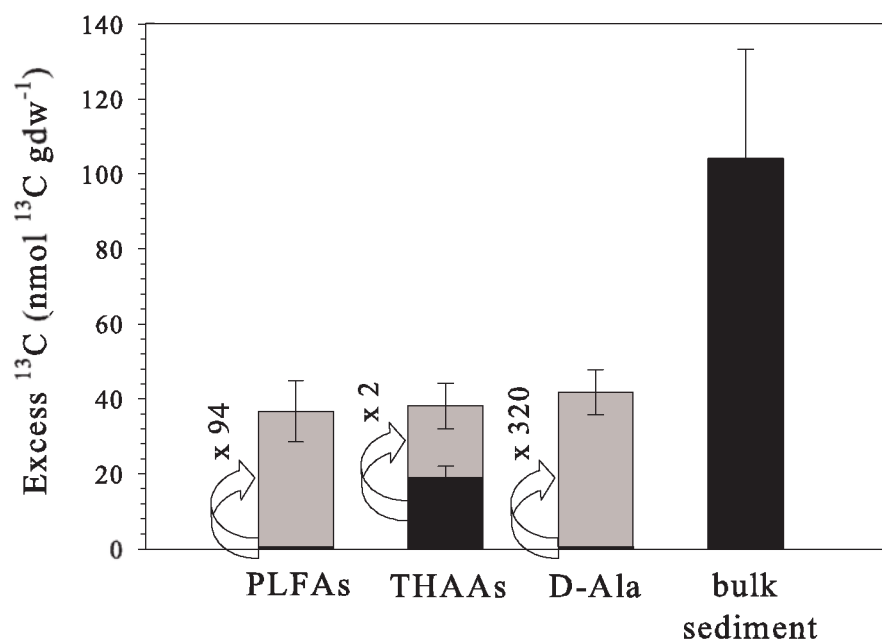


Figure 6.4: Excess ^{13}C in bacteria-specific PLFAs, THAAs, D-Ala and bulk sediment (black bars) and resulting estimates of total bacterial excess ^{13}C (grey bars) for day 6-18 (average \pm stdev). Numbers are used conversion factors (see text).

excess ^{13}C of ~ 86 nmol ^{13}C gdw $^{-1}$, which is considerably higher than estimates from bacteria-specific PLFAs and THAAs (Fig. 6.4). Therefore, a new conversion factor for D-Ala was derived from three separate steps that involve relatively consistent values. The first step is from D-Ala to L-Ala. Since bacteria appear to have a relatively stable D/L-Ala ratio of $\sim 5\%$ (Fig. 6.2B and Veuger et al. (2005) + references therein), we used a conversion of $\times 20$. The second step is from L-Ala to THAA. Cowie and Hedges (1992) found Ala to be 9-15 mole % of the THAA pool of three bacterial cultures (5-9 % C-based). We used a somewhat higher value of 12.6 % (C-based), which was the average contribution of ^{13}C -L-Ala to the ^{13}C -THAA pool for day 6-18 in this study (Fig. 6.5A). Resulting conversion for step 2 is $\times 8$. The third step is from THAA to total bacterial-C, which requires a conversion of $\times 2$, as already discussed above. The three steps together result in a total conversion of $\times 320$, yielding an estimate of total bacterial excess ^{13}C very similar to those from bacteria-specific PLFAs and THAAs (Fig. 6.4). This internal consistency between the different estimates is excellent given the underlying assumptions (as discussed above) and the general uncertainties typically associated with this kind of conversions (e.g. dependence on bacterial cell size, community composition and environmental conditions).

Comparison of estimates of total bacterial excess ^{13}C from excess ^{13}C in bacteria-specific PLFAs, THAAs and D-Ala (Fig. 6.4) served as a useful validation of the use of bacteria-specific PLFAs and D-Ala as bacterial biomarkers and their accompanying conversion factors in ^{13}C labeling studies. Furthermore, it also supports the feasibility of using D-Ala as a bacterial biomarker in ^{15}N labeling studies, although results indicate that the N-based conversion factor of $\times 400$ presented in Veuger et al. (2005) may be somewhat too large.

The average estimate of total excess ^{13}C incorporated by bacteria (39 nmol ^{13}C

gdw⁻¹) was considerably lower than the measured excess ¹³C for the whole sediment (110 nmol ¹³C gdw⁻¹), indicating that a considerable pool of ¹³C was present in the sediment next to the ¹³C incorporated in bacterial biomass. Since the presence of a substantial pool of ¹³C labeled cell remnants is not likely for days 6-18 (as discussed in following paragraphs) this pool probably comprised ¹³C-glucose adsorbed to the sediment, which is supported by modeling results (Chapter 4). In addition, ¹³C labeled compounds excreted by bacteria may also have contributed to this extracellular ¹³C pool.

6.3.3 Fate of bacterial ¹³C: General trends

After the positive validation of using excess ¹³C incorporated in the different bacterial components to estimate total bacterial excess ¹³C, we now focus on the fate of the bacterial ¹³C, especially ¹³C-labeled proteins (¹³C-THAAs) and peptidoglycan (¹³C-D-Ala), in the 4.5 months after labeling.

In general, excess ¹³C in the bacterial components remained high until day 18. After day 18, excess ¹³C in PLFAs decreased gradually while excess ¹³C in D-Ala (Fig. 6.2B) and $\Delta\delta^{13}\text{C}$ values (Fig. 6.1) showed a less rapid and less consistent decrease. For all components, a considerable fraction of the initial excess ¹³C remained present until day 71. Excess ¹³C at day 136 was very low for all bacterial components (Fig. 6.1, 6.2 and 6.3), indicating that the bulk of the ¹³C labeled bacterial biomass had disappeared after 136 days. Loss processes for bacterial ¹³C in this experiment included cell death, grazing and resuspension. Modeling results for the whole 0-10 cm layer showed that resuspension and grazing only contributed 10 % and 30 % to total loss respectively (Chapter 4). Although the 2-5 cm layer was not in direct contact with the overlying water, resuspension may still have contributed to the removal of bacterial biomass from this layer since the sediment was thoroughly mixed by bioturbating animals (Chapter 5). As these loss processes contributed only ~ 40 % to total loss, this implies that most bacterial ¹³C was not removed as whole cells but instead remained in the sediment after cell death. These dead bacteria likely provided a pool of fresh organic matter readily available for degradation. In the following paragraphs, we further discuss the fate of the different ¹³C-labeled bacterial components, especially after 136 days, in more detail.

6.3.4 Fate of bacterial ¹³C: ¹³C-THAAs

A first indication as to whether the ¹³C labeled bacterial biomass had been subject to degradation is provided by the composition of the ¹³C-THAA pool (Fig. 6.5). Various studies (e.g. Cowie and Hedges, 1992; Keil et al., 2000; Pantoja and Lee, 2003) found that the THAA pool composition of organic matter shows consistent changes during degradation. Therefore, the composition of the THAA pool can be used as an indicator for the extent of organic matter degradation ('diagenetic state') (Dauwe et al., 1999).

The composition of the total sediment THAA pool (i.e. concentrations) remained stable throughout the entire sampling period (data not shown), indicating that the diagenetic state of total sediment organic matter did not change during the experiment. This is consistent with observations that changes in composition of the total sediment THAA pool typically occur at longer time scales since this pool is a mixture of different pools of fresh and degraded organic matter (e.g. Dauwe and Middelburg, 1998). However, the ¹³C-glucose labeling in this study only tagged a specific pool (bacteria active at the time of labeling) within the total sediment organic matter pool (i.e. no bias from other pools). Therefore, changes in composition of the ¹³C-THAA pool appeared at a much shorter time

scale (months) than for the total sediment THAA pool: The relative composition of the ^{13}C -THAA pool remained stable until day 71 (except for some variation during the first few days), indicating that no substantial degradation occurred before day 71 (Fig. 6.5). Conversely, a clear change did occur between days 71 and 136 (Fig. 6.5): the relative abundance of Glu+Phe, D-Ala, Ser, Pro and Gly increased while L-Ala, Asp, Leu and Ile decreased in abundance and Tyr and Thr+Val disappeared completely. This decrease for amino acids like Leu and Ile and the increased relative abundance of Gly and Ser are typical for organic matter degradation (Dauwe and Middelburg, 1998; Dauwe et al., 1999; Keil et al., 2000). Therefore, these changes show that the ^{13}C -THAA pool (i.e. bacterial proteins) had been subject to substantial degradation between days 71 and 136. The relatively sudden shift from predominantly living bacteria at day 71 to clearly degraded bacterial remnants at day 136 is striking. However, available data do not allow further clarification.

When considering the differences in relative abundance at day 136 versus day 6-18 (Fig. 6.5B) in more detail, Gly, and to a lesser extent Ser and Pro, actually showed a considerably stronger increase than D-Ala. The refractory behavior of Gly is generally attributed to its presence in diatom cell walls and/or bacterial peptidoglycan (Dauwe and Middelburg, 1998; Keil et al., 2000). The first can be excluded in this study as we specifically labeled bacterial biomass. If Gly would have accumulated only because of its presence in (refractory) peptidoglycan, one would expect it to show a similar refractory behavior as D-Ala since the latter is unique to peptidoglycan. The fact that the increase for Gly (as well as Ser and Pro) was considerably stronger than for D-Ala (Fig. 6.5B) indicates that another mechanism was involved in the preservation of Gly. Potential mechanisms include the presence of Gly in another bacterial component (more refractory than peptidoglycan) and/or accumulation of Gly as a degradation product (Dauwe and Middelburg, 1998). The latter would involve a similar principle as the one underlying the production of non-protein amino acids (γ -ABA en β -Ala) as degradation products (Lee and Cronin, 1982; Cowie and Hedges, 1994; Keil et al., 2000). This is supported by results of Keil and Fogel (2001) who compared natural abundance $\delta^{13}\text{C}$ values for various HAAs in different pools of marine organic matter and found that $\delta^{13}\text{C}$ values for Gly showed a different behavior than other HAAs and bulk $\delta^{13}\text{C}$. This different behavior was attributed to relatively intensive microbial reworking of Gly. Results from Ziegler and Fogel (2003) suggest that similar mechanisms may apply for Ser, which is consistent with the refractory behavior of Ser in this study (Fig. 6.5B).

In addition, Pro showed a refractory behavior similar to Gly and Ser. Although Pro is usually not included in other studies (since it cannot be measured with typically used HPLC methods), results from a previous (^{15}N labeling) experiment also indicated a refractory behavior of Pro (Veuger et al., 2005). While Gly and Ser are relatively simple amino acids (2 and 3 C atoms, respectively), Pro is a larger (5 C atoms), more complex, secondary amino acid that therefore seems less likely to accumulate as a degradation product like Gly and Ser. This is supported by results from Keil and Fogel (2001) where $\Delta\delta^{13}\text{C}$ values for Pro did not indicate relatively intensive microbial reworking, while values for Gly did. Therefore, it seems most likely that Pro accumulated because it was relatively resistant to degradation (rather than due to accumulation as a degradation product), which might be related to the molecular structure (including a cyclic side group) of this secondary amino acid.

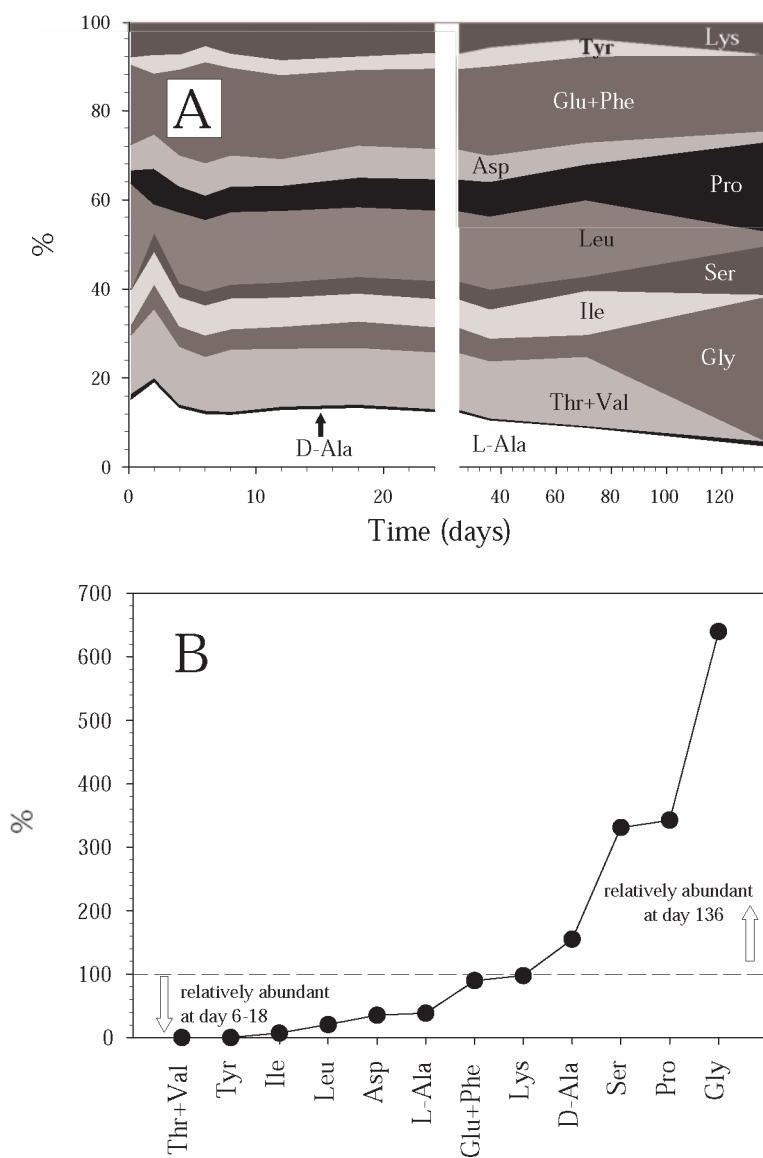


Figure 6.5: A) Relative composition of ^{13}C -THAA pool. B: Comparison of relative abundance of individual ^{13}C -HAAs in ^{13}C -THAA pool for days 6-18 versus day 136. Dashed line at 100 % indicates same abundance at days 6-18 and 136. All amino acids are L-enantiomers, except D-Ala. Glu+Phe and Thr+Val are combined since their GC-c-IRMS peaks overlapped.

6.3.5 Degradation of bacterial proteins versus peptidoglycan

After finding that bacterial ^{13}C -proteins had been subject to substantial degradation, we now discuss how degradation affected ^{13}C -peptidoglycan. A direct comparison of degradation of ^{13}C -labeled proteins versus peptidoglycan is provided by the ^{13}C D/L-Ala

ratio (Fig. 6.2B) where D- and L-Ala represent peptidoglycan and proteins respectively: Until day 71, the excess ^{13}C D/L-Ala ratio remained stable at $\sim 5\%$, which is typical for living marine bacteria (Veuger et al., 2005). This indicates that ^{13}C -D-Ala and ^{13}C -L-Ala (i.e. proteins and peptidoglycan) were mainly present in living (active and dormant) bacteria or intact dead bacteria until day 71. Between day 71 and 136, the excess ^{13}C D/L-Ala ratio increased to 22 %, which means that ^{13}C -L-Ala disappeared faster than ^{13}C -D-Ala. This relative accumulation of D-Ala is consistent with results from various other studies that found increasing D/L-Ala ratios with increasing degradation (McCarthy et al., 1998; Amon et al., 2001; Dittmar et al., 2001) and sediment depth (Pedersen et al., 2001; Grutters et al., 2002). Although preferential degradation of free L-AAs relative to D-AAs has been shown in soils (O'Dowd et al., 1999), our results concern hydrolyzable (i.e. bound) amino acids, meaning that results reflect differences in degradability of the components containing these HAAs. Therefore, the increased ^{13}C D/L-Ala ratio shows that bacterial proteins (L-Ala) were degraded more rapidly than peptidoglycan (D-Ala). Precise quantification of the difference in degradability of peptidoglycan versus total protein is difficult, since the individual protein HAAs showed a range in degradability (Fig. 6.5B). However, the use of L-Ala as a representative for the whole THAA seems justified by its 'average' behavior during degradation (Fig. 6.5). Given the range from Fig. 6.5B, results indicate that the degradability of peptidoglycan was 1.6 to 23 times lower than that of the bacterial proteins (based on Lys and Ile, respectively). This range is consistent with results by Nagata et al. (2003), who found degradation of peptidoglycan in marine waters to be 2 to 21 times lower than that of proteins. Our results confirm the semi-labile character of peptidoglycan (Jorgensen et al., 2003; Nagata et al., 2003), which is thought to be due to the strong bonds in the polysaccharide matrix and the presence of D-Ala and other D-AAs in the peptide cross links, since peptides containing D-AAs cannot be cut with 'common' enzymes that are used to cut 'common' peptides and proteins (Koch, 1990; McCarthy et al., 1998; Nagata et al., 2003).

6.3.6 Importance of peptidoglycan as a long term sink for bacterial ^{13}C

In order to investigate whether the relatively refractory peptidoglycan served as an important long term sink for the bacterial ^{13}C , we compared excess ^{13}C in different bacterial components for freshly labeled bacterial biomass (average for day 6-18) versus the leftovers at day 136 (Fig. 6.6). Total ^{13}C incorporation in living bacteria for day 6-18 is the average estimate from bacteria-specific PLFAs, D-Ala and THAA (see Fig. 6.4). For day 136, this value was estimated from excess ^{13}C in bacteria-specific PLFAs (being an indicator for living bacteria). Subsequently, fractions of ^{13}C -THAA and ^{13}C -D-Ala present in living bacteria were estimated from excess ^{13}C in living bacteria, using the reversed conversion factors from Fig. 6.4. Excess ^{13}C in peptidoglycan was estimated from excess ^{13}C in D-Ala using a conversion factor of $\times 12$ (i.e. C in D-Ala = 8 % of total peptidoglycan-C), which was based on the typical composition of peptidoglycan (containing equal amounts of D-Ala, L-Ala, D-Glu, DAP and the two sugar derivatives NAG and NAM, De Leeuw and Largeau (1993) and Madigan et al. (2000)).

Comparison of excess ^{13}C remaining in the different bacterial components at day 136 with the original excess ^{13}C in freshly labeled bacteria (Fig. 6.6) shows that, at day 136, only $\sim 1\%$ (0.44/39) of the originally labeled bacterial biomass was still present as living bacteria while most of the ^{13}C -THAA and ^{13}C -D-Ala were present in bacterial remnants (87 % and 92 %, respectively). Furthermore, excess ^{13}C in peptidoglycan at day 136

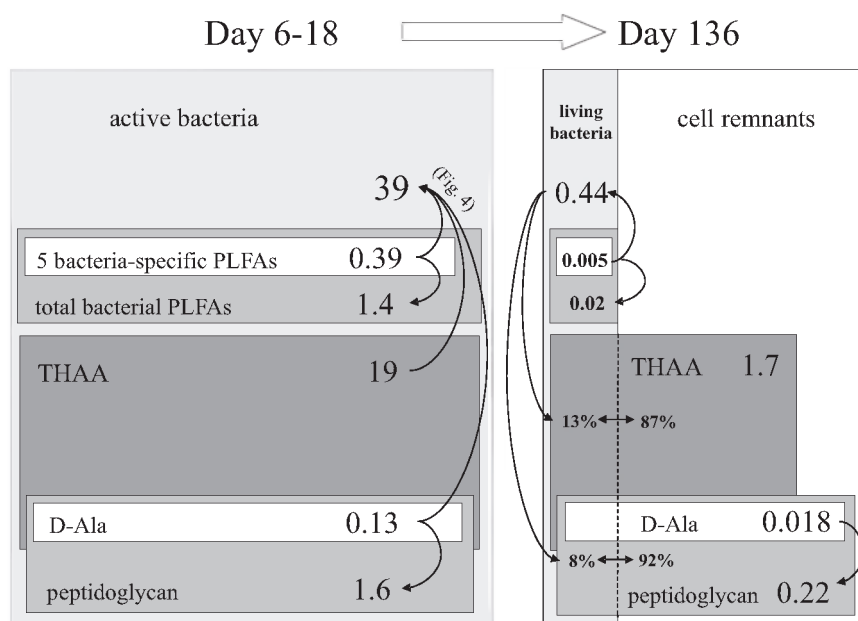


Figure 6.6: Overview of excess ^{13}C ($\text{nmol } ^{13}\text{C gdw}^{-1}$) in different bacterial components at day 6-18 (freshly labeled bacteria) versus day 136 (after degradation). Excess ^{13}C in D-Ala, THAAs and bacteria-specific PLFAs were measured. Excess ^{13}C in active/living bacteria, total bacterial PLFAs and peptidoglycan were estimated using conversion factors from Fig. 6.4.

was only 0.6 % (0.22/39) of the original total bacterial ^{13}C at day 6-18. Even if these estimates are corrected for a 3 times lower degradability of the polysaccharide component of peptidoglycan relative to the peptide component (Nagata et al., 2003), excess ^{13}C in peptidoglycan at day 136 still represented only a very small (< 2 %) fraction of the original bacterial ^{13}C .

6.3.7 Substantial contribution of peptidoglycan to total sediment OC?

Although peptidoglycan did not serve as an important long-term sink for bacterial ^{13}C , it might still have been a relatively important contributor to the total sediment OC pool, since this pool consists of a mixture of fresh organic matter (living bacteria and other organisms) and accumulated leftovers that escaped degradation (enriched in D-Ala/peptidoglycan like the ^{13}C pool at day 136). In addition, further recycling of sediment organic matter by bacteria may further increase the contribution of peptidoglycan to the total sediment OC pool. To test this, we compared different (bacterial) C pools in the sediment using measured concentrations of D-Ala, THAA, bacteria-specific PLFAs and total OC (Fig. 6.7). Carbon in living bacteria and peptidoglycan was estimated from bacteria-specific PLFAs and D-Ala respectively using the same conversion factors as in Fig. 6.4. Estimates were tested for potential bias from 18:1 ω 7c in algae (as discussed before), which was found to be negligible. Unlike for the ^{13}C -THAA pool in Fig. 6.6, the total sediment THAA pool can be derived from various organisms and was therefore not treated as a bacterial-C pool in Fig. 6.7.

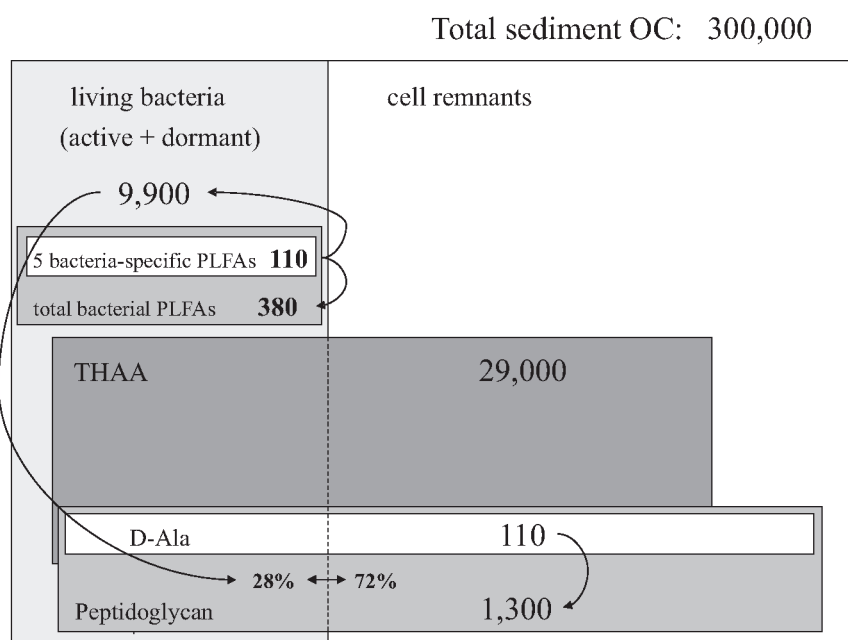


Figure 6.7: Overview of (bacterial) C pools in the whole sediment (averages for day 6-18 in $\mu\text{mol C gdw}^{-1}$). Concentrations of D-Ala, THAAs, bacteria-specific PLFAs and total OC were measured. Total C in living bacteria, total bacterial PLFAs and peptidoglycan as well as the fraction of D-Ala (and peptidoglycan) in living bacteria were estimated using conversion factors from Fig. 6.4.

The overview in Fig. 6.7 shows that living bacteria were only 3.3 % (9,900/300,000) of the total OC in the sediment and that most D-Ala (72 %) was present in cell remnants. The latter is confirmed by the difference between $\Delta\delta^{13}\text{C}$ values for the bacteria-specific PLFAs versus D-Ala (Fig. 6.1), where the 3.5 \times lower values for D-Ala were the result of dilution of ^{13}C -D-Ala in living bacteria by an (unlabeled) background pool of D-Ala from cell remnants (while no such background pool exists for PLFAs given their rapid turnover). The 3.5 \times difference indicates that the background D-Ala pool was 2.5 \times larger than the D-Ala pool in living bacteria. This means that D-Ala in living bacteria was 29 % of total D-Ala, which is very similar to the calculated 28 % in Fig. 6.7. This fraction of D-Ala in living bacteria is larger than the fraction ^{13}C -D-Ala in living bacteria at day 136 (8 %, Fig. 6.6), which is consistent with the total sediment D-Ala pool being a mixture of D-Ala in living bacteria (like ^{13}C -D-Ala at days 6-18) and bacterial remnants (like ^{13}C -D-Ala at day 136).

Figure 6.7 also shows that D-Ala was only ~ 0.4 % (110/29,000) of the THAA pool while THAAs were only ~ 10 % (29,000/300,000) of the total sediment OC pool. The latter is consistent with values for shallow marine sediments reported by Dauwe and Middelburg (1998) and Keil et al. (2000). Together, this means that D-Ala was only ~ 0.04 % of the total sediment OC pool, suggesting that the contribution of peptidoglycan was only ~ 0.5 % (0.04 \times 12). Although these values might be underestimates given the higher degradability for the peptide fraction of peptidoglycan compared to the polysaccharide fraction (Nagata et al., 2003), these results clearly show that peptidoglycan-C was only a minor fraction (< 2 %) of the total sediment OC pool. This low contribution is consistent

with other HAA-based estimates by Keil et al. (2000), Pedersen et al. (2001) and Grutters et al. (2002), who also found peptidoglycan to be only a minor fraction of total sediment organic matter. Moreover, a similar conclusion was drawn by Sinninghe Damsté and Schouten (1997) who used a number of alternative approaches to show that there is no evidence for a substantial contribution of bacterial biomass to sediment OC.

6.4 In summary

1. ^{13}C from ^{13}C -glucose was readily incorporated into the different cellular components of the sediment bacteria, while uptake by other organisms was negligible.
2. Estimates of total bacterial ^{13}C incorporation from excess ^{13}C in bacteria-specific PLFAs, D-Ala and THAAs yielded very similar results, which served as a positive validation of the use of bacteria-specific PLFAs and D-Ala as bacterial biomarkers, and their accompanying conversion factors, to estimate total bacterial incorporation of ^{13}C - and ^{15}N -labeled substrates.
3. ^{13}C -labeled bacterial biomass could be traced up to 136 days and changes in composition of the ^{13}C -THAA pool showed that ^{13}C -bacterial biomass was degraded substantially.
4. Degradation resulted in an increased relative abundance of ^{13}C -D-Ala compared to ^{13}C -L-Ala and ^{13}C -THAAs, indicating that ^{13}C -peptidoglycan was more resistant to degradation than ^{13}C -proteins. However, in spite of the relatively low degradability of peptidoglycan, it did neither serve as an important long term sink for bacterial ^{13}C nor as an important contributor to total sediment OC.

Bibliography

- Aller, R. C. and J. Y. Yingst, 1985. Effects of the marine deposit-feeders *Heteromastus filiformis* (Polychaeta), *Macoma balthica* (Bivalvia), and *Tellina texana* (Bivalvia) on averaged sedimentary solute transport, reaction rates, and microbial distributions. *Journal of Marine Research* **43**: 615–645.
- Alongi, D. M., 1994. The role of bacteria in nutrient recycling in tropical mangrove and other coastal benthic ecosystems. *Hydrobiologia* **285**: 19–32.
- , 1995. Decomposition and recycling of organic matter in muds of the Gulf of Papua, Northern Coral Sea. *Continental Shelf Research* **15**: 1319–1337.
- Alperin, M. J., D. B. Albert, and C. S. Martens, 1994. Seasonal variations in production and consumption rates of dissolved organic carbon in an organic rich coastal sediment. *Geochimica et Cosmochimica Acta* **58**: 4909–4930.
- Amon, R. M. W., H. P. Fitznar, and R. Benner, 2001. Linkages among the bioreactivity, chemical composition, and diagenetic state of marine dissolved organic matter. *Limnology and Oceanography* **46**: 287–297.
- Anderson, T. R., 1992. Modeling the influence of food CN ratio, and respiration on growth and nitrogen excretion in marine zooplankton and bacteria. *Journal of Plankton Research* **14**: 1645–1671.
- Anderson, T. R. and P. J. L. Williams, 1999. A one-dimensional model of dissolved organic carbon cycling in the water column incorporating combined biological-photochemical decomposition. *Global Biogeochemical Cycles* **13**: 337–349.
- Andresen, M. and E. Kristensen, 2002. The importance of bacteria and microalgae in the diet of the deposit-feeding polychaete *Arenicola marina*. *Ophelia* **56**: 179–196.
- Arifin, Z. and L. I. Bendell-Young, 1997. Feeding response and carbon assimilation by the blue mussel *Mytilus trossulus* exposed to environmentally relevant seston matrices. *Marine Ecology Progress Series* **160**: 241–253.
- , 2001. Cost of selective feeding by the blue mussel (*Mytilus trossulus*) as measured by respiration and ammonia excretion rates. *Journal of Experimental Marine Biology and Ecology* **260**: 259–269.
- Armstrong, R. A. and R. McGehee, 1980. Competitive exclusion. *American Naturalist* **115**: 151–170.

Bibliography

- Arnarson, T. S. and R. G. Keil, 2005. Influence of organic-mineral aggregates on microbial degradation of the dinoflagellate *Scrippsiella trochoidea*. *Geochimica et Cosmochimica Acta* **69**: 2111–2117.
- Arnosti, C. and M. Holmer, 1999. Carbohydrate dynamics and contributions to the carbon budget of an organic-rich coastal sediment. *Geochimica et Cosmochimica Acta* **63**: 393–403.
- Athias, V., P. Mazzega, and C. Jeandel, 2000. Selecting a global optimization method to estimate the oceanic particle cycling rate constants. *Journal of Marine Research* **58**: 675–707.
- Azam, F., T. Fenchel, J. G. Field, J. S. Gray, L. A. Meyer-Reil, and F. Thingstad, 1983. The ecological role of water-column microbes in the sea. *Marine Ecology Progress Series* **10**: 257–263.
- Azam, F. and A. Z. Worden, 2004. Microbes, molecules, and marine ecosystems. *Science* **303**: 1622–1624.
- Bachok, Z., P. L. Mfilinge, and M. Tsuchiya, 2003. The diet of the mud clam *Geloina coaxans* (Mollusca, Bivalvia) as indicated by fatty acid markers in a subtropical mangrove forest of Okinawa, Japan. *Journal of Experimental Marine Biology and Ecology* **292**: 187–197.
- Baker, J. H. and L. A. Bradnam, 1976. Role of bacteria in the nutrition of aquatic detritivores. *Oecologia* **24**: 95–104.
- Banse, K. and S. Mosher, 1980. Adult body mass and annual production/biomass relationships of field populations. *Ecological Monographs* **50**: 355–379.
- Benner, R., M. A. Moran, and R. E. Hodson, 1986. Biogeochemical cycling of lignocellulosic carbon in marine and freshwater ecosystems: Relative contributions of procaryotes and eucaryotes. *Limnology and Oceanography* **31**: 89–100.
- Berg, M., P. C. De Ruiter, W. Didden, M. Janssen, T. Schouten, and H. Verhoef, 2001. Community food web, decomposition and nitrogen mineralisation in a stratified Scots pine forest soil. *Oikos* **94**: 130–142.
- Bersier, L. F., C. Banasek-Richter, and M. F. Cattin, 2002. Quantitative descriptors of food-web matrices. *Ecology* **83**: 2394–2407.
- Bird, D. F. and C. M. Duarte, 1989. Bacteria organic-matter relationship in sediments - A case of spurious correlation. *Canadian Journal of Fisheries and Aquatic Sciences* **46**: 904–908.
- Blackburn, T. H. and K. Henriksen, 1983. Nitrogen cycling in different types of sediments from Danish waters. *Limnology and Oceanography* **28**: 477–493.
- Blair, N. E., L. A. Levin, D. J. DeMaster, and G. Plaia, 1996. The short-term fate of fresh algal carbon in continental slope sediments. *Limnology and Oceanography* **41**: 1208–1219.

- Bock, M. J. and D. C. Miller, 1999. Particle selectivity, gut volume, and the response to a step change in diet for deposit-feeding polychaetes. *Limnology and Oceanography* **44**: 1132–1138.
- Boon, A. R., G. C. A. Duineveld, E. M. Berghuis, and J. A. van der Weele, 1998. Relationships between benthic activity and the annual phytopigment cycle in near-bottom water and sediments in the southern North Sea. *Estuarine Coastal and Shelf Science* **46**: 1–13.
- Borch, N. H. and D. L. Kirchman, 1999. Protection of protein from bacterial degradation by submicron particles. *Aquatic Microbial Ecology* **16**: 265–272.
- Boschker, H. T. S., 2004. Linking microbial community structure and functioning: Stable isotope (^{13}C) labeling in combination with PLFA analysis. *In* G. A. Kowalchuk, F. J. De Bruijn, I. M. Head, A. D. Akkermans, and J. D. Van Elsas, eds., *Molecular microbial ecology manual II*. Kluwer Academic Publishers, Dordrecht.
- Boschker, H. T. S., J. F. C. De Brouwer, and T. E. Cappenberg, 1999. The contribution of macrophyte-derived organic matter to microbial biomass in salt-marsh sediments: Stable carbon isotope analysis of microbial biomarkers. *Limnology and Oceanography* **44**: 309–319.
- Boschker, H. T. S. and J. J. Middelburg, 2002. Stable isotopes and biomarkers in microbial ecology. *FEMS Microbiology Ecology* **40**: 85–95.
- Boschker, H. T. S., S. C. Nold, P. Wellsbury, D. Bos, W. De Graaf, R. Pel, R. J. Parkes, and T. E. Cappenberg, 1998. Direct linking of microbial populations to specific biogeochemical processes by ^{13}C -labelling of biomarkers. *Nature* **392**: 801–805.
- Boudreau, B. P., 1999. A theoretical investigation of the organic carbon-microbial biomass relation in muddy sediments. *Aquatic Microbial Ecology* **17**: 181–189.
- Bouillon, S., T. Moens, N. Koedam, F. Dahdouh-Guebas, W. Baeyens, and F. Dehairs, 2004. Variability in the origin of carbon substrates for bacterial communities in mangrove sediments. *FEMS Microbiology Ecology* **49**: 171–179.
- Breed, G. A., G. A. Jackson, and T. L. Richardson, 2004. Sedimentation, carbon export and food web structure in the Mississippi River plume described by inverse analysis. *Marine Ecology Progress Series* **278**: 35–51.
- Brinch-Iversen, J. and G. M. King, 1990. Effects of substrate concentration, growth state, and oxygen availability on relationships among bacterial carbon, nitrogen and phospholipid phosphorus content. *FEMS Microbiology Ecology* **74**: 345–355.
- Burdige, D. J., W. M. Berelson, K. H. Coale, J. McManus, and K. S. Johnson, 1999. Fluxes of dissolved organic carbon from California continental margin sediments. *Geochimica et Cosmochimica Acta* **63**: 1507–1515.
- Burke, R. A., M. Molina, J. E. Cox, L. J. Osher, and M. C. Piccolo, 2003. Stable carbon isotope ratio and composition of microbial fatty acids in tropical soils. *Journal of Environmental Quality* **32**: 198–206.

Bibliography

- Calow, P., 1977. Conversion efficiencies in heterotrophic organisms. *Biological Reviews* **52**: 385–409.
- Cammen, L., 1991. Annual bacterial production in relation to benthic microalgal production and sediment oxygen uptake in an intertidal sandflat and intertidal mudflat. *Marine Ecology Progress Series* **71**: 13–25.
- Cammen, L. M., 1980. The significance of microbial carbon in the nutrition of the deposit feeding polychaete *Nereis succinea*. *Marine Biology* **61**: 9–20.
- Canfield, D. E., B. B. Jorgensen, H. Fossing, R. Glud, J. Gundersen, N. B. Ramsing, B. Thamdrup, J. W. Hansen, L. P. Nielsen, and P. O. J. Hall, 1993. Pathways of organic-carbon oxidation in three continental-margin sediments. *Marine Geology* **113**: 27–40.
- Capriulo, G. M., 1990. Feeding-related ecology of marine protozoa. *In* G. M. Capriulo, ed., *Ecology of marine protozoa*, pp. 186–259. Oxford University Press, New York.
- Carman, K. R., 1990. Mechanisms of uptake of radioactive labels by meiobenthic copepods during grazing experiments. *Marine Ecology Progress Series* **68**: 71–83.
- Cebrian, J., 2004. Role of first-order consumers in ecosystem carbon flow. *Ecology Letters* **7**: 232–240.
- Ceccherelli, V. U. and M. Mistri, 1991. Production of the meiobenthic harpacticoid copepod *Canuella perplexa*. *Marine Ecology Progress Series* **68**: 225–234.
- Chanton, J. and F. G. Lewis, 2002. Examination of coupling between primary and secondary production in a river-dominated estuary: Apalachicola Bay, Florida, USA. *Limnology and Oceanography* **47**: 683–697.
- Chardy, P. and J.-C. Dauvin, 1992. Carbon flows in a subtidal fine sand community from the western English Channel: A simulation analysis. *Marine Ecology Progress Series* **81**: 147–161.
- Chardy, P., P. Gros, H. Mercier, and Y. Monbet, 1993. Benthic carbon budget for the Bay of Saint-Brieuc (Western Channel). Application of inverse method. *Oceanologica Acta* **16**: 687–694.
- Cheng, I. J. and G. R. Lopez, 1991. Contributions of bacteria and sedimentary organic matter to the diet of *Nucula proxima*, a deposit-feeding protobranchiate bivalve. *Ophelia* **34**: 157–170.
- Chisholm, S. W., 2000. Oceanography - Stirring times in the Southern Ocean. *Nature* **407**: 685–687.
- Christensen, V. and D. Pauly, 1992. Ecopath-II - A software for balancing steady-state ecosystem models and calculating network characteristics. *Ecological Modelling* **61**: 169–185.
- Clough, L. M. and G. R. Lopez, 1993. Potential carbon sources for the head down deposit-feeding polychaete *Heteromastus filiformis*. *Journal of Marine Research* **51**: 595–616.

- Cohen, J. E., R. A. Beaver, S. H. Cousins, D. L. Deangelis, L. Goldwasser, K. L. Heong, R. D. Holt, A. J. Kohn, J. H. Lawton, N. Martinez, R. Omalley, L. M. Page, B. C. Patten, S. L. Pimm, G. A. Polis, M. Rejmanek, T. W. Schoener, K. Schoenly, W. G. Sprules, J. M. Teal, R. E. Ulanowicz, P. H. Warren, H. M. Wilbur, and P. Yodzis, 1993. Improving food webs. *Ecology* **74**: 252–258.
- Cole, J. J., S. R. Carpenter, J. F. Kitchell, and M. L. Pace, 2002. Pathways of organic carbon utilization in small lakes: Results from a whole-lake C-13 addition and coupled model. *Limnology and Oceanography* **47**: 1664–1675.
- Conover, R. J., 1961. The turnover of phosphorus by *Calanus finmarchicus*. *Journal of the Marine Biological Association of the United Kingdom* **41**: 484–488.
- , 1966. Factors affecting the assimilation of organic matter by zooplankton and the question of superfluous feeding. *Limnology and Oceanography* **11**: 346–354.
- Cowie, G. L. and J. I. Hedges, 1992. Sources and reactivities of amino acids in a coastal marine environment. *Limnology and Oceanography* **37**: 703–724.
- , 1994. Biochemical indicators of diagenetic alteration in natural organic matter mixtures. *Nature* **369**: 304–307.
- , 1996. Digestion and alteration of the biochemical constituents of a diatom (*Thalassiosira weissflogii*) ingested by an herbivorous zooplankton (*Calanus pacificus*). *Limnology and Oceanography* **41**: 581–594.
- Dauwe, B. and J. J. Middelburg, 1998. Amino acids and hexosamines as indicators of organic matter degradation state in North Sea sediments. *Limnology and Oceanography* **43**: 782–798.
- Dauwe, B., J. J. Middelburg, and P. M. J. Herman, 2001. Effect of oxygen on the degradability of organic matter in subtidal and intertidal sediments of the North Sea area. *Marine Ecology Progress Series* **215**: 13–22.
- Dauwe, B., J. J. Middelburg, P. M. J. Herman, and C. H. R. Heip, 1999. Linking diagenetic alteration of amino acids and bulk organic matter reactivity. *Limnology and Oceanography* **44**: 1809–1814.
- De Leeuw, J. W. and C. Largeau, 1993. A review of macromolecular organic compounds that comprise living organisms and their role in kerogen, coal, and petroleum formation. *In* M. H. Engel and S. A. Macko, eds., *Organic geochemistry: Principles and applications*, pp. 23–72. Plenum Press, New York.
- De Ruiter, P. C., A. M. Neutel, and J. C. Moore, 1995. Energetics, patterns of interaction strengths, and stability in real ecosystems. *Science* **269**: 1257–1260.
- del Giorgio, P. A. and J. J. Cole, 1998. Bacterial growth efficiency in natural aquatic systems. *Annual Review of Ecology and Systematics* **29**: 503–541.
- DeNiro, M. J. and S. Epstein, 1977. Mechanisms of carbon isotope fractionation associated with lipid synthesis. *Science* **197**: 261–263.
- Diehl, S. and M. Feissel, 2001. Intraguild prey suffer from enrichment of their resources: A microcosm experiment with ciliates. *Ecology* **82**: 2977–2983.

Bibliography

- Diffendorfer, J. E., P. M. Richards, G. H. Dalrymple, and D. L. DeAngelis, 2001. Applying linear programming to estimate fluxes in ecosystems or food webs: An example from the herpetological assemblage of the freshwater Everglades. *Ecological Modelling* **144**: 99–120.
- Dittmar, T., H. P. Fitznar, and G. Kattner, 2001. Origin and biogeochemical cycling of organic nitrogen in the eastern Arctic Ocean as evident from D- and L-amino acids. *Geochimica et Cosmochimica Acta* **65**: 4103–4114.
- Dixon, J. L. and C. M. Turley, 2001. Measuring bacterial production in deep-sea sediments using ³H-thymidine incorporation: Ecological significance. *Microbial Ecology* **42**: 549–561.
- Dobbs, F. C., J. B. Guckert, and K. R. Carman, 1989. Comparison of 3 techniques for administering radiolabeled substrates to sediments for trophic studies - Incorporation by microbes. *Microbial Ecology* **17**: 237–250.
- Donali, E., K. Olli, A.-S. Heiskanen, and T. Andersen, 1999. Carbon flow patterns in the planktonic food web of the Gulf of Riga, the Baltic Sea: A reconstruction by the inverse method. *Journal of Marine Systems* **23**: 251–268.
- Eldridge, P. M. and G. A. Jackson, 1993. Benthic trophic dynamics in California coastal basin and continental slope communities inferred using inverse analysis. *Marine Ecology Progress Series* **99**: 115–135.
- Engelberg-Kulka, H. and G. Glaser, 1999. Addiction modules and programmed cell death and antideath in bacterial cultures. *Annual Review of Microbiology* **53**: 43–70.
- Epstein, S. S., 1997a. Microbial food webs in marine sediments. 1. Trophic interactions and grazing rates in two tidal flat communities. *Microbial Ecology* **34**: 188–198.
- , 1997b. Microbial food webs in marine sediments. 2. Seasonal changes in trophic interactions in a sandy tidal flat community. *Microbial Ecology* **34**: 199–209.
- Epstein, S. S., I. V. Burkovsky, and M. P. Shiaris, 1992. Ciliate grazing on bacteria, flagellates, and microalgae in a temperate zone sandy tidal flat: Ingestion rates and food niche partitioning. *Journal of Experimental Marine Biology and Ecology* **165**: 103–125.
- Epstein, S. S. and M. P. Shiaris, 1992. Rates of microbenthic and meiobenthic bacterivory in a temperate muddy tidal flat community. *Applied and Environmental Microbiology* **58**: 2426–2431.
- Fauchald, K. and P. A. Jumars, 1979. The diet of worms: A study of polychaete feeding guilds. *Oceanography and Marine Biology Annual Review* **39**: 193–284.
- Feller, R. J., 1982. Empirical estimates of carbon production for a meiobenthic harpacticoid copepod. *Canadian Journal of Fisheries and Aquatic Sciences* **39**: 1435–1443.
- Fenchel, T., 1982. Ecology of heterotrophic microflagellates. II Bioenergetics and growth. *Marine Ecology Progress Series* **8**: 225–231.
- Fenchel, T., G. M. King, and T. H. Blackburn, 1998. Bacterial biogeochemistry. The ecophysiology of mineral cycling. Academic Press, San Diego.

- Findlay, S., J. Tank, S. Dye, H. M. Valett, P. J. Mulholland, W. H. McDowell, S. L. Johnson, S. K. Hamilton, J. Edmonds, W. K. Dodds, and W. B. Bowden, 2002. A cross-system comparison of bacterial and fungal biomass in detritus pools of headwater streams. *Microbial Ecology* **43**: 55–66.
- Fischer, H., S. C. Wanner, and M. Pusch, 2002. Bacterial abundance and production in river sediments as related to the biochemical composition of particulate organic matter (POM). *Biogeochemistry* **61**: 37–55.
- Fischer, U. R., C. Wieltchnig, A. K. T. Kirschner, and B. Velimirov, 2003. Does virus-induced lysis contribute significantly to bacterial mortality in the oxygenated sediment layer of shallow oxbow lakes? *Applied and Environmental Microbiology* **69**: 5281–5289.
- Fleeger, J. W. and M. A. Palmer, 1982. Secondary production of the estuarine, meiobenthic copepod *Microarthridion littorale*. *Marine Ecology Progress Series* **7**: 157–162.
- Flemming, B. W. and M. T. Delafontaine, 2000. Mass physical properties of muddy intertidal sediments: Some applications, misapplications and non-applications. *Continental Shelf Research* **20**: 1179–1197.
- Fox, J. W. and E. Olsen, 2000. Food web structure and the strength of transient indirect effects. *Oikos* **90**: 219–226.
- Friedrichs, M. A. M., 2002. Assimilation of JGOFS EqPac and SeaWiFS data into a marine ecosystem model of the central equatorial Pacific Ocean. *Deep-Sea Research Part II-Topical Studies in Oceanography* **49**: 289–319.
- Fry, B., 1991. Stable isotope diagrams of freshwater food webs. *Ecology* **72**: 2293–2297.
- Fuhrman, J., 2000. Impact of viruses on bacterial processes. *In* D. L. Kirchman, ed., *Microbial ecology of the oceans*, pp. 327–350. Wiley-Liss, New York.
- Gaedke, U., 1995. A comparison of whole-community and ecosystem approaches (biomass size distributions, food web analysis, network analysis, simulation models) to study the structure, function and regulation of pelagic food webs. *Journal of Plankton Research* **17**: 1273–1305.
- Gaedke, U., S. Hochstadter, and D. Straile, 2002. Interplay between energy limitation and nutritional deficiency: Empirical data and food web models. *Ecological Monographs* **72**: 251–270.
- Gannes, L. Z., D. M. Obrien, and C. M. delRio, 1997. Stable isotopes in animal ecology: Assumptions, caveats, and a call for more laboratory experiments. *Ecology* **78**: 1271–1276.
- Gelman, A., J. B. Carlin, H. S. Stern, and D. B. Rubin, 2003. *Bayesian Data Analysis*. Texts in Statistical Science Series. Chapman & Hall/CRC, Boca Raton.
- Gerlach, S. A., 1971. On the importance of marine meiofauna for benthos communities. *Oecologia* **6**: 176–190.
- , 1978. Food-chain relationships in subtidal silty sand marine sediments and role of meiofauna in stimulating bacterial productivity. *Oecologia* **33**: 55–69.

Bibliography

- Gilks, W. R., S. Richardson, and D. J. Spiegelhalter, 1998. Markov chain Monte Carlo in practice. Chapman & Hall/CRC, Boca Raton.
- Glud, R. N. and M. Middelboe, 2004. Virus and bacteria dynamics of a coastal sediment: Implications for benthic carbon cycling. *Limnology and Oceanography* **49**: 2073–2081.
- Goto, N., T. Kawamura, O. Mitamura, and H. Terai, 1999. Importance of extracellular organic carbon production in the total primary production by tidal-flat diatoms in comparison to phytoplankton. *Marine Ecology Progress Series* **190**: 289–295.
- Graf, G., 1992. Benthic-pelagic coupling - A benthic view. *Oceanography and Marine Biology* **30**: 149–190.
- Grossmann, S. and W. Reichardt, 1991. Impact of *Arenicola marina* on bacteria in intertidal sediments. *Marine Ecology Progress Series* **77**: 85–93.
- Grutters, M., W. van Raaphorst, E. Epping, W. Helder, J. W. de Leeuw, D. P. Glavin, and J. Bada, 2002. Preservation of amino acids from in situ-produced bacterial cell wall peptidoglycans in northeastern Atlantic continental margin sediments. *Limnology and Oceanography* **47**: 1521–1524.
- Hall, R. O. and J. L. Meyer, 1998. The trophic significance of bacteria in a detritus-based stream food web. *Ecology* **79**: 1995–2012.
- Hall, R. O., J. B. Wallace, and S. L. Eggert, 2000. Organic matter flow in stream food webs with reduced detrital resource base. *Ecology* **81**: 3445–3463.
- Hall, S. J. and D. G. Raffaelli, 1993. Food webs - Theory and reality. *Advances in Ecological Research* **24**: 187–239.
- Hamels, I., T. Moens, K. Mutylaert, and W. Vyverman, 2001a. Trophic interactions between ciliates and nematodes from an intertidal flat. *Aquatic Microbial Ecology* **26**: 61–72.
- Hamels, I., K. Muylaert, G. Casteleyn, and W. Vyverman, 2001b. Uncoupling of bacterial production and flagellate grazing in aquatic sediments: A case study from an intertidal flat. *Aquatic Microbial Ecology* **25**: 31–42.
- Hamels, I., K. Sabbe, K. Muylaert, C. Barranguet, C. H. Lucas, P. M. J. Herman, and W. Vyverman, 1998. Organisation of microbenthic communities in intertidal estuarine flats, a case study from the Molenplaat (Westerschelde Estuary, The Netherlands). *European Journal of Protistology* **34**: 308–320.
- Hamels, I., K. Sabbe, K. Muylaert, and W. Vyverman, 2004. Quantitative importance, composition, and seasonal dynamics of protozoan communities in polyhaline versus freshwater intertidal sediments. *Microbial Ecology* **47**: 18–29.
- Hamilton, S. K., J. L. Tank, D. E. Raikow, E. R. Siler, N. J. Dorn, and N. E. Leonard, 2004. The role of instream vs allochthonous N in stream food webs: Modeling the results of an isotope addition experiment. *Journal of the North American Benthological Society* **23**: 429–448.

- Hamilton, S. K., J. L. Tank, D. F. Raikow, W. M. Wollheim, B. J. Peterson, and J. R. Webster, 2001. Nitrogen uptake and transformation in a midwestern US stream: A stable isotope enrichment study. *Biogeochemistry* **54**: 297–340.
- Hart, D., L. Stone, A. Stern, D. Straile, and U. Gaedke, 1997. Methods for constructing and balancing ecosystem flux charts: New techniques and software. *Environmental Modeling and Assessment* **2**: 23–28.
- Hart, D. R., L. Stone, and T. Berman, 2000. Seasonal dynamics of the Lake Kinneret food web: The importance of the microbial loop. *Limnology and Oceanography* **45**: 350–361.
- Hayes, J. M., 2001. Fractionation of carbon and hydrogen isotopes in biosynthetic processes. In J. Valley and D. Cole, eds., *Stable Isotope Geochemistry*, volume 43 of *Reviews in Mineralogy and Geochemistry*, pp. 225–277. Mineralogical Society of America, 1st edition.
- Heip, C., P. M. J. Herman, and A. Coomans, 1982. The productivity of marine meiobenthos. *Academiae Analecta* **44**: 1–20.
- Heip, C., M. Vincx, and G. Vranken, 1985. The ecology of marine nematodes. *Oceanography and Marine Biology Annual Review* **23**: 399–489.
- Heip, C. H. R., N. K. Goosen, P. M. J. Herman, J. Kromkamp, J. J. Middelburg, and K. Soetaert, 1995. Production and consumption of biological particles in temperate tidal estuaries. *Oceanography and Marine Biology Annual Review* **33**: 1–149.
- Henrichs, S. M. and A. Doyle, 1986. Decomposition of ¹⁴C-labelled organic substances in marine sediments. *Limnology and Oceanography* **31**: 765–778.
- Henrichs, S. M. and S. F. Sugai, 1993. Adsorption of amino-acids and glucose by sediments of Resurrection Bay, Alaska, USA - Functional-group effects. *Geochimica et Cosmochimica Acta* **57**: 823–835.
- Herman, P. M. J. and C. Heip, 1985. Secondary production of the harpacticoid copepod *Paronychocamptus nanus* in a brackish-water habitat. *Limnology and Oceanography* **30**: 1060–1066.
- Herman, P. M. J., C. Heip, and B. Guillemijn, 1984. Production of *Tachidius discipes* (Copepoda: Harpacticoida). *Marine Ecology Progress Series* **17**: 271–278.
- Herman, P. M. J., C. Heip, and G. Vranken, 1983. The production of *Cyprideis torosa* Jones 1850 (Crustacea, Ostracoda). *Oecologia* **58**: 326–331.
- Herman, P. M. J., J. J. Middelburg, and C. H. R. Heip, 2001. Benthic community structure and sediment processes on an intertidal flat: Results from the ECOFLAT project. *Continental Shelf Research* **21**: 2055–2071.
- Herman, P. M. J., J. J. Middelburg, J. Van de Koppel, and C. H. R. Heip, 1999. Ecology of estuarine macrobenthos. *Advances in Ecological Research* **29**: 195–240.
- Herman, P. M. J., J. J. Middelburg, J. Widdows, C. H. Lucas, and C. H. R. Heip, 2000. Stable isotopes as trophic tracers: Combining field sampling and manipulative labelling of food resources for macrobenthos. *Marine Ecology Progress Series* **204**: 79–92.

Bibliography

- Herman, P. M. J. and G. Vranken, 1988. Studies of the life-history and energetics of marine and brackish-water nematodes. 2. Production, respiration and food uptake by *Monhystera disjuncta*. *Oecologia* **77**: 457–463.
- Hewson, I. and J. A. Fuhrman, 2003. Viriobenthos production and virioplankton sorptive scavenging by suspended sediment particles in coastal and pelagic waters. *Microbial Ecology* **46**: 337–347.
- Holmes, R. M., B. J. Peterson, L. D. Deegan, J. E. Hughes, and B. Fry, 2000. Nitrogen biogeochemistry in the oligohaline zone of a New England estuary. *Ecology* **81**: 416–432.
- Hondeveld, B. J. M., R. P. M. Bak, and F. C. Van Duyl, 1992. Bacterivory by heterotrophic nanoflagellates in marine sediments measured by uptake of fluorescently labeled bacteria. *Marine Ecology Progress Series* **89**: 63–71.
- Hondeveld, B. J. M., G. Nieuwland, F. C. Van Duyl, and R. P. M. Bak, 1995. Impact of nanoflagellate bacterivory on benthic bacterial production in the North Sea. *Netherlands Journal of Sea Research* **34**: 275–287.
- Hummel, H., R. H. Bogaards, G. Bachelet, F. Caron, J. C. Sola, and C. Aimard-Triquet, 2000. The respiratory performance and survival of the bivalve *Macoma balthica* (L.) at the southern limit of its distribution area: A translocation experiment. *Journal of Experimental Marine Biology and Ecology* **251**: 85–102.
- Ikeda, T., Y. Kanno, K. Ozaki, and A. Shinada, 2001. Metabolic rates of epipelagic marine copepods as a function of body mass and temperature. *Marine Biology* **139**: 587–596.
- Iverson, S. J., C. Field, W. D. Bowen, and W. Blanchard, 2004. Quantitative fatty acid signature analysis: A new method of estimating predator diets. *Ecological Monographs* **74**: 211–235.
- Jackson, G. A. and P. M. Eldridge, 1992. Food web analysis of a planktonic system off Southern California. *Progress in Oceanography* **30**: 223–251.
- Jahnke, R. A. and D. B. Craven, 1995. Quantifying the role of heterotrophic bacteria in the carbon cycle: A need for respiration rate measurements. *Limnology and Oceanography* **40**: 436–441.
- Johnson, J. B. and K. S. Omland, 2004. Model selection in ecology and evolution. *Trends in Ecology & Evolution* **19**: 101–108.
- Jordana, E., F. Charles, A. Gremare, J. M. Amouroux, and M. J. Chretiennot-Dinet, 2001. Food sources, ingestion and absorption in the suspension-feeding polychaete, *Ditrupea arietina* (O.F. Muller). *Journal of Experimental Marine Biology and Ecology* **266**: 219–236.
- Jorgensen, N. O. G., R. Stepanouk, A. G. U. Pedersen, M. Hansen, and O. Nybroe, 2003. Occurrence and degradation of peptidoglycan in aquatic environments. *FEMS Microbiology Ecology* **46**: 269–280.

- Jumars, P. A., D. L. Penry, J. A. Baross, M. J. Perry, and B. W. Frost, 1989. Closing the microbial loop - Dissolved carbon pathway to heterotrophic bacteria from incomplete ingestion, digestion and absorption in animals. *Deep-Sea Research Part I-Oceanographic Research Papers* **36**: 483–495.
- Kasibhatla, P., M. Heimann, P. Rayner, N. Mahowald, R. G. Prinn, and D. E. Hartley, 1999. Inverse methods in global biogeochemical cycles, volume 114 of *AGU Geophysical Monograph Series*. AGU.
- Keil, R. G. and M. L. Fogel, 2001. Reworking of amino acid in marine sediments: Stable carbon isotopic composition of amino acids in sediments along the Washington coast. *Limnology and Oceanography* **46**: 14–23.
- Keil, R. G., E. Tsamakis, and J. I. Hedges, 2000. Early diagenesis of particulate amino acids in marine systems. *In* G. A. Goodfriend, M. J. Collins, M. L. Fogel, S. A. Macko, and J. F. Wehmiller, eds., *Perspectives in amino acid and protein geochemistry*. Oxford University Press, New York.
- Kemp, P. F., 1987. Potential impact on bacteria of grazing by a macrofaunal deposit-feeder, and the fate of bacterial production. *Marine Ecology Progress Series* **36**: 151–161.
- , 1990. The fate of benthic bacterial production. *Aquatic Sciences* **2**: 109–124.
- Kendall, B. E., C. J. Briggs, W. W. Murdoch, P. Turchin, S. P. Ellner, E. McCauley, R. M. Nisbet, and S. N. Wood, 1999. Why do populations cycle? A synthesis of statistical and mechanistic modeling approaches. *Ecology* **80**: 1789–1805.
- Klepper, O. and J. P. G. Van de Kamer, 1987. The use of mass balances to test and improve the estimates of carbon fluxes in an ecosystem. *Mathematical Biosciences* **85**: 37–49.
- , 1988. A definition of the consistency of the carbon budget of an ecosystem, and its application to the Oosterschelde-Estuary, SW Netherlands. *Ecological Modelling* **42**: 217–232.
- Koch, A. L., 1990. Growth and form of the bacterial cell wall. *American Scientist* **78**: 327–340.
- Kones, J., K. Soetaert, D. Van Oevelen, J. O. Owino, and K. Mavuti, Accepted. Gaining insight into food webs reconstructed by the inverse method. *Journal of Marine Systems* .
- Kooijman, S. A. L. M., 2000. *Dynamic energy and mass budgets in biological systems*. Cambridge University Press, Cambridge, 2nd edition.
- Kristensen, E., 1989. Oxygen and carbon dioxide exchange in the polychaete *Nereis virens*: Influence of ventilation activity and starvation. *Marine Biology* **101**: 381–388.
- Lajtha, K. and R. H. Michener, eds., 1994. *Stable isotopes in ecology and environmental science*. Methods in ecology. Blackwell Scientific Publications, Oxford.
- Landry, M. R., R. P. Hassett, V. Fagerness, J. Downs, and C. J. Lorenzen, 1983. Effect of food acclimation on assimilation efficiency of *Calanus pacificus*. *Limnology and Oceanography* **29**: 361–364.

Bibliography

- Langdon, C., 1993. The significance of respiration in production measurements based on oxygen. *ICES Mar. Sci. Symp.* **197**: 69–78.
- Lary, D. J., 1999. Data assimilation: A powerful tool for atmospheric chemistry. *Philosophical Transactions of the Royal Society of London Series A-Mathematical Physical and Engineering Sciences* **357**: 3445–3457.
- Lawson, C. L. and R. J. Hanson, 1995. Solving Least Squares Problems, volume 15 of *Classics in Applied Mathematics*. SIAM, Philadelphia.
- Lawson, L. M., E. E. Hofmann, and Y. H. Spitz, 1996. Time series sampling and data assimilation in a simple marine ecosystem model. *Deep-Sea Research Part II-Topical Studies in Oceanography* **43**: 625–651.
- Lee, C. and C. Cronin, 1982. The vertical flux of particulate organic nitrogen in the sea: Decomposition of amino acids in the Peru upwelling area and the equatorial Atlantic. *Journal of Marine Research* **40**: 227–251.
- Legendre, L. and F. Rassoulzadegan, 1995. Plankton and nutrient dynamics in marine waters. *Ophelia* **41**: 153–172.
- Leguerrier, D., N. Niquil, N. Boileau, J. Rzeznik, P. G. Sauriau, O. Le Moine, and C. Bacher, 2003. Numerical analysis of the food web of an intertidal mudflat ecosystem on the Atlantic coast of France. *Marine Ecology Progress Series* **246**: 17–37.
- Leguerrier, D., N. Niquil, A. Petiau, and A. Bodoy, 2004. Modeling the impact of oyster culture on a mudflat food web in Marennes-Oleron Bay (France). *Marine Ecology Progress Series* **273**: 147–161.
- Lehman, J. T., R. Foy, and D. A. Lehman, 2001. Inverse model method for estimating assimilation by aquatic invertebrates. *Aquatic Sciences* **63**: 168–181.
- Levin, L. A., N. E. Blair, D. J. DeMaster, G. Plaia, W. Fornes, C. Martin, and C. J. Thomas, 1997. Rapid subduction of organic matter by malvanid polychaetes on the North Carolina slope. *Journal of Marine Research* **55**: 595–611.
- Levin, L. A., N. E. Blair, C. M. Martin, D. J. DeMaster, G. Plaia, and C. J. Thomas, 1999. Macrofaunal processing of phytodetritus at two sites on the Carolina margin: In situ experiments using ¹³C-labeled diatoms. *Marine Ecology Progress Series* **182**: 37–54.
- Li, L. N., C. Kato, and K. Horikoshi, 1999. Bacterial diversity in deep-sea sediments from different depths. *Biodiversity and Conservation* **8**: 659–677.
- Lindeman, R. L., 1942. The trophic-dynamic aspect of ecology. *Ecology* **23**: 399–417.
- Loo, L.-O. and R. Rosenberg, 1996. Production and energy budget in marine suspension feeding populations: *Mytilus edulis*, *Cerastoderma edule*, *Mya arenaria* and *Amphiura filiformis*. *Journal of Sea Research* **35**: 199–207.
- Lopez, G. R. and I.-J. Cheng, 1983. Synoptic measurements of ingestion rate, ingestion selectivity, and absorption efficiency of natural foods in the deposit-feeding molluscs *Nucula annulata* (Bivalvia) and *Hydrobia totteni* (Gastropoda). *Marine Ecology Progress Series* **11**: 55–62.

- Lopez, G. R. and J. S. Levinton, 1987. Ecology of deposit-feeding animals in marine sediments. *The Quarterly Review of Biology* **62**: 235–260.
- Lyche, A., T. Andersen, K. Christoffersen, D. O. Hessen, P. H. B. Hansen, and A. Klynsner, 1996a. Mesocosm tracer studies. 1. Zooplankton as sources and sinks in the pelagic phosphorus cycle of a mesotrophic lake. *Limnology and Oceanography* **41**: 460–474.
- , 1996b. Mesocosm tracer studies. 2. The fate of primary production and the role of consumers in the pelagic carbon cycle of a mesotrophic lake. *Limnology and Oceanography* **41**: 475–487.
- MacGinitie, G. E., 1932. The role of bacteria as food for bottom animals. *Science* **76**: 490.
- MacIntyre, H. L., R. J. Geider, and D. C. Miller, 1996. Microphytobenthos: The ecological role of the "secret garden" of unvegetated, shallow-water marine habitats. 1. Distribution, abundance and primary production. *Estuaries* **19**: 186–201.
- Madigan, M. T., M. J. M., and J. Parker, 2000. Brock biology of microorganisms, volume 9th edition. Prentice-Hall.
- Maranger, R. and D. E. Bird, 1996. High concentrations of viruses in the sediments of Lac Gilbert, Quebec. *Microbial Ecology* **31**: 141–151.
- Martin, W. R. and G. T. Banta, 1992. The measurement of sediment irrigation rates - A comparison of the Br⁻ tracer and ²²²Rn/²²⁶Ra disequilibrium techniques. *Journal of Marine Research* **50**: 125–154.
- Mayer, L. M., P. A. Jumars, M. J. Bock, Y.-A. Vetter, and J. L. Schmidt, 2001. Two roads to sparagmos: Extracellular digestion of sedimentary food by bacterial inoculation versus deposit-feeding. *In* J. Y. Aller, S. A. Woodin, and R. C. Aller, eds., *Organism-Sediment Interactions*, pp. 335–347. University of South Carolina Press, Columbia.
- McCann, K., A. Hastings, and G. R. Huxel, 1998. Weak trophic interactions and the balance of nature. *Nature* **395**: 794–798.
- McCarthy, M. D., J. I. Hedges, and R. Benner, 1998. Major bacterial contribution to marine dissolved organic nitrogen. *Science* **281**: 231–234.
- McIntosh, P. C. and S. R. Rintoul, 1997. Do box inverse models work? *Journal of Physical Oceanography* **27**: 291–308.
- Mei, M. L. and R. Danovaro, 2004. Virus production and life strategies in aquatic sediments. *Limnology and Oceanography* **49**: 459–470.
- Meile, C., C. M. Koretsky, and P. Van Kapellen, 2001. Quantifying bioirrigation in aquatic sediments: An inverse modelling approach. *Limnology and Oceanography* **46**: 164–177.
- Menke, W., 1984. Geophysical data analysis: Discrete inverse theory. Academic Press, New York.
- Meyer-Reil, L. A., 1986. Measurement of hydrolytic activity and incorporation of dissolved organic substrates by microorganisms in marine sediments. *Marine Ecology Progress Series* **31**: 143–149.

Bibliography

- Meziane, T., L. Bodineau, C. Retiere, and G. Thoumelin, 1997. The use of lipid markers to define sources of organic matter in sediment and food web of the intertidal salt-marsh-flat ecosystem of Mont-Saint-Michel Bay, France. *Journal of Sea Research* **38**: 47–58.
- Meziane, T. and M. Tsuchiya, 2000. Fatty acids as tracers of organic matter in the sediments and food web of a mangrove/intertidal flat ecosystem, Okinawa, Japan. *Marine Ecology Progress Series* **200**: 49–57.
- Middelboe, M., L. Riemann, G. F. Steward, V. Hansen, and O. Nybroe, 2003. Virus-induced transfer of organic carbon between marine bacteria in a model community. *Aquatic Microbial Ecology* **33**: 1–10.
- Middelburg, J. J., 1989. A simple rate model for organic matter decomposition in marine sediments. *Geochimica et Cosmochimica Acta* **53**: 1577–1581.
- Middelburg, J. J., C. Barranguet, H. T. S. Boschker, P. M. J. Herman, T. Moens, and C. H. R. Heip, 2000. The fate of intertidal microphytobenthos: An in situ ^{13}C labeling study. *Limnology and Oceanography* **45**: 1224–1234.
- Minagawa, M. and E. Wada, 1984. Stepwise enrichment of ^{15}N along food chains: Further evidence and the relation between $\delta^{15}\text{N}$ and animal age. *Geochimica et Cosmochimica Acta* **48**: 1135–1140.
- Moens, T., C. Luyten, J. J. Middelburg, P. M. J. Herman, and M. Vincx, 2002. Tracing organic matter sources of estuarine tidal flat nematodes with stable carbon isotopes. *Marine Ecology Progress Series* **234**: 127–137.
- Moens, T. and M. Vincx, 1997. Observations on the feeding ecology of estuarine nematodes. *Journal of the Marine Biological Association of the United Kingdom* **77**: 211–227.
- Montagna, P. A., 1995. Rates of metazoan meiofaunal microbivory: A review. *Vie Milieu* **45**: 1–9.
- Moodley, L., H. T. S. Boschker, J. J. Middelburg, P. M. J. Herman, E. De Deckere, and C. H. R. Heip, 2000. The ecological significance of benthic Foraminifera: ^{13}C labelling experiments. *Marine Ecology Progress Series* **202**: 289–295.
- Moodley, L., J. J. Middelburg, H. T. S. Boschker, G. C. A. Duineveld, R. Pel, P. M. J. Herman, and C. H. R. Heip, 2002. Bacteria and Foraminifera: Key players in a short-term deep-sea benthic response to phytodetritus. *Marine Ecology Progress Series* **236**: 23–29.
- Moodley, L., J. J. Middelburg, K. Soetaert, H. T. S. Boschker, P. M. J. Herman, and C. H. R. Heip, 2005. Similar rapid response to phytodetritus deposition in shallow and deep-sea sediments. *Journal of Marine Research* **63**: 457–469.
- Moore, J. C., E. L. Berlow, F. C. Coleman, P. C. De Ruiter, Q. Dong, A. Hastings, N. Collins, K. McCann, K. Melville, P. Morin, K. Nadelhoffer, A. Rosemond, D. M. Post, J. Sabo, K. Scow, M. Vanni, and D. Wall, 2004. Detritus, trophic dynamics and biodiversity. *Ecology Letters* **7**: 584–600.

- Muller, W. A. and J. J. Lee, 1969. Apparent indispensability of bacteria in Foraminiferan nutrition. *Journal of Protozoology* **16**: 471–478.
- Nagata, T., B. Meon, and D. L. Kirchman, 2003. Microbial degradation of peptidoglycan in seawater. *Limnology and Oceanography* **48**: 745–754.
- Neira, C. and T. Höpner, 1993. Fecal pellet production and sediment reworking potential of the polychaete *Heteromastus filiformis* show a tide dependent periodicity. *Ophelia* **37**: 175–185.
- , 1994. The role of *Heteromastus filiformis* (Capitellidae, Polychaeta) in organic carbon cycling. *Ophelia* **39**: 55–73.
- Nielsen, A. M., N. T. Eriksen, J. J. L. Iversen, and H. U. Riisgård, 1995. Feeding, growth and respiration in the polychaetes *Nereis diversicolor* (facultative filter-feeder) and *N. virens* (omnivorous) - A comparative study. *Marine Ecology Progress Series* **125**: 149–158.
- Niquil, N., G. A. Jackson, L. Legendre, and B. Delesalle, 1998. Inverse model analysis of the planktonic food web of Takapoto Atoll (French Polynesia). *Marine Ecology Progress Series* **165**: 17–29.
- Nomaki, H., P. Heinz, T. Nakatsuka, M. Shimanaga, and H. Kitazato, 2005. Species-specific ingestion of organic carbon by deep-sea benthic foraminifera and meiobenthos: In situ tracer experiments. *Limnology and Oceanography* **50**: 134–146.
- Novitsky, J. A., 1986. Degradation of dead microbial biomass in a marine sediment. *Applied and Environmental Microbiology* **52**: 504–509.
- O'Dowd, R. W., D. Barraclough, and D. W. Hopkins, 1999. Nitrogen and carbon mineralization in soil amended with D- and L-leucine. *Soil Biology & Biochemistry* **31**: 1573–1578.
- Odum, E. P., 1969. The strategy of ecosystem development. *Science* **164**: 262–279.
- Oksanen, L., S. D. Fretwell, J. Arruda, and P. Niemel, 1981. Exploitation ecosystems in gradients of primary productivity. *American Naturalist* **118**: 240–261.
- Pace, M. L., J. J. Cole, S. R. Carpenter, J. F. Kitchell, J. R. Hodgson, M. C. Van de Bogart, D. L. Bade, E. S. Kritzberg, and D. Bastviken, 2004. Whole-lake carbon-13 additions reveal terrestrial support of aquatic food webs. *Nature* **427**: 240–243.
- Pantoja, S. and C. Lee, 2003. Amino acid remineralization and organic matter lability in Chilean coastal sediments. *Organic Geochemistry* **34**: 1047–1056.
- Parkes, R. J., 1987. Analysis of microbial communities within sediments using biomarkers. *In* M. Hatcher, R. T. G. Gray, and J. G. Jones, eds., *Ecology of microbial communities*, pp. 147–177. Cambridge University Press, Cambridge.
- Parkes, R. J., B. A. Cragg, J. M. Getliff, S. M. Harvey, J. C. Fry, C. A. Lewis, and S. J. Rowland, 1993. A quantitative study of microbial decomposition of biopolymers in recent sediments from the Peru Margin. *Marine Geology* **113**: 55–66.

Bibliography

- Parmelee, R. W., R. S. Wentsel, C. T. Phillips, M. Simini, and R. T. Checkai, 1993. Soil microcosm for testing the effects of chemical-pollutants on soil fauna communities and trophic structure. *Environmental Toxicology and Chemistry* **12**: 1477–1486.
- Paul, J. H., J. B. Rose, S. C. Jiang, C. A. Kellogg, and L. Dickson, 1993. Distribution of viral abundance in the reef environment of Key Largo, Florida. *Applied and Environmental Microbiology* **59**: 718–724.
- Pauly, D., V. Christensen, J. Dalsgaard, R. Froese, and F. Torres, 1998. Fishing down marine food webs. *Science* **279**: 860–863.
- Pearson, T. H., 2001. Functional group ecology in soft-sediment marine benthos: The role of bioturbation. *Oceanography and Marine Biology Annual Review* **39**: 233–267.
- Pedersen, A. G. U., T. R. Thomsen, B. A. Lomstein, and N. O. G. Jorgensen, 2001. Bacterial influence on amino acid enantiomerization in a coastal marine sediment. *Limnology and Oceanography* **46**: 1358–1369.
- Pelz, O., A. Chatzinotas, A. Zarda-Hess, W. R. Abraham, and J. Zeyer, 2001. Tracing toluene-assimilating sulfate-reducing bacteria using ^{13}C -incorporation in fatty acids and whole-cell hybridization. *FEMS Microbiology Ecology* **38**: 123–131.
- Pelz, O., L. A. Cifuentes, B. T. Hammer, C. A. Kelley, and R. B. Coffin, 1998. Tracing the assimilation of organic compounds using $\delta^{13}\text{C}$ analysis of unique amino acids in the bacterial peptidoglycan cell wall. *FEMS Microbiology Ecology* **25**: 229–240.
- Persson, L., D. Claessen, A. M. De Roos, P. Bystrom, S. Sjogren, R. Svanback, E. Wahlstrom, and E. Westman, 2004. Cannibalism in a size-structured population: Energy extraction and control. *Ecological Monographs* **74**: 135–157.
- Peters, R. H., 1983. *The ecological implications of body size*. Cambridge University Press.
- Peterson, B. J. and B. Fry, 1987. Stable isotopes in ecosystem studies. *Annual Review of Ecology and Systematics* **18**: 293–320.
- Peterson, B. J. and R. W. Howarth, 1987. Sulfur, carbon, and nitrogen isotopes used to trace organic matter flow in the salt-marsh estuaries of Sapelo Island, Georgia. *Limnology and Oceanography* **32**: 1195–1213.
- Peterson, B. J., R. W. Howarth, and R. H. Garritt, 1986. Sulfur and carbon isotopes as tracers of salt-marsh organic matter flow. *Ecology* **67**: 865–874.
- Phillips, D. L., 2001. Mixing models in analyses of diet using multiple stable isotopes: A critique. *Oecologia* **127**: 166–170.
- Phillips, D. L. and J. W. Gregg, 2003. Source partitioning using stable isotopes: Coping with too many sources. *Oecologia* **136**: 261–269.
- Pimm, S. L., J. H. Lawton, and J. E. Cohen, 1991. Food web patterns and their consequences. *Nature* **350**: 669–674.
- Plante, C. J., P. A. Jumars, and J. A. Baross, 1989. Rapid bacterial growth in the hindgut of a marine deposit feeder. *Microbial Ecology* **18**: 29–44.

- Plante, C. J. and L. M. Mayer, 1994. Distribution and efficiency of bacteriolysis in the gut of *Arenicola marina* and three additional deposit feeders. *Marine Ecology Progress Series* **109**: 183–194.
- Polis, G. A. and S. D. Hurd, 1996. Linking marine and terrestrial food webs: Allochthonous input from the ocean supports high secondary productivity on small islands and coastal land communities. *American Naturalist* **147**: 396–423.
- Polis, G. A. and D. R. Strong, 1996. Food web complexity and community dynamics. *American Naturalist* **147**: 813–846.
- Pomeroy, L. R., 1974. The ocean's food web, a changing paradigm. *Bioscience* **24**: 499–504.
- Post, D. M., 2002. Using stable isotopes to estimate trophic position: Models, methods, and assumptions. *Ecology* **83**: 703–718.
- Press, W. H., S. A. Teukolsky, W. T. Vetterling, and B. P. Flannery, 1992. *Numerical Recipes in Fortran. The art of scientific computing.* Cambridge University Press, Cambridge, 2nd edition.
- Price, W. L., 1979. A controlled random search procedure for global optimization. *Computer Journal* **20**: 367–370.
- Prunet, P., J. F. Minster, D. Ruiz-Pino, and I. Dadou, 1996. Assimilation of surface data in a one-dimensional physical-biogeochemical model of the surface ocean 1. Method and preliminary results. *Global Biogeochemical Cycles* **10**: 111–138.
- Ricciardi-Rigault, M., D. F. Bird, and Y. T. Prairie, 2000. Changes in sediment viral and bacterial abundances with hypolimnetic oxygen depletion in a shallow eutrophic Lac Brome (Quebec, Canada). *Canadian Journal of Fisheries and Aquatic Sciences* **57**: 1284–1290.
- Richardson, T. L., G. A. Jackson, and A. B. Burd, 2003. Planktonic food web dynamics in two contrasting regions of Florida Bay, US. *Bulletin of Marine Science* **73**: 569–591.
- Richardson, T. L., G. A. Jackson, H. W. Ducklow, and M. R. Roman, 2004. Carbon fluxes through food webs of the eastern equatorial Pacific: An inverse approach. *Deep-Sea Research Part I-Oceanographic Research Papers* **51**: 1245–1274.
- Ritchie, M. E., 1998. Scale-dependent foraging and patch choice in fractal environments. *Evolutionary Ecology* **12**: 309–330.
- Ritchie, M. E. and H. Olff, 1999. Spatial scaling laws yield a synthetic theory of biodiversity. *Nature* **400**: 557–560.
- Robertson, A. I., 1979. The relationship between annual production : biomass ratios and lifespans for marine macrobenthos. *Oecologia* **38**: 193–202.
- Rosenzweig, M. L., 1971. Paradox of enrichment: Destabilization of exploitation ecosystems in ecological time. *Science* **171**: 385–387.

Bibliography

- Rossi, F., P. M. J. Herman, and J. J. Middelburg, 2004. Inter- and intra-specific variation of $\delta^{13}\text{C}$ and $\delta^{15}\text{N}$ in deposit- and suspension-feeding bivalves (*Macoma balthica* and *Cerastoderma edule*): Evidence of ontogenetic changes in feeding mode of *Macoma balthica*. *Limnology and Oceanography* **49**: 408–414.
- Ryther, J. H., 1969. Photosynthesis and fish production in the sea. *Science* **166**: 72–76.
- Saager, P. M., J. P. Sweerts, and H. J. Ellermeijer, 1990. A simple pore-water sampler for coarse, sandy sediments of low porosity. *Limnology and Oceanography* **35**: 747–751.
- Sander, B. C. and J. Kalff, 1993. Factors controlling bacterial production in marine and freshwater sediments. *Microbial Ecology* **26**: 79–99.
- Sawyer, T. E. and G. M. King, 1993. Glucose uptake and end-product formation in an intertidal marine sediment. *Applied and Environmental Microbiology* **59**: 120–128.
- Schallenberg, M. and J. Kalff, 1993. The ecology of sediment bacteria in lakes and comparisons with other aquatic ecosystems. *Ecology* **74**: 919–934.
- Scheffer, M., 2001. Climatic warming causes regime shifts in lake food webs. *Limnology and Oceanography* **46**: 1780–1783.
- Schiemer, F., 1982. Food dependence and energetics of freeliving nematodes 1. Respiration, growth and reproduction of *Caenorhabditis briggsae* (Nematoda) at different levels of food supply. *Oecologia* **54**: 108–121.
- , 1983. Comparative aspects of food dependence and energetics of freeliving nematodes. *Oikos* **41**: 32–42.
- Schiemer, F., A. Duncan, and R. Z. Klekowski, 1980. A bioenergetic study of a benthic nematode, *Plectus palustris* de Man 1880, throughout its life cycle. *Oecologia* **44**: 205–212.
- Schluter, M., E. Sauter, H. P. Hansen, and E. Suess, 2000. Seasonal variations of bioirrigation in coastal sediments: Modelling of field data. *Geochimica et Cosmochimica Acta* **64**: 821–834.
- Schmidt, J. L., J. W. Deming, P. A. Jumars, and R. G. Keil, 1998. Constancy of bacterial abundance in surficial marine sediments. *Limnology and Oceanography* **43**: 976–982.
- Schwinghamer, P., 1981. Characteristic size distributions of integral benthic communities. *Canadian Journal of Fisheries and Aquatic Sciences* **38**: 1255–1263.
- Schwinghamer, P., B. Hargrave, D. Peer, and C. M. Hawkins, 1986. Partitioning of production and respiration among size groups of organisms in an intertidal benthic community. *Marine Ecology Progress Series* **31**: 131–142.
- Sherr, E. B., 1988. Direct use of high molecular-weight polysaccharide by heterotrophic flagellates. *Nature* **335**: 348–351.
- Silfer, J. A., M. H. Engel, S. A. Macko, and E. J. Jumeau, 1991. Stable carbon isotope analysis of amino acid enantiomers by conventional isotope ratio mass spectrometry and combined gas chromatography isotope ratio mass spectrometry. *Analytical Chemistry* **63**: 370–374.

- Sinninghe Damsté, J. S. and S. Schouten, 1997. Is there evidence for a substantial contribution of prokaryotic biomass to organic carbon in Phanerozoic carbonaceous sediments? *Organic Geochemistry* **26**: 517–530.
- Sleigh, M. A. and M. V. Zubkov, 1998. Methods of estimating bacterivory by protozoa. *European Journal of Protistology* **34**: 273–280.
- Smith, K. L., 1973. Respiration of a sublittoral community. *Ecology* **54**: 1065–1075.
- Sobczak, W. V., J. E. Cloern, A. D. Jassby, and A. B. Muller-Solger, 2002. Bioavailability of organic matter in a highly disturbed estuary: The role of detrital and algal resources. *Proceedings of the National Academy of Sciences of the United States of America* **99**: 8101–8105.
- Soetaert, K., V. deClijpele, and P. M. J. Herman, 2002. FEMME, a flexible environment for mathematically modelling the environment. *Ecological Modelling* **151**: 177–193.
- Soetaert, K., M. Vincx, J. Wittoeck, and M. Tulkens, 1995. Meiobenthic distribution and nematode community structure in 5 European estuaries. *Hydrobiologia* **311**: 185–206.
- Sprung, M., 1993. Estimating macrobenthic secondary production from body weight and biomass: A field test in a non-boreal intertidal habitat. *Marine Ecology Progress Series* **100**: 103–109.
- Starink, M., I. N. Krylova, M. J. Bargilissen, R. P. M. Bak, and T. E. Cappenberg, 1994. Rates of benthic protozoan grazing on free and attached sediment bacteria measured with fluorescently stained sediment. *Applied and Environmental Microbiology* **60**: 2259–2264.
- Steele, J. H., 1974. *The structure of marine ecosystems*. Cambridge University Press, Cambridge.
- Steele, J. H. and E. W. Henderson, 1992. The role of predation in plankton models. *Journal of Plankton Research* **14**: 157–172.
- Sterner, R. and J. Elser, 2002. *Ecological Stoichiometry. The biology of elements from molecules to the biosphere*. Princeton University Press, Princeton Oxfordshire.
- Steyaert, M., J. Vanaverbeke, A. Vanreusel, C. Barranguet, C. Lucas, and M. Vincx, 2003. The importance of fine-scale, vertical profiles in characterising nematode community structure. *Estuarine Coastal and Shelf Science* **58**: 353–366.
- Stone, L., T. Berman, R. Bonner, S. Barry, and S. W. Weeks, 1993. Lake Kinneret: A seasonal model for carbon flux through the planktonic biota. *Limnology and Oceanography* **38**: 1680–1695.
- Straile, D., 1997. Gross growth efficiencies of protozoan and metazoan zooplankton and their dependence on food concentration, predator-prey weight ratio, and taxonomic group. *Limnology and Oceanography* **42**: 1375–1385.
- Sun, N.-Z., 1994. Inverse problems in groundwater modeling, volume 6 of *Theory and applications of transport in porous media*. Kluwer academic publishers.

Bibliography

- Sundback, K., P. Nilsson, C. Nilsson, and B. Jonsson, 1996. Balance between autotrophic and heterotrophic components and processes in microbenthic communities of sandy sediments: A field study. *Estuarine Coastal and Shelf Science* **43**: 689–706.
- Talin, F., C. Tolla, C. Rabouille, and J. C. Poggiale, 2003. Relations between bacterial biomass and carbon cycle in marine sediments: An early diagenetic model. *Acta Biotheoretica* **51**: 295–315.
- Tank, J. L., J. L. Meyer, D. M. Sanzone, P. J. Mulholland, J. R. Webster, B. J. Peterson, S. A. Woodin, and N. E. Leonard, 2000. Analysis of nitrogen cycling in a forest stream during autumn using a ¹⁵N-tracer addition. *Limnology and Oceanography* **45**: 1013–1029.
- Teal, J. M., 1962. Energy flow in the salt marsh ecosystem of Georgia. *Ecology* **43**: 614–649.
- Teece, M. A., M. L. Fogel, M. E. Dollhopf, and K. H. Nealson, 1999. Isotopic fractionation associated with biosynthesis of fatty acids by a marine bacterium under oxic and anoxic conditions. *Organic Geochemistry* **30**: 1571–1579.
- Thompson, M. L. and L. C. Schaffner, 2001. Population biology and secondary production of the suspension feeding polychaete *Chaetopterus* cf. *variopedatus*: Implications for benthic-pelagic coupling in lower Chesapeake Bay. *Limnology and Oceanography* **46**: 1899–1907.
- Tobias, C. R., M. Cieri, B. J. Peterson, L. A. Deegan, J. Vallino, and J. Hughes, 2003. Processing watershed-derived nitrogen in a well-flushed New England estuary. *Limnology and Oceanography* **48**: 1766–1778.
- Tobias, C. R., S. A. Macko, I. C. Anderson, E. A. Canuel, and J. W. Harvey, 2001. Tracking the fate of a high concentration groundwater nitrate plume through a fringing marsh: A combined groundwater tracer and in situ isotope enrichment study. *Limnology and Oceanography* **46**: 1977–1989.
- Toolan, T., 2001. Coulometric carbon-based respiration rates and estimates of bacterioplankton growth efficiencies in Massachusetts Bay. *Limnology and Oceanography* **46**: 1298–1308.
- Torsvik, V., R. Sorheim, and J. Goksoyr, 1996. Total bacterial diversity in soil and sediment communities - A review. *Journal of Industrial Microbiology* **17**: 170–178.
- Tsuchiya, M. and Y. Kurihara, 1979. The feeding habits and food sources of the deposit feeding polychaete, *Neanthes japonica* (Izuka). *Journal of Experimental Marine Biology and Ecology* **36**: 79–89.
- Ulanowicz, R. E., 1986. *Growth and Development: Ecosystems Phenomenology*. Springer-Verlag, New York.
- Underwood, G. J. C. and J. Kromkamp, 1999. Primary production by phytoplankton and microphytobenthos in estuaries. *Advances in Ecological Research* **29**: 93–153.
- Vallino, J. J., 2000. Improving marine ecosystem models: Use of data assimilation and mesocosm experiments. *Journal of Marine Research* **58**: 117–164.

- Van de Koppel, J., P. M. J. Herman, P. Thoolen, and C. H. R. Heip, 2001. Do alternate stable states occur in natural ecosystems? Evidence from a tidal flat. *Ecology* **82**: 3449–3461.
- Van den Meersche, K., J. J. Middelburg, K. Soetaert, P. Van Rijswijk, H. T. S. Boschker, and C. H. R. Heip, 2004. Carbon-nitrogen coupling and algal-bacterial interactions during an experimental bloom: Modeling a ^{13}C tracer experiment. *Limnology and Oceanography* **49**: 862–878.
- Van Duyl, F. C. and A. J. Kop, 1990. Seasonal patterns of bacterial production and biomass in intertidal sediments of the western Dutch Wadden Sea. *Marine Ecology Progress Series* **29**: 249–261.
- Vander Zanden, M. J. and J. B. Rasmussen, 1999. Primary consumer $\delta^{13}\text{C}$ and $\delta^{15}\text{N}$ and the trophic position of aquatic consumers. *Ecology* **80**: 1395–1404.
- Vanni, M. J., 2002. Nutrient cycling by animals in freshwater ecosystems. *Annual Review of Ecology and Systematics* **33**: 341–370.
- Vedel, A. and H. U. Riisgård, 1993. Filter-feeding in the polychaete *Nereis diversicolor* - growth and bioenergetics. *Marine Ecology Progress Series* **100**: 145–152.
- Verity, P. G., 1985. Grazing, respiration, excretion, and growth rates of tintinnids. *Limnology and Oceanography* **30**: 1268–1282.
- Veuger, B., J. J. Middelburg, H. T. S. Boschker, and M. Houtekamer, 2005. Analysis of ^{15}N incorporation into D-alanine: A new method for tracing nitrogen uptake by bacteria. *Limnology and Oceanography: Methods* **3**: 230–240.
- Vézina, A. F., F. Berreville, and S. Loza, 2004. Inverse reconstructions of ecosystem flows in investigating regime shifts: Impact of the choice of objective function. *Progress in Oceanography* **60**: 321–341.
- Vézina, A. F., S. Demers, I. Laurion, T. Sime-Ngando, S. K. Juniper, and L. Devine, 1997. Carbon flows through the microbial food web of first-year ice in Resolute Passage (Canadian High Arctic). *Journal of Marine Systems* **11**: 173–189.
- Vézina, A. F. and M. L. Pace, 1994. An inverse model analysis of planktonic food webs in experimental lakes. *Canadian Journal of Fisheries and Aquatic Sciences* **51**: 2034–2044.
- Vézina, A. F. and M. Pahlow, 2003. Reconstruction of ecosystem flows using inverse methods: How well do they work? *Journal of Marine Systems* **40**: 55–77.
- Vézina, A. F. and T. Platt, 1988. Food web dynamics in the ocean. I. Best-estimates of flow networks using inverse methods. *Marine Ecology Progress Series* **42**: 269–287.
- Vézina, A. F. and C. Savenkoff, 1999. Inverse modeling of carbon and nitrogen flow in the pelagic food web of the northeast subarctic Pacific. *Deep-Sea Research II* **46**: 2909–2939.
- Vézina, A. F., C. Savenkoff, S. Roy, B. Klein, R. Rivkin, J.-C. Therriault, and L. Legendre, 2000. Export of biogenic carbon and structure and dynamics of the pelagic food web in the Gulf of St. Lawrence Part 2. Inverse analysis. *Deep-Sea Research II* **47**: 609–635.

Bibliography

- Vidal, J., 1980. Physiology of zooplankton. IV. Effects of phytoplankton concentration, temperature, and body size on the net production efficiency of *Calanus pacificus*. *Marine Biology* **56**: 203–211.
- Vranken, G. and C. Heip, 1986. The productivity of marine nematodes. *Ophelia* **26**: 429–442.
- Vranken, G., P. M. J. Herman, and C. Heip, 1986. A re-evaluation of marine nematode productivity. *Hydrobiologia* **135**: 193–196.
- Wang, B., X. L. Zou, and J. Zhu, 2000. Data assimilation and its applications. *Proceedings of the National Academy of Sciences of the United States of America* **97**: 11143–11144.
- Weinbauer, M. G., 2004. Ecology of prokaryotic viruses. *FEMS Microbiology Reviews* **28**: 127–181.
- Westrich, J. T. and R. A. Berner, 1984. The role of sedimentary organic matter in bacterial sulfate reduction: The G model tested. *Limnology and Oceanography* **29**: 236–249.
- Widdows, J., A. Blauw, C. H. R. Heip, P. M. J. Herman, C. H. Lucas, J. J. Middelburg, S. Schmidt, M. D. Brinsley, F. Twisk, and H. Verbeek, 2004. Role of physical and biological processes in sediment dynamics of a tidal flat in Westerschelde Estuary, SW Netherlands. *Marine Ecology Progress Series* **274**: 41–56.
- Widdows, J., M. D. Brinsley, P. N. Salkeld, and C. H. Lucas, 2000. Influence of biota on spatial and temporal variation in sediment erodability and material flux on a tidal flat (Westerschelde, The Netherlands). *Marine Ecology Progress Series* **194**: 23–37.
- Wieltschnig, C., A. K. T. Kirschner, A. Steitz, and B. Velimirov, 2001. Weak coupling between heterotrophic nanoflagellates and bacteria in a eutrophic freshwater environment. *Microbial Ecology* **42**: 159–167.
- Wild, C., H. Roy, and M. Huettel, 2005. Role of pelletization in mineralization of fine-grained coastal sediments. *Marine Ecology Progress Series* **291**: 23–33.
- Witte, U., F. Wenzhofer, S. Sommer, A. Boetius, P. Heinz, N. Aberle, M. Sand, A. Cremer, W. R. Abraham, B. B. Jorgensen, and O. Pfannkuche, 2003. In situ experimental evidence of the fate of a phytodetritus pulse at the abyssal sea floor. *Nature* **424**: 763–766.
- Wolfstein, K., J. F. C. de Brouwer, and L. J. Stal, 2002. Biochemical partitioning of photosynthetically fixed carbon by benthic diatoms during short-term incubations at different irradiances. *Marine Ecology Progress Series* **245**: 21–31.
- Woombs, M. and J. Laybourn-Parry, 1984. Feeding biology of *Diplogasteritus nudicapitatus* and *Rhabditis curvicaudata* (Nematoda) related to food concentration and temperature, in sewage treatment plants. *Oecologia* **64**: 163–167.
- , 1985. Energy partitioning in three species of nematode from polysaprobic environments. *Oecologia* **65**: 289–295.
- Wunsch, C., 1978. The North Atlantic general circulation west of 50°W determined by inverse methods. *Reviews of Geophysics and Space Physics* **16**: 583–620.

- , 1996. The ocean circulation inverse problem. Cambridge University Press, New York.
- Wunsch, C. and J. F. Minster, 1982. Methods for box models and ocean circulation tracers: Mathematical programming and nonlinear inverse theory. *Journal of Geophysical Research* **87**: 5647–5662.
- Yarmolinsky, M. B., 1995. Programmed cell death in bacterial populations. *Science* **267**: 836–837.
- Ziegler, S. E. and M. L. Fogel, 2003. Seasonal and diel relationships between the isotopic compositions of dissolved and particulate organic matter in freshwater ecosystems. *Biogeochemistry* **64**: 25–52.
- ZoBell, C. E., 1938. Studies on the bacterial flora of marine bottom sediments. *Journal of Sedimentary Petrology* **8**: 10–18.
- ZoBell, C. E. and C. B. Feltham, 1937. Bacteria as food for certain marine invertebrates. *Journal of Marine Research* **4**: 312–327.
- Zubkov, M. V. and M. A. Sleight, 1999. Growth of amoebae and flagellates on bacteria deposited on filters. *Microbial Ecology* **37**: 107–115.

Summary

The rich benthic community of estuarine and coastal sediments thrives in an environment where organic carbon inputs of different origins are diluted with inedible sediment particles. Our knowledge on how the different carbon inputs are partitioned within the benthic community is limited, because of the intractability of the benthic environment, in particular due to difficulties with accessibility and sampling, and high heterogeneity. In this thesis, we combine stable isotope techniques with quantitative modeling approaches to gain additional insight in the structure of marine benthic food webs.

Chapter 2 is a review of applications of linear inverse modeling (LIM); a data assimilation technique that is used to reconstruct food web flows from incomplete data sets. The review discusses three aspects.

First, we make explicit account of the different elements that form a LIM: 1) five types of ecological information, 2) three linear equations and 3) two optimization norms. Differences among LIM applications can be explained by differences in the way these elements are combined, which can be translated to 1) a different appraisal of the quality of different information types and 2) differences in the chosen optimization norm.

Second, common practice in ecological modeling is to solve the LIM and discuss the results in terms of the food web flows. Typically, no or only limited attention is paid to the properties of the LIM solution. Five LIMs of food webs that differ in number of food web compartments, flows and available data were investigated with especial emphasis on the properties of their solutions. Strikingly, it appeared that the uncertainty surrounding the recovered flows was high. However, the uncertainty clearly differed among the LIMs and were directly related to the ratio of data to number of food web flows, the lower this ratio the higher the uncertainty. Moreover, it appeared that the linear optimization criteria did not always lead to one unique solution, but several alternative solutions may exist. Since the quadratic optimization criterium should always lead to a unique optimal solution, we recommend the use of this criterium in future studies. The gained insights in LIM problems showed that the analysis of the LIM solution is valuable and should be routinely included in LIM food web studies.

Finally, the large uncertainty in the reconstructed food webs pinpoints to the need for additional data resources that may reduce this uncertainty. We demonstrate that stable isotope signatures were very successful in reducing the uncertainty of the food web flows of a benthic food web (Chapter 3). Other data types, such as ecological stoichiometry and quantitative fatty acid signature data, are expected to be similarly effective and we suggest that LIM offers a ideal platform to integrate traditional data types (e.g. biomass data) with these modern data types to reduce the uncertainty in food web reconstructions.

Chapter 3 is a case-study of LIM to recover the carbon flows in an intertidal sediment. Conventional LIM methodology accommodates data on biomass and total carbon processing (e.g. primary production, community respiration). In this chapter we

Summary

extended the existing methodology such that natural abundance and tracer stable isotope data can also be added. Dedicated uncertainty analysis clearly demonstrated that these data additions decreased the uncertainty in the recovered food web: the uncertainty range for 60% of the flows decreased with > 50%. Moreover, the conventional methodology uses a minimization criterium to solve the inverse model, this criterium has been questioned because it lacks a biological justification and introduces a bias in the reconstruction. In the extended methodology, the model is solved by assimilating tracer isotope data and therefore makes the arbitrary minimization criterium redundant.

Carbon flows in the intertidal food web were dominated by bacteria, both in terms of secondary production and respiration. Bacteria acquired carbon predominantly (85 %) from semi-labile detritus and the remainder from dissolved organic carbon. Only a limited fraction (9 %) of the bacterial carbon production was grazed by the benthos, the remainder was recycled back to detritus and dissolved organic carbon. Microbenthos was the second contributor to total secondary production. Its dominant carbon sources were detritus or dissolved organic carbon, the results from the inverse model did however not allow to quantify the importance of the sources individually. Surprisingly, bacteria contributed only a few percent to the total carbon requirements of microbenthos. Larger benthos, consisting of nematodes, meiobenthos and macrobenthos, fed selectively and relied primarily on microphytobenthos and phytoplankton. Surprisingly, detritivory was negligible for these larger benthic fauna. These observations suggest that the microbial community (i.e. bacteria and possibly microbenthos) is supported by semi-labile detritus with limited transfer to higher trophic levels, whereas local primary production by microphytobenthos and phytoplankton supported the meiobenthic and macrobenthic communities. This separation suggested that the detrital-microbial and algal-grazer pathways function rather autonomously.

Chapter 4 builds on the conclusion from chapter 3 that only a limited fraction of bacterial carbon production is grazed by the benthic community, but instead recycles back to detritus or dissolved organic carbon. This chapter reports on a dedicated in situ isotope labeling study that was conducted to quantify the fate of bacterial carbon in sediments on a time scale ranging from days to months. ^{13}C -glucose was injected in the surface 10 cm of an intertidal sediment and traced into specific bacterial polar-lipid-derived fatty acid (PLFA) biomarkers, particulate organic carbon (POC), dissolved inorganic carbon (DIC), meiobenthos and macrobenthos. A dynamic model describing the C and ^{13}C transfers in the sediment was successfully fitted to the C and ^{13}C observations of the different compartments. The model output was subsequently used to recover total bacterial carbon production and the importance of its potential fates: grazing, resuspension or recycling to dissolved organic carbon.

The model contained parameters describing bacterial growth, bacterial grazing, resuspension and growth efficiency. The values of these parameters were used in a published mechanistic relation that predicts the ratio $\frac{\text{bacterial carbon}}{\text{particulate organic carbon}}$. The ratio prediction based on the model parameter was 0.005, and compared reasonably, although at the lower end, with the observed ratios (0.005 - 0.24). This correspondence suggests that mechanistic modeling may be used to model bacterial carbon dynamics, rather than the statistical regression models that are more commonly employed.

Total bacterial production was $67 \text{ mmol C m}^{-2} \text{ d}^{-1}$. The primary fate of bacterial production was mortality, accounting for 65 % of the bacterial production, thus forming a recycling carbon in the bacteria - dissolved organic carbon loop. The major loss from this loop is bacterial respiration. Grazing of bacteria by meiobenthos (3 %) and macrobenthos (24 %) accounted for 27 % of the bacterial production. Due to the high meiobenthic and

macrobenthic biomass at the study site, we surmise that grazing pressure is high when compared to other systems. Therefore grazing on bacteria by benthos is not expected to be a major controlling factor of bacterial biomass in marine sediments.

The results from this experiment were also used in chapters 5 and 6.

Chapter 5 aims to answer the question: How much of their carbon requirements do intertidal meiobenthos and macrobenthos derive from bacterial carbon? To answer this question, the bacterial community in an intertidal sediment was labeled with ^{13}C , following the injection of ^{13}C -glucose. The appearance of label in bacteria (based on label incorporation in bacterial-specific phospholipid-derived fatty acids) and subsequent transfer to meiobenthos (group level) and macrobenthos (species level) was followed over a period of 36 days. The label dynamics of the benthos were either fitted with a simple isotope model or evaluated against enrichment of bacteria, to derive the importance of bacteria in the carbon budget of the meiobenthic and macrobenthic community. Bacteria constituted a maximum of 20 % and generally < 10 % of total carbon demands of the different members of the meiobenthic and macrobenthic community. Therefore the trophic significance of bacterial carbon for intertidal meiobenthos and macrobenthos is limited.

The amount of labile carbon usually decreases with sediment depth. We therefore hypothesized that deeper dwelling benthos relies more on labile bacterial carbon than surface dwelling benthos that have direct access to other labile carbon sources. Contrary to this hypothesis, meiobenthos and macrobenthos living deeper in the sediment did not show a comparatively higher dependence on bacterial carbon. Possibly, benthic fauna cannot process sediment particles, with attached bacterial community, quickly enough to exploit the present bacterial carbon to a greater extent. If one assumes indiscriminate feeding on a homogeneous mix of sediment and bacteria, the expected removal of bacterial carbon at our study site is $0.36\% \text{ d}^{-1}$. The resulting carbon flows is well below the maintenance requirements of benthic fauna, and therefore we expect that bacterivory is limited by the processing rates of sediment particles. However, our observations do show that $6\times$ more bacterial carbon is removed than expected from indiscriminate feeding, which clearly demonstrates selective feeding by benthic fauna.

Bacteria assimilate and respire both fresh and semi-labile organic carbon. The low dependence on bacterial carbon suggests that benthic fauna competes with bacteria for labile organic carbon, as labile carbon assimilated by bacteria is effectively lost for the faunal food web. Alternatively however, ingestion of bacteria might provide a means through which otherwise indigestible semi-labile detrital organic matter might enter the metazoan food web. Local circumstances, in particular the availability of labile organic carbon, will determine whether competition or subsidy dominates. The weak interaction between bacteria and benthic fauna implies that this interaction should not be viewed as a predatory, but as a competitive interaction for labile organic matter in the benthic food web.

In chapter 4 the most important fate of benthic bacterial carbon production was found to be mortality (65 %). Bacteria are made up of different compounds that different degrees of degradability, which may result in a build up of refractory compounds in the sediment. In **chapter 6** we evaluate the results from a ^{13}C -glucose labeling experiment and compared ^{13}C of different bacterial biomarkers. Polar-lipid-derived fatty acids (PLFAs) rapidly degrade in sediments and were therefore used as a marker for living bacteria. D-alanine (D-Ala) is a compound unique to peptidoglycan, a constituent of bacterial cell walls, which is known for its refractory nature. Therefore, D-Alanine is used as a marker for both living bacteria and bacterial remnants. Finally, since label uptake was dominated by bacteria, the label dynamics of individual amino acids (AAs) were assumed to be derived from bacteria

Summary

and were compared with amino acids that have been used as markers to quantify organic matter quality.

Dynamics in $\Delta\delta^{13}\text{C}$ were very similar for PLFAs, D-Alanine and AA in the first weeks after labeling, indicating simultaneous production of the different biomarkers, which is expected when new bacterial cells are produced. Levels of $\Delta\delta^{13}\text{C}$ were however lower for D-Ala and THAAs as compared to PLFAs, presumably due to the presence of an inactive background pool for D-ala and THAA that dilutes the $\Delta\delta^{13}\text{C}$ signal of the living bacteria.

Surprisingly however, the $\Delta\delta^{13}\text{C}$ dynamics were similar during the 4.5 months after labeling. If burial would have been an important sink of bacterial carbon, $\Delta\delta^{13}\text{C}$ values of D-Ala and some AAs are expected to be relatively higher when compared to PLFAs. The correspondence in $\Delta\delta^{13}\text{C}$ values between D-Ala and PLFAs therefore implies that burial of comparatively recalcitrant bacterially derived compounds is not a major sink of bacterial carbon. This is further indicated by the low contribution (< 1 %) of D-Ala carbon to total sediment organic carbon.

Absolute incorporation rates of ^{13}C for bacteria, inferred from conversion from the different biomarkers, are in good agreement and therefore provide an important validation for the use of biomarkers as a tool to quantify bacterial tracer incorporation.

Notable differences in the dynamics of $\Delta\delta^{13}\text{C}$ and ^{13}C among the HAAs were only found 4.5 months after labeling. These differences confirmed the refractory nature of peptidoglycan, as more ^{13}C -D-Ala persisted when compared to the ^{13}C -L-Ala. Moreover the HAAs glycine (Gly), serine (Ser) and proline (Pro) behaved relatively refractory. Interestingly, these AAs have previously been linked to progressive states of organic matter degradation.

Samenvatting

De diverse bodemgemeenschap van estuariene- en kustsedimenten floreert in een omgeving waar organisch koolstof van verschillende herkomst wordt verdund met sedimentpartikels op het moment dat het organisch koolstof het sediment bereikt. Onze kennis van de manier waarop het organisch koolstof wordt 'verdeeld' binnen de bodemgemeenschap is zeer beperkt. Dit komt doordat mariene sedimenten moeilijk te bereiken en bemonsteren zijn en doordat ze gekenmerkt worden door een grote ruimtelijke variabiliteit. In dit proefschrift combineren we het gebruik van stabiele isotopen methoden en kwantitatieve modellen om nieuwe inzichten te verkrijgen in de structuur van mariene benthische voedselwebben.

Hoofdstuk 2 is een overzicht van gepubliceerde lineaire inverse modellen (LIM); een modelleertechniek waarin data worden samengevoegd in een voedselweb model om vanuit incomplete datasets alle relaties in een voedselweb te reconstrueren. Dit overzicht bestaat uit drie delen.

Allereerst ontleden we een LIM in verschillende onderdelen, te weten: 1) vijf soorten ecologische informatie, 2) drie lineaire vergelijkingen, 3) twee soorten optimalisatiecriteria. Verschillen tussen LIM toepassingen kunnen worden teruggevoerd op de wijze waarop deze onderdelen worden gecombineerd. De belangrijkste keuzes die moeten worden gemaakt in het combineren van de onderdelen, blijken terug te brengen tot 1) waardering van de kwaliteit van de diverse informatietypen en 2) de keuze van het optimalisatiecriterium.

Ten tweede, in de meeste gevallen wordt in de ecologie een LIM gebruikt om een voedselweb te reconstrueren en gaat de discussie vooral over de structuur van het voedselweb. Echter, over het algemeen wordt geen, of slechts in beperkte mate, aandacht geschonken aan de eigenschappen van de LIM oplossing. Vijf LIMs van voedselwebben die verschillen in het aantal compartimenten, voedselwebrelaties en beschikbare data werden onderzocht en de meeste aandacht ging hierbij uit naar de eigenschappen van de LIM oplossing. Opvallend genoeg bleek dat de onzekerheid van de gereconstrueerde voedselwebrelaties in alle voedselwebben hoog was. De onzekerheid bleek gerelateerd aan de verhouding van het aantal observaties tot het aantal voedselwebrelaties. Hoe lager deze ratio, hoe hoger de onzekerheid. Bovendien bleek dat lineaire minimalisatiecriteria niet altijd tot één unieke oplossing leiden, maar dat deze criteria ruimte over laten voor andere gelijkwaardige oplossingen. Omdat kwadratische minimalisatiecriteria wel altijd tot een unieke oplossing leiden, wordt aangeraden deze te gebruiken in toekomstige studies. Op grond van de analyse van de LIM oplossingen adviseren we een dergelijke analyse voortaan routinematig uit te voeren.

Ten derde, de grote onzekerheid binnen gereconstrueerde voedselwebben maakt duidelijk dat extra databronnen nodig zijn om deze onzekerheid te verkleinen. Uit een studie naar een benthisch voedselweb bleek dat het toevoegen van stabiele isotopen

Samenvatting

data leidde tot een aanmerkelijke reductie van de onzekerheid (Hoofdstuk 3). Andere databronnen, zoals stochiometrie en kwantitatieve vetzuur analyse, zouden vergelijkbaar effectief kunnen zijn. We stellen dat LIM een ideale manier is om traditionele gegevens (bijvoorbeeld biomassa data) te integreren met meer moderne gegevens en zodoende de onzekerheid in voedselwebreconstructies kan verkleinen.

Hoofdstuk 3 beschrijft een casus waarin LIM wordt toegepast om de koolstofstromen in een intergetijdesediment te kwantificeren. In de conventionele LIM-methode bestaat de mogelijkheid om biomassa's en data van procesmetingen (bijvoorbeeld primaire productie, respiratie door de hele gemeenschap) te integreren. In dit hoofdstuk breiden we de bestaande methodologie uit, zodat ook stabiele isotopen data, op natuurlijk en tracer niveau, kunnen worden ingebracht. De onzekerheidsanalyse laat duidelijk zien dat deze toegevoegde data de onzekerheid in het gereconstrueerde voedselweb sterk verminderen: de onzekerheidsmarge in 60 % van de relaties nam af met meer dan 50 %. De conventionele methode maakt bovendien gebruik van een minimalisatiecriterium om het LIM op te lossen. Het gebruik hiervan is bekritiseerd in de literatuur, omdat een duidelijke verantwoording voor het gebruik ervan ontbreekt. In de hier uitgebreide methodologie wordt het model opgelost door tracer isotopen data toe te voegen wat het gebruik van het arbitraire minimalisatiecriterium overbodig maakt.

De koolstofstromen in het intergetijde voedselweb, in termen van secundaire productie en respiratie, werden gedomineerd door bacteriën. Bacteriën haalden hun koolstof voornamelijk van het semi-labele detritus (85 %), aangevuld met opgelost organisch koolstof. Maar een beperkte fractie (9 %) van de bacteriële productie wordt begraasd door het benthos, het grootste gedeelte werd gerecycleerd naar detritus en opgelost organisch koolstof. Microbenthos had de op een na hoogste secundaire productie. De dominante koolstofbronnen waren detritus en opgelost organisch koolstof. De resultaten maakten het echter niet mogelijk om het belang van de afzonderlijke bronnen vast te stellen. Opmerkelijk echter was het feit dat bacteriën voor slechts enkele procenten in de koolstofbehoefte van het microbenthos voorzien. Het grotere benthos, bestaande uit nematoden, ander meiobenthos en macrobenthos, bleek zich zeer selectief te voeden en is primair afhankelijk van de primaire productie van microphytobenthos en phytoplankton. Verrassend genoeg bleek dat het grotere benthos geen of nauwelijks koolstof opneemt van het semi-labele detritus. Deze bevindingen suggereren dat de microbiële gemeenschap (bacteriën en wellicht microbenthos) afhankelijk is van semi-labele detritus en dat maar weinig koolstof wordt doorgegeven aan hogere trofische niveaus, terwijl lokale primaire productie door microphytobenthos en phytoplankton van groot belang is als voedsel voor de meiobenthische en macrobenthische gemeenschappen. Dit suggereert dat de koolstofstromen tussen detritus-microben en algen-grazers gescheiden zijn en dat deze stromen onafhankelijk van elkaar functioneren.

Hoofdstuk 4 bouwt voort op de conclusie uit hoofdstuk 3 dat slechts een beperkte hoeveelheid van de bacteriële koolstofproductie wordt begraasd door de benthische gemeenschap en dat het grootste deel wordt gerecycleerd naar detritus of opgelost organisch koolstof. In dit hoofdstuk wordt een labelingsexperiment met stabiele isotopen beschreven dat is uitgevoerd om het lot van bacterieel koolstof in het sediment te kwantificeren. ^{13}C -glucose werd geïnjecteerd in de bovenste 10 cm van een intergetijdesediment en gevolgd in specifieke bacteriële polaire vetzuren (PLFAs), particulier organisch koolstof (POC), opgelost anorganisch koolstof (DIC), meiobenthos en macrobenthos. Een dynamisch model, met daarin de koolstof (C) en ^{13}C stromen in het sediment, werd gebruikt om de observaties van C en ^{13}C in de verschillende compartimenten te beschrijven. Dit model werd vervolgens gebruikt om de bacteriële

productie te bepalen en om te kwantificeren wat het belang was van de verliesprocessen begrazing, resuspensie en recycling naar detritus en opgelost organisch koolstof.

Het model bevat parameters voor resuspensie, bacteriële groei en begrazing en bacteriële groei efficiëntie. De parameterwaarden werden ingevoerd in een mechanistische vergelijking die op basis hiervan de ratio $\frac{\text{bacterieel koolstof}}{\text{particulair organisch koolstof}}$ voorspelt. De voorspelling op basis van de parameterwaarden uit het model was 0.005 en ligt in dezelfde orde als de geobserveerde ratio's (0.005 - 0.24). Het feit dat de voorspelling redelijk goed overeenkomt met de metingen suggereert dat mechanistische vergelijkingen kunnen worden gebruikt om de dynamiek van bacterieel koolstof te modelleren, in plaats van de empirische statistische modellen die over het algemeen worden gebruikt.

De bacteriële productie bedroeg $67 \text{ mmol C m}^{-2} \text{ d}^{-1}$. Het belangrijkste lot van bacteriële productie bleek mortaliteit te zijn (65 %). Hieruit blijkt dat er een lus tussen bacteriën en opgelost organisch koolstof bestaat, waarin koolstof wordt gerecycleerd. Het belangrijkste verliesproces van deze lus is bacteriële respiratie. Meiobenthos (3 %) en macrobenthos (24 %) begraasden 27 % van de bacteriële productie. Aangezien de meiobenthische en macrobenthische biomassa's hoog zijn in dit intergetijdesediment, verwachten we dat de graasdruk relatief hoog is ten opzichte van andere benthische systemen. Deze resultaten suggereren dat begrazing onbelangrijk is als controlerende factor van de bacteriële biomassa in mariene sedimenten.

De resultaten van dit experiment vormen eveneens de basis voor de hoofdstukken 5 en 6.

In **Hoofdstuk 5** staat de volgende vraag centraal: Hoeveel van hun koolstofbehoefte halen meiobenthos en macrobenthos uit bacteriën? Om deze vraag te beantwoorden werd de bacteriële gemeenschap van een intergetijdesediment gemerkt met een ^{13}C isotopen label, door ^{13}C -glucose in het sediment te injecteren. Het label werd gevolgd in bacteriën (via metingen aan labelopname in vetzuren specifiek voor bacteriën (PLFAs)) en in het meiobenthos (op groep niveau) en macrobenthos (op soort niveau) gedurende een periode van 36 dagen. Om het belang van bacterieel koolstof in het koolstofbudget van benthische organismen te kunnen vaststellen, werd de ^{13}C label opname in het benthos gemodelleerd met een simpel isotoop model en vergeleken met de verrijking aan ^{13}C in bacteriën. Bacterieel koolstof levert maximaal 20 % en over het algemeen < 10 % van de totale koolstofbehoefte van de verschillende meiobenthische en macrobenthische organismen. Het trofische belang van bacteriën voor meiobenthos en macrobenthos in intergetijdesedimenten is daarom beperkt.

De hoeveelheid labiel koolstof neemt over het algemeen af met toenemende diepte in het sediment. Vandaar dat we de hypothese stelden dat benthische organismen die dieper in het sediment leven, in hogere mate afhankelijk zijn van labiel bacterieel koolstof dan organismen die aan het sedimentoppervlak leven en direct toegang hebben tot andere bronnen van labiel koolstof. In tegenstelling tot onze hypothese, bleek dat meiobenthische en macrobenthische soorten die dieper in het sediment leven niet voor een relatief groter deel afhankelijk zijn van bacterieel koolstof. Mogelijk kunnen benthische organismen niet meer van het beschikbare bacterieel koolstof opnemen, omdat sedimentkorrels, met daarop de bacteriën, niet snel genoeg kunnen worden verwerkt in het maag-darmstelsel. Onder de aanname dat benthische organismen willekeurig een homogeen mengsel van sedimentkorrels en bacteriën eten, zou de hele benthische gemeenschap ongeveer 0.36 % van de beschikbare hoeveelheid bacterieel koolstof per dag eten. Dit ligt beneden de basisbehoefte aan koolstof van de benthische organismen en daarom lijkt het er inderdaad op dat een hogere opname van bacteriën simpelweg beperkt wordt door de snelheid waarmee sedimentkorrels kunnen worden verwerkt. Toch laten de gegevens ook zien

Samenvatting

dat de opgenomen hoeveelheid bacterieel koolstof 6 maal hoger is dan mag worden verwacht wanneer willekeurig gegeten zou worden. Dit toont duidelijk aan dat benthische organismen hun voedsel selectief opnemen.

Bacteriën assimileren en respireren labiel en semi-labiel organisch koolstof, terwijl uit eerder onderzoek (zie onder andere hoofdstuk 3) blijkt dat benthische fauna voornamelijk labiel organisch koolstof prefereert. De lage afhankelijkheid van bacterieel koolstof van benthische organismen suggereert dat competitie plaatsvindt voor het labiele koolstof en dat wanneer labiel koolstof eenmaal is geassimileerd door bacteriën dit in feite verloren is voor de fauna. Echter, de opname van bacterieel koolstof maakt het mogelijk dat semi-labiel koolstof, dat normaliter niet eetbaar is, alsnog voor de benthische fauna beschikbaar komt. Waarschijnlijk bepalen lokale omstandigheden, met name de beschikbaarheid van labiel koolstof, welk scenario zal domineren. De zwakke interactie tussen bacteriën, meiobenthos and macrobenthos betekent dat deze relatie niet als een predator-prooi relatie, maar als een competitie relatie voor labiel organisch koolstof moet worden gezien in het benthische voedselweb.

In hoofdstuk 4 bleek mortaliteit het belangrijkste lot van bacteriële koolstof productie. Aangezien bacteriën bestaan uit componenten met een verschillende afbreekbaarheid, zou tengevolge van de mortaliteit een opbouw kunnen plaatsvinden van de slecht afbreekbare componenten. In **hoofdstuk 6** bekijken we het lot van verschillende bacteriële biomarkers in het eerder beschreven ^{13}C -glucose labelingsexperiment. Vetzuren (PLFAs) worden relatief snel afgebroken in het sediment en staan daarom model voor levende bacteriën. D-Ala komt alleen voor in bacterieel peptidoglycaan, een bestanddeel van de celwand, wat bekend staat om zijn slechte afbreekbaarheid. Daarom gebruiken we D-Ala als een marker voor levende bacteriën en voor overblijfselen van dode bacteriën. Als laatste wordt de ^{13}C dynamiek in individuele aminozuren (AAs) vergeleken met AAs die in eerdere studies gerelateerd bleken te zijn aan de kwaliteit van het organisch materiaal.

De dynamiek van $\Delta\delta^{13}\text{C}$ in PLFAs, D-Ala en AAs bleek zeer vergelijkbaar in de eerste weken na labeling, wat betekent dat de verschillende biomarkers in gelijke hoeveelheden werden geproduceerd. Dit valt te verwachten wanneer nieuwe bacteriële cellen worden geproduceerd. De $\Delta\delta^{13}\text{C}$ was echter lager voor D-Ala en THAAs in vergelijking met PLFAs, dit komt waarschijnlijk doordat een grote inactieve achtergrond pool van D-Ala en THAAs de $\Delta\delta^{13}\text{C}$ van de levende bacteriën verlaagt.

Verrassend genoeg bleek echter dat de $\Delta\delta^{13}\text{C}$ dynamiek van PLFAs, D-Ala en AAs vergelijkbaar bleef gedurende de gehele experimentele periode van 4.5 maand. Indien de opbouw van slecht afbreekbare stoffen een belangrijk lot zou zijn na bacteriële mortaliteit, dan zou een relatieve verhoging van de $\Delta\delta^{13}\text{C}$ van D-Ala ten opzichte van de $\Delta\delta^{13}\text{C}$ van PLFAs met de tijd te verwachten zijn. Het gelijk blijven van de $\Delta\delta^{13}\text{C}$ dynamiek van PLFAs en D-Ala betekent daarom dat de opbouw van slecht afbreekbare stoffen geen belangrijk lot is van bacteriële koolstof productie. Het feit dat het organisch koolstof in het sediment maar voor $< 1\%$ uit koolstof van D-Ala bestaat, vormt aanvullend bewijs voor deze stelling.

Schattingen voor de absolute hoeveelheid ^{13}C opgenomen door bacteriën op basis van PLFAs, D-Ala en THAAs komen goed met elkaar overeen. Dit betekent een validatie van de methode om vanuit bacteriële biomarkers de totale opname van een stabiele isotopen tracer door bacteriën te kwantificeren.

Duidelijke verschillen in de dynamiek van $\Delta\delta^{13}\text{C}$ en ^{13}C tussen de verschillende THAAs werden pas 4.5 maand na de ^{13}C -glucose injectie gevonden. De verschillen bevestigen dat peptidoglycaan (bepaald via D-Ala) slecht afbreekbaar is, omdat meer ^{13}C -D-Ala aanwezig was dan ^{13}C -L-Ala. Bovendien leken de HAAs glycine (Gly), serine

(Ser) en proline (Pro) slecht afbreekbaar. Juist deze AAs zijn in eerdere studies goede indicatoren gebleken voor gevorderde stadia van afbraak van organisch materiaal.

Dankwoord

Dan nu het dankwoord, volgens mij een van de meest gelezen onderdelen van een proefschrift en niet zonder reden. Want ondanks dat het schrijven ervan betrekkelijk gemakkelijk is, wordt hier recht gedaan aan de niet onaanzienlijke bijdrage die anderen hebben geleverd aan dit proefschrift.

Allereerst bedank ik mijn promotor Carlo, voor het geven van veel vrijheid, het voorzien in zeer goede onderzoeksfaciliteiten en niet in de laatste plaats voor de mogelijkheid om mijn onderzoek voort te zetten in het EU-project HERMES. Jack, ook jij heel erg bedankt, voor de vele opmerkingen, suggesties en aanmoedigingen, de altijd snelle response op manuscripten, maar ook voor het houden van de nodige druk op de ketel in de laatste schrijfmaanden middels het regelmatig uitspreken van het simpele zinnetje "En Dick, hoe staat het met je stukken?". Karline, de enige die ik ken die 8 uur lang onverstoort aan een PC kan werken, heel erg bedankt voor je grote en uiteenlopende bijdrage aan dit proefschrift. Je hulp met onder andere de inverse and Bayesian analyses was onmisbaar. Nu alleen nog de overstap naar \LaTeX ... Peter, begeleider in de eerste jaren van mijn aio-schap, bedankt voor je input en bemoedigende woorden in het moeizame proces van publiceren. Ook kwam volgens mij het idee om de stabiele isotopen data in de inverse analyse vergelijkingen in te bouwen van jou. Ook jij bedankt Leon, bedankt voor de vele praktische tips aangaande het doen van experimenten, in het bijzonder tijdens de Pelagia en Trophos tochten, en het commentaar op mijn manuscripten waarin jij meestal voorstelde om alles volledig om te gooien (major re-juggling zoals jij dat noemt).

Naast begeleiders ook aan collega-aio's geen gebrek in dit dankwoord. Ed, Imola, Paul, Iris en Han bedankt voor de collegialiteit en gezelligheid. Met name aan het voetbal op dat hobbelige handbalveldje en het squashen heb ik goede herinneringen. De 'cups' die veroverd zijn tijdens de NIOO-voetbaltoernooien laten zien dat al die training niet voor niets was.

Op het moment dat ik zelf als aio begon was dat nog een 'nieuwje' op het CEME. Kort daarop vond een heuse aio-boom plaats en werden er in een periode van enkele jaren zo'n 20 nieuwe aio's aangesteld. Veel Nederlanders zaten er niet bij, maar dat maakt het zeker zo gezellig. In het bijzonder wil ik Bart, Karel, Sandra, Bregje en Jeroen noemen en natuurlijk Henrik en Maria. Maria bedankt voor het opofferen van enkele weekenden om monsters voor mij door te meten op het lab. Ik hoop dat we elkaar zo af en toe blijven zien, ofwel in het kneuterige Zweden of in het met kleine natuurgebieden bezaaide Nederland.

Voor de vele hulp, praktische oplossingen en vakantie verhalen wil ik Pieter graag bedanken. Ute, bedankt voor het voorzien van de benodigde algenkweken. De bootbemanning, laboratorium crew en huishoudelijke dienst zorgden altijd voor een prettige sfeer. In het bijzonder wil ik hier Els noemen, een dag begon vrijwel altijd met een praatje met Els in de keuken en het is er nu een stuk stiller. De manier waarop je bent afgeschreven in de reorganisatie staat in geen enkele verhouding tot je inzet voor NIOO;

Dankwoord

Els bedankt voor je gezelligheid. Ook wil ik Cynthia en de studenten Ria en Ehsan, die mij met veel enthousiasme hebben geholpen in mijn werk, bedanken.

Mathieu, kamergenoot in het eerste jaar en begeleider tijdens mijn afstudeervak, bedankt voor je gezellige en energieke aanwezigheid en vele verhalen over je rugzaktochten. Ik kan je vertellen dat Patagonië heel mooi is. Ook Filip bedankt, kamergenoot sinds enkele jaren, voor je gevatte gevoel voor humor en voor het feilloos vinden van gaten in mijn ogenschijnlijk waterdichte redeneringen.

Mijn paranimfen komen niet van het CEME en dat is niet omdat er geen geschikte kandidaten zijn. Nee, ik heb 2 vrienden bereid gevonden om die taak op zich te nemen en ik kan me geen betere wensen. Otto, met jou heb ik veel beleefd: het studentenleven in Vlissingen en Wageningen, een verre stage in Costa Rica, een fantastische vakantie in Patagonië en duiken in Nederland en Egypte. Ik hoop dat dit rijtje over enkele jaren verder uitgebreid zal kunnen worden. Maarten, we zijn begonnen als afdelingsgenoten in Wageningen en uitgegroeid tot vrienden, mede dankzij vele avonden kletsen en discussiëren in de bank of in de kroeg. Die avonden gaven en geven veel stof tot nadenken, hopelijk blijven ze dat doen.

Als laatste wil ik het thuisfront enorm bedanken. Pa en ma voor het blijven steunen van mijn voortdurende ambities om te blijven studeren; dit proefschrift is mede daaraan te danken. Lisette, je hebt me vaak door dipjes en dippen heen moeten slepen, vooral tijdens de laatste loodjes en dat deed je altijd glansrijk, heel erg bedankt daarvoor en nog meer voor de grote rest. Thijs, het is een fantastisch gevoel als jij met een grote glimlach op me af komt lopen als ik 's avonds thuiskom; een hele dikke knuffel.

Curriculum Vitae

Dick van Oevelen graduated from the study Aquatic Ecotechnology (Higher Professional Education) at the Hogeschool Zeeland in Vlissingen. He did one practical period in Costa Rica (Universidad Nacional, Heredia) where he worked on the reduction of pesticide pollution from banana plantations. He did another practical period at the Institute of Nature Conservation (Brussels, Belgium) on the integration of the Barbierbeek brook in the controlled inundation area Kruikeke-Bazel-Rupelmonde, which is developed along the Schelde estuary in Belgium. He continued his studies at the Wageningen University (WUR) and graduated *cum laude* in 2000 as an aquatic ecologist. One MSc project concerned modeling bulrush growth along the Schelde estuary and was carried out at the NIOO-CEME in Yerseke. In another MSc project, the effect of sedimentation on coral recovery rates was quantified during a field experiment carried out at the field station of the Marine Science Institute of the University of the Philippines. After his graduation he worked for half a year at the Institute of Nature Conservation in Brussels on a bibliographic synthesis of estuarine restoration projects. He started his PhD project in August 2000 at the NIOO-CEME, which resulted in the thesis "Structure of marine benthic food webs: Combining stable isotope techniques and inverse modeling". He also participated in the TROPHOS project (<http://www.vliz.be/projects/trophos/index.php>), in which the benthic-pelagic coupling was investigated of two contrasting sites at the Belgian Continental Shelf. He continues his scientific work in the frame of the HERMES project (Hotspot Ecosystem Research along the Margins of European Seas, <http://www.soc.soton.ac.uk/CHD/HERMES/intro.html>), which involves the construction of carbon and nitrogen budgets of several deep-sea ecosystems.

List of publications

- Van Oevelen D, Middelburg JJ, Soetaert K and Moodley L. The fate of bacterial carbon in an intertidal sediment: Modeling an in situ isotope tracer experiment. Accepted by Limnology and Oceanography.
- Van Oevelen D, Moodley L, Soetaert K and Middelburg JJ. The trophic significance of bacterial carbon in a marine intertidal sediment: Results of an in situ stable isotope labeling study. In revision for Limnology and Oceanography.
- Veuger B, Van Oevelen D, Middelburg JJ and Boschker HTS. Fate of ^{13}C labeled bacterial proteins and peptidoglycan in an intertidal sediment. In revision for Limnology and Oceanography.
- Van Oevelen D, Soetaert K, Middelburg JJ, Herman PMJ, Moodley L, Hamels I, Moens T and Heip CHR. Carbon flows through a benthic food web: Integrating biomass, isotope and tracer data. Submitted to Journal of Marine Research
- Kones J, Soetaert K, Van Oevelen D, Owinoa JO, Mavutic K. Gaining insight into aquatic food webs reconstructed by the inverse method. Accepted by Journal of Marine Systems.
- Van der Meer J, Heip CHR, Herman PMJ, Moens T and Van Oevelen D, 2005. Measuring the flow of energy and matter in marine benthic animal populations, p. 326-408. In Eleftheriou A and McIntyre A (eds.), Methods for the study of marine benthos. 3Rev ed. Blackwell Science
- Soetaert K, Hoffmann M, Meire P, Starink M, Van Oevelen D, Van Regenmortel S, Cox T, 2004. Modeling growth and carbon allocation in two reed beds (*Phragmites australis*) in the Scheldt estuary. Aquatic Botany 79: 211-234



Royal Netherlands
Academy of Arts
and Sciences